



The University of  
**Nottingham**

UNITED KINGDOM • CHINA • MALAYSIA

Shen, Jingyi (2017) Chemical and isotopic analysis in the investigation of glazes from Northern China and the Middle East, 7th-14th centuries AD. PhD thesis, University of Nottingham.

**Access from the University of Nottingham repository:**

<http://eprints.nottingham.ac.uk/48201/1/Jingyi%20Shen%20thesis%20corrected.pdf>

**Copyright and reuse:**

The Nottingham ePrints service makes this work by researchers of the University of Nottingham available open access under the following conditions.

This article is made available under the University of Nottingham End User licence and may be reused according to the conditions of the licence. For more details see:

[http://eprints.nottingham.ac.uk/end\\_user\\_agreement.pdf](http://eprints.nottingham.ac.uk/end_user_agreement.pdf)

For more information, please contact [eprints@nottingham.ac.uk](mailto:eprints@nottingham.ac.uk)

UNIVERSITY OF NOTTINGHAM

**Chemical and isotopic analysis in the  
investigation of glazes from Northern China  
and the Middle East, 7th-14th centuries AD**

by

**Jingyi Shen**

**BSc, MA**

**March 2017**



Thesis submitted to The University of Nottingham for the degree of Doctor of Philosophy



## Abstract

Both Chinese and Islamic glazed ceramics played a significant role in the history of ancient ceramic production. Moreover, it was innovation in glazes that made the Chinese and Islamic ceramics constantly innovative in various categories with different manufacturing techniques. This study applies chemical and isotopic analyses to investigate the manufacturing techniques and provenances of different types of glazes from Northern China and the Middle East, and extends the use of Sr isotopic analysis to investigate raw materials and glaze recipes used to making lime/alkaline glazes in Northern China and the Middle East for the first time.

By chemical compositions of the lead glazes, the glazing techniques used to produce Chinese Tang Sancai lead glazes and splashed lead glazes from the Middle East have been identified. The mixture of lead oxide plus quartz/quartz sand was used for making both Chinese Tang Sancai glazes and Islamic splashed lead glazes. Besides, for the Chinese lead glazes, the trace element and lead isotopic analyses of them have been effective in grouping glazes made in different production kiln sites, and hence associating the Tang Sancai wares excavated from archaeological sites of unknown origin with their production centres. Furthermore, by comparing the lead isotopic ratios of Islamic lead glazes and those of lead ore deposits, the possible sources of lead used for making lead glazes can be determined, although more than one source was suggested due to the overlap of Pb isotopic ratios of different lead ore sources in some cases.

This study is the first time that Sr isotopic analysis has been applied to the lime/alkaline glazes from Northern China and the Middle East. It has revealed that Sr isotopic compositions of lime/alkaline glazes from Northern China and the Middle East have been very effective in providing information on the glaze recipes and characteristics of raw materials used for

making them. Based on Sr isotopic compositions, the case study of Northern Chinese lime glaze has identified that the Yaozhou celadon glaze was probably produced by local 'Fuping glaze stone' combined with botanic ash. Besides, the case study of the Middle East alkaline glaze has suggested that the Raqqa ware glaze was probably made by 'Cenozoic sand' containing a certain content of limestone grains and feldspar and that botanic ash was used as a flux.

**Keywords:** Tang Sancai lead glaze, Islamic splashed lead glaze, Yaozhou celadon glaze, Raqqa ware glaze, Northern China, the Middle East, chemical composition analysis, Pb isotopic analysis, Sr isotopic analysis

## **Acknowledgement**

I would like to express my sincerest gratitude to my supervisor, Professor Julian Henderson, for his guidance, understanding, support and encouragement during my PhD study. His great supervision and constant passion for archaeological research has enlightened my research and will benefit my future career in archaeology undoubtedly. I think that my PhD study went so well was because Professor Henderson always gives the helpful instruction whenever I need it.

My sincere thanks also extend to Dr Jane Evans of the NERC Isotope Geosciences and Dr Simon Chenery of the Analytical Geochemical Laboratories in British Geological Survey, for their professional guidance and endless patience during my laboratory training in lead and strontium analysis, trace element analysis, and preparation of my sample. They also gave me academic suggestions and comments on my research. I would also like to thank Dr Edward Faber at the Department of Archaeology for his support and assistance during the EPMA-WDS analysis.

The ceramic samples analysed in this project came from some museums and institutes, and each one was extremely helpful. Sincerely thanks to: Department of Cultural Heritage, the Northwest University, China; Xi'an City Institute of Archaeology, China; Ashmolean Museum, Oxford, UK.

I am also grateful for NERC Isotope Geosciences Laboratory, British Geological Survey for funding Professor Julian Henderson and Doctor Jane Evans to carry out this PhD training project for me on the lead and strontium analysis, and special gratitude is also given the University of Nottingham for funding me to fulfil my dream to study ceramics as a PhD student.

I also appropriate all my friends and the members of the Department of Archaeology who have supported me and helped me a lot in both academic and life.

Finally, I would like to express my thanks and love to my parent, for their endless love and support for me during my PhD study aboard. I am also indebted to my beloved husband JI-Peng Wang, for his tireless support and caring.

# Table of Contents

Abstract .....	I
Acknowledgement .....	III
Table of Contents .....	V
Chapter 1 Introduction .....	1
1.1 Background.....	1
1.2 Aims, objectives and research questions .....	6
1.3 The research subjects and thesis structure .....	7
Chapter 2 The Introduction to glazed ceramics from Northern China and the Middle East .....	10
2.1 Introduction .....	10
2.2 The introduction to Chinese lead glazed ceramics .....	11
2.2.1 Chinese lead glazed ceramics .....	11
2.2.2 Tang Sancai wares .....	14
2.2.3 Introduction to Chinese sites where the Tang Sancai lead glazes in this study were excavated.....	18
2.2.4 Previous scientific studies of Tang Sancai wares .....	23
2.3 Islamic glazed ceramics from the Middle East.....	26
2.3.1 Islamic glazed ceramics .....	26
2.3.2 Coloured monochrome-glazed wares.....	31
2.3.3 Lead-glazed splashed ceramics .....	32
2.3.4 Introduction to archaeological sites of Syria and Iraq where the Islamic glazes in this study were excavated from .....	34
2.3.5 Previous scientific studies of glazes from Al-Raqqah, Kish and Hira .....	40
2.4 The introduction to green stoneware of Northern China .....	42
2.4.1 The brief history of green stoneware of Northern China .....	42
2.4.2 Introduction to the Yaozhou Kiln complex.....	45
2.4.3 The archaeology of Yaozhou Kiln complex .....	55



2.4.4 Historical records and scientific studies of Yaozhou celadon wares and their production techniques .....	57
<b>Chapter 3 Methodology and previous work .....</b>	<b>63</b>
3.1 Introduction .....	63
3.2 Major and minor chemical composition analysis .....	63
3.2.1 Introduction.....	63
3.2.2 Sample preparation for analysis by electron microprobe.....	64
3.2.3 The significant elements to be measured .....	65
3.2.4 Analysis and standards.....	65
3.2.5 Relevant literature review .....	67
3.3 Trace elemental analysis.....	70
3.3.1 Introduction.....	70
3.3.2 Sample preparation for analysis by LA-ICP-MS .....	72
3.3.3 The trace elements to be measured .....	72
3.3.4 Analysis and standards.....	72
3.3.5 Relevant literature review .....	74
3.4 Lead isotope analysis.....	78
3.4.1 Introduction.....	78
3.4.2 The basic hypothesis of Pb isotopic application to provenance ancient glaze materials .....	79
3.4.3 MC-ICP-MS instrumentation.....	80
3.4.4 Sample preparation for Pb isotopic analysis .....	81
3.4.5 Analyses and standards .....	82
3.4.6 The precise and accuracy of MC-ICP-MS analysis .....	86
3.4.7 Relevant literature review .....	87
3.5 Strontium isotopic analysis.....	90
3.5.1 Introduction.....	90
3.5.2 The basic hypothesis of Sr isotopic application to provenance ancient glass or glaze materials.....	91

3.5.3 The TIMS technique for Sr isotope analysis and the standard used .....	93
3.5.4 Preparation of samples for Sr isotopic analysis .....	94
3.5.5 Relevant literature review .....	96
<b>Chapter 4 Chemical and lead isotopic analysis of lead glazes from Northern China and the Middle East, 7th-14th centuries AD .....</b>	<b>101</b>
4.1 Introduction .....	101
4.2 Samples.....	101
4.2.1 Tang Sancai glaze samples from Northern China.....	101
4.2.2 The Islamic glaze samples from Syria and Iraq .....	102
4.3 Results and discussion of major elemental composition.....	102
4.3.1 The major elemental compositions of Tang Sancai lead glaze samples .....	103
4.3.2 The major chemical compositions of lead glazes from the Middle East (Syria and Iraq) .....	110
4.3.3 Comparison of high lead glazes from Northern China and the Middle East .....	115
4.4 Trace elemental compositions of Chinese Tang Sancai and Islamic lead glazes from Syria and Iraq.....	118
4.4.1 The trace elements of Chinese Tang Sancai lead glaze samples.....	119
4.4.2 The trace elements of Islamic splashed lead glaze samples excavated in Syria and Iraq .....	125
4.4.3 The trace element compositional comparison of Chinese Tang Sancai lead glazes and Islamic lead glazes of Syria and Iraq .....	126
4.5 Results and discussion of lead isotope analysis of Chinese Tang Sancai and Islamic glazes from Syria and Iraq.....	129
4.5.1 Tang Sancai lead glazes .....	130
4.5.2 Islamic splashed lead glazes from Syria and Iraq .....	137
4.5.3 The lead isotope comparison of Chinese Tang Sancai lead glazes and Islamic lead glazes of Syria and Iraq.....	150
4.6 Conclusions .....	151
<b>Chapter 5 The chemical and Sr isotopic analysis of Yaozhou celadon glaze from Northern China.....</b>	<b>153</b>

5.1 Introduction .....	153
5.2 Samples.....	154
5.3 Results .....	155
5.3.1 The major elemental compositions of Yaozhou celadon glaze samples .....	155
5.3.2 The rare earth elemental compositions of Yaozhou celadon glaze samples .....	158
5.3.3 The Sr isotopic compositions of Yaozhou celadon glaze samples.....	164
5.4 Discussion.....	168
5.4.1 The possible flux type used in Yaozhou celadon glaze based on major chemical compositions .....	168
5.4.2 The changes in glaze recipes in Yaozhou celadon glaze in the three successive periods .....	170
5.4.3 The clues from historical records and REE distribution curves of glaze stone used in Yaozhou celadon glazes.....	171
5.4.4 The Sr isotopic composition pattern of Yaozhou celadon glaze and the suggested flux used in Yaozhou celadon glazes .....	173
5.4.5 The possible contribution of glaze stone to the Sr isotopic composition and the characteristics of glaze stone.....	177
5.4.6 Possible explanations for the wide spread of $^{87}\text{Sr}/^{86}\text{Sr}$ signatures in Yaozhou celadon glaze .....	180
5.4.7 The Sr isotopic composition as a method of comparing the glaze recipes.....	182
5.5 Conclusions .....	185
<b>Chapter 6 A pilot study of the Sr isotopic composition of ceramic glazes from Al-Raqqa, Syria.....</b>	<b>186</b>
6.1 Introduction .....	186
6.2 The archaeology of Tell Zujaj and Tell Aswad in the Al-Raqqa industrial complex, northern Syria .....	186
6.2.1 Introduction to Tell Zujaj.....	187
6.2.2 Introduction to Tell Aswad.....	188
6.3 Samples.....	189
6.4 Results .....	189

6.4.1 The major elemental composition of Al-Raqqa turquoise monochrome glaze samples .....	189
6.4.2 The Sr isotopic composition of Al-Raqqa turquoise monochrome glaze samples.....	191
6.5 Discussion.....	193
6.5.1 The Sr isotopic compositional pattern of Al-Raqqa alkaline glaze and the flux of Al-Raqqa alkaline glaze suggested by it .....	193
6.5.2 The possible contribution of siliceous raw material to the Sr isotopic composition of Al-Raqqa alkali glaze and the characteristics of the siliceous raw material used.....	197
6.5.3 The connection between the glass production and glazed ceramic production in Al-Raqqa .....	201
6.6 Conclusions .....	204
Chapter 7 Conclusions and future work .....	206
Bibliography.....	215
APPENDIX I Data tables.....	237
APPENDIX II The photos of samples.....	267



# Chapter 1 Introduction

## 1.1 Background

Chinese glazed ceramic techniques, dating back to the Shang dynasty (16th -11th centuries BC), show a continuous development and innovation during its long history. Chinese glazed ceramics were not only one of the most important inventions in ancient China, but also influenced Islamic pottery production tracing back to at least the 8th century AD of the Tang dynasty (AD618-907). A number of studies have proven that Tang imported glazed ceramics and their techniques, traded by the Silk Road and Maritime Silk Route, rekindled the inspiration of the Islamic potters, and stimulated the innovation of early Islamic pottery techniques (Lane 1947, 12; Mason and Tite 1997; Tite et al. 1998; Kerr and Wood 2004, 732-733; Watson 2014, 47).

In the long history of both Chinese and Islamic glazed ceramic production, technological breakthroughs occurred one after another, and with it came a great variety of glazed ceramic types produced in different kiln sites and areas. Compared to ceramic body, ceramic glazes were produced by more complicated processes. It is ancient Chinese glaze that made Chinese ceramics outstanding in the world. Besides, glaze was one of the key factors that made the Chinese and Islamic ceramics constantly innovate producing various categories with different manufacturing techniques. Therefore, the glaze is an indispensable research subject in ancient ceramic studies, and the ancient Chinese and Islamic glazes are research subjects of this present study.

Glaze can be basically divided into two categories: low-fired lead based glaze and high-fired glaze including lime/alkali glaze, alkali glaze and high lime glaze due to their significantly

different glaze recipes. Within each category, some sub-groups can be found by different manufacturing techniques (e.g. different raw material selections, glaze recipes and decoration techniques) and it is hard to study all of them within one piece of research. Therefore, several typical glaze types which represent ancient lead glaze and lime/alkaline glaze from Northern China and the Middle East were selected as research subjects in this study.

Normally two questions are particularly important for ancient ceramic studies. The first is concerned with the manufacturing techniques of ceramics as well as evolution and transformation of the manufacturing process (Tite et al. 1984, 140; Pollard and Hatcher 1994; Tite 2008). The second question focuses on provenance and dating (Leung and Luo 2000; Bartle and Watling 2007; Tite 2008). Provenance studies try to discuss whether ceramics were locally produced or imported, and if the latter, to determine the origin of production centre and/or the source of the raw materials used (Tite 2008). The studies on the manufacturing technology and provenance of ancient Chinese and Islamic glazes also are the main research objectives of this present work.

Over the past decades, chemical composition analysis has been used widely as a useful tool to group glazes with distinct characteristics and identify possible glaze recipes used. The use of lead isotopic analysis can provide information on the possible sources of lead used in the production of glazes. The application of Sr isotopic analysis is a relatively new technique of archaeological material studies. Some studies have already proven its potential for providing useful information about raw material sources of a range of archaeological materials (e.g. Freestone et al. 2003; Montgomery et al. 2003; Henderson et al. 2005a; Ma et al. 2016). In this present work, the different types of isotopic analysis will combine with the chemical composition analysis to investigate the different glaze types and corresponding research objectives.

## **Chemical and lead isotope analyses on lead glazes**

To identify whether a lead compound by itself or a mixture of a lead compound with silica was used in glaze making is one of the most important research objectives in lead glazing techniques. By previous studies (Hurst and Freestone 1996, Tite et al. 1998, Walton and Tite 2010), it has been proven that the interaction between the glaze and the body might provide evidence for this research objective, which can be identified by a comparison of the body and glaze chemical compositions. By chemical composition analysis, De Benedetto et al. (2004) and Waksman et al. (2007) have provided information on the glazing technology of high-lead glazes for the Roman period and the Byzantine period respectively. In this study, the glazing techniques of some lead glazes from Northern China and the Middle East during the periods from the 7th to the 14th centuries AD will be identified by chemical analysis.

Lead glaze, is characterised by its high composition of PbO (usually more than 40%), which makes it ideal to use lead isotope analysis to study the provenance of the glaze. Comparison of the lead isotope ratios for the glazes with those for lead ores, one can provide information on the possible sources of the lead used in the glaze production. In this study, the possible sources of the lead used in the glaze production of some Chinese and Islamic lead-glazed ceramics will be discussed. Besides, the method using lead isotope ratios of glazes to provenance the glazed ceramics with unknown origin also will be discussed. However, it needs to be pointed out that the overlap of lead isotopic signatures among some different lead ore sources in different areas makes the lead isotope analysis have a limitation in provenancing the lead source in some cases.

According to the Goldschmidt's Rule in Geochemistry (Goldschmidt 1937), all the elements in periodic table of the elements could be divided into four categories: lithophile elements, chalcophile/sulfophile elements, siderophile elements and atmophile elements. The elements



which belong to the same category have the similar geochemical characteristics, and they enrich mutually during the processing of crust formation, smelt, ore-forming and other geochemical processes. By this, the contents of chalcophile trace elements (e.g. As, Sn and Sb) in the lead glaze, which are the common accompanying elements of lead ore deposits, were mainly introduced by lead flux. Therefore, by compositions of these trace elements in the glazes, information on the lead sources used in glaze production might be suggested. In this study, the trace elemental analysis will be undertaken on Chinese and Islamic glazes to identify whether this method can be used as a complementary tool to provenance the lead-glazed ceramics.

### **Chemical and Sr isotope analyses on lime/alkaline glazes**

To identify the recipe used in ancient glaze production is one of the most important research objectives in manufacturing technology study.

The lime/alkaline glaze is composed of two parts- the siliceous raw material (usually clay or weathered rock for Chinese glaze, quartz or sand for Islamic glaze) and the flux. The siliceous raw material is the major raw material of both ceramic body and glaze. Because of the inconvenience of transport in ancient times, the availability of siliceous raw materials was always the priority for the location selection of ceramic production kilns. This means that siliceous raw materials of ancient ceramic production would be inferred relatively easily by studying both the glazed ceramic samples and minerals nearby. Over the past decades, by comparing the major chemical compositions of the ceramic samples with local minerals which were probably used as siliceous raw materials of ceramic making, the siliceous raw materials used for ceramic making of some important kilns have been understood clearly.

However, with regards to the other part of glaze- flux, the chemical composition analysis seems to be not so effective. For the Chinese lime glazes, the limestone and botanic ash were normally used as the fluxes, and for the Islamic alkaline glaze, the natron and botanic ash were the possible fluxes used. In some previous chemical compositional studies, the contents of  $P_2O_5$ , MgO and sometimes MnO were used to identify the flux, because only botanic ash could provide a significant amount of  $P_2O_5$ , MgO and MnO. However, this method has not been proven very well, because no standard contents of  $P_2O_5$ , MgO and MnO have been identified with which to judge whether the flux should be suggested as plant ash. In recent years, Sr isotopic analysis has been proven to be a helpful method to identify the raw material sources in ancient glasses (Freestone et al. 2003; Henderson et al. 2005a; Brems et al. 2013). Besides, Ma and Henderson et al. (2014) did the pioneering work to apply Sr isotope analysis in the study on lime glazes of Southern China and demonstrated that Sr isotopic analysis is a potential method to identify the flux.

The Chinese ceramic technologies of South China and North China have developed along their own courses mainly due to the different raw materials used (Wood 2011, 27). Despite having the same important role in the Chinese ceramic history, northern ceramics are not so well studied as their southern counterparts due to fewer historical records and fewer available raw material samples. Until now, the recipes of many glazes from Northern China have not been identified clearly. In this study, the Sr isotopic analysis is undertaken on lime glazes from Northern China to explore if the Sr isotopic compositions of Northern China glazes could identify the raw materials used in their production. Similarly, a pilot Sr isotopic analysis also is conducted on the alkaline glazes from the Middle East to explore whether it could be used as a method for suggesting the characteristics of raw materials used in Islamic glaze production.

## **1.2 Aims, objectives and research questions**

This thesis aims to combine the chemical and isotopic analyses to investigate manufacturing techniques and provenance of lead glazes from Northern China and the Middle East and to extend the application of Sr isotopic analysis to investigate glaze recipes used to make lime/alkaline glazes in Northern China and the Middle East.

### **Aims and objectives**

1. To identify and compare the glazing techniques of lead glazes from Northern China and the Middle East.
2. To combine chemical and lead isotopic analyses to determine the possible sources of lead used in the production of the glazes and provide information on the possible provenance of glazed ceramics.
3. To determine what kind of Sr isotopic composition patterns lime glazes from Northern China and alkaline glazes from the Middle East contain.
4. To use Sr isotope composition to characterise raw materials used in glaze production and suggest the glaze making recipes of glazes from Northern China and the Middle East.

### **Research questions**

1. How do the chemical compositions of lead glazes from Northern China and the Middle East help to identify and compare the raw materials and glazing techniques used?

2. Is it possible to determine the possible sources of lead used in the production of lead glazes from the Middle East?
3. How do chemical and lead isotopic analyses of lead glazes excavated from ceramic production kilns help to provide information on the provenance of glazed ceramics with unknown origin?
4. How does Sr isotopic analysis of Northern China and the Middle East glazes help to characterise raw materials used in glaze production and determine the glaze recipes?
5. How does Sr isotopic analysis of Northern China and the Middle East glazes help to trace the raw materials used for glaze production?

### **1.3 The research subjects and thesis structure**

The initial starting point of this study is to apply different analytical methods to investigate the manufacturing techniques and provenances of selected Chinese and Islamic glazes. Based on the different glaze types selected in this study-low-fired lead glazes and high-fired lime/alkaline glazes, this study can generally be divided into two parts.

The first part uses chemical and lead isotopic analyses to investigate the glazing techniques and lead sources used in lead glaze production. Besides, the origin of the lead-glazed wares and the interactions between different ceramic production centres are also discussed (in chapter 4). In this chapter, the Tang Sancai lead glazes from Northern China and Islamic splashed lead glazes from the Syria and Iraq are selected as the research subjective. Tang Sancai, a type of ceramics covered with multi-coloured lead-glazes, were mainly produced in Northern China during the Tang Dynasty (AD618-907). Tang Sancai is quite unusual in Chinese ceramic history because of its unique low-fired lead glaze. Besides, the export Tang

Sancai wares also became popular in the Islamic world because of the prosperous Silk Road trade. The famous Islamic ceramic family called ‘lead-glazed splashed wares’ are thought to be influenced by Chinese Tang Sancai wares. The Tang Sancai lead glaze samples in this study were collected from the two most significant Tang Sancai production kiln sites- Huangye kiln in Henan province and Huangpu kiln in Shaanxi province, and two Tang dynasty tombs from the Xi’an city of Shaanxi province with unknown origin. For the Islamic glaze samples, the fragments of splashed lead-glazed wares (8th-14th centuries AD) were collected from the Al-Raqqa in Northern Syria and Kish and Hira in Iraq.

The second part of this study is using chemical and strontium isotopic analyses to provide information on the glaze recipes used in making high-fired lime/alkaline glazes from the Northern China and Syria. Since the raw materials and glazing techniques used in them are different, the glaze making techniques used on each site are discussed in two separate case studies in this thesis.

The northern green stoneware manufactured in Yaozhou kiln from Shaanxi province, called as ‘Northern Yaozhou style Celadon’ by modern archaeological scholars, is thought to be the best representative of Northern China greenware. Until now, the siliceous raw materials and especially the flux used in Yaozhou celadon glaze are still unresolved clearly. Thus the Yaozhou celadon glazes made from the Tang dynasty (AD618-907) to the Northern Song dynasty (AD960-1127) were selected as the research subjective studied in chapter five. The identification of the raw materials and the glaze recipe of Yaozhou celadon glaze, as well as the changes of glaze recipes of Yaozhou celadon made in different periods are discussed by Sr isotopic compositions in this chapter.

The glazes of turquoise monochrome ‘Raqqa ware’ (8th-9th centuries AD) from Al-Raqqa of Northern Syria, which was one of the typical Islamic alkaline-glazed ceramics, were selected

as Islamic glaze samples studied in chapter six. The identification of the raw material characteristics used in 'Raqqqa ware' production is discussed by Sr isotopic compositions in this chapter. Because the Sr isotope analysis had been carried out on plant ash glasses excavated from Al-Raqqqa by Henderson et al. (2015a), in this study, the raw material sources used in glass and glaze production in Al-Raqqqa also can be compared by their Sr isotopic compositions.

The glazes from Northern China and the Middle East discussed in this study were produced in a long-term time span stretching from the 7th century AD to the 14th century AD, and the glazes are selected from several archaeological sites in different regions and belong to different types of ceramic ware. Therefore, a brief ceramic history relevant to these glazes is introduced in chapter two to help understand their history context. The archaeological sites of Northern China and the Middle East where the glazes in this study were excavated are introduced in details. Besides, the previous scientific studies on these glazes are reviewed.

The methodology of this thesis is introduced in chapter three. The basic methodology, the instruments used, the experimental procedures and reviews of previous work of chemical composition analysis, Pb isotopic analysis and Sr isotopic analysis are introduced.

Chapter seven is the overall conclusions generalised from the three case studies and the future work that needs to be done.

# **Chapter 2 The Introduction to glazed ceramics from Northern China and the Middle East**

## **2.1 Introduction**

In the long history of both Chinese and Islamic glazed ceramic production, technological breakthroughs occurred one after another, and with it came a great variety of ceramic and glaze types. The Chinese and Islamic glazes discussed in this study were in a long-term time span stretching from the 7th century AD to 14th century AD, and the glazes are from several archaeological sites in different regions and belong to different types of ceramic ware. In particular, the Tang Sancai lead glaze and Yaozhou celadon from Northern China are Chinese samples chosen in this study, while the glazes of monochrome glazed Raqqa ware and splashed lead-glazed ware from Syria and Iraq are the Middle Eastern samples selected in this study. Therefore, a brief ceramic history relevant to these glazes is presented in this chapter to help understand their historical context. The archaeological sites of Northern China and the Middle East where the glazes were derived from in this study are also described.

## **2.2 The introduction to Chinese lead glazed ceramics**

### **2.2.1 Chinese lead glazed ceramics**

The earliest glaze found in China is high-fired lime glaze fused to the proto-porcelain<sup>1</sup> body, which was first produced in the early Bronze Age Shang dynasty (the middle of the second millennium BCE) (Li 1998, 69). However, it was not until the Western Han dynasty (BC206-AD9) that the first low-fired lead glaze in Chinese ceramic history was born, which was fused to pottery bodies and named as Han lead glaze (Li 1998, 465). The lead glaze uses lead compounds as a flux to reduce the melting temperature of glaze to approximately 700-900°C (Zhang and Zhang 1980). Han lead-glazed pottery developed rapidly during the whole Han Dynasty (BC206-AD220). The archaeological findings indicate that Han lead glazed ceramics were mainly produced as funerary objects like bowls, boxes, models of houses and livestock statues (Ye 1989, 100-102; Jiang 2009, 8-13). Han lead-glazed pottery is mainly decorated by monochrome-coloured glaze, and green is the most common colour.

In the subsequent 200 years, with the Han Empire dying out, Han lead-glazed pottery experienced a decline too. Until the beginning of Northern Wei dynasty (AD386-534), lead-glazed pottery became popular again in Northern China, and its glazing technique improved a lot compared to that of the Han dynasty lead-glazed pottery. Specifically, almost all the Han lead glazed ceramics are a monochrome green colour, whereas, since the Northern Wei dynasty, some lead-glazed pottery had been decorated with an added

---

<sup>1</sup> Proto-porcelain, referring to early high-fired glazed ceramics dating back to the Shang and Zhou dynasties (BC1600-BC256), is a kind of glazed stoneware which has a dense hard body made from porcelain stone alone and has low porosity (Luo and Li 1998, 647; Li 1998, 69; Kerr and Wood 2004, 11).



green colour on its yellow or white background glaze; even yellow, green and brown colours had been used together. The appearance of multicolour glaze is a significant development of Chinese glazed ceramics. Moreover, it lays the foundation for the transition to the new famous lead-glazed ceramic family called Tang Sancai (AD618-907) (Feng 1982, 171).

Tang Sancai, as its name suggests, is the famous Chinese glazed ceramic produced during the Tang Dynasty (AD618–907). It is also the most important type of low-fired glaze ceramics throughout all the Chinese ceramic history. Sancai refers to its three dominant glaze colours, namely, green, yellow and white, but it was not limited to them. Many other colours, such as blue, brown and so on, are also used in its glazes (Yu and Zhang 1994). Similar to Han lead-glazed ceramic mentioned above, Tang Sancai also use white kaolin clay or yellowish loessic clay as the raw material to produce the pottery body and cover with low-temperature lead glaze. Tang Sancai wares, famous for its exquisite and bright glazing decoration, were widely traded along the Maritime Silk Route between China and the Islamic lands. The Tang Sancai shards have been found in present-day Japan, Sri Lanka, Iran, Egypt and Iraq (Rawson et al., 1989). Some of them were decorated with Islamic shape and decoration style, for example, the shape of ‘Tang Sancai wares with phoenix-head spout’ imitated the features of Persia silverwares (Watson 2004, 47).

With the decline of the Tang Empire, the production of lead glazed Tang Sancai also was on the wane. The main reason for the decline of Tang Sancai production is that, during the Tang dynasty, the manufacture of various high-fired lime glaze stonewares and porcelains also developed rapidly and became the mainstream ceramic. Compared to low-fired lead glaze, the high-fired lime glaze has more compact and stable characteristics and

can be used for various glaze types. Therefore, the production of low-temperature lead glaze went downhill gradually with the decline of Tang Empire. Although the lead-glazed Sancai wares re-appeared in the next Liao dynasty (AD916-1125), Song dynasty (AD960-1279) and Jin dynasty (AD1115-1234), the production of them cannot be compared with that of Tang Sancai both in scale and the diversity of shape (Li 1998, 470). Moreover, the Sancai wares made in Liao, Song and Jin dynasties almost had the same manufacturing technique with that of Tang Sancai wares (Li 1998, 470).

During the Ming dynasty (AD1368-1644) and Qing dynasty (AD1636-1912), by the lead glazing techniques, Chinese ceramic craftsmen created several new low-temperature glaze types. The first one is Fahua ceramics. The term Fahua 法华 refers to Chinese wares use coloured glazes of deep blue, turquoise, purple, green, yellow and white applied within areas enclosed by thin lines of raised clay. Because this decoration technique is similar with that of cloisonné metalwork, Fahua wares are regarded as the ceramic versions of cloisonné Fahua wares, first made in the Shanxi Province of Northern China, started from the late Yuan dynasty (AD1271-1368). The Fahua wares of Northern China fused glaze on low-fired pottery or stoneware (Li 1998, 474). The Fahua decoration style spread to Southern China in the mid-15th century of Ming dynasty (AD1368-1644), where the glaze was fused on high-fired porcelain (Wood 2011, 218). Most Fahua glazes belong to low-fired  $\text{SiO}_2\text{-PbO-K}_2\text{O}$  glaze system, using the potassium oxide and lead compound together as their main flux. Other Fahua glazes belong to  $\text{SiO}_2\text{-K(Na)}_2\text{O}$  system and  $\text{SiO}_2\text{-K}_2\text{O-CaO}$  system (Li 1988, 474).

The second one is low-fired overglazed wares of different types. Overglaze is a kind of glaze-decoration applied after porcelain wares have been glazed (Zhang 2000, 92). Low-fired overglazes using a lead compound as flux first made in Hebei Province of Northern

China during the Northern Song dynasty (AD960-1127), which are the red or green colours fused on the white glazed porcelains (Li 1998, 478). The overglaze spread to Jingdezhen in South China in the 14th Century of Ming dynasty (AD1368-1644), where the porcelain craftsmen created the innovated glaze 'Doucai 斗彩' by combining the overglaze with blue-and-white underglaze together (Li 1998, 479). 'Wucan 五彩', another famous overglaze, first appeared during the reign of the Emperor Jiajing who ruled the Chinese empire between AD1521 and 1567 of Ming dynasty. The manufacture of 'Wucan 五彩' continued into the succeeding Qing dynasty (AD1644-1911). Red, green, yellow and purple were the main overglaze colours of the Ming dynasty 'Wucan 五彩', and during the Qing dynasty, the colours of blue and black were added. The major composition of overglaze 'Wucan' is  $\text{SiO}_2\text{-PbO-K}_2\text{O}$  (Zhang 2000, 139). Besides, 'Fencan 粉彩' and 'Enamel 珐琅彩' are also important overglaze types in Chinese ceramic history. Similar to 'Wucan 五彩', the chemical composition of 'Fencan 粉彩' also belongs to the  $\text{SiO}_2\text{-PbO-K}_2\text{O}$  system, however, different from 'Wucan 五彩', 'Fencan 粉彩' is a kind of opaque overglaze using arsenous oxide as its opacifier (Li 1998, 482). Similarly, arsenous oxide also is an opacifier in 'Enamel 珐琅彩'. However, 'Enamel 珐琅彩' has its distinct glaze composition which is a  $\text{SiO}_2\text{-PbO-B}_2\text{O}_3$  system (Li 1998, 481).

### **2.2.2 Tang Sancai wares**

Sancai is the name given to the ceramics made with white kaolin clay or yellowish loessic clay and covered with multi-coloured lead-glaze. Sancai wares were made by two firings: firstly the unglazed biscuit was fired at 1000-1100°C to get fairly consolidated; and then after applying the glaze, the wares were fired again at a low temperature varying between 700 °C and 900 °C to vitrify the glaze (Zhang and Zhang 1983, 32).

Tang Sancai was produced during the Tang dynasty (AD618-907), which is China's most prosperous dynasty. Most of the Tang Sancai wares and fragments were excavated from Chinese Tang tombs. Therefore, they are thought as tomb objects which were served for burial rituals. The types of Tang Sancai include utensil objects, human male and female figures, animal figures, miniature furniture and so on (Miao and Lu 2001). Besides, Tang Sancai wares and shards were also found in the ruins of palaces, temples and sites outside China (Jiang 2009, 98-100; 149). The utensil-shaped Sancai wares found in these places has raised the question whether these Tang Sancai wares were made for daily use. Watson (1984) inferred that the Sancai vessels found in the ruins of palace might be produced for daily use. Li (1986) suggested that the export Sancai wares found outside China were made for daily use because some sets of Sancai vessels were excavated from kiln sites. However, Narasaki (2000b) and Jiang (2009) suggested that the utensil-shaped Tang Sancai wares found in palace or temple were produced as containers for ritual offerings.

As mentioned above, the overwhelming majority of Tang Sancai items were excavated from Chinese Tang tombs as burial objects. Tang Sancai wares were firstly unearthed in the Luoyang City of Henan Province in 1899 when the Qing government built the Longhai Railway (Feng et al. 2005). Most of the tombs having Tang Sancai wares were excavated officially in the recent fifty years, the amount of which are around 30 in total (Jiang 2009, 20). Most tombs were located near the two capitals of Tang dynasty: Chang'an (present-day Xi'an) in Shaanxi Province and Luoyang in Henan Province. Three tombs of which were found in Taiyuan City of Shanxi Province. In Beijing City, Jilin Province and Hebei Province, one tomb having Tang Sancai wares was excavated respectively. All the tombs mentioned above are located in the north part of China. So far, only two tombs containing Tang Sancai wares were found in Southern China; one is in Hunan Province, the other is in Hubei Province (Jiang 2009, 20).

Besides tombs, Tang Sancai shards were also found in the ruins of Tang imperial palace sites and temple sites located at or around the Xi'an City and Luoyang City which were the two capitals of Tang dynasty. Specifically, Tang Sancai wares and architectural fragments were excavated from the Daming Palace 大明宫, the Jiucheng Palace 九成宫, the Jianfu Temple 荐福寺 and the Qinglong Temple 青龙寺 in Xi'an City as well as the Shangyang Palace 上阳宫 of Luoyang City (Jiang 2009, 98-100).

Moreover, Tang Sancai wares and fragments also have been found outside China. Fragments of Tang Sancai ware were excavated in Japan, Fustat in Egypt and Samarra of Iraq. To be specific, almost 300 Tang Sancai wares and shards were found at 48 sites in Japan, including the ruins of cities, villages, temples and tombs (Narasaki 2000b, 66). The shapes of unearthed Tang Sancai include figures, pillows, utensils like dishes, bowls, cups, pots, jars and ewers (ibid, 66). The manufacture of Japanese Sancai wares started from the middle of 8th Century in Nara in Japan influenced by imported Chinese Tang Sancai (Narasaki 2000a, 61). Around four thousands ceramic shards were found in the ruins of Fustat in Egypt between 1964 and 1972. Within these unearthed ceramic sherds, 381 were Sancai fragments. By studying the shapes, patterns and colours of these Sancai shards, Gyllensv ärd suggested that these Sancai fragments might be made in the Liao dynasty (AD916-1125) of China (Gyllensv ärd 1973). At the Samarra ruins in Iraq, Friedrich Sarre (1925) found some glazed ceramics with bright multi-colours and inferred that these ceramics might be imported Tang Sancai wares from China. Rawson et al. (1989) compared the lead-glazed shards found in Iraq with Chinese Tang Sancai by their firing temperatures, major chemical compositions of bodies and glazes. Their study proved that some lead-glazed shards found in Samarra were indeed made in China. All these Tang sancai wares and fragments found outside China reflect the export trade of Tang Sancai

by the maritime trade between the Persian Gulf and China. Furthermore, the Tang Sancai trade also can be reflected by the Tang Sancai wares and fragments found in Yangzhou, an important export port in the Tang period, and by the Belitung cargo, a sunken trade ship found on the western coast of Indonesia which carried massive Chinese ceramics destined to the Middle East (Guy 2011-2012).

So far, in China, four kiln sites producing Tang sancai ceramics have been discovered. All of them are located in Northern China: the Huangye kiln in the Henan Province; the Huangpu kiln and the Liqianfang kiln in the Shaanxi Province; the Neiqiu kiln in the Hebei Province. Liqianfang kiln sites are located at the west of Chang'an City (now Xi'an City), the capital of the Tang dynasty. Shaanxi Provincial Institute of Archaeology excavated this site in 1999, and four kiln sites, ten ash pits, ten thousands of different kinds of Tang Sancai ceramics, porcelain fragments, residual glass/glaze chunks and remains of bone tools were found. The four kiln sites have similar features which are composed of fire gate, burning chamber, kiln bed and funnel, and the types of Tang Sancai ceramics and fragments include utensils, pillows, Buddhist figurines, human figurines and animal figurines (Shaanxi Provincial Institute of Archaeology, 2008). Neiqiu kiln sites are located in the Neiqiu County and Lincheng County of the Hebei Province. During the surveys and archaeological excavations between 1987 and 1991, three Sancai kilns were found amongst 21 other kilns which produced the white Xing ware. It needs to be pointed that, only Sancai shards and kiln tools were found at the Neiqiu kiln sites, but no excavation of the actual Sancai firing kiln has been made. At the Neiqiu kilns, only Tang Sancai shards of utensil-shaped wares have been found, such as jars, pots and plates (Archaeological Institute of Neiqiu, 1987). In this study, the Tang Sancai glazes excavated from Huangpu kiln and Huangye kiln are selected as the major

research subjects. Therefore, the introduction of these two sites is presented in details in following Section 2.2.3.

### **2.2.3 Introduction to Chinese sites where the Tang Sancai lead glazes in this study were excavated**

The Tang Sancai glazes unearthed from Huangpu kiln, Huangye kiln and two tombs (Weilaichubanshe tomb and Nankezhhan tomb) are the major Chinese research subjects of this study, a brief introduction of these archaeological sites are presented below, and the location map of them is shown in Figure 2.1.



**Figure 2.1 the location of Tang Sancai kiln sites and tombs in this study**

**(WL Tang tomb for Weilaichubanshe tomb and NKZ Tang tomb for Nankezhhan tomb)**

### **2.2.3.1 Huangpu Kiln sites and its Archaeology**

The Huangpu kiln complex sites were the highest yielding kiln sites for Tang Sancai production in China. It is located in the Huangpu town of Tongchuan City, which is around 80 km north of the Xi'an City, Shaanxi Province. The Huangpu kiln is not only famous for Tang Sancai production, but Yaozhou celadon ware also is the representative product of the Huangpu Kiln. The Yaozhou celadon is discussed in Chapter 5, and its glaze-making sites are introduced in Section 2.4.2. In this section, only the Huangpu kiln sites relevant to Tang Sancai production are introduced here. Although the active period of the Huangpu kiln lasts around 700 years from Tang dynasty (AD618-907) to Yuan dynasty (AD1271-1368), the Tang Sancai production mainly runs within the narrow period of Tang Dynasty.

The Huangpu kiln had been excavated in three phases. The first and second phases were small-scale trial excavation in 1959 and 1972 when a large number of Tang Sancai shards were discovered. The third excavation was conducted systematically during the 1984 and 1990 when several Tang Sancai kiln sites were found. The archaeological findings of Tang Sancai kiln sites were reported in 1992 by the book named 'Excavations of the Tang Kiln-Site at Huangpu in Tongchuan, Shaanxi' (Shaanxi Provincial Institute of Archaeology 1992).

During the third phase of excavation, one integrated workshop for Tang Sancai making, and three Tang Sancai firing kilns were unearthed. According to archaeological report, this Tang Sancai ware making workshop covered an area of 636 square meters. It was composed by seven cave-like chambers, and each chamber was used for different purposes. The first chamber was used as the dwelling for craftsmen and keepers. The second one was used for drying the vessels or glazing. The third chamber was the place



where the vessels were shaped. The fourth chamber was the final moulding area. The fifth one was exclusively used to produce the base of Tang Sancai lamps. The sixth and seventh chambers were the places where mainly the ewers were manufactured. The excavation of this workshop infers that the Tang Sancai wares were produced by a well-organized working procedure. Besides, hundreds of unglazed wares also were found in this workshop, which suggests that it had a large scale of production.

Three Tang Sancai kilns were unearthed close to the workshop. All these kilns were the cross-draught type with steamed bun shape called mantou kilns. This kind of kiln was widely adopted in Northern China. The Tang Sancai wares found in Huangpu kiln had a variety of shapes, including ewers, jars, figurines and others. Moulds with the shapes of lions, dragons, and bodhisattvas as well as other figures were also excavated. The monochromatic-glazed Tang Sancai with brown or green colour occupied about half the number of all Tang Sancai wares, the others were the mixed brown, yellow, green colours or white; no blue coloured glaze was found. The Tang Sancai with the white coloured body and pinky-white coloured body both were discovered in the Huangpu kiln.

Using archaeological findings, the earliest Tang Sancai production in the Huangpu kiln could be in the Prospering period (AD649–756) of the Tang Dynasty. Then Tang Sancai production reached to its peak period during the Middle (AD756–846) and early time of Late period (AD846–907) within the Tang Dynasty. Finally, it declined during the late time of Late period of Tang Dynasty (Wang and Kato 2002).

### **2.2.3.2 Huangye Kiln sites and its Archaeology**

The Huangye kiln complex is the first Tang Sancai kiln that was discovered and excavated. It is located five kilometres east of Gongyi City, which is in the middle of

Henan province. Similar to the Huangpu kiln, the Huangye kiln is also a comprehensive ceramic-making site, producing Tang Sancai wares as its dominating products, besides, green wares, white wares were also produced. The production period of the Huangye kiln began in the Sui Dynasty (AD581-618), reached its peak time during the the Prospering period (AD649–756) and Middle period (AD756–846) of Tang Dynasty. Then it went into decline and finally faded out in the several years later at the end of the Northern Song dynasty (AD1127). Tang Sancai wares, as the major products of the Huangye kiln, shared the same development process.

The Huangye kiln sites were excavated in two phases. The first step was a small-scale trial excavation during the 1976 and 1983 when a large number of Tang Sancai shards, kiln furniture, moulds and several incomplete kilns were discovered. Also, the main area of the Huangye kiln was determined. The Huangye Tang Sancai kiln sites were scattered in the Big Huangye village and the Small Huangye village, and located on both banks of the Huangye River, which flows through Huangye city and is a tributary of the Luo River which is a tributary of the Yellow River. Like the terrestrial environment in which the Huangpu kiln sites are located, the Huangye kiln sites are also distributed in the hilly and gully area of loess plateau, where abundant kaolin clay and coal mines were available. The archaeological findings were reported in 2000 in the book named ‘Excavations of the Tang Sancai Kiln at Huangye’ (Gongyi City Institute of Cultural Relics 2000).

The second excavation was conducted comprehensively during 2002 and 2003. By this excavation, nine Sancai firing kilns, four Sancai workshops, two elutriation and sedimentation tanks, seven ditches, 107 pits, hundreds of complete and restored Sancai utensils, thousands of Sancai glazed and unglazed sherds, as well as various kiln furniture, were unearthed. The glazes of Tang Sancai wares were the mixed colour of brown, green,

white or blue. Moreover, Tang Sancai wares were made by white coloured body, grey-white coloured body and pinky-white coloured body. The archaeological findings and preliminary study of this phase were reported in 2005 in the book named ‘The new archaeological discovery at the Huangye kiln site’ (Henan Provincial Institute of Archaeology et al. 2005).

### **2.2.3.3 Tang Sancai in tombs of Tang Dynasty**

As referred to in Section 2.2.2, Tang Sancai wares mainly were used as funerary objects in the tombs during Tang period. In this study, some Tang Sancai glaze samples deriving from two Tang period tombs both located in the Xi’an City of Shaanxi Province were analysed. The brief introduction of these two tombs is presented below.

#### **A. Chengnankeyunzhan Tang tomb**

The Chengnankeyunzhan Tang tomb was located eight kilometres south of the central place-Tell Tower of Xi’an City. It was excavated by the Xi’an City Institute of Archaeology in 2010. This tomb was robbed heavily. Approximately thirty complete and restored utensils, as well as hundreds of ceramic shards, were unearthed, including Tang Sancai wares, figures, horses and camels, pottery wares and pottery figurines. Using archaeological findings, this tomb was dated to the Prospering period (AD649–756) of Tang Dynasty.

#### **B. Weilaichubanshe Tang tomb**

The Weilaichubanshe Tang tomb was located thirteen kilometres south-east to the central place-Tell Tower of Xi’an city, excavated by the Xi’an City Institute of Archaeology in 2008. This tomb was also robbed heavily. Approximately fifty complete and restored

utensils, as well as hundreds of ceramic shards were unearthed, including Tang Sancai wares, Tang Sancai figurines, pottery wares, pottery figurines, white-glazed wares and black-glazed wares. The main shapes of Tang Sancai artefacts are various tomb figures including male alien-looking standing figures, alien-looking grooms, female figures mounted on horseback, female standing figures, as well as horses. By archaeological findings, this tomb also was dated to the Prospering period (AD649-756) of Tang Dynasty.

#### **2.2.4 Previous scientific studies of Tang Sancai wares**

A large number of chemical composition studies of the body of Tang Sancai wares have been conducted to provenance the Tang Sancai wares excavated in different kilns, tombs and relics.

Li and Zhao (2002), Yang et al. (2008) analysed the trace element compositions of Tang Sancai shards and Yaozhou celadon shards unearthed in the Huangpu kiln. The results indicate that the Tang Sancai wares and Yaozhou celadon wares made in the Huangye kiln used the same source of clay.

Lei and Feng (2002) analysed the chemical compositions of Tang Sancai shards unearthed in both Huangye kiln and Huangpu kiln. The different trace element characteristics indicate that the bodies of Sancai wares in these two kilns were made by different clay raw materials collected in their local places separately.

Miao and Lu (2001), Lei (2007) and Yang (2007) studied the trace element compositions of the body of Tang Sancai samples excavated from the four most famous Tang Sancai kilns- the Huangye kiln in Henan Province, the Huangpu kiln and Liquanfang kiln in Shaanxi Province and the Xing kiln in Hebei Province. The results suggest that all the

Tang Sancai samples from the Huangye, the Huangpu and the Xing kilns were manufactured in their local places using local raw materials (local kaolin) separately. With regards to the Tang Sancai samples of Liqianfang kiln, they can be grouped into two types—white body ceramics and red body ceramics. All the red bodied samples are found to use local raw materials, whereas all the white-bodied samples are thought to use the clay imported from Huangye kiln and Huangpu kiln.

The results above set up the chemical composition database of the body of Tang Sancai wares from different kilns which are beneficial to their provenance study. Based on this, archaeologists have already successfully identified the source of some Tang Sancai unearthed in some tombs and relics, mainly including: Tang Sancai samples unearthed in the Shaanxi Province (Lihui Tomb, Lifu Tomb, Jiehan prince Tomb, Zhanghuai prince Tomb, M32 subordinate tomb of Zhaoling Mausoleum, Tombs 1 to the south of Xi'an, Tombs 3 to the south of Xi'an, Tombs 25 to the south of Xi'an, Tombs 31 to the south of Xi'an, Tombs 36 to the south of Xi'an and Daming Palace Relics); Tang Sancai samples unearthed in Henan Province (Luoyang City Relics, Aifei Tomb, Guanlin Tomb and Lixiang Tomb); and Tang Sancai samples unearthed in Yangzhou City (Yangzhou City Relics and Kangwentong Tomb). By the body trace element compositions of all these Tang Sancai samples, some research findings have been inferred, including:

(1) All the Tang Sancai samples unearthed in the tombs of Henan Province and Yangzhou city mentioned above were made in the Huangye kiln in Henan province. It means that some Tang Sancai products manufactured in the Huangye kiln were traded to Yangzhou City, which was the largest harbour for overseas export in the Tang Dynasty. Archaeological evidence show that the Huangye kiln was the closest Tang Sancai kiln

found so far to Yangzhou city, and the transport routes between them were quite convenient (Miao and Lu 2001, Lei et al. 2005a, Xiao 2007, Jia et al. 2006).

(2) Within the 11 tombs of Shaanxi Province, both white-bodied and red-bodied Tang Sancai samples have been found. All the red-bodied samples were made in Liquanfang kiln in the Xi'an City of Shaanxi Province and used local raw materials. For the white-bodied samples, some of them were made in the Huangpu kiln of Shaanxi Province, while the others were either made in the Huangye kiln of Henan Province or made of the raw materials imported from the Huangye kiln (Miao and Lu 2001; Lei et al. 2005b; Lei 2007; Ma et al. 2014a).

(3) The production centre of Tang Sancai wares was thought to shift from the Huangye kiln of Henan Province to the Huangpu kiln of Shaanxi Province in the year AD705 when Empress Wuzetian gave up the throne. Since that year, the political and economic centres shifted to Xi'an City in Shaanxi Province from Luoyang City of Henan Province (Lei 2007).

The glazes of Tang Sancai wares are low-fired lead glazes. Some major chemical analyses have shown that the Tang Sancai glaze belongs to the system  $\text{PbO-SiO}_2\text{-Al}_2\text{O}_3$ . The main colouring elements of them are limited to Fe, Cu, and Co. Fe is the main colourant element of yellow colour, while Cu is the main colourant element of the green colour. The brown colour is due to the mixture of Fe and Cu elements. Co is the main colourant element of blue colour (Zhang and Zhang 1980, Zhang 2000, 130, Feng et al. 2005, Wu et al. 2010).

Up to now, only a little work has been done on the sources of Tang Sancai glaze making. Feng et al. (2005) studied the chemical compositions of the Sancai glazes excavated in

the three important Tang Sancai kilns mentioned above: the Huangye kiln, the Huangpu kiln and the Liquanfang kiln. The results show that the distribution of elemental contents of Al, Si, K, Ca, Ti and Pb all are homogeneous in the glazes. It also indicates that the contents of K, Si and Pb are different in Tang Sancai glazes made in these three different kilns.

So far the most important glaze provenance study on Tang Sancai wares was conducted by Cui and Lei (2010). The lead isotopic ratios of 19 Tang Sancai glazes unearthed from the Huangye and Huangpu kiln sites were analysed by MC-ICP-MS (Multi-collector-inductively coupled plasma mass spectrometry). They found that the glazes made in these two kilns could be grouped separately by their distinct lead isotopic ratios, suggesting different lead ore sources were used for glaze making. The  $^{206}\text{Pb}/^{204}\text{Pb}$  ratios of glazes made in the Huangpu kiln indicate that the lead used for making the glazes might collect from the Northern China geochemical province, while the  $^{206}\text{Pb}/^{204}\text{Pb}$  ratios of Huangye kiln glazes suggest their lead source might come from the Yangtze geochemical province.

## **2.3 Islamic glazed ceramics from the Middle East**

### **2.3.1 Islamic glazed ceramics**

During the centuries under discussion (7th-14th centuries AD), the ceramic production of the Islamic world, which extended across a vast region from Inner Asia to the Atlantic Ocean and endured the rise or fall of several dynasties, reveals a large variety of glazing styles and techniques.

Before the 9th century AD, two major types of decorated ceramic wares were in use in the Islamic world. One is the moulded decoration earthenware deriving from the late

Greco-Roman models or motifs of the Sasanian origin. The other is the stamped and incised decorated ceramic ware which has Eastern prototypes. Both types are found in either glazed or unglazed kind (Jenkins 1983, 5). Since the beginning of 9th century AD, the ceramic production included works of art. This transformation can be shown by the innovations of various glazed ceramic types mainly appearing in two specific regions: the capital of the Abbasid caliphate in Iraq and the northeastern provinces of Khorasan and Transoxiana (Atil 1973, 2). The most significant contributions of early Islamic ceramic production were the application of the tin-opacification and luster-painting decoration to ceramics.

The beginning of the true tin-opacified glazes firstly developed in Iraq during the second half of the 8th century AD (Vendrell et al. 2000). The origin of this glaze has been traditionally related to attempts to imitate Chinese porcelain by use of tin oxide as an opacifier (Vendrell et al. 2000). Tin-opacification was used continuously by Islamic potters to innovate various types of decoration such as luster painting. The first lustre-decorated ceramics were produced in Basra in Iraq during the 9th century AD, which is also adding the mixture of tin and lead oxide to the alkaline glaze (Mason 2004; Pradell et al. 2008b). Lustre-decorated ceramics are characterised by the metallic shine of glaze due to the reduction of silver, gold and copper oxides (Pradell et al. 2008a; Borgia et al. 2002). The necessary changes and improvements in the lustre process from the beginning of the lustre production (Iraq 9th and 10th centuries AD), through the Fatimid (Egypt 11th and 12th centuries AD) and to the later Syrian and Iranian (late 12th and 13th centuries AD) productions are thus exposed (Pradell et al. 2008c). The Abbasid lustres of 9th century AD was polychrome showing two to four lustre colours of olive green, brown, orange, yellow, black and red, then during the beginning of the 10th century AD, an olive-green monochrome golden lustre production started (Pradell et al. 2008a).



Another important type of glazed ware appearing during the early Islamic period is known as 'splashed sgraffito ware', which are manufactured with a clay pottery body with a white slip coating under a transparent lead glaze. Their surfaces are splashed or mottled with yellow, green and brown colours. When first excavated at Samarra, lead-glazed splashed wares were thought to have an immediate connection with Chinese Tang Sancai by archaeologists, because of the apparent similarities between them with the same materials (lead glaze with metallic pigments) (Watson 2004, 47). The technology of the early glazed ceramic production travelled with Iraqi craftsmen and immigrants to the regional centres of new governing classes around the late of the 9th century, such as Nishapur in Iran, Merv in Turkmenistan, and Samarkand in Transoxania. The important ceramic production centres of Nishapur and Samarkand produced some different types of underglaze-painted wares during the Samanid rule (AD819-1005). Specifically, the Nishapur wares include the distinctive polychrome figural decoration covered on buff paste (Bulliet 1992, 78). Moreover, a distinct glazing decoration style named as 'slip-painted epigraphic pottery' first produced in Samarkand and Nishapur. The buff paste of this group was covered by a white engobe on which slips of brown, black or red colours were used for inscriptions which convey messages and decorate the objects (Atil 1973, 4). Excavations of Samarkand and Nishapur show that splash-glazed wares and lustre wares also were commonly produced in both sites (ibid, 4).

By the end of the Samanid period in the early 11th century, the different parts of caliphate fell apart and were under the control of several independent dynasties. The Seljuk Turks (AD1038-1194) controlled Khurasan and Iran in the early 11<sup>th</sup> century and eventually the whole eastern caliphate. The Fatimid dynasty (AD909-1171), centred in Egypt, controlled the whole of Islamic North Africa and the Levant area since the 11th century. Moreover, the Ayyubid dynasty (AD1171-1260), centred in Egypt, ruled many regions of the Middle

East. Then during the first quarter of the 13th century, the Mongols arrived from the East, and the Ayyubid Empire declined due to the Mongol invasion.

During this period from the 11th century to the mid-13th century, the technique of lustre painting continued in Egypt, Spain, Syria and Iran. Egypt picks up the lustre technique during the 10th century possibly due to the transfer of Iraqi ceramists to Fatimid Cairo during this time (Mason 2004, 78). The earliest dated Egypt lustre fragments are found in Fustat and can be dated back to AD1000 and the Fustat lustre production lasted until the end of the Fatimid dynasty (Philon 1980; Watson 1985). The Fatimid lustrewares have new painting motifs of a central figure line-drawn on a plain background (Philon 1980). The use of incised lustre decorated style dated back to around AD 1100 (Philon 1980; Mason 2004). In the mid-12th century, with the fall of the Fatimid dynasty, lustre-painted ware was spread and produced in Iran and Syria. Typical Syrian lustre-painted ware is characterised by copper-greenish tinge lustre applied to transparent alkali glazes (Pradell et al. 2008b). Since the late 12th and early 13th century period of Syria, Iran and Spain the lustre-painting technique was combined with underglaze painting (Jenkins 1983, 24). Moreover, during the 13th century, the lustre-painting ware with a chocolate brown and yellowish green tinge was produced in Al-Raqqa in Syria (Porter and Watson 1987; Mason 2004). In addition to luster-painted ware, moulded slip- and in-glaze-painted ware also continued to be made, along with some innovations.

One of the most significant innovations during the period from the 11th century to the mid-13th century was the re-discovery of 'faience' (also referred to as quartz-frit, fritware), which was made in an attempt to imitate the appearance of Chinese Song white porcelain. It is characterised by the stonepaste technology which was a partially vitrified body made of a quartz-rich paste, were first produced in Egypt during the 11th century

AD (Mason and Tite 1994). During the end of the 11th century AD, the stonepaste technology also was used in Iran and Syria, after that a large majority of finewares made in the Islamic Middle East were stonepaste (Tite et al. 2011). Most of the fritware objects seem to be exclusively covered with alkaline glazes in Syria during the 12th to 14th century and in Iran during the late 14th to early 18th century. However, during the 11th to the mid-14th century, the stonepaste ceramics were also covered by lead glazes in Iran (Jenkins 1983, 13).

The production of ceramics in the Near East halted temporarily due to the destruction of some important ceramic centres such as Nishapur, Al-Raqqa and Rayyan by the Mongols. The Mongol invasion disrupted lustre production, and there is no known dated lusterware between AD 1226 and 1261 (Watson, 1985). Then it was revived to some extent between AD 1260 and 1280 during the Ilkhanid reign (AD1256-1353), a limited production of lustre ceramics begins again, this shows new influences from Chinese porcelains (Pradell et al, 2008b).

Several new styles and techniques of ceramic production also appeared in late 13th century. Sultanabad ware was an innovation during this period. It is characterised by covering with a grey engobe on which the design was applied with a thick white slip and outlined in black (Atil 1973, 8). Besides, this glazed pottery type often was decorated with Chinese decoration style of lotus blossoms and phoenix. The lajvardina ceramic type also was an innovation by Iranian potters during the Ilkhanid period, which was overglaze-painted ware often decorated with gold leaf over a monochrome dark blue or turquoise glaze (ibid, 8).

During the Ottoman rule (AD1281-1923), the famous blue-and-white wares of the Ottomans named as Iznik pottery appeared from towards the end of the 15th century onwards, initially as a substitute for imported Chinese Blue-and-white porcelain (Carswell 1998). It was produced from a white stonepaste body that was decorated with designs in brightly coloured pigments applied under a transparent lead–alkali glaze (Paynter et al. 2004). Besides, various glazed ceramic types, such as polychrome-painted wares, had been made during earlier periods and continued to be produced during the Ottoman Empire too. This long-time period also saw the decline of the ceramic-making industry, by the end of this period, the production of Islamic ceramics had totally lost its vitality (Jenkins 1983, 41).

### **2.3.2 Coloured monochrome-glazed wares**

Since the 6th century BC and during the following pre-Islamic periods of the Neo-Babylonian (BC626-539), the Achaemenid (BC550-330), the Seleucid (BC312-63), the Parthian (BC247-AD224) and the Sasanian (AD224-651), coloured monochrome glazed wares were produced as the major type of glazed wares in sites of Iraq and Iran (Hedges and Moorey 1975; McCarthy et al. 1995). Moreover, this ceramic making tradition continued into the early Islamic period (Pace et al. 2008). Until the 9th century AD, profound changes took place in the production of Islamic glazed pottery, which is the shift from alkaline-based glaze to lead-based glaze (Tite et al. 1998). After that, the lead glazed wares with various decoration styles developed rapidly and instead the role of monochrome glazed wares.

Coloured monochrome-glazed wares are characterised by having a transparent alkaline glaze layer on slipped coarse earthenware, and their most common glaze colours ranging

from turquoise to blue (Al-Ziad 2002). Sometimes, incised decoration under the glaze layer was shown in the monochrome-glazed ware. Hedges and Moorey (Hedges and Moorey 1975; Hedges 1976) undertook a scientific study on coloured monochrome-glazed wares collected from Iraqi sites of Kish, Nineveh and Nippur manufactured between BC600 and AD600. The results showed that the reason for these predominant blue and blue-green glazed colours is the presence of copper or the mixture of copper and iron. All monochrome-glazed wares under study are covered with alkaline glazes, and lead oxides rarely reached 1% weight; some glazes were rich in copper. The local alkaline glazing technique persisted unchanged over around 1200 years (BC600 to AD 600). Besides, Ziad (2002) and Pace et al. (2008) studied some Islamic coloured monochrome-glazed shards, collected from the Dohaleh site of Northern Jordan and Veh Ardašīr site in Iran, using chemical analysis. The results inferred that all the monochrome-glazed shards under study were typically alkaline in composition, with considerable amounts of soda used as the main flux, and also a certain amount of lime.

### **2.3.3 Lead-glazed splashed ceramics**

As mentioned in Section 2.3.2 above, during the 9th century AD, the production of Islamic glazed ceramics, especially in the Middle East, changed a lot to imitate the appearance of imported Chinese ceramics (Lane 1947, 11; Fleming et al. 1992). And the major change of glazing techniques in the Middle East is the shift from alkaline glaze to lead glaze (Tite et al. 1998). It was at the same time that the splashed lead-glazed ceramics (also known as ‘splashed sgraffito ware’) were produced in some Middle East sites. At present, splashed lead-glazed wares and fragments have been found in profusion on sites from Iraq to eastern Iran and Egypt (Lane 1947; 12). Splashed lead-glazed wares are typically produced by a clay pottery body with a white slip coating under a

transparent lead glaze. Their surfaces are typically splashed or mottled with yellow, green and brown colours. When first excavated at Samarra site of Iraq, Islamic lead splashed wares were thought to have an immediate connection with Chinese Tang Sancai by some archaeologists, because some of them have a similar appearance and making materials (lead glaze with metallic pigments) with those of Chinese Tang Sancai wares (Watson 2014; 47). The production of Islamic splashed lead glazed wares lasted a long time until the 14th century AD. Their decoration styles were enhanced by the incised decorations into the slip which initially were simple scrolls, but later included elaborate designs, such as eagles and other animals (Watson 2015). Therefore, the Islamic splashed ware was also named as 'splashed sgraffito ware'. Besides, the quartz-based slip also was used to produce certain 'splashed sgraffito ware' in some sites of Iraq, including Basra and Baghdad (Mason and Tite 1994). There has been long-term debate on the role of Chinese Sancai wares in the development of Islamic lead splashed wares. Islamic lead splashed wares were considered as imitations of imported Chinese splashed Sancai wares, which is supported by some Chinese Sancai fragments were found at Samarra in Iraq and Fustat in Egypt (Lane 1947, 12; Rawson et al, 1989). However, how far-reaching the influence of Chinese Sancai on Islamic splashed wares is still to be established and is without secure foundations due to a lack of detailed study of the Islamic wares as well as of the imported Chinese wares (Watson 2014; 199).

Friedrich Sarre (1925) grouped the shards of lead splashed ware that were excavated at Samarra in Iraq into two categories by chemical composition analysis, which are 'Mesopotamische Keramik' and 'Ostasiatisches Steinzeug'. He demonstrated that the brightly coloured ware of the latter group was Chinese Tang Sancai.

Rawson et al. (1989) studied on a small number of splashed ware samples from Samarra in Iraq, Fustat in Egypt, Mantai in Sri Lanka and Luoyang in China. They demonstrated that there is an evident difference in composition between Chinese Sancai and Islamic origin. The bodies of Chinese Sancai sherds were made from clays with high alumina (around 30%  $\text{Al}_2\text{O}_3$ ) which are characteristic of porcelain and stonewares made in North China, while, local Samarra wares were made from calcareous clays (around 20%  $\text{CaO}$  and less than 15%  $\text{Al}_2\text{O}_3$ ), which were extensively used for the ceramic production in Iraq. Besides, the local Islamic splashed glazes under study are of the medium lead type (24-40%  $\text{PbO}$ ), containing significant amount of alkali (less than 6-9%  $\text{K}_2\text{O}$  plus  $\text{Na}_2\text{O}$ ) and lime (around 5%  $\text{CaO}$ ), while the imported Chinese Sancai glazes are of the high lead type (50-60%  $\text{PbO}$ ), containing negligible alkali (less than 1%  $\text{K}_2\text{O}$  plus  $\text{Na}_2\text{O}$ ) but significant alumina (around 6%  $\text{Al}_2\text{O}_3$ ). They also identified that the Chinese lead-glazed wares with green-on-white decoration, quite different from that of typical Chinese Tang Sancai, and some pieces decorated in a single colour dated to Liao period (AD907-1119) named as 'Liao Sancai' in China also were found to export from China to Samarra and Fustat.

### **2.3.4 Introduction to archaeological sites of Syria and Iraq where the Islamic glazes in this study were excavated from**

The Islamic monochrome-glazed ware and splashed lead-glazed ware unearthed from the Al-Raqqa complex sites in Syria, Kish and Hira and Kish-shaal Ghazna in Iraq are the main origins of Islamic ceramics in this study. A brief introduction of these archaeological sites is presented below, and the location map of them is shown in Figure 2.2.



**Figure 2.2 the location of Islamic archaeological sites excavated lead glazes in this study**

#### **2.3.4.1 Al-Raqqa complex of Syria**

The Al-Raqqa complex sites are located in northern central Syria. Between the short periods AD796-808, Al-Raqqa became the capital of the Abbasid Empire (AD750-1258) under the caliph Harun al-Rashid. Since the Abbasid period onwards the city shows evidence for comprehensive industrial activity including the manufacture of various glazed pottery wares, unglazed pottery, as well as the glass production. Al-Raqqa was eventually abandoned when the Mongols invaded in the mid-thirteenth century. And the production of Al-Raqqa wares which were widely distributed in the Islamic world also was halted during that period (Henderson et al. 2005).

The earliest investigation of the sites in Al-Raqqa goes back to the period 1903-1906 by the former Imperial Ottoman Museum. After that, several attempts at surveying the presence of pottery workshops at Al-Raqqa were made. A pottery kiln, some pottery



shards as well as pottery wasters were collected by Friedrich Sarre and Ernst Herzfeld in 1907-1908, Gertrude Bell in 1921 and Eustache de Lorey in 1924 (Tonghini and Henderson 1998).

The pioneer archaeological research in Al-Raqqa complex was conducted by the Deutsches Archäologisches Institut in Damascus under the direction of Michael Meinecke between 1982 and 1993 (Meinecke 1991). They mainly conducted the excavation on the Abbasid town, finding an Abbasid palace and some other early Islamic structures of the 8th and 9th centuries. The debris of pottery and glass and two destroyed pottery kilns also were found which show that Al-Raqqa was an important production centre for Islamic pottery and glass during the Abbasid period (Tonghini and Henderson 1998).

Since 1994, under the direction of Julian Henderson, the extensive excavation of the early Islamic industrial complex sites at Al-Raqqa was conducted as part of the Raqqa Ancient Industry Project. The archaeological findings included many glasses, glazed and unglazed pottery wares and shards, metalwork as well as the remains of kilns and furnaces. These findings revealed the Islamic glass and glaze production complex in Al-Raqqa. Specifically, a pottery production site which could be dated back to the 11th century was found at Tel Fukhkhar. It contains both domestic and industrial shards including wasters and kiln furniture, various types of pottery wares (Tonghini and Henderson 1998). A production site of both glass and glaze making traced back to 11th -12th centuries was found at Tel Bellor (Henderson et al. 2002). Some glass-production debris, including large (up to 150cm) fragments of the tank-furnace floor, glass-blowing waste and glass frit, as well as the remains of fritting ovens, were found at the Tel Bellor (Henderson et al. 2002). The site of Tel Zujaj was an 8th to 9th centuries glass workshop. Many hundreds of Abbasid glass vessel fragments provided evidence for glass working in Tell Zujaj, and

glass making in Tel Zujaj could be proved by the findings that the raw glass blocks attached to tank furnace fragments and fragments of semi-vitrified frit. Pottery wares and shards also were unearthed from Tell Zujaj, evidencing that the production of Abbasid glazed wares and unglazed plain and stamp-decorated pottery in Tell Zujaj (Henderson 1999; Henderson et al. 2005). The site of Tel Abu Ali which is dated back to 8th-9th centuries provided limited evidence for pottery production. The main evidence is 'high status' occupation with fragments of fine ceramics and glass (Henderson 2000).

#### **2.3.4.2 Kish and Hira, Iraq**

##### **A. Kish**

The region of Kish is located around 100 km south of Baghdad and approximate 17 km east of Babylon. The ancient city of Kish held a significant position during the early periods of Mesopotamian history. The earliest and largest scale investigation of the sites in Kish could go back to the period 1923-1933 by the Oxford-Chicago expedition. On the basis of their excavation report, the ruins of ancient Kish and its dependencies are about nine miles. The various temples, palaces, tombs, street areas and mounds are distributed in ancient Kish, and their surfaces are covered with pottery fragments (Field 1929). Besides, in association with the superhighway construction, small scales of investigations were made on two mounds (Mound X and Mound A) by the Iraqi State Organization of Antiquities & Heritage. The Kokushikan University Archaeological team from Japan commenced the excavation at Kish mainly in the area of Tell Uhaimir in 1988, 2000 and 2001 (Matsumoto 1991; Matsumoto and Oguchi 2002; Matsumoto and Oguchi 2004).

The shards of glazed pottery found in Kish stretch a long period from the late 10th or early 11th century AD to the beginning of the 14th century AD. The Kish region unearthed various types of pottery wares and shards. However, no remains of kilns or their accompanying wasters were found (Reitlinger 1935). The unearthed pottery shards at present are mainly collected in Ashmolean Museum and the Victoria and Albert Museum (V&A). Some mottled glazed pottery and the incised 'Sgraffiato' pottery were found in Kish. Besides, large fragments with a somewhat celadon colouring glaze and partly vitrified fired body are common on the surface of Hira, and white and grey fragments of the porcelain type having painted designs in blue and green colours also were found. However, very few lustre ware was found in Kish (Reitlinger 1935).

### **B. Kish-Shaal Ghazna sites**

The Shaal Ghazna sites are located at the extreme western end of the Kish. It was in the area of the town built in the Nebuchadnezzar period (BC630-561) and partly reoccupied in the 11<sup>th</sup> century. A large number of pottery fragments were found on the surface of this area. The pottery wares and fragments which were found in the Islamic site of Shaal Ghazna are mostly of one type, a yellow slip ware with sgraffiato decoration and mottled painting. Besides, two types of glaze found in Shaal Ghazna suggest a Chinese origin. The first glaze is evidently intended to imitate the porcelain with pale bluish colour which seems to be alike between the crackled Ko ware which one of the 'Five Great Wares' during the Chinese Song Dynasty (AD 960-1279) and Ying Ch'ing ware produced in the Jingdezhen kiln sites. Another glaze type seems to be an imitation of a Chinese glaze called 'Temmoku'(天目釉 in Chinese), famous for its rich black-brown colour and the hares-fur marking decorations (Reitlinger 1935).

### **C. Hira**

Hira was an important ancient city in pre-Islamic Arab history. It is located south of present-day Kufa city in south-central Iraq, about 50 miles to the south of ancient Babylon. The ancient city of Hira was founded in the around 2nd or 3rd century AD, then it thrived in the following four or five centuries, not only as the capital of the Lakhmid kingdom but also as a trading city and river port (Rice 1932).

The large-scale excavation at Hira was conducted by the team of Oxford University directed by Gerald Reitlinger and D. Talbot Rice in 1931 (Rice 1932; Rice 1934). The Hira site excavations consisted of trenches placed into the small mounds and their intervening areas (Mason 1997). Some houses, churches and mounds were excavated thoroughly. A large fortified building with Sasanian foundations was uncovered in Mound I. Mound I extended for a long period until the 8th century which was dated by coins of AD769, AD773 and AD783 as well as a further twenty coins of the 8th century AD. Some well-constructed courtyard houses were unearthed at Mound IH-IV, and some coins of the 8th century also were found there. Some glazed wares and shards were uncovered in these mounds and collected by the Ashmolean Museum. The restricted nature of these glazed ware assemblage in the Ashmolean Museum would seem to suggest that it was deposited at about the same date as the coins (Mason 1997). Most glazed pottery fragments were collected from the surface, which belongs to the Islamic period and are similar to the glazed pottery types from Samarra, Susa and elsewhere (Rice 1932). It needs to be pointed that, Hira was supposedly abandoned in the later 8th century according to the dates of recovered coins. However, the unearthed late Sgraffiato fragments in Hira suggest that continuous occupation at Hira up to at least the 11th -12th centuries AD. For the lack of the 9th century coins at Hira, it can be explained by the widespread phenomenon that a decline in coin finds from archaeological contexts of the 9th -12th centuries across much of the Middle Eastern areas (Priestman 2011).

### **2.3.5 Previous scientific studies of glazes from Al-Raqqa, Kish and Hira**

Early Islamic glazes (AD700-1250) unearthed from different sites with various glazed pottery types have been studied on the respect of their provenance, typology, dating and technology transfer. To discuss these issues, some stylistic studies, major and trace elemental composition analyses and petrographic analyses of ceramic bodies have been conducted on various glazed ceramic types from some representative sites in Egypt, Iran, Iraq and Syria (Reitlinger 1935; Mason and Keall 1991; Mason 1995). Some elemental compositions and lead isotope analysis for the Islamic glazes also had been conducted (Mason et al. 1992; Wolf et al. 2003; Hill et al. 2004). With regards to the scientific analyses on the glazes from Al-Raqqa, Hira and Kish which will be discussed in this research, only a few analytical studies have been conducted.

Hedges and Moorey (1975) analysed the major elements of the glazed pottery samples excavated from Kish, Hira and Nineveh. The Kish glaze samples were unearthed from the mound W and Tell Ingharra dated to Neo-Babylonian and Achaemenid periods (BC600-BC330), Tell Bandar traced back to Parthian period (BC150-AD250) and Tell H and Tell Ingharra dated back to the Sasanian period (AD250-650). The glaze samples excavated in Hira are Islamic shards of 9th to 10th centuries AD. They found that all the analysed pre-Islamic glazes are the alkaline type. There is comparatively little compositional variation in the glaze composition throughout the 1200 years from BC600 to AD600. Besides, the constancy of the glazing technique is paralleled in the constancy of body composition, which is typical of the alluvial deposits in Iraq. The Islamic glazes from Hira of 9th to 10th centuries AD show varied glaze compositions, some of which were splashed glazes with relatively high lead oxide contents of 28%-36% (Hedges and Moorey 1975).

Borregaard (2000) analysed the major chemical compositions of 25 glazed pottery samples dating from 8th to 12th centuries AD unearthed in the Al-Raqqā Islamic industrial complex to determine the evolution of its glazing technology over time. She found that all three glaze types-alkaline, lead-alkaline and high lead glaze were produced at Al-Raqqā's industrial complex. The alkali glazes are either lustre glazes or turquoise glazes all dated to the Early Period of Al-Raqqā (8th-9th centuries AD). All the lead-alkaline are dated to the Late period (11th-12th centuries AD). The lead glazes were produced in both Early Period and Late Period. All the tin-opaque glaze samples were covered by high lead glaze, which is different from the opaque glazes unearthed in other Islamic production sites (such as Bagdad and Basra), which were covered by lead-alkali glaze. This suggests that Al-Raqqā's industry was an independent production centre compared to other Islamic production sites.

Smith (2006) analysed the bulk compositions of the body of some early-thirteen-century ceramics known as Raqqā ware with stonepaste body and alkaline glaze. He compared them with some reference samples from relevant sites. He found that the variations in the compositions of analysed ceramic bodies might be associated with the production date, technique and workshop rather than geography.

Tite (2011) conducted comparative work on major chemical compositional data of both the glazes and bodies of some 1200 glazed Islamic ceramics which were analysed by Alexander Kaczmarczyk during the 1980s. The analysed glazes include the sherds unearthed from Al-Raqqā, Kish and Hira. The others glazes were from Egypt (Fustat and the Cairo area, Qusier, Aswan), Iran (Susa), Iraq (Samarra, Nineveh) and Syria (Ma'arrat al Numan, Queiq, Meskene), and spanned the period from the 8th to the 14th centuries AD. By the major chemical compositions, he preliminarily concluded the basic

development of glaze types (alkali-lime, lead-alkali, high-lead and tin-opacification), body type (quartz or stonepaste, calcareous clay, and non-calcareous clay) and colourants of Islamic glazed pottery making. He inferred that the potters in different periods chose different glaze and body recipes to produce ceramics mainly depending on the availability of raw materials.

## **2.4 The introduction to green stoneware of Northern China**

### **2.4.1 The brief history of green stoneware of Northern China**

The development of green stoneware of North and South China, like other Chinese ceramics, had their own courses with influences between each other on some degree (Kerr and Wood 2004, 50). The reason is that the raw materials with different geological natures were used to produce Chinese ceramics of South and North China. The green stoneware was a ceramic tradition of South China. Proto-porcelain is regarded as the predecessor of later South China green stoneware. The earliest known Chinese proto-porcelain kiln can date back to the late Xia (c.2070– c.1600 BC), the first dynasty of China, which was excavated in the Piaoshan kiln site in Huzhou city in Zhejiang Province (Li et al., 2015). Yue wares started from the late Eastern Han dynasty (AD25-220) is the initiator and representative of South China green stoneware. The green stoneware of South China lasted over a thousand years until the Yuan dynasty (AD1271-1368). Here we mainly focus on the history of North China green stoneware since Yaozhou celadon of North China is the research object of this study.

The earliest evidence of northern green stoneware were unearthed from tombs dated to the late Qi (AD550-577) to early Sui (AD581-618) dynasties. During the years of 1955 and 1956, some wares having greyish white bodies and greenish glaze were found in the

tombs located in the Jing County of Hebei Province, the Xinxiang City and Anyang City of Henan Province. The shape and decoration style of some unearthed green stonewares are different from those of South China Yue green stonewares. Therefore, Chen (1956) and Feng (1958) demonstrated that these unearthed green stonewares were made in North China and named them 'early northern green stoneware'. During the following years of 1976-1996, some ceramic production kilns of North China which also are dated to the late Qi to early Sui dynasties were found in the Shandong Province, Henan Province and Hebei Province. A large number of green stonewares also were excavated from these kiln sites, which reconfirm the production of 'early northern green stoneware' of North China during this period. The 'early green stoneware' of North China were initially influenced by southern green stonewares of Yue kiln in glazing techniques and developed gradually into their own characteristics by using their local raw materials. Early northern celadon wares bear greenish- or amber- tinge glazes applied to kaolinitic clays. The glazes are high in content of CaO and belong to high lime glaze (Kerr and Wood 2004, 539).

During the following Tang Dynasty (AD618-907) and Five Dynasties and Ten Kingdoms period (AD907-979), the production of green stoneware in North China went through their downturn stage for two reasons. Firstly, the white porcelain production developed rapidly and finally dominated in the ceramic production of North China during the Tang Dynasty, because the sedimentary clay in North China was fully suitable as raw material for the white porcelain production. Secondly, green stonewares with high quality represented by Yue green stonewares of Yue kiln flourished in South China. During the Tang dynasty, the so-called 'Southern green-Northern white' ceramic situation defined by scholars have been established (Liu 1999, 86). However, although in this context, there were still several kilns in North China, represented by the Yaozhou kilns in Shaanxi province, persisted in the production of northern green stoneware and laid the foundation



for the golden era of Northern green stoneware in the following Northern Song dynasty (AD960-1127).

After a short turbulent period, due to the overturn of Tang Empire, the Northern Song dynasty (AD960-1127) reunited China in AD960. The Northern Song Empire found their capital in the Kaifeng City, Henan Province of North China, which means that their political centre of authority was set up in North China. In this situation, ceramic production of North China flourished. Amongst the ‘five famous kilns in Song dynasty’, two of them produced northern green stoneware, which are the Ru kiln and Jun kiln in Henan Province. This means that green stonewares of North China finally ushered in their golden era during Northern Song dynasty. The Yaozhou kilns located in Shaanxi province were the pioneer of the northern green stonewares production. Then the production of green stonewares spread rapidly in North China by imitation. Some kilns for green stonewares making were set up in succession, such as Ru kilns, Linru kilns, Qingliangsi kilns and Jun kilns (Feng 1982, 255). Most of these kiln sites locate in today's Henan province of North China. By imitating Yaozhou style green stonewares, the potters in other kilns, particular in Jun kilns and Ru kilns, also brought in their own craft and created new style celadon wares. For example, Ru wares made in Ru kilns are a type of green stoneware with occasional crazes, and their glaze colours are ranged from sky blue to olive green. The shapes of Ru wares often imitated those of contemporary silver wares (Li 1998, 271). It needs to be pointed that, these northern green stonewares that initially appeared in Yaozhou kilns starting from Tang period are also called as “celadon” by modern archaeological scholars.

The Northern Song dynasty constantly suffered the invasions from northern minority regimes-the Khitan Liao kingdom, the Jurchen Jin kingdom and the Tangut Western Xia

kingdom. After the Jurchen Jin-Northern Song war in AD1127, the Northern Song Empire lost the entire North China to the Jurchen Jin. Remnants of the Northern Song ruling officials retreated to the South China, and set up Southern Song Empire (AD1127-AD1279). During Southern Song dynasty, for the reasons that political centre of authority was moved to South China, and the ceramic production of North China was severely damaged by the invasions, the production centre of green stonewares was moved to South China again. The ceramics production of South China kept prosperous in the following dynasties, in contrast, the ceramics making of North China including Northern style celadon wares has never actually recovered again.

#### **2.4.2 Introduction to the Yaozhou Kiln complex**

The Yaozhou kiln complex, being one of the most important ceramic production centres in ancient China, is most famous for its celadon ware with unique decorative techniques of incised and carved flower patterns. The Yaozhou kiln is a general name of the kiln complexes around Tongchuan City, Shaanxi Province in North China. The Huangpu kiln complex is the representative and the production centre of Yaozhou kiln. Besides, the nearby kiln sites distributed in the area of Shangdian, Lidipo, Chenlu and Tapo also belong to Yaozhou kiln complex. The production period of Yaozhou kiln complex extended over 700 years. With the high quality of celadon quality and its aesthetic value, the Yaozhou celadon wares were widely popular and were imitated by nearby ceramic workshops, such as Xin'an and Yiyang in Henan Province also located in Northern China, as well as by Yongfu in Guangxi Province and Xicun in Guangdong Province which are distributed in the Southern China (Zuo 1999). Undoubtedly, the Yaozhou kiln complex plays a unique role in the ceramic history of China. Because Yaozhou celadon glazes

made in three successive periods are the major research focus of this study, a brief introduction to the Yaozhou kiln complex is presented below.

#### **2.4.2.1 The beginning and early innovation period of the Yaozhou Kiln complex-the Tang dynasty (AD618-907)**

To discuss the beginnings of the Yaozhou kiln complex, we need to refer to a local historical stele set up in the 7th year of Yuanfeng Emperor (AD1084) of the Northern Song dynasty, called ‘the stele of Deying Hou’ (‘Marquis of Deying’ 德应侯碑). It is informative about the development and manufacture of Yaozhou ceramics, describing that a ceramic specialist called Bolin who lived during the time of Yonghe Emperor (AD345-356) of Jin Dynasty (AD266-420) introduced advanced ceramic making techniques into the Yaozhou area. After this the Yaozhou kiln complex developed gradually. According to the stele, some scholars infer that the beginnings of Yaozhou kilns could go back to the Jin dynasty (4th century AD). However, this historical record cannot be proved by the archaeological excavation. According to archaeological survey, the earliest pottery making practice of the Yaozhou kiln emerged in the area of present-day Huangpu town during the Tang dynasty (AD618-907). The Huangpu kiln complex is the original and most productive Yaozhou ceramic making centre lasting from the Tang dynasty to the Yuan dynasty (AD1271-1368). The Huangpu kiln sites have been identified for around five miles along the Qishui River in Huangpu town of Tongchuan City. It needs to be clarified that, it is not until the Northern Song dynasty (AD960-1127) that the Yaozhou kiln was named officially, because during that period, the Song imperial government set up the state of Yaozhou in this area so that the kiln sites were called Yaozhou kilns. For those kiln sites set up before the Northern Song dynasty (that is the kiln sites set up in the Tang and the period of Five dynasties and Ten kingdoms), the

archaeologists nowadays conventionally call them Huangpu kilns because of the important role of the Huangpu kiln complex in the Yaozhou kiln system.

The Tang dynasty was literally the most thriving and powerful empire in the world at that time. Because social prosperity, an economic boom, as well as abundant trade along the famous Silk Road started in this period, the demand for the ceramic wares both at home and abroad went up radically. Therefore, ceramic production developed significantly in both North and South China during this period. ‘Southern green and Northern white’ are the widely accepted terms for Tang dynasty ceramic production. Specifically, the Southern kilns were famous for their green glazed stoneware, and the new white ware was the representative product of Northern China.

At such a time, the Huangpu kiln located in the vicinity of the capital (at present Xi’an City) of the Great Tang emerged and developed. The Tang Dynasty Huangpu kiln ceramic products are the most diverse, the main kinds being lead-glazed Tang Sancai wares, black-glazed porcelain wares, tea-dust glaze porcelain wares as well as white-glazed porcelain wares. Specifically, the Huangpu kiln is the most representative and productive kiln to produce Sancai wares in Chinese ceramic history, and the carved flower on black glaze wares made in Huangpu kiln are the original founder of the famous carved flower on black glaze wares made in later Cizhou kiln in Northern Song dynasty. However, the local raw materials called ‘Gantu’ used in Huangpu kiln for ceramic making have a high content of  $\text{Fe}_2\text{O}_3$ , which makes the colour of white glaze a creamy colour and not white enough. Therefore, the white-glazed porcelain wares made in the Huangpu kiln were thought to have had a lower quality than that of other white-glazed ones manufactured in other Northern ceramic kilns (Liang et al. 1997 and Zhuo 2008).

To produce porcelain with a higher quality, in practice the potters in the Huangpu kiln gradually learnt about the characteristics of the local materials, and finally realised that the local ‘Gantu’ was suitable for celadon glaze making. During the Tang dynasty, Yue kilns were undoubtedly the leaders of green glazed stoneware production in the whole of China. The potters in Huangpu kiln then learned the advanced green glaze making techniques from contemporary Yue kiln. Through these efforts, the Huangpu kiln produced Yaozhou style celadon wares eventually and formed a path of development which suited them. It needs to be pointed out that, the archaeologists have reached an agreement that Yue kiln celadon wares had a deep influence on the celadon making in the Huangpu kiln regarding firing technique. Specifically, the use of M-shaped sagger, the glaze-coated foot and the ‘bead-bearing firing method’ that three small piles of sand grain are provided at the points where the ring foot of the ware contacts with the sagger so as to set off the ware and avoid adhering to the sagger while firing all influenced by the Yue kiln firing technology (Wang and Eiji 2005). Moreover, it is the crucial impulsion that the celadon wares became the most significant products of Yaozhou kilns finally. However, the question whether the glaze recipe in Huangpu kiln also imitated that in Yue kiln is still not resolved.

The mid-Tang period was the initial and immature stage for celadon ware making in the Huangpu kiln. The coarse celadon body, uneven glaze layer, brown-yellow coloured celadon wares are the characteristics of the products during this period. Furthermore, a layer of slip was added before glazing, so as to hide defects in the porcelain body. During the late-Tang period, the technique of celadon making made progress. Due to the improvement of the pulverisation and washing process for clay raw materials and the stability of firing process, compared to early time Yaozhou celadon, the porcelain body of

late-Tang period celadon became finer, and its glaze layer became more homogeneous and transparent (Zhuo 2008).

Generally, in the Tang period, the decorative techniques of celadon wares included incising, stamping, appliqué and painting. The shaping techniques included throwing, moulding and pinching. The celadon wares were fired in the semi-downdraft dome kiln with the shape of steamed bun called the ‘Mantou kiln’ in a reducing atmosphere. Wood was used as the fuel. Its firing principle was that the rising flame in the combustion chamber was transmitted to the rear of the heating chamber and it reached the top. Then the smoke entered the bottom of the chimney and was expelled by the drawing force of the chimney itself. Its structure and transmission way of the flame in the kiln were beneficial to the control of the atmosphere which created a reducing atmosphere (The Shaanxi Provincial Institute of Archaeology 1997, 314). Basket-shaped saggars holding several vessels at a time were used in firing. Bowl and plate-type utensils were stacked up, using triangular setters, so that after firing the vessels retained three spurs from the setters. The celadon wares made in the Tang dynasty, in the beginning and during early innovation, laid a solid foundation for the later peak of Yaozhou celadon wares.

#### **2.4.2.2 The development and Maturation period of Yaozhou Kiln complex- the Five dynasties and Ten kingdoms (AD907-960)**

The Five dynasties and Ten kingdoms period lasted for only 53 years, from AD907 to AD960. This was an era of political upheaval when five states followed one another in quick succession in Northern China, while ten regimes ruled separate regions of Southern China during the same period. Due to the frequent wars occurring in both North and South, it is inevitable that the trade which conveyed the Yue green glazed stoneware from South to North suffered a blow. However, there was great demand for the Yue green

glazed stoneware. Under these circumstances, the celadon glazed wares from the Huangpu kilns saw a great development mainly revealed in the following aspects.

Firstly, during this period, celadon glazed wares became the mainstream products of Huangpu kiln. According to archaeological excavations by the Shaanxi Provincial Institute of Archaeology, the amount of celadon glazed wares was 84.5% of all the ceramics unearthed wares dates to the Five dynasties and Ten kingdoms period.

Secondly, during this period, the Huangpu kiln successfully produced sky-blue celadon ware and pioneered sky-blue glazed wares in the context of Chinese ceramic history. However, its production only lasted decades until the early Northern Song dynasty. One reason for the creation of the sky-blue coloured glaze is that a better reduced firing atmosphere was developed during this period due to the improvement of kiln structure. Compared to the kiln in the Tang dynasty, the firing chamber of the kiln was higher during the Five dynasties and Ten kingdoms period, which meant that the height difference between the firing chamber and the combustion chamber became larger. Under these circumstances, firing in the chamber increased more rapidly as a result and suited the firing of celadon with a finer reducing flame (The Shaanxi Provincial Institute of Archaeology 1997, 22). Kerr and Wood (2004) inferred that low levels of titania in the glaze might be another factor in the development of fine bluish celadon colours, but they also demonstrated that the evidence here is still not clear enough. Although low titania compositions were certainly used at Huangpu kiln for sky-blue glaze making during the Five dynasties and Ten kingdoms period, similar low titania levels also were found in some Northern Song dynasty green glazed wares (Kerr and Wood 2004, 586-587).

Thirdly, the firing technique at the Huangpu kiln also improved. On the one hand, each sagger contained only one object to be fired; the loaded saggars were built into tall

columns and fired in the kilns (Kerr and Wood 2004, 341). The ‘one sagger one object’ setting method helped to keep the wares away from fuel ash and protect the wares from stress forces between them (Kerr and Wood 2004, 342). On the other hand, the support beneath the base of the wares, which mainly has the shape of trifurcate spur, became thinner and more pointed. In this way, almost no traces of the spur were left on the bottoms of the fired wares (The Shaanxi Provincial Institute of Archaeology 1997, 243).

#### **2.4.2.3 The golden age of Yaozhou Kiln complex- the Northern Song dynasty (AD960-1127)**

After a short turbulent phase during the Five dynasties and Ten kingdoms period, the Northern Song dynasty (AD960-1127) reunified China back in 960 AD. During the Northern Song period, China passed through a phase of economic growth that was unprecedented in earlier Chinese history. The prosperity of commercialization and civilisation brought increased craft production throughout China (Curtin 1984, 109-110). Therefore, ceramic production, including the Yaozhou kiln complex, in this period also developed prosperously. The Yaozhou kilns became the best representative of the Northern China kilns during this period. And the peak of ceramic production of the Yaozhou kilns finally came during the middle period of Northern Song dynasty (The Shaanxi Provincial Institute of Archaeology and Yaozhou kiln Museum 1998, 541). The expansion of ceramic production scale, the great increase of ceramic types and various decorative techniques could all be the evidence for the great prosperity of Yaozhou kilns during this period. More important, a large amount of Yaozhou celadon wares of advanced quality and exquisite incised and carved flower pattern decoration were made during this period. Yaozhou celadon glaze became well known during that time and made a great impact on other kilns all over the county, such as Xin’an of Henan Province in



North China, as well as Xicun of Guangdong Province, which was in the south of China (Kerr and Wood 2004, 435-436). The creation of these amazing celadon wares should be attributed to a range of technological improvements during this period.

First of all, the raw material selection became more rigorous for the Yaozhou kilns during the Northern Song dynasty. The potters only selected the certain kind of 'Gantu' clays which has light colour as the raw material of celadon wares body making. By this, only white-bodied wares were made during the Northern dynasty. Also the slip layer applied by potters before Northern Song period to hide the defect of ceramic body was no longer necessary. The Northern Song celadon wares usually had an anorthite inner layer which was formed by the interaction between the glaze and their body during the long soaking time. This interaction layer not only supplies a unique waxen cast to the glaze surface, but also tightly bound the glaze to their body paste (The Shaanxi Provincial Institute of Archaeology and Yaozhou kiln Museum 1998, 550 and 553).

Secondly, the Northern Song Yaozhou kiln developed the paste preparation processes dramatically. The improved larger stone troughs were used to grind raw materials and the potters let the livestock haul the grinding stone instead of men. In this way, the large grains of minerals are seen less in the bodies of Yaozhou wares made in Northern Song period. The more sophisticated washing processes for paste preparation were also a reason for the finer body of Northern Song Yaozhou wares to develop (The Shaanxi Provincial Institute of Archaeology and Yaozhou kiln Museum 1998, 550 and 553).

Thirdly, the most important glazing technique advance of Northern Song Yaozhou celadon was the thickened glaze. The glaze colour became stable with an olive-green hue during the Northern Song dynasty. To achieve such a colour, the wares were always applied in two layers of glaze slip before being fired (Guo and Li 1984). Previous studies

inferred that the thicker Yaozhou glaze tends not to re-oxidise during the cooling periods and made it easier to produce a more olive-green hue (Kerr and Wood 2004, 594). However, so far, no data shows that to what extent the Yaozhou celadon glaze layer of the Northern Song dynasty thicker than the earlier celadon glaze

Finally, the biggest technical change of Yaozhou Kilns during the Northern Song period was the revolution of firing techniques. The kiln remains found in the Yaozhou kiln sites showed a fuel transition from wood to coal during this period (Kerr and Wood 2004, 319). The possible cause of this change might be the lack of wood after long-term deforestation and abundant coal resource in Northern China (Kerr and Wood 2004, 165). Using coal as the fuel has both advantages and disadvantages. Better thermal efficiency and availability are the main benefits. However, atmospheres in coal-fired kilns tend to produce less efficient reduction (Kerr and Wood 2004, 590). Furthermore, the flame became more difficult to sustain and keep stable, producing uneven kiln temperatures (Kerr and Wood 2004, 318). However, after a period of practice, the potters in the Yaozhou kiln improved the firing method by using the longer soaking period with a relatively lower temperature. As a result, a more evenly and stable fire atmosphere could be obtained.

#### **2.4.2.4 The decline of Yaozhou Kiln complex**

The Song dynasty suffered constant invasions from northern minorities, such as the Jurchen, the Khitan, the Tartar and the Mongols. In AD1127, the Northern Song Empire lost the control of North China due to the Jurchen's invasion. In this year, the Song Empire retreated to the south of the Yangtze and established its capital at Lin'an (present-day Hangzhou) in the Southern Song dynasty. In the meantime, North China was ruled by Jurchen and called the Jin Dynasty. However, the newly formed Southern Song Empire and Jin Empire did not last for long. The Southern Song Empire suffered massive

aggression by the powerful Mongols during the period of AD1235-1267 and finally perished in AD1279. The Jin Dynasty died out in 1234 AD.

During this period, on the one hand, ceramic production in Yaozhou Kilns was affected to a certain degree due to social upheaval. On the other hand, because the Yaozhou kilns were the best-known kiln controlled by the Jin Empire, the market demands for Yaozhou celadon wares increased dramatically. This saw the scale of ceramic production of celadon expand, and some new kiln sites were set up during this period in Chenlu Town where about 20 kilometres away from the central area of Yaozhou kilns. The refined manufacturing and firing techniques of the Northern Song were partly inherited by the potters in Jin dynasty. The most notable innovation of the Jin dynasty Yaozhou potters was creating a whitish toned glaze called ‘Yuebai’ (月白), literally meaning a moon white colour tone. The glaze layer was thicker and had a jade-like glossy quality.

The celadon ware of Yaozhou kiln severely declined starting from the following Yuan dynasty (AD1271-1368). During this period, northern ceramic production largely diminished because of a prolonged war in North China and the ceramic production centre re-shifted from the North to South. Besides, from this period, a new trend in Chinese ceramics emerged. People were no longer in favour of celadon ware with pure and clear appearance. Instead, they preferred coloured and decorated wares, such as the notable blue-and-white porcelain (Fang 2011, 50). In this situation, the Yaozhou kiln reached its lowest ebb in history. The Huangpu kiln complex, which was the ceramic production centre of Yaozhou kiln system, finally stopped during the late Yuan to early Ming dynasties.

During the following Ming dynasty (AD1358-1644), Qing dynasty (AD1644-1912) and Republic of China period (AD1912-1949), the ceramic production of the Yaozhou kiln

complex still continued. Both the prosperity of the Yaozhou kiln system and celadon ware production never really recovered. The output of celadon wares decreased dramatically, in terms of the types and decoration. Furthermore, their quality declined with the coarser ceramic body and dull glaze colours with yellowish hues. During these periods, the ceramic production centre was moved to the Lidipo kiln, the Shangdian kiln and the Chenlu kiln in Chenlu Town around 20 kilometres from its previous kiln firing center-Huangpu kiln complex. Besides, with the decline of the Yaozhou celadon industry, many other types of ceramics such as the black-and-white wares and yellow glazed wares replaced celadon as the primary ceramic types.

### **2.4.3 The archaeology of Yaozhou Kiln complex**

The archaeological works in Yaozhou kiln complex (see Fig 2.3) can be divided into two phases. During the first phase from 1984 to 1992, the Huangpu kiln sites which were the ceramic production centre of Yaozhou kiln from Tang dynasty (AD618-907) to Yuan dynasty (AD1271-1368) were excavated comprehensively. During the second phase between 2002 and 2004, systematic excavations were conducted of the Lidipo kiln, Shangdian kiln and Chenlu kiln which developed into the ceramic production centre of Yaozhou kiln during the Ming dynasty (AD1358-1644) and continued into Republic of China period (AD1912-1949).

From 1984 to 1992, the archaeological works mainly focused on the area of the Huangpu kiln sites. These excavations were directed by the Shaanxi Provincial Institute of Archaeology. Seventy-three workshops, 61 porcelain-firing kilns, 78 ash-pits and 51 tombs in total were unearthed and a large amount of artefacts of the Tang, Five dynasties and Ten kingdoms, Song, Jin and Yuan periods were found. The overall context of the

Yaozhou ceramic manufacturing history was obtained from these efforts and some survey reports were published.

The Tang remains which were the earliest cultural layer included one workshop and three kilns for making low-fired Tang Sancai wares, eight workshops and five kilns for making high-fired wares, seven ash-pits and seven Tang tombs. These archaeological findings of the Tang period were reported in 1992 named 'Excavations of the Tang Kiln-Site at Huangpu in Tongchuan, Shaanxi' (The Shaanxi Provincial Institute of Archaeology 1992). For the Five dynasties and Ten kingdoms period, four workshops and six kilns for porcelain-making, sixteen ash-pits and around seventy thousand stoneware samples were found. A number of restorable shards of exquisite celadon wares incised with character '官'(which means 'official') were unearthed, which had great significance for the study of the kilns in Five dynasties and Ten kingdoms period. These archaeological materials have been published in 1997 called 'Excavations of the Five Dynasties period Kiln-Site at Huangpu in Tongchuan, Shaanxi' (The Shaanxi Provincial Institute of Archaeology 1997). With regards to the Northern Song dynasty, 35 workshops and 23 kilns for porcelain-making, 2 kilns for glaze making, 16 ash-pits and a lot of exquisite celadon wares. These archaeological materials have been published in 1998 called 'Excavations of the Song period Kiln-Site at Huangpu in Tongchuan, Shaanxi' (The Shaanxi Provincial Institute of Archaeology and Yaozhou kiln Museum 1998).

Since the 1950s, the Shaanxi Archaeological Research Institute conducted some excavations of the Lidipo kiln, the Shangdian kiln and the Chenlu kiln in Chenlu Town and dated the kiln sites to the Jin dynasty (AD1115-1234) and Yuan dynasty (AD1271-1368), and some survey reports were published accordingly. During the 2002 to 2004 period, systematic excavation works were conducted in the above three kiln sites by a

cooperative team of the Yaozhou kiln Museum, the Shaanxi Provincial Institute of Archaeology and the Tongchuan City Institute of Archaeology. According to the investigation, 16 porcelain-firing kilns were found and 6 of them were excavated completely. Specifically, three of them were dated to Jin dynasty (AD1115-1234), one of them belonged to Yuan dynasty (AD1271-1368) and two were dated to Qing dynasty (AD1636-1912). These archaeological works have been published in 2004 called ‘Yaozhou kiln site at Lidipo and Shangdian’ (Yaozhou kiln Museum, The Shaanxi Provincial Institute of Archaeology and Tongchuan city Institute of Archaeology 2004).



Fig 2.3 the location map of the Yaozhou kiln complex sites

#### 2.4.4 Historical records and scientific studies of Yaozhou celadon wares and their production techniques

Historical literature tells us the clay sources used to manufacture the body of Yaozhou celadon wares were local white and fine clay called ‘Gantu’, collected from Huangpu

town and Chenlu town nearby the Yaozhou kilns. Over the years a number of scientific analyses have been made of the bodies of Yaozhou style celadon wares (Li 1998; Zhang 2000; Zhu 2011; Kerr and Wood 2004). These results showed that the characteristic of Yaozhou celadon body is in keeping with the nature of all northern ceramics- a relatively higher alumina content (20%-30%) and a lower silica content. The local raw material ‘Gantu’ mainly contains kaolinitic clay minerals, including a certain amount of quartz, feldspar, mica and apatite. The raw materials need to be pulverised, ground, washed and precipitated to produce fine clay suitable for the production of Yaozhou celadon bodies (Li 1998, 261).

Here I mainly focus on the historical records and scientific studies of celadon glazes and the raw materials used for making them. Yaozhou celadon wares have been described in some famous historical notes which record products, ancient laws and regulations, and customs during the Northern Song Dynasty (AD960-1127) and the Southern Song Dynasty (AD1127AD-1279) written by scholars at that time, such as ‘QingYi Lu’清异录 written by Tao Gu, ‘LaoXueAn BiJi’老学庵笔记 written by Lu You, ‘QingBo ZaZhi’清波杂志 by Zhou Hui and ‘TanZhanBiHeng’坦斋笔衡 by Ye Zhi. These historical records mention that the kilns which made Yaozhou celadon wares were located in Huangpu County in Shaanxi province in North China. And sometimes Yaozhou celadon is mistaken for Yue celadon made in Zhejiang Province in South China because their glazes have similar colour tones. However, the raw materials and glaze making procedures of Yaozhou celadon are seldom mentioned in detail in historical records.

The most detailed historical record of the raw materials used in Yaozhou celadon glaze was written in the ‘The Great Gazetteer of Tongguan ·Minguo’ 同官县志·民国志 where

the Yaozhou celadons were manufactured, which was compiled in AD1944 during the Republican period of China by Li Jinxi. It records 'the clay for making stoneware bodies called 'Ganzi', a kind of clay with a cyan or reddish-yellow colour in a Permo-Carboniferous age. The raw material for glaze making collected from the Mingyue Mountain in Fuping county (around 30 kilometres southeast of Yaozhou kiln), is a kind of shale generated within Ordovician limestone.

Using this historical record, some researchers have inferred that the glaze stone from the local Fuping county might be the main raw material for Yaozhou celadon glaze production, and they named it 'Fuping glaze stone' (Guo and Li 1984; Guo 1984; Li 1998, 260; Kerr and Wood 2004, 592). Analysis of Fuping glaze stone shows that it is a kind of shale, which is mainly composed of kaolinite and calcite (20%-25%), a certain content of quartz (5%-10%) and feldspar, a small amount of biotite, as well as some trace minerals, such as apatite, zircon and leucosene (Li and Guan 1979; Guo 1984; Li 1998, 260). 'Fuping glaze stone' is suitable for making glaze by minor additions of silica, clay and a calcium-rich flux (Kerr and Wood 2004, 592). However, there is no historical record referring to what kinds of raw materials were used to flux the Yaozhou celadon glaze. Some chemical studies on the fluxing agent of Yaozhou celadon glazes were performed during the past decades.

The first scientific study which focused on Yaozhou celadon ware samples was done by Guo and Guan (1979). They successfully reproduced celadon from local clay minerals ('Gantu') and 'Fuping glaze stone' in the reducing firing atmosphere. They also analysed chemically Yaozhou celadon samples of Northern Song dynasty, finding that the  $\text{Al}_2\text{O}_3/\text{SiO}_2$  ratio of body is between 1/4 and 1/5.36, and the  $\text{SiO}_2/\text{Al}_2\text{O}_3$  ratio of glaze is around 8.0.



Guo and Li (1984) analysed the major chemical compositions of both body and glaze of five Yaozhou celadon samples and four celadon samples made in the Linru kilns (located in modern-day Ruzhou City, Henan Province), and also the major chemical compositions of two feldspar samples and one wood ash sample collected near the Linru kilns. They inferred that the high CaO content (31.12%) in wood ash samples might be the main source of the CaO content in Yaozhou and Linru celadon glaze samples, and the high K<sub>2</sub>O content in two feldspar samples (9.68% and 10.51% respectively) might be the major provenience of the K<sub>2</sub>O in Yaozhou and Linru celadon glaze samples. They concluded that it is possible to use wood ash and feldspar as the fluxing agent in the Yaozhou and Linru celadon glazes.

Guo and Guan (1979) and Li (1998) analysed the mineral compositions of a local limestone material called 'Liaojiang Stone', they found that the Liaojiang stone is primarily composed of calcite particles, and a small quantity of quartz, feldspar, mica and chlorite clastic inclusion. They inferred from this that the limestone 'Liaojiang stone' might be the main fluxing raw material in the Yaozhou celadon glaze. According to 'The Great Gazetteer of Tongguan · Minguo' 同官县志·民国志, 'Liaojiang stone' is a kind of Ordovician limestone which is distributed in the nearby areas of Yaozhou kiln. Beside, in the book 'The Yaozhou Kiln Site of Song period' edited by the Shaanxi Provincial Institute of Archaeology and Yaozhou kiln Museum who conducted the excavation of Yaozhou kilns, limestone also was regarded as a possible fluxing raw material (The Shaanxi Provincial Institute of Archaeology and Yaozhou kilns Museum 1998, 553).

Liang et al. (1997) studied 83 Yaozhou celadon glazes from the Tang dynasty (AD618-907) to the Yuan dynasty (AD1271-1368) analysed by Energy-Dispersive X-Ray Fluorescence (EDXRF) and used statistical analysis of their major elemental

compositions. They found that almost all Yaozhou celadon belonged to a lime glaze with high CaO content, and the glazes of Song Dynasty (AD960-1280) and later have higher K<sub>2</sub>O contents and lower CaO contents than those of the earlier period. Yang et al. (2010) also analysed the major chemical composition of 30 Yaozhou ware samples by proton induced X-ray emission (PIXE). They found the similar results for the Northern Song dynasty, a transitional period when the raw materials recipe of both the body and glaze changed.

Ling et al. (2008) analysed both major and trace elemental composition (only Rb<sub>2</sub>O, SrO and ZrO for trace elements) of 20 Yaozhou celadon samples from the Tang dynasty (AD618-907) to the Jin dynasty (AD1115-1234) by EDXRF (Energy-Dispersive X-Ray Fluorescence). They found that both the contents of SiO<sub>2</sub> and Al<sub>2</sub>O<sub>3</sub> in glaze increased gradually from the Tang dynasty to the Northern Song dynasty and then had a slight decrease from Northern Song to Jin Dynasty, while the content of CaO+MgO+K<sub>2</sub>O+Na<sub>2</sub>O had the opposite trend, and there is no difference in trace elements compositions. This could be interpreted by the changes in the proportion or types of fluxing agents in the glaze making during different periods. They also found that the CaO content was negatively correlated with the K<sub>2</sub>O content in glazes during different periods. They infer that for those glazes with relatively high K<sub>2</sub>O content and low CaO content, the potassium-rich botanic ash might be used as their fluxing agent.

Zhu et al. (2010) analysed seven pieces of celadon samples of the Northern Song dynasty from the Yaozhou kiln. They found that the P<sub>2</sub>O<sub>5</sub> content in the Yaozhou celadon glazes is much higher than that of the corresponding body. Therefore, they suggested that the two Yaozhou kilns employed plant ash as the main flux.

The coloration mechanism of the celadon in Yaozhou kiln was studied by Zhang et al. (1995), Zhang and Gao (2002) and Li (2003). The elemental composition of colourant in the glaze was analysed by the neutron activation analysis (NAA) and femtosecond laser ionisation time-of-flight (FS-LI-TOFMS). And the chemical states of iron in glaze were analysed by Mössbauer spectroscopy. They found that the major colouring element in Yaozhou celadon is iron. The different glaze colour hues of Yaozhou celadon mainly depend on the  $Fe^{2+}/Fe^{3+}$  ratio value in the glaze. The  $Fe^{2+}/Fe^{3+}$  ratio value further depends on firing atmosphere and the firing temperature in the kiln.

According to the aforementioned studies on Yaozhou celadon glazes, it can be seen that only a small number of preliminary studies on the glaze recipe of Yaozhou celadon have been done. The Yaozhou celadon glaze is a calcium glaze. The local stone named 'Fuping glaze stone' is inferred as the most likely siliceous raw material for glaze making, consisting of kaolinite, calcite, quartz, feldspar, clay minerals and calcium carbonate. And as for the fluxing agent, botanic ash and limestone could be the candidates. The glaze recipes in northern glazes present a rather more complex problem than with southern glazes because of the deficiency of historical records. Therefore, a deeper and more systemic study needs to be carried out.

## **Chapter 3 Methodology and previous work**

### **3.1 Introduction**

Both the chemical and isotopic analyses were carried out in this study to obtain the scientific data to discuss the raw material, technique and provenance of the glazes from Northern China and the Middle East. Specifically, the bulk chemical composition analysis of this study was carried out by the Electron microprobe wavelength dispersive X-ray spectrometry (EPMA-WDS), the trace element composition data was determined using laser ablation-inductively coupled plasma-mass spectrometry (LA-ICP-MS). The lead isotopic analysis was carried out using laser ablation-multi collector-inductively coupled plasma-mass spectrometry (LA-MC-ICP-MS) and solution MC-ICP-MS, and the Thermal ionisation mass spectrometry (TIMS) was applied to analyse the Sr isotopic compositions of glazes. In this chapter, the basic methodology, the experimental procedures and review of previous work of each analysis are introduced.

### **3.2 Major and minor chemical composition analysis**

#### **3.2.1 Introduction**

Chemical analysis is a basic method to study and characterise ceramic bodies and glazes. In this study, by major and minor chemical composition analysis, the raw materials and manufacturing techniques used for making some glazes from Northern China and the Middle East can be discussed.

The bulk and minor elemental compositions of glazes in this study were determined using a JEOL JXA-8200 electron microprobe with four wavelength-dispersive spectrometers located in the Department of Archaeology in the University of Nottingham and Cameca

SX100 microprobe located in the Open University. The electron microprobe uses X-ray spectrometry to identify and measure the concentrations of elements in the specimen. Both energy dispersive (EDS) and wavelength dispersive spectrometers (WDS) are available to do the chemical composition analysis. Comparing to the technique of EDS, the WDS takes longer. However, it provides more accurate and precise elemental compositions. In this study, the WDS technique was used.

### **3.2.2 Sample preparation for analysis by electron microprobe**

Electron microprobe analysis is a micro-destructive analytical method for archaeological samples. Only small sizes of ceramic shards are needed, and the analytical process itself only destroys a microscopic area of around 50 $\mu$ m and even smaller.

In sample preparation, small sub-samples (around 5mm $\times$ 5mm in size) were cut from each ceramic shard ensuring that the cross-sections of them included all the glaze colours will be analysed. The sub-sample fragments were mounted in cross-section in epoxy resin blocks. Once the ceramic samples were mounted, they are next prepared for grinding and polishing to a 0.25  $\mu$ m diamond paste finish, the purpose of which is to obtain the necessary take-off angle for analysis. For qualitative analysis only, the sample needs to be coated with double-stick conductive carbon tape to prevent surface charging and any distortion and deflection of the electron beam during analysis. The mounted samples can be reanalysed again by electron microprobe or other techniques, for example the LA-ICP-MS technique which also is used in this study.

### **3.2.3 The significant elements to be measured**

Quantitative analysis with WDS technique requires prior knowledge about which elements are present in the sample to be measured. By the electron microprobe analysis, the main questions to be answered using the compositional characterisation of the glazes are the determination of the raw materials and glaze recipes used to produce them. Therefore, a selection of major and minor oxide components was included in this study, partly based on published information. Moreover, based on the different glaze types, different oxides were considered in the final analysis. For the lead glaze type, SiO<sub>2</sub>, Al<sub>2</sub>O<sub>3</sub>, PbO, Na<sub>2</sub>O, K<sub>2</sub>O, CaO, FeO, MgO, MnO, CuO, TiO<sub>2</sub>, Sb<sub>2</sub>O<sub>5</sub> and ZnO were analysed. While for the lime and alkaline-lime glaze type, SiO<sub>2</sub>, Al<sub>2</sub>O<sub>3</sub>, Na<sub>2</sub>O, K<sub>2</sub>O, CaO, FeO, MgO, CuO, TiO<sub>2</sub>, MnO and P<sub>2</sub>O<sub>5</sub> were considered. The raw data of chemical compositions of these elements of each sample are listed in the Appendix I Tables A1-A4, and the final data used in each chapter are the average of the raw data.

### **3.2.4 Analysis and standards**

A total of 76 glaze samples were analysed using EPMA-WDS. Each sample was analysed at least three times for each colour at 20 kV accelerating voltage and 50 nA incident beam current with a 50µm defocused electron beam. A defused beam is used to reduce the effect of the migration of alkalis and other volatile elements within the samples (Henderson et al. 2016; 30). The counting time was 30 seconds on the peak (20s for sodium) and 20 seconds on the background (10s for sodium).

The EPMA-WDS was calibrated against a series of certified mineral, pure metal and synthetic standards. Analytical results were corrected using a commercial ZAF program as the matrix corrections. Moreover, as the external standards, Corning B reference glass

and Corning C reference glass were analysed both at the start and end of each analytical run to check the accuracy and precision of the samples. In total, replicate analyses (n=36) of Corning B reference glass were used to assess the precision of alkali-lime and lime glaze analysis, and 48 replicate analyses of Corning C reference glass were used to check the precision of lead glaze analysis. The average analytical results, the calculated standard deviations and relative standard deviation (RSD%) of the replicate measurements of reference glasses were presented in Table 3.1, combined with the known values of Corning B and Corning C reference glasses. By this, the precision and accuracy of the measurements can be assessed.

	Corning B glass					Corning C glass				
	Measures Mean	Known	St. Dev	% RSD	% Bias	Known	Measures Mean	St. Dev	% RSD	% Bias
SiO <sub>2</sub>	60.40	61.55	1.45	2.40	-1.87	34.87	36.61	1.02	2.77	4.99
Al <sub>2</sub> O <sub>3</sub>	4.47	4.36	0.06	1.43	2.52	0.87	0.90	0.02	2.34	3.45
Na <sub>2</sub> O	17.67	17.00	0.21	1.19	3.94	1.07	1.20	0.03	2.38	12.15
K <sub>2</sub> O	1.01	1.00	0.02	1.73	1.00	2.84	2.82	0.03	1.05	-0.70
CaO	8.85	8.56	0.10	1.08	3.39	5.07	5.19	0.04	0.75	2.37
MgO	1.13	1.03	0.02	1.80	9.71	2.76	3.15	0.04	1.18	14.13
ZnO	0.18	0.19	0.03	17.51	-5.26	0.05	0.05	0.01	25.35	0.00
TiO <sub>2</sub>	0.09	0.09	0.01	5.73	0.00	0.79	0.91	0.04	3.22	15.19
PbO	0.21	0.16	0.03	6.90	31.25	36.7	35.22	0.42	1.34	-4.03
FeO	0.31	0.34	0.01	3.68	-8.82	0.34	0.31	0.01	3.15	-8.82
MnO	0.25	0.25	0.01	3.97	0.00	0.82	0.70	0.13	18.48	-14.63
CuO	2.79	2.66	0.03	1.17	4.89	1.13	1.18	0.02	1.95	4.42
Sb <sub>2</sub> O <sub>5</sub>	0.47	0.46	0.05	10.9	2.17	0.03	0.04	0.01	27.32	33.33
P <sub>2</sub> O <sub>5</sub>	0.74	0.82	0.06	8.85	-9.76	0.14	0.11	0.01	13.55	-21.43

**Table 3.1 the analytical results of the Corning B and Corning C archaeological reference glass (The known values for Corning B and Corning C glasses were published by Brill (Brill et al. 1999))**

For Corning B glass used to assess the accuracy of analyses for alkali-lime and lime glaze types, the precisions of SiO<sub>2</sub>, Al<sub>2</sub>O<sub>3</sub>, Na<sub>2</sub>O, K<sub>2</sub>O, CaO, MgO, FeO, MnO and CuO are ideal (RSD<5%). For the oxide of minor elements Sb<sub>2</sub>O<sub>5</sub>, P<sub>2</sub>O<sub>5</sub>, TiO<sub>2</sub>, PbO and ZnO, the

RSD of them are above 5% but below 18%. Moreover, the accuracies for all the elements ranged between -10 and +10% except Pb (+31.25%). The percentage error of 20% is seen as a critical value to check whether an analytical data is acceptable as a quantitative result and in any case these errors would be expected to be a bit higher for low levels in the samples. The percentage error of element PbO is above 20%, which is assessed as a semi-quantitative result. For Corning C glass used to assess the accuracy of analyses for lead glaze type, the precisions of most elements are ideal, only the RSD of ZnO and Sb<sub>2</sub>O<sub>5</sub> are above 20%. Moreover, the accuracies for all the elements ranged between -15% and +15% except Sb<sub>2</sub>O<sub>5</sub> and P<sub>2</sub>O<sub>5</sub> which are assessed as a semi-quantitative result. Thus, the overall accuracy of the measurements is sound. The analytical data of PbO in alkaline-lime/lime glazes, ZnO, Sb<sub>2</sub>O<sub>5</sub> and P<sub>2</sub>O<sub>5</sub> in lead glazes will not be used for data discussion.

### **3.2.5 Relevant literature review**

The application of electron microprobe analysis on the compositions of glazes started to appear in the late 1970s and early 1980s. Many types of chemical analysis techniques have been used by these studies, for example, the energy dispersive X-ray spectrometer (EDS) fitted to the early equipment. In this study, the Electron microprobe wavelength dispersive X-ray spectrometry (EPMA-WDS) is used to obtain the major and minor chemical compositions of our glaze samples from Northern China and the Middle East.

Henderson et al. (1989) studied the chemical compositions of 24 Chinese cloisonné enamels dating from the early 16th century AD to middle 17th century AD by EPMA-WDS, combined with the scanning-electron microscope with an energy dispersive spectrometer (SEM-EDS), and the X-ray diffractometer (XRD). The results of EPMA-WDS compositional analysis show that the basic chemical compositions of the enamels



can be seen as the lead oxide was added to an existing glass, or to the sintered raw material having the chemical composition of glass. Both transparent, translucent and opacity enamels can be found. Calcium fluoride was found to exist in some enamel colours to produce opacity (e.g. opaque white colour) or translucent colour (e.g. translucent turquoise colour). Besides, in general, the cloisonné enamels were produced by a gradually reduced level of lead oxide and correspondingly increasing silica content during the period of early 16th century AD to middle 17th century AD.

Pradell et al. (2008a) studied the chemical compositions of four glazes of Iraqi lustre ceramics covering 9th century AD polychrome and 10th century AD monochrome lustre by EPMA-WDS. Besides, the Synchrotron Radiation Micro X-ray Diffraction (SR- $\mu$ XRD) analysis was used to determine the crystalline species within both glazes and lustre layers, the X-ray Absorption Near Edge Spectroscopy (XANES) and Extended X-ray Absorption Fine Structure (EXAFS) was applied to study the oxidation state and local coordination of Cu and Ag in the lustre layers. They found that, for the early Iraqi polychrome lustrewares, when the glaze contains PbO content above 10%, the silver-rich green lustre glaze shows metal shines. However, for the mixed Cu/Ag amber and brown lustre glazes having PbO contents of 10-15%, the metal shine does not appear. This suggests that the metal shine in the mixed Cu/Ag amber and brown lustre glazes need relatively high PbO content. Therefore, they inferred that the increase of the lead content in the glazes is the key parameter in the success of obtaining a golden lustre for the monochrome lustre decorations.

Pradell et al. (2008b) studied the chemical compositions of the glazes of lustre ceramics dating from the late 10th century AD to the second half of the 13th century AD from Egypt, Syria and Iran by EPMA-WDS, also combined with the SR- $\mu$ XRD analysis, the

XANES and the EXAFS. The results of the EPMA-WDS chemical analysis show that the earliest Iraqi wares were produced by lead-alkaline glazes with relatively low lead contents and decorated by lustre paints with different copper and silver compositions. The later Iraqi lustre wares of the 10th century shifted from polychrome to the monochrome green-golden and had higher lead contents. The development of the golden shine is associated with silver rich lustres and higher lead glazes. The monochrome Fatimid lustres are silver rich too. These glazes have high lead contents (the highest contents of all lustre productions) which provide sufficient firing temperatures and reducing atmospheres for the production of a golden metallic shine. The Syrian lustrewares studied covered with alkali glazes followed an existing local tradition of the area.

Yin et al. (2011) studied the chemical compositions of the bodies and glazes of 54 proto-porcelain samples and 18 fragments of stamped pottery and kiln walls from the Shang (BC1700-1027) and Zhou (BC1027-221) dynasties production sites in Deqing, Zhejiang province by EPMA -WDS. The results of EPMA -WDS chemical analysis show that the glazes of proto-porcelain samples are characterised by the high contents of calcium oxide (10-20 wt.%) and low levels of alkali with 2-3 wt.%  $K_2O$  and around 1 wt.%  $Na_2O$ . The contents of magnesia (1-3 wt.%) and phosphate (around 1 wt.%) also were detected in their glazes which are higher than those in their bodies. Processed wood ashes, high in lime and low in potash, were inferred as having been added as the flux for making these lime-based glazes. The fluctuation of lime contents in the different ceramic glazes is suggested as an indication of the potters' early attempt to explore the ideal glaze formula. The exact compositions of glazes were determined by a temperature-controlled mechanism, by which the glazes were selectively absorbed into the ceramic bodies.

Tseng and Xu (2012) studied the chemical compositions on the glazes of Ye Wang's Koji pottery from Taiwan by EPMA-WDS. Ye Wang (1826-1887) was the most famous Koji pottery artist of Taiwan. The results of EPMA showed that the gem-blue glaze of Ye Wang's Koji pottery belongs to the  $\text{PbO-K}_2\text{O-B}_2\text{O-Na}_2\text{O-SiO}_2$  system. It contains high levels of potassium and lead as fluxes, besides, the existence of boron as a supplementary flux in Ye Wang's Koji glaze also is confirmed by the chemical analysis. EPMA-WDS analysis combined with spectroscopic analysis further suggested that the unique gem-blue colour of Ye Wang's Koji glaze due to the combination of copper, iron, manganese and cobalt. The glaze chemical compositional characteristics of Ye Wang's Koji pottery are similar to those of the Chinese Fahua formulae, which was popular in the mid-late Ming Dynasty (AD1368-1633) around the Shanxi area of Northern China.

### **3.3 Trace elemental analysis**

#### **3.3.1 Introduction**

The ceramics produced in different places can use raw materials with different types and sources, which may have had distinct chemical traces in the final ceramic products (Resano et al. 2010). Therefore, the chemical compositions of ceramics, especially the trace elements detected in ceramic pastes and glazes which have less than 1000ppm (parts per million), can provide useful hints about the sources of the raw materials and the manufacturing techniques used to produce ceramic bodies and glazes. Besides, by these, the studies of changes in glaze recipes, the origin of the ceramic artefacts and the interactions between different ceramic production centres also might be discussed.

Several techniques can be used to study the trace elemental compositions of glazed ceramics and other archaeological materials. Instrumental Neutron activation analysis

(INAA) has been widely applied in the past decades to conduct the trace element analysis in this field and obtains reliable multi-elemental composition results. During the past several years, the use of laser ablation-inductively coupled plasma-mass spectrometry (LA-ICP-MS) for the studies of the trace elemental characterisations of various archaeological materials has increased steadily. The reason is that LA-ICP-MS has certain advantages over other analytical techniques, such as high accuracy and precision, low detection limits, rapid analytical time, high sample throughput, and minimal destruction of the archaeological materials (Hill et al. 2004).

For trace elemental characterisation of ceramic glazes in this study, LA-ICP-MS was used here. The essential element Pb in glazes which cannot be measured by INAA can be measured by LA-ICP-MS. For many elements such as Sr, Sb, Ba and Zr, the LA-ICP-MS technique has lower detection limits than INAA (Speakman et al. 2002b). Besides, with INAA, the glaze layer must be separated from the ceramic pastes for analysis, while using LA-ICP-MS, glazed surfaces can be analysed without removing the glaze layers from their ceramic bodies (ibid 2002b). Moreover, LA-ICP-MS is flexible enough to achieve high spatial resolution with the highest sensitivity detector (Giussani et al. 2009; Resano et al. 2010).

The trace elemental compositions of glazes in this study were determined using the LA-ICP-MS instrument consisted of a NewWave UP193FX excimer (193 nm) laser system located in the Analytical Geochemical Laboratories of British Geological Survey, under the instruction of Dr Simon Chenery.

### **3.3.2 Sample preparation for analysis by LA-ICP-MS**

As mentioned in Section 3.2.2, the fully-prepared polished glaze-sample discs used for EPMA analysis were also suitable for the analysis by LA-ICP-MS technique. It needs to be pointed that, the samples were cleaned with dilute nitric acid before analysis to remove contamination on the external surface of samples.

### **3.3.3 The trace elements to be measured**

LA-ICP-MS is a suitable analytical technique which can determine the concentrations of tens of elements in different order of magnitude in different matrices simultaneously. By LA-ICP-MS technique, the contents of 35 trace elements were measured in this study, including Li, B, Ti, V, Cr, Rb, Sr, Y, Zr, Nb, Cs, Ba, Hf, Th, U, Zn, As, Sn, Sb, Co, Ni and 14 rare earth elements (La, Ce, Pr, Nd, Sm, Eu, Gd, Tb, Dy, Ho, Er, Tm, Yb and Lu). Every colour in each glaze sample was measured on three sampling positions in order to calculate the average values. These average element concentrations are given as ppm in different colours of the glaze samples used for the data discussion. These data are listed in the Appendix I Tables A5-A7.

### **3.3.4 Analysis and standards**

In LA-ICP-MS, the fully-prepared sample discs were placed inside the sample chamber which had a window. The laser, NewWave UP193FX excimer (193nm) laser system had a built-in microscope imaging system and used to ablate the sample. The chamber is flushed by a stream of helium gas ( $0.80 \text{ L} \times \text{min}^{-1}$ ), mixed with an argon carrier gas ( $0.85 \text{ L} \times \text{min}^{-1}$ ), to the Agilent 7500 series ICP-MS. Laser ablation craters were set at  $70\mu\text{m}$  in diameter, and approximately  $30\mu\text{m}$  deep, the laser was fired for 45 seconds on

sample at 10 Hz and a typical fluence of  $2.8 \text{ Jcm}^{-2}$ . The integrated signal from each ablation was blank subtracted using a ‘gas background’ acquired with the laser not firing on the sample for a period of 30s. Data was recorded in a time-resolved analysis (TRA) mode.

To obtain accurate quantitative results, some suitable standard samples were selected to analyse before and after the analyses of the glaze samples. Calibration of the system was performed using a standard glass of known concentration (NIST SRM610). Moreover, the standard glass NIST SRM612 was used for quality control. The bulk composition of the selected standard should be as similar as possible to that of the target samples. However, the target glaze samples in this study are lead-based glazes, and the suitable matrix-matched standard for this kind glaze is not available in the Analytical Geochemical Laboratories of British Geological Survey. In this case, an internal reference element is imperative to be used to compensate for any variation in the measuring conditions. Specifically, by using the internal reference element (the signal intensity for one selected element), any differences in ablation rates and transport efficiency between samples and sample-standards can be corrected (Resano et al. 2010). In this study, the known Si concentrations of glaze samples determined by EPMA-WDS were used as the internal standard. Calibration and quality control glass standard samples were run with each glaze sample block. Quality control data demonstrated across six analytical sessions and n=96 analyses. Both the average analytical results and the quoted values of NIST SRM612 are presented in Table 3.2. The calculated standard deviations and relative standard deviation (RSD%) of the measurements are also shown in Table 3.2 to check the precision and accuracy of the measurements. As shown in Table 3.2, the precision of the measurements is sound. The precisions of all the elements are as good as can be expected (2-5 RSD%) except Sn and Ti (11.45 and 13.38 RSD% respectively). Moreover, the accuracies for all

the elements ranged between -5 and +3 % except Sn (+13.57%). Although the element Sn has a relatively high percentage error, it is still within the acceptable range as a quantitative result (<20%).

	<b>Li</b>	<b>B</b>	<b>V</b>	<b>Cr</b>	<b>Co</b>	<b>Ni</b>	<b>Zn</b>	<b>As</b>	<b>Rb</b>
<b>Measured NIST612</b>	39.93	35.22	38.56	36.20	34.94	38.90	38.94	33.97	31.62
<b>St.Dev</b>	1.09	1.45	0.99	0.95	0.76	1.21	1.47	1.43	0.84
<b>RSD%</b>	2.73	4.12	2.58	2.62	2.18	3.12	3.78	4.21	2.67
<b>Expected NIST612</b>	40.20	34.30	38.80	36.40	35.50	38.80	39.10	35.70	31.40
<b>%Bias</b>	-0.67	2.69	-0.61	-0.56	-1.58	0.26	-0.41	-4.85	0.69
	<b>Sr</b>	<b>Y</b>	<b>Zr</b>	<b>Nb</b>	<b>Sn</b>	<b>Sb</b>	<b>Cs</b>	<b>Ba</b>	<b>La</b>
<b>Measured NIST612</b>	78.37	38.33	37.93	38.28	43.84	34.17	41.67	39.44	35.95
<b>St.Dev</b>	2.09	1.53	1.54	1.02	5.02	1.02	0.98	1.05	1.15
<b>RSD%</b>	2.67	4.00	4.05	2.67	11.45	2.98	2.36	2.66	3.21
<b>Expected NIST612</b>	78.40	38.30	37.90	38.90	38.60	34.70	42.70	39.30	36.00
<b>%Bias</b>	-0.04	0.07	0.08	-1.60	13.57	-1.52	-2.42	0.37	-0.13
	<b>Ce</b>	<b>Pr</b>	<b>Nd</b>	<b>Sm</b>	<b>Eu</b>	<b>Gd</b>	<b>Tb</b>	<b>Dy</b>	<b>Ho</b>
<b>Measured NIST612</b>	38.32	37.65	35.10	37.51	35.31	37.58	36.75	35.44	37.80
<b>St.Dev</b>	0.94	1.03	1.22	1.22	0.96	1.57	1.40	1.41	1.61
<b>RSD%</b>	2.44	2.72	3.47	3.26	2.73	4.16	3.82	3.99	4.25
<b>Expected NIST612</b>	38.40	37.90	35.50	37.70	35.60	37.30	37.60	35.50	38.30
<b>%Bias</b>	-0.20	-0.66	-1.14	-0.51	-0.81	0.76	-2.26	-0.16	-1.30
	<b>Er</b>	<b>Tm</b>	<b>Yb</b>	<b>Lu</b>	<b>Hf</b>	<b>Th</b>	<b>U</b>	<b>Ti</b>	
<b>Measured NIST612</b>	38.13	36.70	38.10	36.44	36.79	37.48	37.47	44.70	
<b>St.Dev</b>	1.64	1.47	1.48	1.45	1.48	1.34	0.94	5.98	
<b>RSD%</b>	4.30	4.00	3.87	3.98	4.01	3.58	2.52	13.38	
<b>Expected NIST612</b>	38.00	36.80	39.20	37.00	36.70	37.79	37.38	44.00	
<b>%Bias</b>	0.35	-0.28	-2.81	-1.51	0.25	-0.81	0.24	1.60	

**Table 3.2 Measured and expected values (mg/kg), calculated St.Dev values, RSD and Bias values (%) of trace elements for standard reference glass NIST612 by LA-ICP-MS (The expected values for SRM612 were published by GeoRem (Jochum et al. 2011))**

### 3.3.5 Relevant literature review

LA-ICP-MS is a highly sensitive analytical technique for trace element determination. During the past two decades, this technique has been used for the chemical characterisation of many kinds of archaeological materials such as bones and teeth, obsidians and glasses, ceramics and their glazed or painted layers, cherts and other miscellaneous stone materials, ancient documents and metal objects. By these studies, the

use of LA-ICP-MS has been proven as an essential technique for chemistry-based archaeological studies.

Several reviews of the LA-ICP-MS applications in archaeological materials have been published (Gratuze et al. 2001; Neff 2012; Speakman et al. 2002b; Giussani et al. 2009; Resano et al. 2010). These reviews give brief descriptions of the LA-ICP-MS technique especially its features, its basic operating principles, its analytic parameters and calibrations. These reviews also demonstrate an overview of the contributions of LA-ICP-MS in the investigation of various archaeological materials as aforementioned. Moreover, advantages and limitations of the LA-ICP-MS technique also are discussed critically.

The first published application of LA-ICP-MS to ceramics traces back to the paper by Robertson et al. (2002), who carried out a preliminary study on the ceramic standard materials of Ohio Red Clay and NIST SRM612 by both LA-ICP-MS and PIXE techniques. Later papers focused on linking the elemental compositions of ceramics analysed by LA-ICP-MS to the raw material sources and manufacturing techniques used to produce ceramics. Chemical compositional analyses of ceramic bodies and clays have been used widely in provenance studies (Cochrane and Neff 2006; Bartle and Watling 2007; Zhu et al. 2012).

Less compositional analysis by LA-ICP-MS has been used to study glazes and glaze-paints of glazed ceramics. Speakman et al. (2002a) analysed paints on 37 prehistoric Mesa Verde and Mancos Black-on-white pottery from the Mesa Verde Region of the American Southwest using LA-ICP-MS. The results of paint compositions show that Mancos Black-on-white is characterised by having a mineral-based paint derived from an iron-manganese ore, while the Mesa Verde Black-on-white is usually painted by an



organic-based (carbon-based) paint. This work confirmed that the LA-ICP-MS was an appropriate method for distinguishing mineral from carbon-based paints.

Hill et al. (2004) studied the major and trace elemental compositions of the glazes of 175 glazed ceramics from Sasanian and Early Islamic period sites located on the Deh Luran Plain in southwestern Iran by LA-ICP-MS, combined with the INNA analysis determining the ceramic pastes. They identified five compositional groups. The glazes of Group 1 are composed of soda/lime/silica glazes. Group 2 glazes contain trace contents of lead in a soda/lime/silica glaze. The glazes of group 3 and group 4 are all lead-based, and the major discriminating element between these two groups is the existence of copper used as a colourant. The glazed ceramics of Group 3 include blue or green monochrome coloured glazes, green coloured press-moulded glazes and splashed glazes. The glazed ceramics of Group 4 include non-decorated tin-glazed, lustreware glazes and yellow-brown lead stannate coloured glazes. The glazed ceramics of group 5 are high nickel glazes, using cobalt as their colourants. The presence of nickel is thought to be an indicative of the utilisation of the similar ore deposits as for the cobalt.

Resano et al. (2005) investigated the trace and major element compositions of blue-coloured (Co-enriched) glazes of ceramics produced in the Aragon area during the 14th to 18th centuries AD. The results inferred that the differences in the contents of Cu, As and Mn allow the classification of these glazes into three different categories, which could be related to the different ceramic production places and the various possible sources of the Co pigments. The classified results of the glazes are in good agreement with the results obtained by the ICP-AES analysis of the ceramic bodies. In this work, the potential of LA-ICP-MS for obtaining spatially resolved information and for analysing glazed layers was confirmed.

Duwe and Neff (2007) studied the trace and major elemental compositions of glaze-paints of 161 White Mountain Red Ware (WMRW) ceramic samples (AD 1275-1325) from east-central Arizona by the time of flight-laser ablation-inductively coupled plasma-mass spectrometry (TOF-LA-ICP-MS). By PCA analysis of chemical compositions, three different glaze-paint recipes can be determined in the WMRW ceramics by the discriminating elements of iron, copper, antimony, manganese and lead. This work inferred that the TOF-LA-ICP-MS analysis is potential for future studies on glaze-paint of ceramics.

Hao et al. (2013) studied the element concentrations of 13 glazes of Chinese proto-celadon in the Western Han Dynasty (BC202-AD8) excavated in two archaeological sites from Northern China- the Rizhao Cemetery of Shandong Province and the Cuipingshan site of Jiangsu Province, as well as one site from Southern China- the Xiaolongjing Cemetery of Zhejiang Province. The results show that the differences between Northern China proto-celadon glazes and Southern China ones can be found in concentrations of several significant elements of Fe, Ca and Mg. The glazes of Cuipingshan and Rizhao sherds from Northern China have higher content levels of Fe and Ca but lower Mg than Xiaolongjing glazes from Southern China, suggesting a unique manufacture technique in Northern China, differing from the southern ones. Besides, differences of several rare earth elements (Gd, Dy, Ho and Eu) are also remarkable between samples from Northern China and Southern China, implying a distinct feature in the raw material selection of the proto-celadon manufacture between Northern China and Southern China. These results may suggest that Chinese proto-celadon produced in Western Han Dynasty were manufactured both in Southern and Northern China.

## 3.4 Lead isotope analysis

### 3.4.1 Introduction

Lead isotopic analysis can offer useful information for discrimination purposes, especially for those archaeological materials with significant contents of Pb. Lead isotope ratios have been used in some provenance studies of various materials, such as copper, bronze, glass, glaze, faience and pigment (Brill et al. 1979; Gale and Stos-Gale 1982; Barnes et al. 1986; Al-Saa'd 2000; Wolf et al. 2003; Baker et al. 2006; Huntley et al. 2007).

There are several techniques that can be used to measure the lead isotope ratios of archaeological materials. Thermal ionisation mass spectrometry (TIMS) has been widely used in archaeological lead isotope provenance studies (Yener et al. 1991; Stos-Gale et al. 1998; Wolf et al. 2003). With inter-laboratory comparability assured based on replicate analyses of international lead isotope standard SRM 981, the method of using TIMS to determine lead isotope ratios have been suggested to could provide reliable and accurate results (overall reproducibility of  $\pm 0.1\%$  (2 s.d.) for each of the lead isotope ratios) (Baker et al. 2006). The disadvantage of this method is that samples need to be powdered and dissolved before analysis which results in relatively large sample damage, as well as expensive sample preparation. In recent years, the multi-collector inductively coupled plasma mass spectrometry (MC-ICP-MS) has been used in some studies on lead isotope determination in archaeological materials and proven to obtain high-precision isotope ratios (Hirata et al. 2003; Baker et al. 2006; Fenn et al. 2009). Compared to TIMS, the MC-ICP-MS analysis is simpler, quicker and more cost-effective (Baker et al. 2006). With laser ablation, isotope ratios of the sample can be measured in situ without sample

digestion, which is important for the analysis of archaeological materials. Besides, LA-MC-ICP-MS has a potential to obtain spatially-resolved information, which is helpful for the isotopic analysis of some kinds of archaeological materials such as ceramic glazes and pigments.

In this study, 20 fragments of lead-glazed ceramics from Northern China and the Middle East were analysed for lead isotopic ratios of their glazes. By comparing the lead isotope ratios of these glazes with those of some lead ores, information on the possible sources of the lead used to produce these glazes can be discussed. The six Iraqi lead glaze samples supplied by the Ashmolean Museum are small-sized and only are allowed to be analysed by the minimal or non-destructive method. Thus the LA-MC-ICP-MS is the priority technique for them in this study. For the Chinese and Syrian lead glaze fragments, the technique of solution MC-ICP-MS was selected to determine their lead isotope ratios, because these Chinese glazes are big enough to be allowed to remove around 50mg sub-samples for analyses. Besides, the lead isotope ratios of two Chinese lead glaze samples (HPK-5 and HYK-7) were both analysed by LA-MC-ICP-MS and solution-MC-ICP-MS repetitively, to check the accuracy of the lead isotope ratio results in this study.

### **3.4.2 The basic hypothesis of Pb isotopic application to provenance ancient glaze materials**

There are four naturally occurring isotopes of Pb, which are  $^{204}\text{Pb}$ ,  $^{206}\text{Pb}$ ,  $^{207}\text{Pb}$ , and  $^{208}\text{Pb}$ .  $^{204}\text{Pb}$  has no extant progenitor,  $^{206}\text{Pb}$ ,  $^{207}\text{Pb}$  and  $^{208}\text{Pb}$  are produced by the radioactive decay of  $^{238}\text{U}$  ( $T_{1/2}= 4.47 \text{ Ga}^{-1}$ ),  $^{235}\text{U}$  ( $T_{1/2}= 0.704 \text{ Ga}^{-1}$ ) and  $^{232}\text{Th}$  ( $T_{1/2}= 14.0 \text{ Ga}^{-1}$ ) respectively (Albarède et al. 2012). Measurable differences in lead isotope ratios happen naturally because the relative abundances of lead isotopes vary with their respective

progenitors (Gulson 1986; Albarède et al. 2012). Thus, the lead isotope ratios in different ore deposits have distinct characterisations depending on their geological age and the geological region in which it was produced (parent-daughter isotope ratios). This natural variation in lead isotope ratios makes lead isotopic analysis potential to provenance archaeological materials, especially those with significant contents of Pb. Moreover, there is no measurable isotopic fractionation occurring in either the extraction or utilisation of lead ores (Stos-Gale, 1992; Gale and Stos-Gale 2000). Therefore, for the lead glazes which use lead ore deposits for the production of the glazes, lead isotope analysis enables tracing the origins of lead used for glaze production to specific lead ore sources by comparing their lead isotope ratios.

### **3.4.3 MC-ICP-MS instrumentation**

Two different applications of MC-ICP-MS technique were used in this study to do lead isotope analysis- solution analysis of dissolved glaze samples and in situ laser ablation sampling.

A mass spectrometer is a technique which can sort and measure charged atoms and molecules based on their different mass-to-charge ratios. ICP mass spectrometers exploit the inductively coupled plasma to ionise the sample by inductively heating the gas with an electromagnetic conductor, and then these ions are separated and determined by the mass spectrometer. The samples are typically introduced into the ICP plasma as an aerosol, either by aspirating liquid samples or dissolved solid samples with heat and strong acids. With a multi-collector detection system attached to ICP-MS, this advanced technique can monitor ions from the plasma simultaneously through several collectors (generally Faraday cups) and discrete dynode electron multipliers. By measuring the

target isotopes simultaneously, any variations in the conditions should affect all of the signals to a similar extent (Resano et al. 2010). In this way, an improved precision is obtained when measuring the isotope ratios. When laser ablation is used, a laser beam focused on the sample surface generates aerosols by vaporising the materials from the sample. The ablated aerosol then flows into the argon plasma of the ICP-MS instrument following ionisation of the ablated mass.

### **3.4.4 Sample preparation for Pb isotopic analysis**

As mentioned in Section 3.2.2, the fully-prepared polished glaze-sample discs used for EPMA analysis also is suitable for the analysis by LA-MC-ICP-MS technique. Thus in this section, only the sample preparation for solution MC-ICP-MS analysis is introduced in details. The whole procedure of sample preparation for lead isotopic analysis by the solution MC-ICP-MS technique was performed at the NERC Isotope Geosciences Laboratory (NIGL) at the British Geological Survey under the instruction of Professor Jane Evans.

#### **3.4.4.1 Sample pre-treatment**

The samples for lead isotopic analysis by the solution MC-ICP-MS technique were ceramic glazes. Thus, the first step here is removing the glaze layer clearly from their ceramic body. During the whole procedures of sample preparation, the aim of avoiding laboratory contamination for Pb, such as from tools and reagents, should always keep in mind. Firstly, the diamond-edged dental saw was used to cut the glaze layer from the ceramic body, and for each sample, a new dental saw was used. In this step, some ceramic bodies remain in the glaze layer. In the following step, the tungsten carbide dental bur (DFS, Riedenber, Germany) was selected to grind the remaining ceramic body off glaze

clearly. Tungsten carbide is extremely hard so that only introduces negligible Pb and Sr contamination. Therefore, it is suitable for grinding low concentration geological samples such as ceramic glaze before Pb and Sr isotopic measurements (Montgomery 2002, 131). The Tungsten carbide burrs were cleaned before and between sampling by being rinsed ultrasonically with Millipore Alpha-Q H<sub>2</sub>O for 5 minutes. Besides, the clearly ground glaze samples also were cleaned ultrasonically in Millipore Alpha-Q H<sub>2</sub>O for 5 minutes before following sample preparation.

#### **3.4.4.2 Sample dissolution for solution MC-ICP-MS analysis**

Approximately 10mg of each glaze sample was held by an individual, acid-leached Teflon beaker and dissolved in 1-2 mls of Teflon distilled (TD) HNO<sub>3</sub>. Samples were left in nitric acid for around one week to leach the solution. Digested samples were then centrifuged to remove the undissolved samples from the solutions. The clear solution is diluted in a 100 ml flask using deionised water. Before analysis, each sample solution was doped with the thallium (Tl) standard solution-SRM997.

### **3.4.5 Analyses and standards**

#### **3.4.5.1 LA-MC-ICP-MS**

Lead isotopic analyses by the LA-MC-ICP-MS and solution LA-ICP-MS were carried out at the NERC Isotope Geosciences Laboratory (NIGL). Analyses of lead isotopic ratios for a batch of glaze samples were performed using a 193nm excimer-based lasers-ablation system attached to a VG P54 Elemental multi-collector inductively coupled plasma source mass spectrometer (MC-ICP-MS). Ion beams of mass 208 to 201 were collected by static multi-collection in Faraday cups. Nu Plasma time-resolved software was used to establish the average of the background for each analysis and to calculate each ratio using

the background-corrected signals from each time-resolved measurement. Typical ablation spectra were collected for ~60s. The isobaric correction of the contribution of  $^{204}\text{Hg}$  on mass  $^{204}\text{Pb}$  was done by measurement of  $^{202}\text{Hg}$  signal and the natural isotopic abundances of each Hg isotope ( $^{202}\text{Hg}/^{204}\text{Hg}= 0.2299$ ) (de Laeter et al. 2003). However, because this study analysed lead glaze samples with a negligible amount of Hg, the Hg interference was insignificant during the analyses. To minimise the ablated sample volume, the crater diameters and laser energy were kept as small/low as possible. In the case of Standard SRM 610 glass, a laser beam with a diameter of  $100\mu\text{m}$  and a fluence of  $3.0\text{ J/cm}^2$  with 10Hz repetition rate were selected due to its low Pb concentrations. These parameters were reduced to  $35\mu\text{m}$ ,  $2.0\text{ J/cm}^2$  and 5Hz for the Glass Std (P711:15) due to its considerably higher lead content. And for the lead glaze samples, these parameters were reduced to  $10\mu\text{m}$ ,  $0.44\text{ J/cm}^2$  and 5Hz.

Twelve lead glaze samples were analysed for the lead isotopic ratios by LA-MC-ICP-MS. All of these glazes are very rich in Pb (40-65 wt% PbO). The matrix of standard reference materials having similar concentrations with that of analytical samples is vital for the accurate correction of the instrumental mass bias during the LA-MC-ICP-MS analysis. However, there is no international standard reference material with certified Pb isotope ratios have such relatively high lead contents. Therefore, the in-house standard Glass Std (P711:15), which is an archaeological high-lead glass, supplied by the NERC Isotope Geosciences Laboratory (NIGL) at the British Geological Survey was selected in this study for external correction of mass discrimination due to its comparable chemical composition.



Initially, two different standard materials measured for mass discrimination correction were compared using the example of Syria-4 glaze sample: (1) the NIST 610 reference standard glass (National Institute of Standards and Technology, USA), (2) an in-house standard reference material-Glass Std (P711:15) from the NERC Isotope Geosciences Laboratory (NIGL). The results of the two approaches (see Table 3.3) present no significant differences, suggesting these two approaches are in good agreement. Besides, the mass discrimination corrections through the in-house standard Glass Std (P711:15) results were in lower values of  $2\sigma$  (overall analytical error). Finally, because of the comparable concentration levels, the in-house standard Glass Std (P711:15) was used for the external mass bias correction for the lead glaze sample measurements. The lead isotope ratios of standard Glass Std (P711:15) are  $^{206}\text{Pb}/^{204}\text{Pb}=18.3495$ ,  $^{207}\text{Pb}/^{206}\text{Pb}=0.85177$  and  $^{208}\text{Pb}/^{206}\text{Pb}=2.09075$ .

Sample Name	$^{206}\text{Pb}/^{204}\text{Pb}$	$2\sigma$ %	$^{207}\text{Pb}/^{206}\text{Pb}$	$2\sigma$ %	$^{208}\text{Pb}/^{206}\text{Pb}$	$2\sigma$ %
<b>Normalised to NIST 610</b>						
Syria-4(1)	19.1075	0.1503	0.8236	0.1044	2.0693	0.1181
Syria-4(2)	19.1118	0.2088	0.8232	0.1798	2.0663	0.0454
Syria-4(3)	19.1108	0.1317	0.8232	0.0899	2.0692	0.0684
Syria-4(4)	19.1147	0.1694	0.8231	0.1823	2.0690	0.0945
Syria-4(5)	19.1039	0.1599	0.8232	0.1847	2.0685	0.0804
Syria-4(6)	19.1275	0.2488	0.8228	0.1994	2.0681	0.0648
Syria-4(7)	19.0928	0.4134	0.8217	0.2921	2.0651	0.0667
Syria-4(8)	19.1065	0.2592	0.8227	0.1167	2.0650	0.0899
Syria-4(9)	19.1156	0.2088	0.8224	0.1897	2.0669	0.0712
<b>Mean</b>	<b>19.1101</b>	<b>0.2167</b>	<b>0.8229</b>	<b>0.1710</b>	<b>2.0675</b>	<b>0.0777</b>
<b>Normalised to Glass Std (P711:15)</b>						
Syria-4(1)	19.1198	0.1360	0.8240	0.1044	2.0695	0.1160
Syria-4(2)	19.1242	0.1988	0.8236	0.1798	2.0665	0.0397
Syria-4(3)	19.1232	0.1151	0.8236	0.0899	2.0694	0.0648
Syria-4(4)	19.1271	0.1569	0.8235	0.1823	2.0692	0.0919
Syria-4(5)	19.1162	0.1465	0.8237	0.1847	2.0687	0.0774
Syria-4(6)	19.1399	0.2404	0.8232	0.1994	2.0683	0.0609
Syria-4(7)	19.1051	0.4084	0.8222	0.2921	2.0653	0.0630

Syria-4(8)	19.1188	0.2511	0.8231	0.1167	2.0652	0.0872
Syria-4(9)	19.1280	0.1987	0.8228	0.1897	2.0671	0.0678
<b>Mean</b>	<b>19.1225</b>	<b>0.2058</b>	<b>0.8233</b>	<b>0.1710</b>	<b>2.0677</b>	<b>0.0743</b>

**Table 3.3 Pb isotopic ratios of the lead glaze sample-Syria-4 using different standard reference materials for mass discrimination correction**

The standard Glass Std (P711:15) used for external correction for mass discrimination effects was measured at the beginning and the end of every two samples. For each sample, five repeat measurements were carried out at different positions. For every replicate measurement, a transient signal with a duration of 100s was obtained. Only the last 80s were used for quantification purposes since the first 20s were left for signal stabilisation. Replicate analyses (n=59) of standard Glass Std (P711:15) were used to assess an external precision of  $^{206}\text{Pb}/^{204}\text{Pb}=18.3495\pm 0.13\%2\sigma$ ,  $^{207}\text{Pb}/^{206}\text{Pb}=0.8518\pm 0.11\%2\sigma$ ,  $^{208}\text{Pb}/^{206}\text{Pb}=2.0908\pm 0.15\%2\sigma$ . The reproducibility of the standard Glass Std (P711:15) offers the evidence for the stability and the accuracy of the LA-MC-ICP-MS technique (0.13%  $2\sigma$  for  $^{206}\text{Pb}/^{204}\text{Pb}$ , 0.11%  $2\sigma$  for  $^{207}\text{Pb}/^{206}\text{Pb}$ , 0.15%  $2\sigma$  for  $^{208}\text{Pb}/^{206}\text{Pb}$ . Then the  $2\sigma$  values of external reproducibility of the standard were used as error bars on isotope plots for sample discussion.

The average lead isotope ratios calculated by each of the measured Glass Std (P711:15) isotope ratios were then compared to the known ratio values of this standard Glass (provided by NIGL) to normalise all sample data. The Pb isotopic ratios of each glaze sample used for data discussion are average values of five measures per sample.

### **3.4.5.2 Solution MC-ICP-MS**

For solution analyses, prepared lead solutions were conducted using a Nu Instruments Nu plasma MC-ICP-MS. The samples were introduced into the instrument via an ESI 50  $\mu\text{l}/\text{min}$  PFA micro-concentric nebuliser attached to Nu Instruments DSN-100, using argon

as a sweep gas. Ten Chinese lead glaze samples were analysed by solution MC-ICP-MS. For each sample, five ratios were measured simultaneously and three of them ( $^{208}\text{Pb}/^{206}\text{Pb}$ ,  $^{207}\text{Pb}/^{206}\text{Pb}$  and  $^{206}\text{Pb}/^{204}\text{Pb}$ ) were used for data discussion.

During solution analyses, the international standard US National Bureau of Standard NBS981 Pb reference solution (30ppb NBS981 spiked with 3ppb Tl) was used to assess the precision and accuracy of the solution MC-ICP-MS method. The verified lead isotope ratios of the reference standard NIST SRM981 used in this study is  $^{206}\text{Pb}/^{204}\text{Pb} = 16.9417$ ,  $^{207}\text{Pb}/^{206}\text{Pb} = 0.91488$  and  $^{208}\text{Pb}/^{206}\text{Pb} = 2.1677$  (Thirlwall 2002). And the average isotope ratio results of 20 standard NBS 981 runs were:  $^{206}\text{Pb}/^{204}\text{Pb} = 16.9353 \pm 0.010\% 2\sigma$ ;  $^{207}\text{Pb}/^{206}\text{Pb} = 0.9149 \pm 0.005\% 2\sigma$ ;  $^{208}\text{Pb}/^{206}\text{Pb} = 2.1671 \pm 0.007\% 2\sigma$ . The reproducibility of the standard NBS 981 Pb reference solution shows a good stability and accuracy of the solution MC-ICP-MS technique (0.010 %  $2\sigma$  for  $^{206}\text{Pb}/^{204}\text{Pb}$ , 0.005%  $2\sigma$  for  $^{207}\text{Pb}/^{206}\text{Pb}$ , 0.007%  $2\sigma$  for  $^{208}\text{Pb}/^{206}\text{Pb}$ ). The average lead isotope ratios calculated by each of the measured isotope ratios of NBS 981 Pb reference solution were then compared to the known ratio values of this standard to normalise all sample data used for data discussion.

### **3.4.6 The precise and accuracy of MC-ICP-MS analysis**

Lead isotope data of 20 repeat solution-MC-ICP-MS analyses of the standard NBS981 solution shows excellent reproducibility (<0.005%  $2\sigma$ ), better than that for the Glass Std (P711:15) analysed by LA-MS-ICP-MS (<0.11%  $2\sigma$ ). It suggests that the lead isotopic measurements made by solution MC-ICP-MS are more precise than those made using LA-MC-ICP-MS.

The lead isotope ratios of two Chinese lead glaze samples (HPK-5 and HYK-7) were both analysed by LA-MC-ICP-MS and solution MC-ICP-MS repetitively. Comparison of lead

isotopic ratios of these two glaze samples measured by solution MC-ICP-MS and LA-MC-ICP-MS can be seen in Table 3.4. The  $2\sigma$  of lead isotopic ratio of these two methods is less than 0.10% of  $^{207}\text{Pb}/^{206}\text{Pb}$ , 0.13% of  $^{208}/^{206}\text{Pb}$  and 0.15% of  $^{206}\text{Pb}/^{204}\text{Pb}$ , which is suitable for archaeological tracer studies, suggesting that the lead isotope ratios measured by LA-MC-ICP-MS are consistent with those determined by solution MC-ICP-MS. This infers that the lead isotope analysed by LA-MC-ICP-MS is reliable and suitable for archaeological tracer studies.

Sample No.	Analytical Method	$^{208}\text{Pb}/^{206}\text{Pb}$	$^{206}\text{Pb}/^{204}\text{Pb}$	$^{207}\text{Pb}/^{206}\text{Pb}$
HPK-5 green	LA-MC-ICP-MS	2.1913	17.5262	0.8846
HPK-5 green	Solution MC-ICP-MS	2.1920	17.5450	0.8840
<b>2<math>\sigma</math> %</b>		<b>0.05</b>	<b>0.15</b>	<b>0.10</b>
HYK-7 green	LA-MC-ICP-MS	2.1271	18.0479	0.8640
HYK-7 green	Solution MC-ICP-MS	2.1290	18.0610	0.8640
<b>2<math>\sigma</math> %</b>		<b>0.13</b>	<b>0.10</b>	<b>0.00</b>

**Table 3.4 the lead isotope ratios of glaze samples (HPK-5 and HYK-7) measured by Solution MC-ICP-MS and LA-MC-ICP-MS**

### 3.4.7 Relevant literature review

Lead isotope analysis has been proven useful to provide provenance information for various archaeological materials. The application of lead isotope analysis to provenance the source of lead used for lead glaze production is based on the principle that the lead glazes and lead ore deposits from different geological sources can be distinguished by ‘fingerprints’ of their lead isotope ratios. Thus the lead isotope ratio database of ore deposits in the context of the geological backgrounds is crucial for the provenance study by lead isotopic analysis.

Brill and Wampler (1967) studied the lead isotope ratios of 230 lead-containing samples, including 70 ore deposit samples from different ancient mining areas, and 160 archaeological object samples. The lead isotope results of 60 samples were measured at

the Chemistry Department of Brookhaven National Laboratory using a thermal-emission mass spectrometer. The remaining 170 samples were analysed by the authors using a consolidated thermal-emission mass spectrometer. This study suggested that the lead ores collected from three significant ancient mining regions- Greece, England and Spain can be distinguished with each other by their different lead isotope ratios. Moreover, by comparing the lead isotope ratios of archaeological objects and those of ore deposits, the provenance of some archaeological objects had been suggested. Importantly, the source of some archaeological objects cannot be inferred due to the limited lead isotope data of ore deposits.

Brill et al. (1997) summarised the lead isotope ratio results of around twelve hundred ancient lead-containing archaeological artifacts and ores from different areas, including the ores from the Laurion mines in Greece and artifacts of known Greek origins, the leads from Mesopotamia and some from Iran, the leads from Spain, Wales, and Sardinia, the ores from England and certain European areas, some ores and artifacts from Japan and China. The lead isotope ratios of some pigment samples of Buddhist cave paintings and wall paintings from China and other Asian countries were analysed in this study. By comparing the lead isotope ratios of these pigments and those of summarised lead ore sources, the lead sources used in some of these pigments can be inferred.

A large number of lead isotope ratio data for ores from various ore deposits have been summarised in the Oxford Archaeological Lead Isotope Database (OXALID) by the Isotrace Laboratory at the University of Oxford, which are available as Excel files on the OXALID website, at <http://oxalid.arch.ox.ac.uk>. The lead isotope ratio database contains ores from Bulgaria, Spain, Italy, Cyprus, Greece, Turkey and Britain. All data in the Isotrace Laboratory at Oxford was carried out using Multi-collector TIMS. By these data,

some lead isotopic analyses on lead glazes have been used to provenance the lead used for the glaze production.

Wolf et al. (2003) studied the lead isotope ratios of the glazes of Islamic lead glazed ceramics from Fustat, Egypt, dating from the 8th to the 14th century AD using TIMS. The lead isotope ratios of these glazes were compared with those for some lead ores from Egypt, Iran, Tunisia, Anatolia, Greece, Sardinia and Spain in order to provenance the possible sources of the lead used in these glaze making. The results infer that the leads used for making glazes of Islamic Fustat ceramics were probably collected from distant ore sources in Iran or Tunisia, Sardinia, Spain and the Taurus Mountains instead of local Egyptian ore sources. The results also show that the glaze production in different periods used the ore deposits from different areas. Due to the overlap of the lead isotope ratios of some ore sources from different areas, the limited lead isotope data of ores, and the possibility of mixing of lead from different sources, for some glazes, more than one lead source was suggested for the lead used for making them.

Walton and Tite (2010) studied the lead isotope ratios of the glazes of Western Roman lead glazed ceramics during the period from the 1st century AD to the 5th century AD by TIMS. The lead isotope ratios of these glazes were also compared with those of some lead ores from different areas obtained from the Oxford Archaeological Lead Isotope Database (OXALID). The results showed that the lead sources used for the production of the glazes of Western Roman lead-glazed ceramics might be collected from several probable regions, including central Gaul, Italy and, probably, Serbia and Romania.

For the Chinese lead glazes, only a few lead isotope analyses have been carried out to provenance their lead sources. The most significant analysis for Chinese lead glazes by their lead isotope ratios was carried out by Cui et al. (2010). The lead isotope ratios of 19

Tang Sancai lead glazes unearthed from the Huangpu and Huangye kiln sites were analysed by MC-ICP-MS. The glaze samples from these two kiln sites can be grouped separately by their distinct lead isotope ratios. Zhu (1995) divided China into three main geochemical provinces by the lead isotopic characters for ores and rocks from different areas. By comparing lead isotope ratio results of Tang Sancai glazes with those of ores and rocks, Cui et al. (2010) inferred that the lead in the Huangpu kiln glazes might originate from the Northern China geochemical province, while the lead used for making Huangye Kiln glazes were collected from the Yangtze geochemical province.

Nineteen glaze samples of lead glaze ceramics unearthed from Chinese Huangye kiln sites and several Japanese Archaeological sites were studied collaboratively by the Nara National Institute for Cultural Properties and the Henan Provincial Institute of Cultural Relics and Archaeology in 2011 (Nara National Institute for Cultural Properties, Henan Provincial Institute of Cultural Relics and Archaeology 2011). The analysed lead isotope ratios of these glazes were compared to some published lead isotope ratios of bronze artefacts with known Chinese and Japanese origins. The results suggest that the lead isotope ratios of lead glazes made in China and Japan can be distinguished from each other by their different lead isotope ratios. Moreover, some lead glaze ceramics unearthed in Japan might have been made in the Huangye kiln sites and exported to Japan.

## **3.5 Strontium isotopic analysis**

### **3.5.1 Introduction**

The application of combining Sr isotope study with chemical analysis on glass/glaze is potential to understand the raw materials used for glass/glaze production. In this study,

the glazes from Northern China and Syria were analysed for their Sr isotopic compositions by Thermal ionisation mass spectrometry (TIMS).

### **3.5.2 The basic hypothesis of Sr isotopic application to provenance ancient glass or glaze materials**

Strontium has four naturally occurring stable isotopes, which are  $^{84}\text{Sr}$ ,  $^{86}\text{Sr}$ ,  $^{87}\text{Sr}$  and  $^{88}\text{Sr}$ . The amounts of the isotopes  $^{84}\text{Sr}$ ,  $^{86}\text{Sr}$  and  $^{88}\text{Sr}$  are constant in nature, whereas  $^{87}\text{Sr}$  is radiogenic produced by the decay of  $^{87}\text{Rb}$ . Therefore, the Sr isotopic composition of a rock or mineral depends on the age of the rock or mineral and its original Rb/Sr ratio (Faure 1986; 118). Strontium is a member of the alkaline earths of Group IIA, and its ionic radius (1.13 Å) is slightly higher than that of calcium (0.99 Å), which is in the same element group with strontium. Thus,  $\text{Sr}^{2+}$  substitutes  $\text{Ca}^{2+}$  in Ca-bearing minerals like plagioclase, apatite, and calcium carbonate, especially aragonite. Besides,  $\text{Sr}^{2+}$  ions can be captured in place of  $\text{K}^{1+}$  ions by K-feldspar, but this replacement must be coupled by the substitution of  $\text{Si}^{4+}$  by  $\text{Al}^{3+}$  to maintain electrical neutrality (ibid; 117).

Sr isotopic analysis has been widely used in geological studies for a long time, while the use of Sr isotope analysis to discuss the raw materials used in glass and glaze making is a relatively recent method. The use of strontium isotopes in ancient glass and glaze studies are mainly based on two assumptions. Firstly, strontium has low relative mass differences between its isotopes and show radiogenic nuclide (Faure 1986; 118), resulting in no detectable fractionation during production processing. Thus, the Sr isotopic composition of the glass or glaze will be identical, within analytical errors, to the raw materials from which it was derived (Brill and Wampler, 1965). Sr isotopes hence have the potential to understand the different raw materials used in ancient glasses and glazes. Secondly, the



strontium in glass is mainly incorporated with the lime-bearing constituents of the glass recipe (Wedepohl and Baumann, 2000). Besides, the feldspars or heavy minerals in acidic raw material of a glass recipe have a minor Sr contribution to the final Sr isotope composition of glass (Degryse et al. 2009, 19). The raw materials and techniques of glaze production are closely linked with those of glass making. Thus the glaze study by Sr isotopic analysis also can satisfy these two assumptions.

The raw materials used to make ancient glass and glaze are mainly composed of siliceous raw materials (e.g. quartz pebble, lime-bearing sand, coastal sand, glaze stone and clay) and fluxes (e.g. natron, limestone and plant ash). As strontium generally substitutes for calcium, the Sr concentration in the final glass/glaze is mainly contributed by the lime-bearing raw materials used in the glass/glaze recipe, including limestone, plant ash and shell in coastal sand (Wedepohl and Baumann, 2000; Freestone et al. 2003). Besides, calcium-rich minerals present in lime-bearing sands or glaze stones also make a certain contribution to the Sr concentration of glass/glaze. The Sr isotope compositions of these raw materials usually have distinct patterns due to their specific mineralogical and geological characteristics. The  $^{87}\text{Sr}/^{86}\text{Sr}$  ratios of Holocene beach shell reflect that of modern seawater and are close to 0.7092 (Freestone et al. 2003). The Sr isotope compositions of limestone depend on those of the seawater at the time the limestone was deposited, and modified by any diagenetic alteration occurred over geological time (Freestone et al. 2003). In respect of botanic ashes, all plants species growing in a specific geological location have the similar value of  $^{87}\text{Sr}/^{86}\text{Sr}$  isotope ratio, reflecting the geological/surficial environment in which the plants grew (Henderson et al. 2005a; Henderson et al. 2005b). The Sr concentrations of botanic ashes are highly variable due to a range of factors and always have a more concentrated Sr content due to the ashing process of the plants (Henderson et al. 2005b; Barkoudah and Henderson 2006). Thus, the

Sr isotope composition characteristic of the glass/glaze is potential to discuss the recipe and provenance of glass/glaze.

### **3.5.3 The TIMS technique for Sr isotope analysis and the standard used**

Thermal ionisation mass spectrometry (TIMS) is a magnetic sector mass spectrometer which has been widely used as a method for very precise determination of isotope ratios. TIMS is so-named because it exploits the ionisation technique. A chemically purified sample is placed on treated filaments (usually rhenium or tantalum), then heated to cause ionisation of the atoms of the sample by sample evaporation. The resulting ion beam then passes through a magnetic field and then mass-separated by an electromagnet based on different mass to charge ratios. The current of each ion beam is then measured using multi-collector of Faraday cups to calculate precise isotope ratios. The strontium isotope compositions and concentrations of glaze samples in this study were measured by TIMS using a Finnigan Mat 262 multi-collector mass spectrometer at the NERC Isotope Geosciences Laboratory (NIGL).

For Sr isotope analysis, the fully-prepared sample was loaded onto a single Re Filament. The filament is then inserted into the vacuum system, and a current is passed through it to ionise the sample. The international Sr reference standard (NBS 987) was loaded in the same way onto the turret along with the prepared filaments to normalise the measured strontium isotopic ratios of the samples. Typical external precision for NBS 987 Sr standard gave an  $^{87}\text{Sr}/^{86}\text{Sr}$  ratio of  $0.710258 \pm 15$  ( $2\sigma$ ,  $n = 18$ ). The final Sr isotope composition results of glaze samples are presented as ratios and concentrations in parts per million (ppm).

### **3.5.4 Preparation of samples for Sr isotopic analysis**

The whole procedure of sample preparation for Sr isotopic analysis by the TIMS technique was performed at NIGL. The sample preparation for Sr isotopic analysis includes sample pre-treatment, weighing and 'spiking', sample dissolution and separation. The procedure of sample pre-treatment for Sr isotopic analysis is same with that for Pb isotope analysis by solution MC-ICP-MS, which has been described in detail in Section 3.4.4. Thus only the other steps of sample preparation are listed here. The whole procedure of sample preparation was carried out within class 100, HEPA-filtered laboratory facilities at the NERC Isotope Geosciences Laboratory (NIGL).

#### **1). Weighing and 'spiking' of sample**

Around 30.0-90.0mg glaze samples were weight by a balance (Unit: gramme) accurate to the 5<sup>th</sup> decimal digit and held by acid-leached Teflon beakers. Then each sample was spiked with one or two drops (approximate 30.0-60.0mg) of oak ridge <sup>204</sup>Sr enriched tracer and then reweighed, the Sr concentration of which was 1.1593ppm, and its <sup>88</sup>Sr/<sup>86</sup>Sr, <sup>87</sup>Sr/<sup>86</sup>Sr and <sup>84</sup>Sr/<sup>86</sup>Sr were 0.846054, 0.182448 and 937.5584 respectively.

#### **2). Sample dissolution**

- A. Each sample held by the Teflon beaker was soaked with 1-2 mls of Millipore Alpha-Q H<sub>2</sub>O. Then 1-2 mls of Teflon distilled (TD) HNO<sub>3</sub> and 10 mls of HF were added to the Teflon beaker. The lid of each Teflon beaker was screwed tightly and placed the Teflon beakers on the hotplate overnight to dissolve and dry down.
- B. 1-2 mls of TD HNO<sub>3</sub> were added to each Teflon beaker and put on the hotplate uncovered to dryness.

- C. 10 mls of 6M HCl were added to each Teflon beaker and screwed with lids. The Teflon beakers then were put on the hotplate overnight.
- D. Teflon beakers were opened to check whether samples were dissolved completely. If samples were not totally dissolved, the steps of B and C would be repeated. Once samples were completely dissolved, Teflon beakers were put on the hotplate again to dryness.

### **3). Separation**

- A. Prepare columns. Sr ion exchange columns were removed from Savillex container and rinsed with Millipore Alpha-Q H<sub>2</sub>O. After that 6-7 drops of resin (Dowex AG 50W-X8 cation exchange resin) were added, and then columns were washed with 10 mls of Millipore Alpha-Q H<sub>2</sub>O, 10 mls of 6M HCl and 2 mls of Millipore Alpha-Q H<sub>2</sub>O. Then the columns were preconditioned with 3M HCl.
- B. Prepare for column chemistry. 0.5 mls of 2M HNO<sub>3</sub> were added to each beaker to dissolve the sample. Then the samples (now dissolved in 2M HNO<sub>3</sub>) were transferred to labelled centrifuge tubes (make sure that the samples were transferred clearly) to centrifuge.
- C. Using a pipette place 1 ml of the solution from each centrifuge tube onto a column. Then Add 0.5mls of 2M HNO<sub>3</sub>, 2mls of 7M HNO<sub>3</sub> and 3 drops 2M HNO<sub>3</sub> to elute. At the same time, rinse the original Teflon beakers with Millipore Alpha-Q H<sub>2</sub>O, add 6M HCl and put them on the hotplate, then rinse them again with Millipore Alpha-Q H<sub>2</sub>O and put them again on the hotplate to dryness.
- D. When the eluting stage is finished, put the original Teflon beakers under the

corresponding columns, add 1 ml 8M HCL in each column and collect this 1 ml which contain the Sr-rich portion of the solution into clean Savillex bakens, and then put the beakers on the hotplate to dryness.

### **3.5.5 Relevant literature review**

Some strontium isotopic analyses have been carried out on ancient glasses during the past two decades. Moreover, the Sr isotopic analysis has been proved to be useful in the glass studies to discuss the issues of their raw materials and provenance.

The study on ancient glass by Sr isotopic analysis was carried out firstly by Wedepohl and Baumann (2000). This was a pilot work to prove how the  $^{87}\text{Sr}/^{86}\text{Sr}$  isotopic signatures and the concentrations of Sr could be used to identify the raw materials of glass making. They found that strontium concentrations in glass mainly came from the lime-bearing constituents of the raw material. They also inferred that the relatively high strontium concentrations (approx.350-500ppm) and their isotopic composition (approx. 0.70918) in the analysed Roman glasses indicated the general use of shells as raw material. Whereas, a much lower Sr concentration in the glass (approx.100-200ppm) could infer the limestone was used as raw material for glass making.

Freestone et al. (2003) determined the  $^{87}\text{Sr}/^{86}\text{Sr}$  ratios of glasses from four production sites in the Eastern Mediterranean region. They stated that (1) two glass groups from Israel, which are believed to made by the mixtures of Levantine coastal sands and natron, have  $^{87}\text{Sr}/^{86}\text{Sr}$  ratios close to 0.7090 and high elemental strontium. This suggests a high concentration of modern marine shell ( $^{87}\text{Sr}/^{86}\text{Sr}$  ratios  $\approx$ 0.7092) in the raw materials. Moreover, this conclusion is in accordance with that of Wedepohl and Baumann (2000) mentioned above. (2) Natron-based glasses, from a workshop in Middle Egypt, have

$^{87}\text{Sr}/^{86}\text{Sr}$  ratios in the range of 0.70794–0.70798, and low elemental strontium (approx.100-200ppm). This Sr isotope composition characterization is consistent with the use of limestone or limestone-rich sand. (3) The high-magnesia plant ash glasses from Israel have  $^{87}\text{Sr}/^{86}\text{Sr}$  ratios in the range of 0.70772–0.70780 and high contents of Sr around 400ppm. The  $^{87}\text{Sr}/^{86}\text{Sr}$  ratios of plant ash glasses reflect the underlying geology on which the plant used to make plant ash grew. This study proved that the strontium isotope compositions of glasses are potential to identify both the raw materials and the origins of ancient glasses.

Henderson et al. (2005a) was the first study to compare the Sr isotopic compositions of glass samples (4 natron and 7 plant ash glass samples) with those of glass raw materials (2 quartz pebble and 2 plant samples) collected near the glass-making factory site (8th–9th century) at Al-Raqqa, Syria. They found that the Sr isotopic compositions of the quartz pebbles are too low to influence the Sr isotopic composition of glass. The  $^{87}\text{Sr}/^{86}\text{Sr}$  ratios of 2 plant samples are basically same as those of plant ash glass samples. They also found that the Sr isotope compositions can separate the two main glass types successfully. The strontium concentrations of natron glass are basically in the range 385-409 ppm, and  $^{87}\text{Sr}/^{86}\text{Sr}$  ratios are in the range of 0.7092-0.7088, whereas the plant ash glass has a much wider range of Sr concentrations associated with a similar isotopic ratio range (0.7079–0.7084). Strontium concentrations in plant ash glasses often show a considerable range, because the Sr content in the plant ash depends upon the original water content of the plant and the concentrating effect of ashing the plant. This study proved that strontium isotope analysis is useful in distinguishing the sources of raw materials used for making glass.

Degryse et al. (2010) measured the  $^{87}\text{Sr}/^{86}\text{Sr}$  compositions of several plant species and rocks growing on different bedrock types. This study shows that the  $^{87}\text{Sr}/^{86}\text{Sr}$  compositional variations in plant and plant ash are not only determined by local geology, but also by plant species and by the small-scale hydrology from which the plant takes the water consumption. Their research was carried out in an area of very high rainfall. Thus the conclusions may not be valid in all cases such as the semi-desert Middle Eastern environment.

Brems et al. (2013) analysed the Sr isotopic compositions of 77 beach sand samples collected from the coasts of Spain, France and Italy by inductively coupled plasma-optical emission spectrometry (ICP-OES) technique. The results show that these beach sand samples have a wide range of  $^{87}\text{Sr}/^{86}\text{Sr}$  isotope ratios between 0.7075 and 0.7290 and a large variation of Sr concentrations from 30 to 1186ppm. The Sr isotope compositions of these beach sands were then discussed together with their chemical compositions and geological provenances, and compared to the Sr isotope compositions of Roman natron glasses. By this, the question of how the different raw materials contribute to the final Sr isotopic composition of Roman natron glass was determined. The results show that besides the main source of lime in the glass, the Sr isotope ratio in natron glass also is influenced by the silicate fraction of the sand sometimes. In the western Mediterranean, the silicate part of the sand often has high radiogenic Sr concentration, resulting in higher  $^{87}\text{Sr}/^{86}\text{Sr}$  ratios. This might influence the final Sr isotope ratios of glasses made by the sands from the Western Mediterranean. For the sands from the eastern Mediterranean, which are non-carbonate Nile sediments, they have low Sr concentration and their Sr isotopic signature lies around or slightly below that of modern-day seawater. Therefore, for glasses produced by the sands from the eastern Mediterranean, the sands have little contribution to the final Sr isotopic signatures of glasses.

All these studies mentioned above have already demonstrated that strontium isotopic compositions are useful to identify the calcium-rich raw materials associated with sands and fluxes used in ancient glass making. Because the techniques of glass and glaze production are closely linked with each other, Ma and Henderson et al. (2013) was the first work to apply Sr isotope analysis in the study on Chinese high fired ceramic glazes. They determined the strontium isotope compositions of two major ceramic glaze types in Southern China-plant ash glaze from the Yue kilns and limestone glaze from the Jingdezhen kilns. They demonstrated that the Sr isotopic characteristics of limestone glaze and plant ash glaze are completely different. Limestone glaze is characterised by low Sr concentrations (<100 ppm), large  $^{87}\text{Sr}/^{86}\text{Sr}$  ratio variation, and a two-component mixing line. Whereas the ash glaze samples are characterised by a consistent  $^{87}\text{Sr}/^{86}\text{Sr}$  ratio and high Sr concentrations with a large variation, ranging from 100ppm to 400ppm. The differences between the two Sr composition patterns of these two kinds of glazes are mainly due to the different fluxes used in their recipes.

Ma et al. (2016) analysed the Sr isotope compositions of glazes of 'Blanc De Chine' porcelain and blue-and-white porcelain from the Dehua kilns, as well as blue-and-white porcelain from the Taipo kilns in order to investigate the Sr isotope compositions in Southern Chinese glazes. In this study, they found that the strontium to calcium ratio of glaze is also a useful way to explain the raw materials used to make glazes, in the cases that only by using the Sr concentration and  $^{87}\text{Sr}/^{86}\text{Sr}$  ratio of glaze, one cannot be sure whether the plant ash or limestone was used as the flux. They infer that, if the strontium to calcium ratios ( $\text{Sr}\times 10^3/\text{Ca}$ ) of glaze is around 0.71, the limestone might be used as the flux in the glaze, because Turekian and Kulp (1956) reported the strontium to calcium ratios ( $\text{Sr}\times 10^3/\text{Ca}$ ) of over 100 limestones sampled worldwide, showing the average  $\text{Sr}\times 10^3/\text{Ca}$  of them being 0.71. While the average  $\text{Sr}\times 10^3/\text{Ca}$  ratios of 25 plant ashes



analysed by Barkoudah and Henderson (2006) show a high level of 9.6 and the  $\text{Sr} \times 10^3/\text{Ca}$  values in soils are around 10 analysed by Capo et al. (1998). When the  $^{87}\text{Sr}/^{86}\text{Sr}$  ratios, Sr isotope concentrations and strontium to calcium ratios were considered together, the glaze recipes of the 'Blanc De Chine' porcelain and blue-and-white porcelain from the Dehua kilns, and the blue-and-white porcelain from the Taipo kilns can be determined separately.

# **Chapter 4 Chemical and lead isotopic analysis of lead glazes from Northern China and the Middle East, 7th-14th centuries AD**

## **4.1 Introduction**

High lead glazes have been widely used in ancient China and the Middle East. Chinese Tang Sancai lead glaze and Islamic splashed lead glaze have important roles in the lead-glaze making history of China and the Middle East respectively. Besides, the export Tang Sancai wares traded by the Maritime Silk Route have been found in many Islamic countries such as Egypt, Iraq, Iran and Uzbekistan. Tang Sancai ceramics have been proven to stimulate the development of Islamic splashed lead glaze to some extent (Lane 1947, 12; Mason and Tite 1997; Needham 2004, 732-733; Watson 2004, 47). In this chapter, the Chinese Tang Sancai glazes from two important glaze production kilns and two Tang dynasty tombs and Islamic splashed lead glazes from Syria and Iraq are analysed by major, trace element composition analyses and Pb isotope analysis. The lead glazing techniques of them are discussed by major chemical compositions, the provenance of their raw materials are discussed by trace element compositions and Pb isotope signatures. Besides, the origin of lead-glazed wares and the interactions between different ceramic production centres also are discussed.

## **4.2 Samples**

### **4.2.1 Tang Sancai glaze samples from Northern China**

Ten Tang Sancai sherds (HPK-1, HPK-2, HPK-3, HPK-4, HPK-5, HPK-6, HPK-7, HPK-8, HPK-9 and HPK-10) excavated from the Huangpu Kiln, Tongchuan City in Shaanxi

Province were supplied by the Department of Cultural Heritage, the Northwest University, China. Ten Tang Sancai sherds (HYK-1, HYK-2, HYK-5, HYK-7, HYK-8, HYK-9, HYK-10, HYK-11, HYK-13 and HYK-18) unearthed from the Huangye Kiln, Gongyi City in Henan Province were offered by Luoyang Institute of Archaeology, China. All Tang Sancai samples from the Huangpu Kiln and Huangye Kiln are dated to the Tang dynasty (AD618-907). Eight Tang Sancai sherds (NKZ-1, NKZ-2, NKZ-3, NKZ-4, WL-1, WL-2, WL-3 and WL-4) excavated from two Tang tombs-Chengnankeyunzhan Tang tomb (hereinafter referred to as NKZ tomb) and Weilaichubanshe Tang tomb (hereinafter referred to as WL tomb) in Xi'an City, Shaanxi province were provided by Xi'an City Institute of Archaeology, China. The two Tang tombs both are dated to the Prospering period (AD649-756) of Tang Dynasty. The pictures of all these samples are shown in Appendix I-A17.

#### **4.2.2 The Islamic glaze samples from Syria and Iraq**

Two splashed glazed pottery shards (8th-9th centuries AD) excavated from Al-Raqqa in Syria were supplied by Professor Julian Henderson; Sixteen splashed glazed pottery shards excavated from Hira and Kish in Iraq (8th-14th centuries AD) were provided by the Ashmolean Museum, the University of Oxford. The pictures of all these samples are shown in Appendix I A-18.

#### **4.3 Results and discussion of major elemental composition**

The major elemental compositions of Chinese Tang Sancai lead glazes and Islamic glaze samples excavated from several archaeological sites in Syria and Iraq were determined using a JEOL JXA-8200 electron microprobe located in Department of Archaeology, the

University of Nottingham. Each of the reported glaze analyses was determined from an average of at least three points following the methodology described in chapter three.

### 4.3.1 The major elemental compositions of Tang Sancai lead glaze samples

The major elemental compositions of Tang Sancai glaze samples unearthed from the Huangye Kiln (Henan Province), the Huangpu Kiln (Shaanxi Province) and two Tang tombs of Xi'an city (Shaanxi Province) are shown in Table 4.1. The analytical results are given as weight percent in different colours of the glazes

Sample No.	Glaze colour	PbO	SiO <sub>2</sub>	Al <sub>2</sub> O <sub>3</sub>	Na <sub>2</sub> O	K <sub>2</sub> O	CaO	MgO	CuO	FeO	TiO <sub>2</sub>	SnO <sub>2</sub>	MnO	Total
<b>Huangye Kiln, Gongyi City, Henan Province</b>														
HYK-1	green	52.18	36.77	6.17	0.22	0.47	0.65	0.14	2.05	0.39	0.11	b.d.	b.d.	99.15
	white	51.87	38.82	6.37	0.18	0.48	0.48	0.15	0.12	0.28	0.10	b.d.	b.d.	98.85
HYK-2	white	56.36	34.39	5.35	0.17	0.31	1.20	0.12	0.13	0.32	0.03	b.d.	b.d.	98.38
	green	51.14	32.08	7.74	0.28	0.48	1.95	0.33	2.73	1.94	0.24	b.d.	b.d.	98.91
	brown	51.96	30.81	7.74	0.35	0.53	2.08	0.46	0.39	3.00	0.23	b.d.	b.d.	97.55
HYK-5	green	51.72	36.89	5.40	0.23	0.44	1.37	0.13	2.21	0.35	0.15	b.d.	0.02	98.91
	white	48.00	38.57	8.77	0.34	1.15	1.14	0.16	0.72	0.30	0.20	b.d.	0.02	99.37
HYK-7	brown	55.97	33.49	3.25	0.14	0.36	0.99	0.19	0.69	3.42	0.04	b.d.	b.d.	98.54
	green and brown mix	54.50	33.16	4.94	0.21	0.44	1.12	0.24	1.21	2.63	0.13	b.d.	b.d.	98.58
HYK-8	brown	55.35	30.36	6.20	0.21	0.38	2.04	0.42	0.48	2.82	0.16	b.d.	b.d.	98.42
	green	54.53	30.24	7.05	0.26	0.42	1.36	0.26	3.06	0.87	0.20	b.d.	b.d.	98.25
	white	55.14	36.21	5.27	0.14	0.27	0.57	0.09	0.13	0.28	0.03	b.d.	b.d.	98.13
HYK-9	dark brown	53.60	31.60	7.75	0.29	0.50	1.97	0.30	1.06	1.82	0.18	b.d.	0.03	99.10
HYK-10	brown	57.57	31.07	5.94	0.18	0.56	0.95	0.21	0.69	1.09	0.31	0.03	b.d.	98.60
	white and yellow mix	61.58	32.32	3.48	0.03	0.35	0.20	0.13	0.01	0.24	0.13	b.d.	b.d.	98.47
HYK-11	brown	40.03	42.15	9.82	0.24	0.81	1.92	0.51	0.50	2.59	0.37	0.10	b.d.	99.04
	green	40.88	41.78	8.46	0.22	0.63	2.36	0.57	2.39	1.02	0.34	b.d.	b.d.	98.65
HYK-13	green and yellow mix	50.77	36.84	4.15	0.18	0.36	1.24	0.25	1.70	2.10	0.11	b.d.	b.d.	97.70
	brown	48.73	36.87	5.74	0.25	0.50	1.64	0.27	0.22	3.54	0.14	b.d.	b.d.	97.90
HYK-18	brown	49.72	38.42	3.33	0.11	0.23	0.46	0.15	0.06	5.35	0.08	b.d.	0.04	97.95
	green	47.90	37.46	6.88	0.22	0.36	0.45	0.33	3.43	0.63	0.16	b.d.	0.04	97.86

Sample No.	Glaze colour	PbO	SiO <sub>2</sub>	Al <sub>2</sub> O <sub>3</sub>	Na <sub>2</sub> O	K <sub>2</sub> O	CaO	MgO	CuO	FeO	TiO <sub>2</sub>	SnO <sub>2</sub>	MnO	Total
<b>Huangpu Kiln, Tongchuan City, Shaanxi Province</b>														
HPK-1	brown	46.64	39.45	8.59	0.14	0.53	1.01	0.33	0.47	1.60	0.37	0.08	b.d	99.21
	green	47.64	37.88	7.71	0.19	0.50	1.44	0.30	1.46	0.88	0.28	0.28	b.d	98.56
HPK-2	brown	43.76	41.62	8.23	0.17	0.49	0.40	0.30	0.78	2.06	0.34	0.14	b.d	98.29
	green	42.88	41.15	9.57	0.18	0.57	0.44	0.31	1.53	1.25	0.44	0.35	b.d	98.67
HPK-3	brown	39.45	41.68	10.36	0.16	0.85	0.35	0.44	0.15	4.19	0.49	b.d.	b.d	98.12
HPK-4	brown	61.17	29.37	4.02	0.03	0.21	0.18	0.13	0.11	3.78	0.22	0.07	0.02	99.31
HPK-5	green	52.87	35.15	6.85	0.09	0.38	0.68	0.34	1.57	0.90	0.41	0.28	b.d	99.52
	brown	53.82	34.15	6.18	0.05	0.34	0.30	0.24	0.24	4.23	0.37	0.04	b.d	99.96
HPK-6	green	46.79	41.02	5.55	0.10	0.38	0.32	0.36	2.55	0.80	0.29	b.d.	b.d	98.16
HPK-7	green	47.14	40.97	4.28	0.15	0.58	1.18	0.37	2.01	0.76	0.22	b.d.	b.d	97.66
HPK-8	green	49.00	39.05	5.04	0.09	0.27	0.36	0.18	3.03	0.34	0.13	b.d.	b.d	97.49
HPK-9	brown	50.18	35.83	6.35	0.08	0.57	0.55	0.36	0.11	3.51	0.27	0.06	0.02	97.89
HPK-10	green and brown mix	47.19	37.42	6.27	0.16	0.81	0.25	0.28	2.53	1.38	0.30	0.49	b.d	97.08
<b>NKZ tomb, Xi'an City, Shaanxi Province</b>														
NKZ-1	green	48.85	35.78	7.41	0.19	0.59	0.90	0.38	3.70	0.53	0.25	b.d.	b.d	98.58
	dark brown	50.39	34.39	6.10	0.21	0.56	0.97	0.26	1.09	3.12	0.18	b.d.	b.d	97.27
NKZ-2	green	51.26	32.91	6.39	0.19	0.63	0.71	0.27	3.69	2.52	0.32	b.d.	b.d	98.89
	dark brown	54.02	32.00	5.79	0.16	0.53	0.89	0.22	1.19	3.78	0.24	0.08	b.d	98.90
NKZ-3	green and yellow mix	58.45	29.20	5.62	0.18	0.72	1.24	0.19	0.95	2.84	0.26	b.d.	b.d	99.65
NKZ-4	brown	64.34	25.40	4.70	0.06	0.27	1.24	0.14	0.10	3.24	0.18	0.05	b.d	99.72
<b>WL tomb, Xi'an City, Shaanxi Province</b>														
WL-1	dark green	59.88	26.35	5.59	0.10	0.57	1.51	0.63	1.31	1.13	0.31	b.d.	b.d	97.38
WL-2	brown	60.87	29.77	4.38	0.09	0.49	0.27	0.13	0.06	2.23	0.21	b.d.	b.d	98.50
WL-3	green	61.28	27.87	5.16	0.11	0.33	0.42	0.24	1.22	0.43	0.20	b.d.	b.d	97.26
WL-4	brown	48.00	35.98	8.09	0.20	0.73	0.41	0.28	0.19	3.56	0.21	b.d.	b.d	97.65
	white	45.08	41.49	8.28	0.18	0.80	0.50	0.34	0.09	0.39	0.26	b.d.	b.d	97.41

b.d.: Below the detection limits

**Table 4.1 the major elemental compositions of glazes of Tang Sancai samples**

#### 4.3.1.1 The colourants of Tang Sancai glaze

As can be seen from Table 4.1, the dominant colours of Tang Sancai ware samples in this study are green, brown and white. It needs to be pointed that, although cobalt blue decorated shards also were found at the Huangye Sancai kiln and the sites of Yangzhou

City, no Tang Sancai sample with blue colour is included in this study. The green glaze samples have the highest content of copper oxide, ranging from 1.22 wt.% to 3.70 wt.%. This shows that copper oxide has been used as the colouring agent in the green glaze. Most of the brown glazes have relatively high content of iron oxide ranging from 1.09 wt.% to 5.35 wt.%. Besides, the brown glazes could be divided into paler and darker brown variations. The paler brown ones have only a small content of copper oxide (0.06-0.78 wt.%), and the darker brown ones (HYK-9, NKZ-1, NKZ-2) have relatively high contents of copper oxide: 1.06 wt.%, 1.09 wt.% and 1.19 wt.% respectively. This shows that iron oxide had been used as a colouring agent for brown glaze, while the dark brown colour might be caused by the presence of copper and iron oxide together. With regards to the white glazes, the contents of copper oxide and iron oxide both are at the lowest level. The white coloured decoration is actually transparent glaze without adding any colourant. The archaeological reports on Huangye kiln and Huangpu kiln sites demonstrate that white kaolin was the main clay used for Tang Sancai, with lesser uses of loessic clay (Shaanxi Provincial Institute of Archaeology 1992, 15; Sun 2002 3; 10). The white colour shown on Sancai in fact reflects the colour of white kaolin body, which is made from the high alumina (around 30 percent  $\text{Al}_2\text{O}_3$ ) clay, containing low iron oxide less than 2.5%, but relatively high content of titanium dioxide approximately 1% (Tite and Rawson 1988). It needs to be pointed out that there are many intermediate and overlaps in different glaze colours, because in many cases, Tang Sancai wares were splashed with two or three colours and they tended to run and mix together during the process of melting.

#### **4.3.1.2 The glazing techniques of Tang Sancai lead glaze**

As shown in Table 4.1, all glazes have lead oxide as their fluxing agent with the  $\text{PbO}$  contents ranging from 36.45 wt.% to 64.34 wt.%. Besides, they have an average alkali

content ( $\text{Na}_2\text{O}+\text{K}_2\text{O}$ ) of only 0.67 wt.% and average  $\text{Al}_2\text{O}_3$  content of 6.38 wt.%. This is the typical major elemental composition of lead glazes.

By the discussion of Tite et al. (1998), there are several primary methods by which the transparent high lead glazes can be produced. The first method is that the lead compound such as black litharge ( $\text{PbO}$ ), galena ( $\text{PbS}$ ), red lead ( $\text{Pb}_3\text{O}_4$ ) or white lead ( $2\text{PbCO}_3 \cdot \text{Pb}(\text{OH})_2$ ) is applied by itself to the surface of the pottery body as a suspension in water. In the second method, the mixture of lead oxide with silica in the form of quartz sand, ground quartz, chert pebbles or clay is applied. The third method is characterised by pre-fritting the lead compound and silica together and then grinding the frit to powder to be applied. Within each method, a small amount of clay might be added in the glaze suspension.

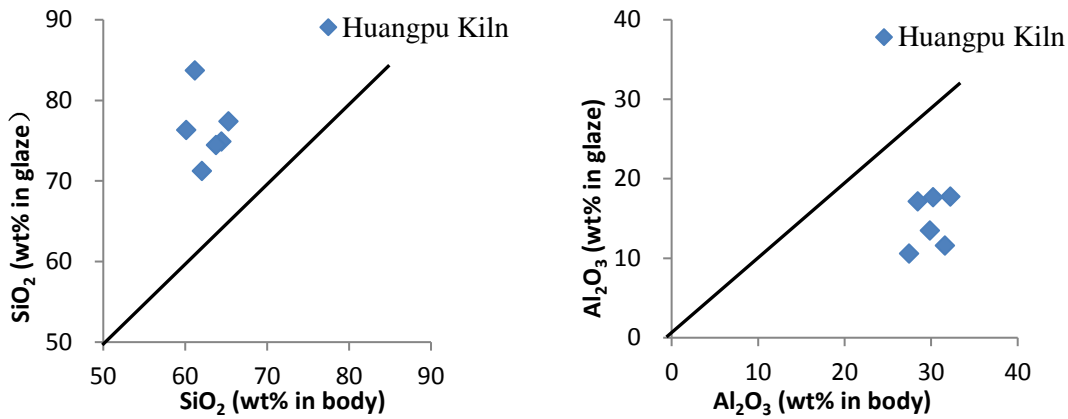
On the basis of previous studies (Hurst and Freestone 1996, Tite et al. 1998, Walton and Tite 2010), it has been proven that the interaction between the glaze and body might provide evidence for the glazing techniques used. The interaction characteristics could be identified by a comparison of the body and glaze chemical compositions. To be specific, if the lead compound itself is applied to the surface of the ceramic body, the lead diffuses into the body during firing and reacts with the body to form a glaze. In this way, the silica and alumina contents in the glaze composition are actually from the body. This suggests that if the contents of lead oxide and any intentionally added colourant (e.g., copper oxide) are subtracted from the glaze composition, and then renormalised it to 100%, the adjusted glaze and body compositions should be similar. Otherwise, if the mixture of lead oxide and silica is applied, the lead and silica would react together with the body during the glazing process. By this, some components of body such as aluminium, calcium, iron and alkalis would diffuse and react with the glaze. It means that the silica content of the recast

glaze should be higher than that of the body, while the alumina and other oxide contents should be lower. It also needs to be pointed out that if the lead compound is mixed with the body clay itself to make the glaze suspension, then the adjusted glaze composition would again tend to match the composition of the body (Walton and Tite 2010). Therefore, by the adjusted glaze composition, we could infer that for the Tang Sancai lead glazes, whether a lead compound is used by itself or a mixture of a lead compound with silica is applied to the ceramic body.

#### **A. The glazing techniques of Tang Sancai glaze produced in the Huangpu Kiln**

To discuss the glazing techniques, the major elemental compositions of the body of six Tang Sancai fragments (HPK-1, HPK-2 HPK-3, HPK-4, HPK-5 and HPK-6) have been analysed in this study by JEOL JXA-8200 electron microprobe. The major elemental compositions of both body and adjusted glaze compositions of these six Tang Sancai shards are given in the Appendix I Table A8. By these compositional data, the plots of the adjusted compositions of Huangpu kiln glazes versus their corresponding body compositions for the contents of silica and alumina are shown in Figures 4.1a and 4.1b. All the adjusted silica contents of Tang Sancai glazes are higher than those of their ceramic bodies, while the alumina contents of glazes are lower than those of their bodies. It suggests that a mixture of lead oxide with silica was used to make Huangpu kiln lead glaze.





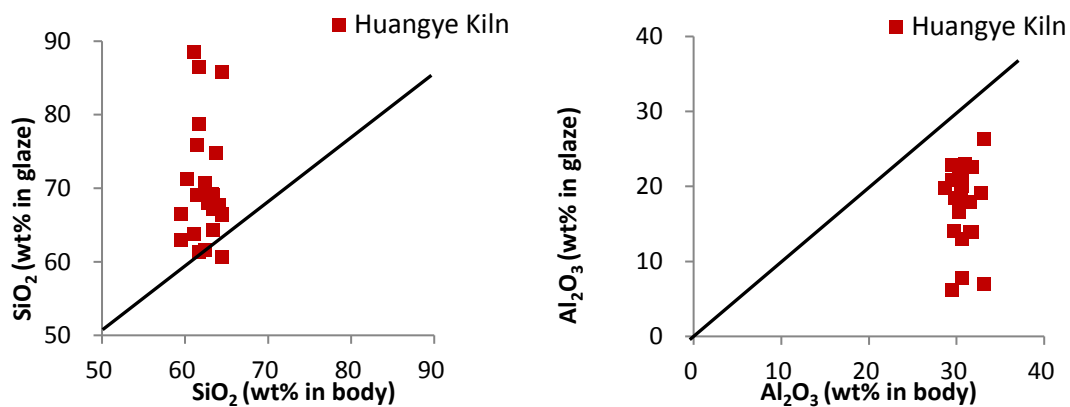
**Figs 4.1a and 4.1b the plots of glaze compositions adjusted by removing the contents of PbO and CuO, versus corresponding body compositions for Tang Sancai glazes produced in Huangpu Kiln**

Furthermore, as seen in Table 4.1, the glazes produced in the Huangpu kiln have a certain amount of alumina with an average content of 6.84 wt.%. Some previous studies (Molera et al. 1997; Tite et al. 1998; Walton and Tite 2010) have shown that when a lead compound with silica mixture is applied, a small amount of alumina from the body would be diffused into the glaze. However, the high content of alumina found in Huangpu kiln glazes infers that, in this case, the alumina might be added to the glaze suspension deliberately in the form of clay.

### **B. The glazing techniques of Tang Sancai glaze produced in the Huangye Kiln**

The major elemental compositions of both glaze and body of Tang Sancai wares were determined by Dong et al. (2008) and are given in the Appendix I Table A9. By these compositional data, the plot of the adjusted glaze compositions for Huangye kiln Tang Sancai glazes versus the corresponding body compositions for the contents of silica and alumina is shown in the Figures 4.2a and 4.2b. It shows that the adjusted silica contents of most Tang Sancai glazes produced in Huangye kiln are higher than those of their ceramic bodies, while the alumina contents of these glazes are lower than those of their bodies. This suggests that a lead oxide with silica glazing mixture was also used in Huangye kiln.

The adjusted silica contents of three samples (HY01-brown, HY04-brown and HY06-brown) are a little lower or similar with those of their ceramic bodies. However, for the other colours of these three samples, the adjusted silica contents of HY01-white, HY01-green, HY04-white, HY04-blue and HY06-green are higher than those of their ceramic bodies. It also can be found that, for samples of HY01-brown, HY04-brown and HY06-brown, they have high contents of iron as their colourants, the adjusted iron contents of them are 10.36%, 8.25% and 6.87% respectively. Therefore, it can be inferred that, the reason for the lower adjusted silica contents of glazes of HY01-brown, HY04-brown and HY06-brown might be that the relatively high iron oxide contents of them were not removed when their glaze compositions were adjusted. This suggests that a lead oxide with silica glazing mixture was also used in these three samples. Besides, the high content of alumina (6.18 wt.% on average in this study- see Table 4.1) found in Huangye Kiln glazes infers that the clay with alumina content might also have been added deliberately to the glaze suspension.



**Figs 4.2a and 4.2b the plots of glaze compositions, adjusted by removing the contents of PbO and CuO, versus body compositions for lead-glazed pottery produced in Huangye Kiln**

### 4.3.2 The major chemical compositions of lead glazes from the Middle

#### East (Syria and Iraq)

The major elemental compositions of Islamic glaze samples excavated from Al-Raqqa sites in Syria, and Kish or Hira sites in Iraq are shown in Table 4.2. The analytical results are given as weight percent in different colours of the glazes.

Sample NO.and Glaze Colour	SiO <sub>2</sub>	Al <sub>2</sub> O <sub>3</sub>	PbO	Na <sub>2</sub> O	K <sub>2</sub> O	CaO	MgO	CuO	FeO	Sb <sub>2</sub> O <sub>5</sub>	MnO	SnO <sub>2</sub>	TiO <sub>2</sub>	ZnO	Total
<b>Al-Raqqa, Syria, 8th-9th Centuries AD</b>															
<b>Syria-4 Green</b>	36.79	1.89	49.91	0.37	0.71	2.48	0.69	2.10	0.86	0.05	0.09	b.d.	0.03	0.77	96.74
<b>Syria-7 green</b>	36.38	1.08	52.16	0.72	0.34	2.25	0.50	3.51	0.13	b.d.	0.74	0.57	0.05	0.01	98.44
<b>Kish-shaal Ghazna, Iraq, 10th-13th Centuries AD</b>															
<b>9913 white</b>	40.05	3.48	46.95	0.78	1.24	3.02	2.10	0.05	0.51	0.05	0.03	0.03	0.25	0.04	98.58
<b>9393 yellow</b>	33.51	3.32	55.37	0.58	1.32	1.62	0.50	0.03	1.83	0.03	0.03	b.d.	0.07	0.02	98.23
<b>9393 green</b>	37.04	3.55	51.25	0.65	1.24	1.62	0.43	2.42	0.78	b.d.	0.06	0.03	0.13	0.23	99.43
<b>9921 yellow</b>	37.19	0.75	53.88	1.07	1.72	1.4	0.44	0.13	1.44	b.d.	0.03	0.15	0.04	0.01	98.25
<b>9921 green</b>	35.03	1.19	54.89	0.99	1.52	1.47	0.40	1.54	0.59	0.08	0.03	0.18	0.09	0.24	98.24
<b>9921 black</b>	31.73	1.13	57.05	0.62	0.69	1.80	0.51	0.83	1.47	b.d.	1.02	0.2	0.10	0.66	97.81
<b>9156 yellow</b>	31.65	3.04	56.35	0.95	1.11	1.53	0.35	0.16	3.85	b.d.	0.01	0.02	0.16	0.04	99.22
<b>9156 green</b>	33.92	1.81	57.85	0.73	0.91	1.66	0.47	1.51	0.55	b.d.	0.03	0.07	0.05	0.21	99.77
<b>9156 white</b>	34.46	0.95	59.95	0.56	0.62	1.74	0.55	0.02	0.66	0.04	0.09	0.10	0.07	0.03	99.84
<b>9161 green</b>	29.29	1.36	64.35	0.09	0.12	1.06	0.23	1.24	0.43	b.d.	0.01	1.33	0.12	0.15	99.78
<b>9161 white</b>	26.99	0.89	68.46	0.01	0.06	0.90	0.28	0.15	0.35	b.d.	0.31	1.09	0.11	0.03	99.63
<b>9147 yellow</b>	24.82	2.25	64.79	0.15	0.21	1.37	0.33	0.35	2.90	0.03	0.01	0.04	0.15	0.04	97.44
<b>9147 green</b>	24.83	2.27	65.26	0.12	0.17	1.37	0.37	1.09	2.58	b.d.	0.02	0.03	0.10	0.10	98.31
<b>9159 brown</b>	28.80	2.98	59.88	0.59	0.72	1.84	0.58	0.17	2.75	b.d.	1.13	0.21	0.16	0.05	99.86
<b>9159 white</b>	32.95	2.83	58.84	0.77	1.07	1.41	0.44	0.05	0.62	0.11	0.05	0.23	0.16	0.06	99.59
<b>9159 yellow</b>	30.41	4.77	56.47	1.02	1.2	0.98	0.3	0.18	4.08	b.d.	0.01	0.15	0.19	0.01	99.77

Sample NO.and Glaze Colour	SiO <sub>2</sub>	Al <sub>2</sub> O <sub>3</sub>	PbO	Na <sub>2</sub> O	K <sub>2</sub> O	CaO	MgO	CuO	FeO	Sb <sub>2</sub> O <sub>5</sub>	MnO	SnO <sub>2</sub>	TiO <sub>2</sub>	ZnO	Total
<b>9915 white</b>	33.72	3.94	56.87	0.58	1.10	1.52	0.37	0.07	0.53	b.d.	0.01	0.34	0.13	0.02	99.20
<b>9915 brown</b>	32.96	4.61	49.83	0.48	0.78	2.93	1.72	0.13	3.15	0.02	1.02	0.34	0.28	0.05	98.30
<b>9915 green</b>	43.10	3.91	39.40	1.44	3.36	2.48	0.51	1.89	0.73	b.d.	0.02	0.39	0.16	0.76	98.15
<b>9162 brown</b>	29.50	2.17	59.87	1.07	1.14	1.45	0.46	0.48	0.74	0.18	2.18	0.01	0.19	b.d.	99.44
<b>9162 green</b>	29.58	2.37	60.15	1.17	1.14	1.62	0.49	1.48	0.85	0.21	0.02.	0.06	0.24	0.16	99.52
<b>9160 green</b>	28.97	3.18	57.94	0.76	0.93	2.37	0.79	1.01	1.35	b.d.	0.12	0.39	0.18	0.2	98.19
<b>9160 brown</b>	33.03	4.70	48.71	1.32	1.90	2.53	0.81	0.32	3.91	b.d.	1.06	0.37	0.28	0.06	99.00
<b>Kish or Hira, 8th-14th Centuries, maybe later than 10th Century</b>															
<b>9312 green</b>	27.2	0.99	64.97	0.41	0.47	1.39	0.23	1.53	0.65	b.d.	0.02	b.d.	0.04	0.32	98.22
<b>9309 yellow</b>	27.35	1.62	62.21	0.36	0.38	1.51	0.46	0.12	3.31	b.d.	0.03	0.42	0.06	0.08	97.91
<b>9309 green</b>	29.69	4.22	55.67	0.20	0.38	1.04	0.23	3.90	0.43	0.03	0.03	0.05	0.17	0.68	96.72
<b>9308 brown</b>	28.31	2.22	62.87	0.47	0.54	1.06	0.17	0.05	1.95	0.03	1.55	b.d.	0.12	0.01	99.35
<b>9308 yellow</b>	28.63	2.46	63.54	0.58	0.70	0.98	0.22	0.03	1.22	b.d.	0.03	b.d.	0.13	0.06	98.58
<b>9808 green</b>	30.24	2.71	60.35	0.81	0.96	1.15	0.24	1.86	0.40	0.02	0.01	0.03	0.13	0.38	99.29
<b>9798 green</b>	40.28	1.10	44.70	2.11	1.51	3.11	1.33	2.54	0.65	b.d.	0.10	0.31	0.08	0.38	98.20
<b>9800 green</b>	35.91	1.13	51.82	2.18	1.02	2.43	0.92	1.32	0.69	b.d.	0.21	1.39	0.11	0.19	99.32
<b>9800 brown</b>	33.42	1.00	52.02	1.42	0.78	2.19	0.75	0.75	0.72	b.d.	2.39	1.85	0.10	0.08	97.47
<b>9807 green</b>	28.12	2.03	59.98	0.76	0.84	1.66	0.47	3.58	0.57	0.18	0.01	0.04	0.11	0.55	98.90

b.d.: Below the detection limits

**Table 4.2 The major elemental compositions of Islamic glazes from Syria and Iraq samples**

#### 4.3.2.1 The colourants of Islamic splashed glaze excavated in Syria and Iraq

The dominant colours used in the decoration of Islamic splashed high lead glazes are green, brown, yellow, white, black and blue. In this case, the green, brown, yellow and white glaze colours are included to determine their colourants. The green coloured glazes have a relatively high content of copper oxide of between 1.01 wt.% and 3.90 wt.%, suggesting that they were coloured by copper oxide. In addition, as seen in Table 4.2, all

the glaze samples with green colours also have relatively higher content of zinc oxide than other coloured glazes. This suggests that copper oxide might be sourced from the oxidise brass. Jābir ibn Ḥayyān, who lived during the Abbasid Caliphate, mentioned that oxidise brass which is a kind of copper compound was used as a glass colourant. And glass and ceramics are close to each other and they have common techniques in pigments and in the methods of colouring (Al-Hassan 2009). All the yellow coloured glazes have relatively high contents of iron oxide ranging from 1.22 wt% to 4.08 wt%. This suggests that iron oxide was used as the main colourant in yellow glazes. For the brown glazes, both high iron contents (0.72-3.91 wt.%) and manganese contents (1.02-2.39 wt.%) are found, suggesting that they are used as the colourants together for the brown glazes. Only one black coloured glaze is included in this case, which has both high contents of iron and manganese oxide (1.47 wt.% and 1.02 wt.% respectively), suggesting that iron plus manganese colourant might also be used in black glaze. Iron oxide might either come from iron ores such as haematite mineral and goethite, or iron rich 'red earths'. Manganese oxide might derive from manganese ores such as pyrolusite or as a component of the red earth burnt umber (Henshaw 2010, 258). The materials to colour a glaze must be in the form of a very fine powder by crushing, powdering, grinding and sifting. A little amount of fine-powdered colourants were then mixed with the prepared silica and lead compound to make the final glaze suspension (Watson 2004, 29).

Two glazes, 9161 and 9800, have SnO<sub>2</sub> contents above 1wt.%. Tin oxide is the common opacifier used in Islamic glaze recipes (Mason and Tite 1997). Although around 1 wt.% SnO<sub>2</sub> is not sufficient to opacify glaze totally, it is enough to make tin oxide exist as particles within the glaze (Tite 2011). Besides, this relatively high content should be

associated with the deliberate addition of tin oxide to the glaze. Therefore, tin-opacified glazes are defined as those containing greater than 1 wt.% SnO<sub>2</sub> in some studies (Tite 2011). On the basis of this standard, in this case, the samples 9161 and 9800 are tin-opacified glazes, and all the remaining glaze samples are transparent glazes. It needs to be pointed out that, in some Islamic green or yellow coloured glazes from the sites in Egypt and Syria, lead antimonate particles are found to have been added deliberately as the colourant and opacifier (Tite 2011). However, all the glazes, in this case, have low contents of Sb<sub>2</sub>O<sub>3</sub> of less than 0.2 wt.%. Such low Sb<sub>2</sub>O<sub>3</sub> concentration is not sufficient to colour and opaque glaze. It infers that the Sb<sub>2</sub>O<sub>3</sub> concentration in the glazes might be incorporated as an impurity with, for example, a lead ore deposit used as the flux.

#### **4.3.2.2 The glazing techniques of Islamic splashed lead glaze excavated in Syria and Iraq**

As shown in Table 4.2, all the Islamic glaze samples have high PbO contents ranging from 40.14 wt.% to 68.72 wt.%. Besides, almost all the glazes have both low levels of alkali (Na<sub>2</sub>O+K<sub>2</sub>O) and lime (CaO+MgO), which are both below 5 wt.%. All Islamic splash-decorated style glazes in this study show typical high-lead glaze characteristics, which is in accord with the common knowledge that high lead flux is the mainstream method to produce such splash-decorated style glaze.

As mentioned in Section 4.3.1.2, the transparent high lead glazes could be produced by several methods, and by the comparison of their body and glaze chemical compositions, one could infer that whether a lead compound by itself or a lead compound with silica mixture is used to make the glaze. In this section, the glazing techniques of Islamic high lead glaze would be discussed by the same method used in the section 4.3.1.2

A large number of Islamic ceramic sherds collected from Egypt (Fustat and the Cairo region, Qusier, Aswan), Iran (Susa), Iraq (Samarra, Nineveh, Kish, Hira), and Syria (Ma'arrat al Numan, Queiq, Meskene, Raqqa) spanning the period from the 8th to 14th centuries AD have been analysed by Kaczmarczyk when working at the University of Oxford during the 1980s. Either atomic absorption spectroscopy (AAS) or proton-induced X-ray emission (PIXE) were applied to analyse their body compositions, and their glaze compositions were analysed by X-ray fluorescence spectrometry (XRF) operated in air. All these analytical data results are available on the Research Laboratory for Archaeology and the History of Art website, and the preliminary study on these analytical data has been done by Tite (2011). He found that, among these samples, the majority of Islamic high-lead glazes (more than 80%) associated with calcareous clay bodies containing CaO contents above 6 wt.%. In this section, the SiO<sub>2</sub> and Al<sub>2</sub>O<sub>3</sub> contents of ceramic bodies of 20 high lead glazes with calcareous clay bodies collected from Hira and Nineveh in Iraq analysed by Kaczmarczyk will be used to compared with adjusted glaze compositions of our analysed high lead glaze samples unearthed in Syria (Al-Raqqa) and Iraq (Hira or Kish). By this, we could infer the lead glaze techniques used. It needs to be pointed out that the reason we could use these body compositions to do the comparative study here is that the alluvial clays with lack differences in major chemical composition have been proven to have been used for Islamic calcareous clay bodies (Hill et al. 2004).

The body compositions of 20 high lead glaze ceramics samples analysed by Kaczmarczyk and our analysed glaze compositions of 18 high lead glaze ceramic sherds with different colours are given in the Appendix I Tables A10 and A11. For the glaze compositions, the lead oxide and added colourant have been removed. Both the compositions of body and glaze are composed of SiO<sub>2</sub>, Al<sub>2</sub>O<sub>3</sub>, CaO, MgO, Na<sub>2</sub>O, K<sub>2</sub>O, FeO, TiO<sub>2</sub> and MnO<sub>2</sub> and renormalised to 100%. The contents of SiO<sub>2</sub> versus Al<sub>2</sub>O<sub>3</sub> of both the body and glaze

compositions mentioned above have been plotted in Figure 4.3.

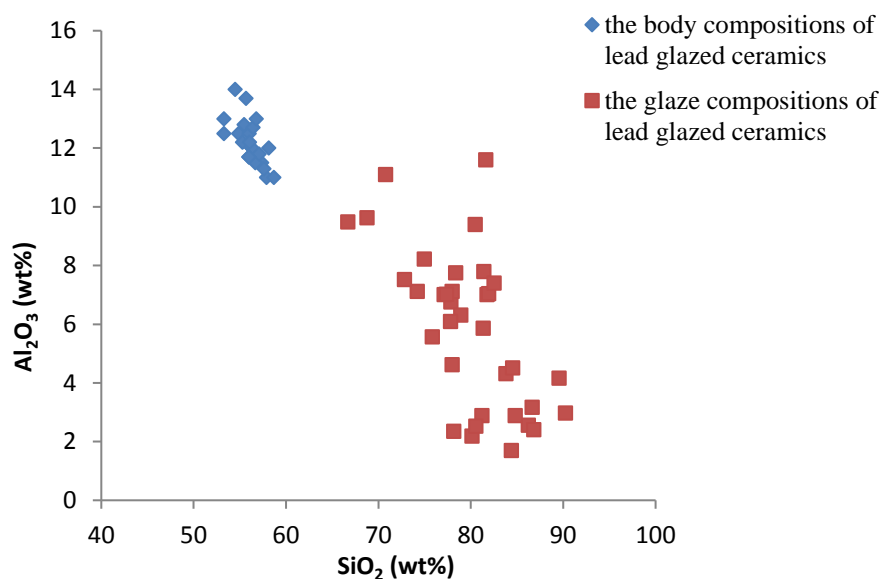


**Fig.4.3 the plot of the contents of SiO<sub>2</sub> versus Al<sub>2</sub>O<sub>3</sub> of the body and glaze compositions of Islamic lead glazed ceramic sherds**

As seen from Figure 4.3, it is evident that all the adjusted silica contents of Islamic high lead glazes are higher than those of Islamic ceramic bodies, while the alumina contents of glaze are lower than those of Islamic ceramic bodies. This suggests, for all the analysed high lead glaze samples in this study, the mixture of lead oxide with silica was used to produce them rather than a powdered lead compound itself was used. Besides, the Al<sub>2</sub>O<sub>3</sub> contents of the Islamic high lead glaze samples in this study range from 0.89 wt.% to 4.70 wt.%, averaging of 2.40 wt.%. The alumina contents of these glazes, in part, may diffusion from the body, and clay may have been added into glaze suspension for those glazes having relatively high Al<sub>2</sub>O<sub>3</sub> content.

### **4.3.3 Comparison of high lead glazes from Northern China and the Middle East**

During the Tang dynasty (AD618-906), Tang imported glazed ceramics traded by



Maritime Silk Route and their techniques have proven to stimulate the changes of early Islamic ceramic techniques to some extent. High lead glazed ceramic-Tang Sancai ware made in North China was one imported Chinese ceramic type which enlightens Islamic potters on applying multiple colours to a pottery's surface often in a semi-haphazard manner (Fleming et al. 1992). A number of Tang Sancai wares and sherds have been found in some Islamic countries such as Fustat in Egypt, Samarra in Iraq, Nishapur in Iran and Samarkand in Uzbekistan (Lane 1947, 12; Needham 2004, 732-733; Watson 2014, 47). The splashed lead glazed wares made in the Middle East starting from around 8th century AD are thought to be probably influenced by imported Tang Sancai wares (Lane 1947, 12; Wood et al. 2009, 154-180; Needham 2004, 732-733; Watson 2004, 47). Hence here a comparison study between Chinese Tang Sancai and Islamic lead glaze is conducted.

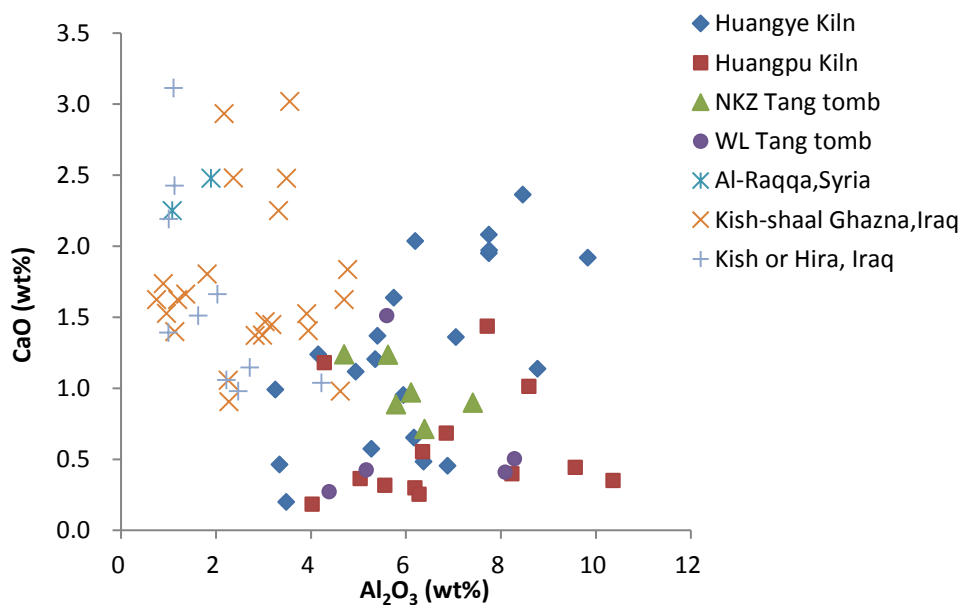


**Fig 4.4 A plot of Al<sub>2</sub>O<sub>3</sub> versus CaO contents of Chinese Tang Sancai glaze samples and Islamic lead glazes excavated in Syria and Iraq**

The main difference between the glazing technique of Chinese Tang Sancai and Islamic lead glaze is that different colourants were used. For the Chinese Tang Sancai glaze, the

iron oxide was used as the colouring agent in the brown glaze, while the iron oxide plus manganese together were used as the colouring agent in the brown colour of Islamic lead glaze. Besides, all Chinese Tang Sancai glazes are transparent, while two Islamic splashed lead glaze samples in this study are found to be tin-opacified, which was used widely by Islamic potters since the second half of the 8th century AD.

As mentioned in Section 4.3.1.2 and 4.3.2.2, both Chinese and Islamic lead glazes analysed in this study have proven to have been produced by a lead-silica mixture. Some replication experiments of high lead glaze production have indicated that the body fabric only makes a minimal contribution to the composition of the glaze due to the sluggish nature of the diffusion from the clay body to glaze when fired (Walton and Tite 2010). Thus the contents of alumina and lime oxide in glaze should mainly represent the raw materials used in fabricating the glaze. As seen in Figure 4.4, the Chinese Tang Sancai lead glazes have higher alumina contents than those of Islamic lead glazes. The high alumina contents (6.36 wt.% on average) found in Tang Sancai glazes infer that the alumina might be added to the glaze suspension deliberately in the form of clay. It is common knowledge that alumina in the glaze recipe is beneficial to the final glazes. On the one hand, it is helpful in controlling the viscosity of the glaze suspension in order to prevent the glaze from being too runny, on the other hand, the alumina is a refractory material which can make the glaze's expansion and contraction coefficient fit better with the ceramic body. Sedimentary secondary clay with a high alumina content was the main raw material of producing ceramic bodies in Northern China. Thus, it is easy for potters to be aware of the benefit of alumina-bearing clay in the glaze recipe during long-time glazed ceramic production. With regards to Islamic lead glazes, they have relatively low  $\text{Al}_2\text{O}_3$  content ranging from 0.75wt.% to 4.77wt.% and averaging on 2.40 wt.%. It

suggests that a part of Islamic lead glazes might be made by adding clay into the glaze suspension. This may also reflect the Islamic potter's selection of suitable raw materials consciously due to a long-time experience.

Based on previous studies, a mixture of lead oxide plus quartz was also found to apply to lead-glaze production in central Italy from the 2nd to 4th centuries AD (Walton and Tite, 2010). Moreover, the application of lead oxide plus quartz/quartz sand can be seen as a natural development from the long-history plant ash glaze production of the Middle East, which using a pre-fritted mixture of plant ash and quartz (Paynter and Tite 2001). Thus, the application of lead-silica mixture in both the lead glaze production of China and the Middle East most probably occurred independently in each region. The Islamic splashed wares mainly attempt to simulate the appearance with multiple splashed colours of Chinese Tang Sancai based on their own lead glazing techniques.

#### **4.4 Trace elemental compositions of Chinese Tang Sancai and Islamic lead glazes from Syria and Iraq**

Using laser ablation inductively coupled plasma mass spectrometry (LA-ICP-MS), trace elemental compositions of Chinese Tang Sancai lead glaze samples and Islamic lead glaze samples excavated in Syria and Iraq were analysed following the methodology described in chapter three. The trace elemental compositions of the tested Chinese and Islamic lead glaze samples are listed in Appendix I Tables A6 and A7. The analytical results are given as ppm by different colours of the glazes.

#### **4.4.1 The trace elements of Chinese Tang Sancai lead glaze samples**

Based on the Goldschmidt's Rule in Geochemistry (Goldschmidt, 1937), all the elements in the periodic table can be divided into four categories: lithophile elements which concentrate in silicate phases; chalcophile/sulfophile elements that concentrate in sulfides; siderophile elements that concentrate in metallic iron; and atmophile elements which naturally occur as gaseous elements such as nitrogen and inert gases. Elements which belong to the same category enrich each other during the process of crust formation, smelting, ore-forming and other geochemical processes, thus have the similar geochemical characteristics. Based on this, all the trace elements in the Tang Sancai glazes measured in this study can be divided into the following three categories: 1) lithophile elements: Li, B, Ti, V, Cr, Rb, Sr, Y, Zr, Nb, Cs, Ba, Hf, Th, U and REE elements; 2) chalcophile elements (sulfophile): Zn, As, Sn and Sb; and 3) siderophile elements: Co and Ni. The Tang Sancai lead glazes made in the Huangpu kiln and Huangye kiln are made with essentially three components: the siliceous raw material (quartz sand/ground quartz as well as clay), the flux (lead compound) and the colorants (copper ore deposits, bronze, brass, ochre or other iron-bearing minerals). Therefore, in light of Goldschmidt's Rule, the contents of lithophile trace elements in Tang Sancai glaze were introduced mainly by the siliceous raw materials of the glaze recipe, and the contents of chalcophile trace elements were mainly introduced by the lead flux and colourants. The trace elements of the glaze samples thus can be divided into subgroups to allow separate discussion of the siliceous raw materials and the lead compound flux.

The chalcophile elements, Zn, As, Sn, and Sb, are common accompanying elements of lead ore deposits. In addition, the copper-bearing and iron-bearing colourant components

of green and brown coloured glaze might also contribute certain concentrations of Zn, As, Sn, and Sb. The primary question to be asked is therefore whether the lead compound or the colourant component is the one dominating the concentrations of Zn, As, Sn, and Sb in the glaze. As mentioned previously, iron oxide was used as a colourant for the general brown glaze, while the dark brown colour is more likely to be caused by the presence of copper and iron oxide together, and the green glaze was coloured with copper oxide. The absolute amounts of Zn and the Zn/As ratios (Figure 4.5) of the glazes show that almost all green and dark brown coloured glazes have evidently higher Zn concentrations than those of brown glazes. In addition, analysis of the trace elemental concentrations of both green and brown coloured areas of glaze samples HYK-11, HPK-2, HPK-5, and NKZ-2 showed that their green coloured areas had evidently higher Zn concentrations than those of the brown coloured areas. These results indicate that, for the green and dark brown coloured glazes, the Zn concentrations are mainly contributed by the copper-bearing colourant component, which may be copper ore deposits with impurities of either zinc or brass.

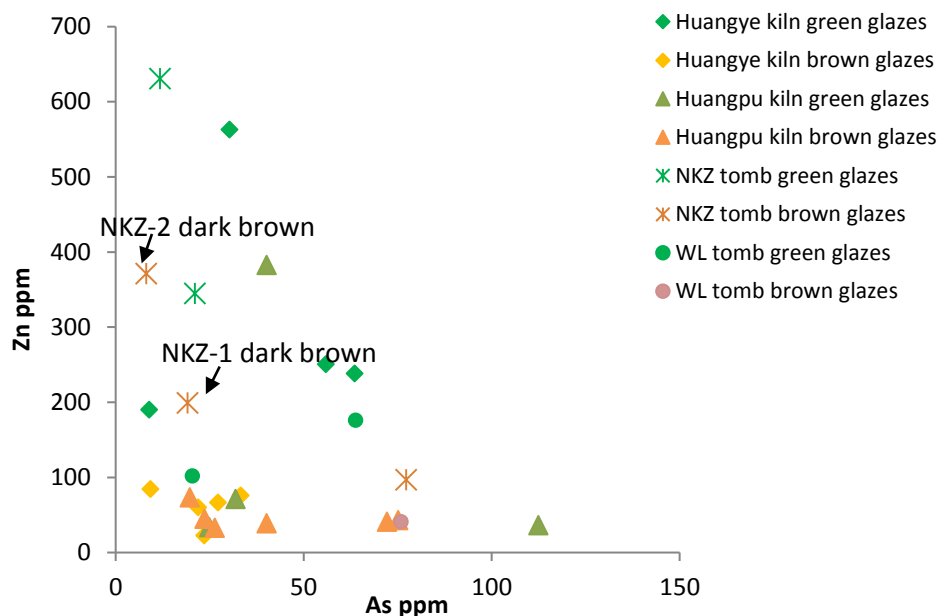


**Fig 4.5 the plot of As (ppm) versus Zn (ppm) of Tang Sancai glaze samples from the Huangye kiln, the Huangpu kiln and two Tang tombs (the NKZ Tang tomb and the WL Tang tomb)**

No similar distinction can be identified among different glaze colours in terms of the concentrations of As, Sn, and Sb in the glazes, and different coloured areas of the same glaze sample have similar concentrations of As, Sn and Sb. This indicates that the concentrations of elements As, Sn, and Sb are mainly affected by the lead compound flux. The Sn/Sb ratios of Tang Sancai lead glazes in this study are shown in Figure 4.6. Huangpu kiln glazes have obviously higher concentration levels of elements Sb and Sn than the Huangye kiln glazes and the glazes excavated from the two Tang tomb sites, yet no distinction in terms of lead oxide content can be identified between the Huangpu kiln glazes and the glazes excavated in the Huangye kiln and two Tang tomb sites. The lead compound used in lead glaze production is extracted and refined from lead sulphide minerals or lead oxide minerals. This suggests that, compared to the source of lead compound used in the Huangye kiln's lead glaze production, the lead ore deposits used to make the Huangpu kiln glazes had higher concentrations of impurities Sb and Sn. In

addition, the relatively low and similar concentrations of Sb and Sn found in the glazes of the NKZ Tang tomb, the WL Tang tomb, and the Huangye kiln suggest that a lead ore deposit with similar geological characteristic was used to produce all of these lead glazes.

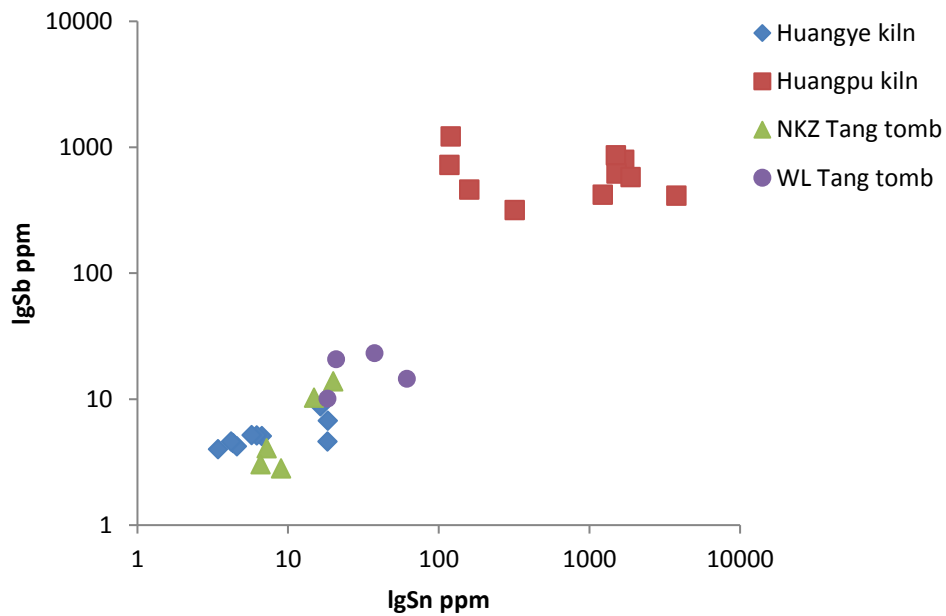


**Fig 4.6 the plot of lgSn (ppm) versus lgSb (ppm) of Tang Sancai glaze samples from the Huangye kiln, the Huangpu kiln and two Tang tombs (the NKZ Tang tomb and the WL Tang tomb)**

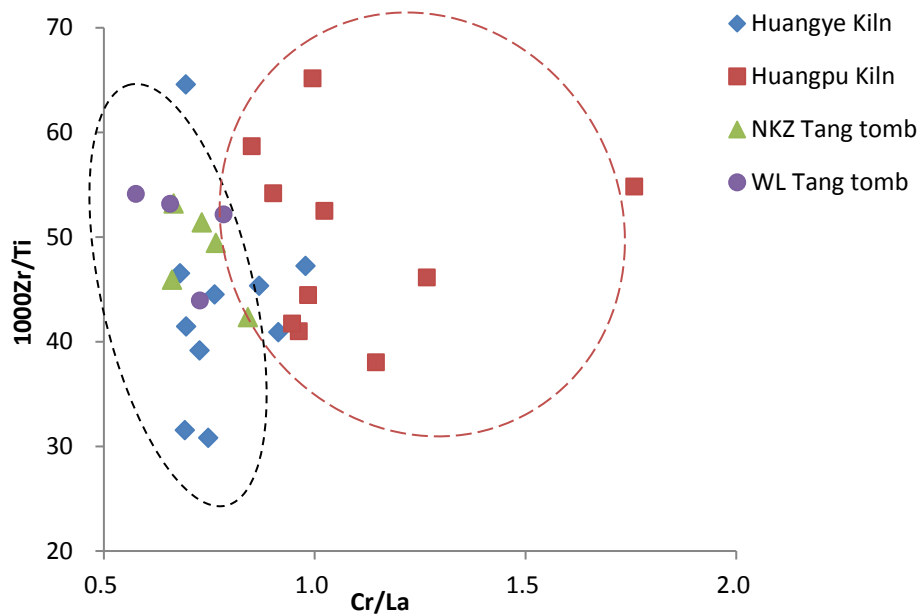


**Fig 4.7** the plot of Cr/La versus 1000Zr/Ti of Tang Sancai glaze samples from the Huangye kiln, the Huangpu kiln and two Tang tombs (the NKZ Tang tomb and the WL Tang tomb)

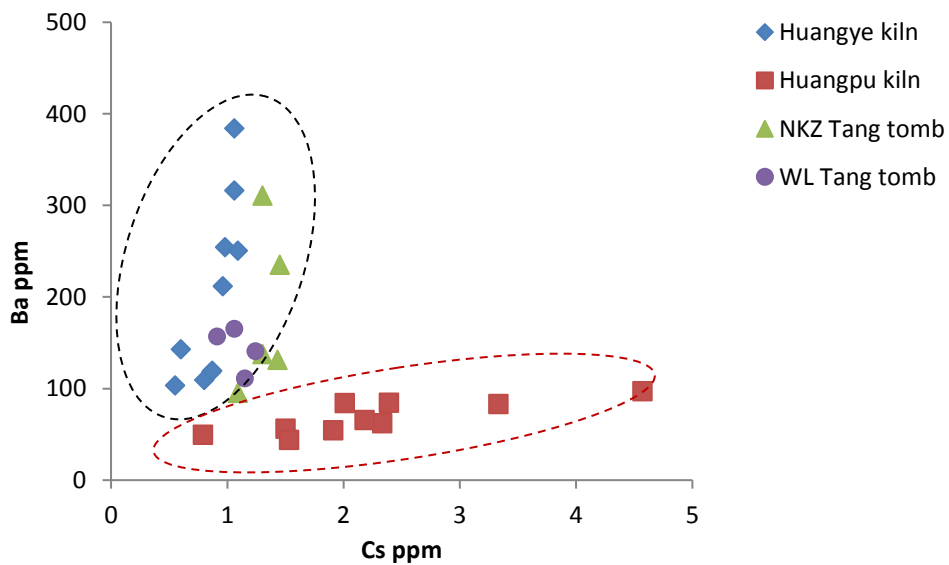


**Fig 4.8** the plot of Cs (ppm) versus Ba (ppm) of Tang Sancai glaze samples from Huangye Kiln, Huangpu Kiln and two Tang tombs (NKZ Tang tomb and WL Tang tomb)

The concentrations of lithophile trace elements in a lead glaze mainly derive from its siliceous raw materials (quartz/sand and clay). It has been proved that some trace



elements have a potential to characterise the siliceous raw materials used for making glasses and ceramic body at different production sites, such as Zr-Ti-Cr-La (Henderson et al., 2016; Shortland et al., 2007) and Zr-Ba (Oikonomou et al., 2016). The elements Zr, Ti, Cr, and La are generally related to various minerals such as zircon (Zr), rutile (Ti), ilmenite (Ti), monazite (La), chromite (Cr) and Barite (Ba). Cs can substitute for K in the mica and K-feldspar of minerals. Thus, their concentration varies in a way that reflects the local geology of the sand and clay precursors used to make the glaze (Oikonomou et al., 2016). The ratio plots of Cr/La versus  $1000\text{Zr/Ti}$  and plot of Cs versus Ba of Tang Sancai glaze samples are shown in Figures 4.7 and 4.8. In Figure 4.7, the Huangpu kiln glazes can be seen to be basically grouped separately from the Huangye kiln glazes based on their relatively higher Cr/La ratios. A more obvious distinction between the lead glazes made in these two kilns can be found in the Cs/Ba ratios (Figure 4.8). These indicate that the lead glazes produced in the Huangpu kiln and Huangye kiln were made from different siliceous raw material sources (probably local sand and clay) and that they can thus be discriminated from each other by means of the trace element ratio plots Cr/La versus  $1000\text{Zr/Ti}$  and Cs versus Ba within the glaze. The glazes of the Tang Sancai fragments excavated from the two Tang tomb sites are grouped within the same distribution area as the Huangye kiln glaze samples (Figures 4.7 and 4.8). This indicates that the siliceous raw materials used to produce these glazes might originate from the same geological region.

Both the lead ore deposits and siliceous raw materials used to make the Tang Sancai glaze samples excavated from the NKZ and WL Tang tombs of Xi'an City have similar geological characteristics to those used in Huangye kiln Tang Sancai glaze production.

This is a strong indication that the Tang Sancai wares found in the NKZ and WL Tang tombs were made in the Huangye kiln near Luoyang City and then traded to Xi'an City.

#### 4.4.2 The trace elements of Islamic splashed lead glaze samples excavated in Syria and Iraq

Similar to the trace element results of Tang Sancai glaze samples, the plots of several lithophile trace elements and chalcophile trace elements also are used to discuss the glaze samples of Syria and Iraq.

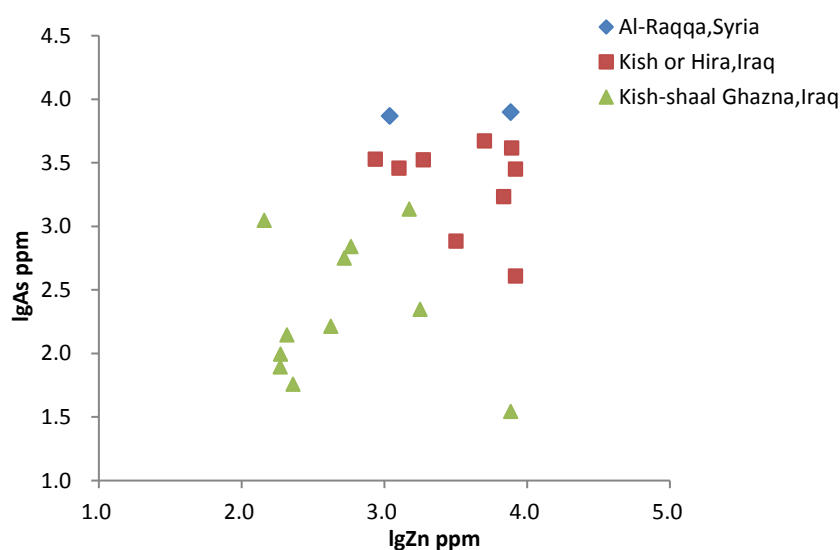


**Fig 4.9** A plot of lgZn versus lgAs of Islamic glazes from the sites in Syria (Al-Raqqa complex) and Iraq (Kish or Hira; Kish-shaal Ghazna site)

As mentioned above, the elements Zn and As both belong to chalcophile elements. The content of As was mainly introduced with the lead compound, and the Zn content seems to correct with copper (copper compound such as brass used as green glaze colourant). As shown in Figure 4.9, the two Al-Raqqa glaze samples have a little higher level of As than those of Iraqi glaze samples from Kish or Hira and Kish-shaal Ghazna site. Also, the

majority of glaze samples of Kish-shaal Ghazna site have lower levels of As than glazes from the two other sites. This may infer that different lead ore sources were used to produce the lead glazes from these three sites. However, because only a limited number of glaze samples from each site was analysed, tentative conclusions can be made here and further research needs to do in future work.

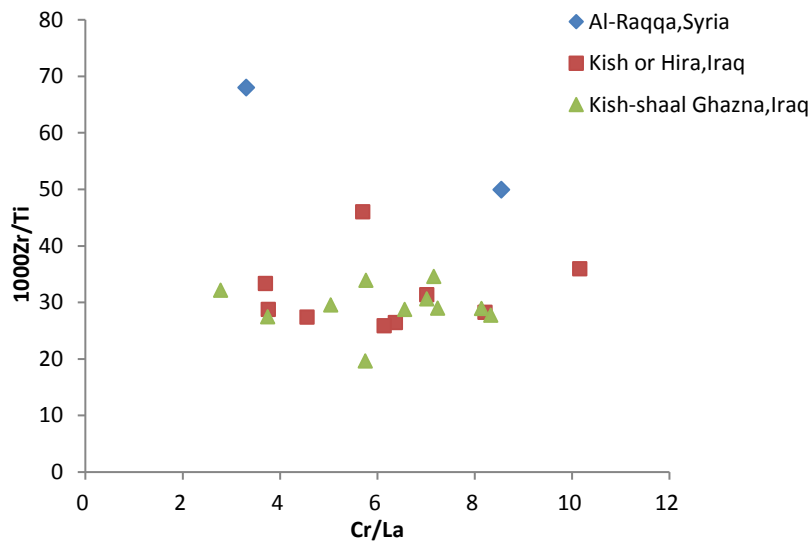


**Fig 4.10 A plot of Cr/La versus 1000Zr/Ti of Islamic glazes from the sites in Syria (Al-Raqqa complex) and Iraq (Kish or Hira; Kish-shaal Ghazna site)**

With regards to the contents of lithophile elements shown in Figure 4.10, the two Al-Raqqa glazes from Syria have a little higher 1000Zr/Ti ratio than those of the Iraqi glaze samples, suggesting different quartz sand sources were used in lead glaze making in Syria and Iraq. For the Iraqi glaze samples, the variation of 1000Zr/Ti ratios and Cr/La ratios appears unable to provide distinction. This suggests that the quartz sands used in these Iraq glazes might have the similar geological characteristic.

### **4.4.3 The trace element compositional comparison of Chinese Tang**

#### **Sancai lead glazes and Islamic lead glazes of Syria and Iraq**

Similar to the major chemical analysis results, the trace element compositions of Chinese

Tang Sancai glazes and Islamic lead glazes are also compared.

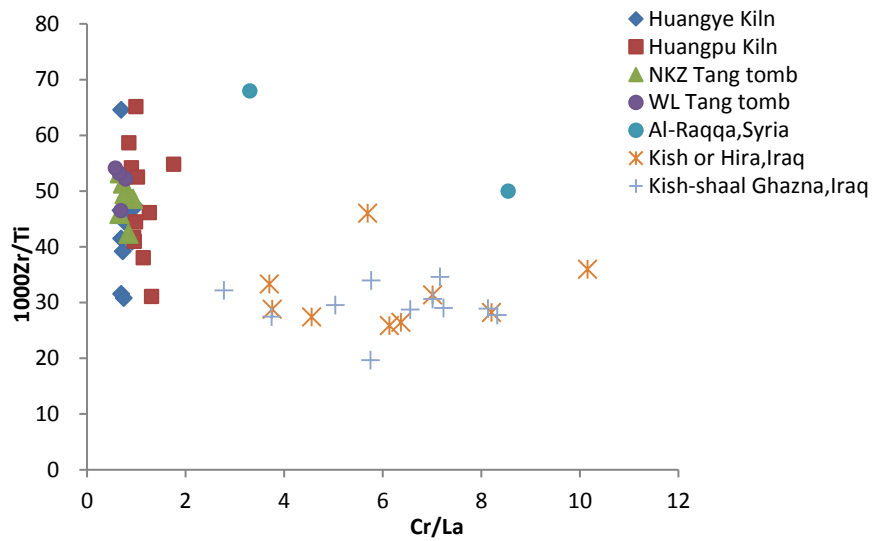


**Fig 4.11 A plot of Cr/La versus 1000Zr/Ti of Chinese Tang Sancai glazes and Islamic lead glazes from Syria and Iraq**

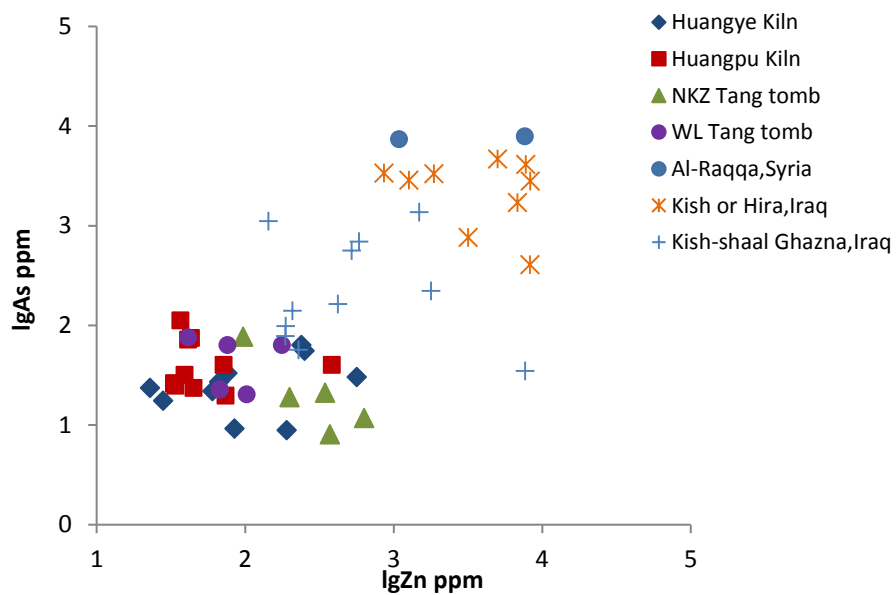


**Fig 4.12 the plot of lgZn versus lgAs of Chinese Tang Sancai glazes and Islamic lead glazes from Syria and Iraq**

In the plot of Cr/La versus 1000Zr/Ti shown in Figure 4.11, the distinction between Chinese Tang Sancai glazes and Islamic lead glazes is clear. The low Cr/La ratios and

highly variable Zr/Ti of Tang Sancai glazes contrast with the low Zr/Ti of the Islamic glazes combined with their variable and higher Cr/La ratios. Zr, Ti, Cr and La are thought to be related to various minerals such as zircon (Zr), rutile (Ti), ilmenite (Ti), monazite (La) and chromite (Cr). Therefore, their concentration variations can reflect the geological characteristics of siliceous raw materials used in glaze production.

From the plot of lgZn versus lgAs shown in Figure 4.12, the distinction of lead compounds used in Chinese Tang Sancai glazes and Islamic glazes of Syria and Iraq can be found. Islamic glazes tend to have both higher contents of Zn and As than in Chinese glazes. It suggests that the lead compound used in Islamic lead glaze making might be extracted from the lead ore with higher content of As as its accompanying elements. And copper compound used as colourant in Islamic lead glaze making has higher content of As as its accompanying elements. From the discussion above, trace element analysis is potentially distinguishing Chinese Tang Sancai glazes from Islamic glazes from Syria and Iraq, and they reflect the geographical and geological variations of raw materials used to make them.

The lead glaze is composed of three parts-siliceous raw material, lead compound and colourant. Although the contents of lithophile elements in glaze were introduced mainly from the siliceous raw material of glaze, a small content of them may derive from the lead compound. Besides, a small part of trace element composition of glaze may diffuse from the clay body, although normally the same clay source should be used in the glaze and its ceramic body. Thus, the multiple components of glaze may weaken the trace element distinctions of the raw materials with different geographical and geological sources used in different production sites. However, the trace element analysis still might be able to be used as a complementary method to distinguish the different sources of raw materials

used in some cases based on the discussion of this case study.

## 4.5 Results and discussion of lead isotope analysis of Chinese Tang Sancai and Islamic glazes from Syria and Iraq

By both LA-MC-ICP-MS and Solution MC-ICP-MS, the lead isotopic ratios of thirteen Chinese Tang Sancai lead glaze samples, and seven Islamic glaze samples excavated in Syria and Iraq were analysed following the methodology described in Chapter three. The lead isotopic ratios ( $^{208}\text{Pb}/^{206}\text{Pb}$ ,  $^{207}\text{Pb}/^{206}\text{Pb}$  and  $^{206}\text{Pb}/^{204}\text{Pb}$ ) of the tested samples are listed in Table 4.3 for Chinese Tang Sancai lead glaze samples and in Table 4.4 for Syria and Iraq lead glaze samples.

Sample No.	Date	Excavated	Produced	$^{208}\text{Pb}/^{206}\text{Pb}$	$^{207}\text{Pb}/^{206}\text{Pb}$	$^{206}\text{Pb}/^{204}\text{Pb}$	Analytical Method
HPK-4 brown	7th-9th Centuries	Huangpu Kiln	Huangpu Kiln	2.201	0.884	17.557	Solution- MC-ICP-MS
HPK-5 green				2.191	0.885	17.526	LA- MC-ICP-MS
HPK-5 brown				2.191	0.885	17.523	LA- MC-ICP-MS
HPK-5 green				2.192	0.884	17.545	Solution- MC-ICP-MS
HPK-6 green				2.176	0.881	17.613	LA- MC-ICP-MS
HPK-8 green				2.175	0.880	17.656	Solution- MC-ICP-MS
HYPK-1 brown				7th-9th Centuries	Huangye Kiln	Huangye Kiln	2.126
HYPK-2 green	2.127	0.864	18.048				LA- MC-ICP-MS
HYPK-3 green	2.129	0.864	18.061				Solution- MC-ICP-MS
HYPK-4 brown	2.127	0.864	18.074				LA- MC-ICP-MS
HYPK-5 green	2.127	0.864	18.076				LA- MC-ICP-MS
HYPK-6 green	2.129	0.864	18.069				Solution- MC-ICP-MS
HYPK-7 brown	2.131	0.865	18.053				Solution- MC-ICP-MS

NKZ-3 green and yellow mix	8th Century	NKZ Tang tomb	unknown	2.128	0.864	18.068	Solution- MC-ICP-MS
NKZ-4 brown			unknown	2.129	0.865	18.058	Solution- MC-ICP-MS
WL-1 green	8th Century	WL Tang tomb	unknown	2.129	0.864	18.066	Solution- MC-ICP-MS
WL-2 brown				2.131	0.865	18.048	Solution- MC-ICP-MS
WL-4 white				2.130	0.865	18.049	Solution- MC-ICP-MS

**Table 4.3 the lead isotopic ratios of Chinese Tang Sancai lead glaze samples**

Sample No.	Date	Excavated	$^{207}\text{Pb}/^{206}\text{Pb}$	$^{208}\text{Pb}/^{206}\text{Pb}$	$^{206}\text{Pb}/^{204}\text{Pb}$	Analytical Method
Syria-4 green	8th-9th Centuries	Al-raqqa, Syria	0.823248	2.067487	19.12322	LA-MC-ICP-MS
9798 green	8th-14th Centuries, maybe after 10th century	Hira or kish, Iraq	0.829704	2.060745	18.93978	LA-MC-ICP-MS
9800 green			0.830473	2.058005	18.91526	LA-MC-ICP-MS
9807 green			0.836225	2.08082	18.81116	LA-MC-ICP-MS
9156 green	10th-13th Centuries	Kish-shaal, Ghazna,Iraq	0.861539	2.108865	18.17585	LA-MC-ICP-MS
9921 green			0.840984	2.080655	18.62768	LA-MC-ICP-MS
9915 green			0.841999	2.082375	18.60122	LA-MC-ICP-MS

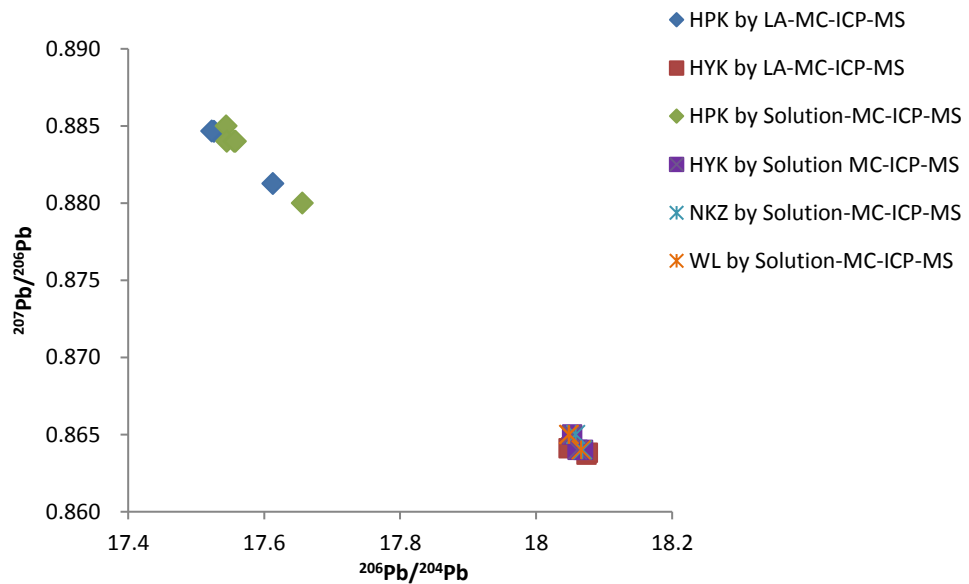
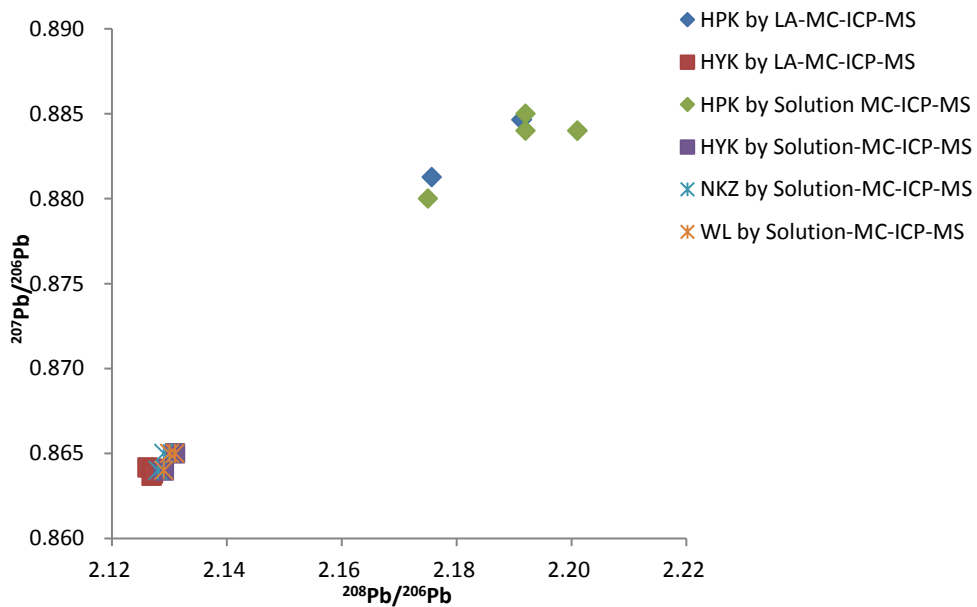
**Table 4.4 the lead isotopic ratios of Islamic lead glaze samples excavated in Syria and Iraq**

## 4.5.1 Tang Sancai lead glazes

### 4.5.1.1 Results

Four Tang Sancai lead glaze samples from Huangpu Kiln, four samples from Huangye Kiln and five samples from two Tang tombs of Xi'an City have been analysed in this study. The data are shown on the  $^{208}\text{Pb}/^{206}\text{Pb}$  versus  $^{207}\text{Pb}/^{206}\text{Pb}$  and  $^{206}\text{Pb}/^{204}\text{Pb}$  versus  $^{207}\text{Pb}/^{206}\text{Pb}$  plots in Figures 4.13a and 4.13b. It is evident from Figures 4.13a and 4.13b, the Tang Sancai glazes produced in the two kilns can be grouped separately according to their different lead isotope ratios. Besides, the lead isotope data of glaze samples for the

two kilns are both plotted in a narrow range, especially for the Huangye Kiln glazes. With regards to the five samples excavated from two tomb sites of Xi'an City, all of them are distributed within the Huangye Kiln sample group.



**Figs 4.13a and 4.13b Lead isotope ratios of Tang Sancai lead glazes from Huangpu Kiln (HPK), Huangye Kiln (HYK), two Tang tombs of Xi'an City (NKZ for Nankezhao Tang tomb, WL for Weilaichubanshe Tang tomb)**



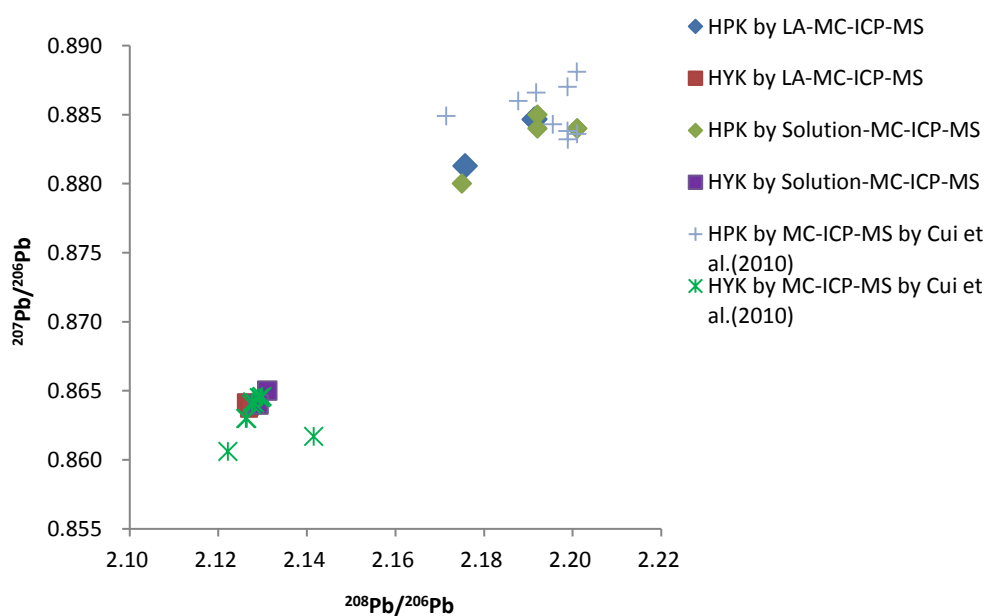
#### **4.5.1.2 Using lead isotopic analysis of glaze to provenance the Tang Sancai artefacts to their producing kilns**

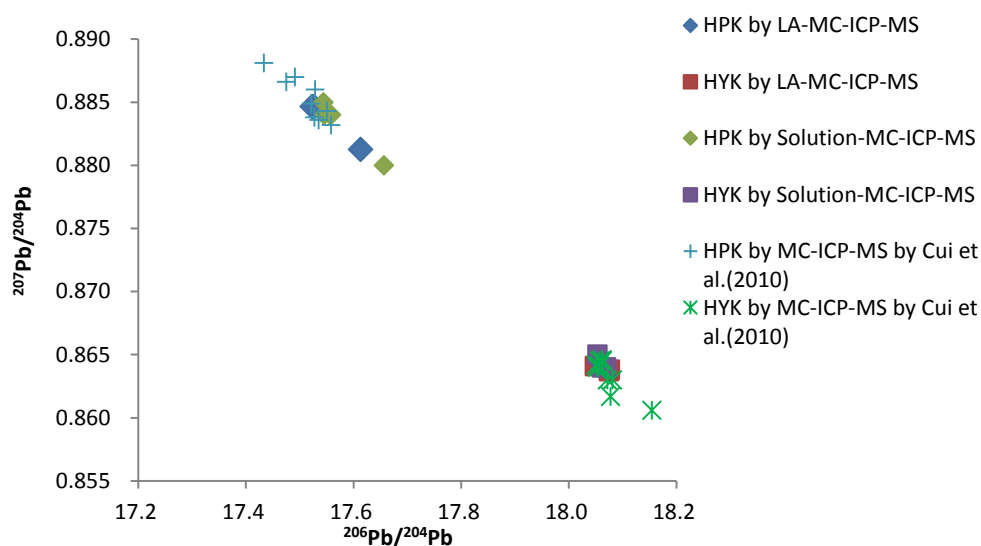
Based on the Pb isotopic ratios comparison of ores and rocks from different areas of China, Zhu (1995, 2001) found that three main geochemical provinces can be distinguished within China: Southern China block with  $^{206}\text{Pb}/^{204}\text{Pb} > 18.4$ ; Yangtze block with  $^{206}\text{Pb}/^{204}\text{Pb}=17.8$  to  $18.3$ ; Northern China block with  $^{206}\text{Pb}/^{204}\text{Pb} < 17.8$ . Cui et al. (2010) analysed the lead isotopic ratios of 19 Tang Sancai glaze samples and found that Tang Sancai lead glazes from the Huangpu Kiln probably used lead ore deposits from the Northern China province, while the lead sources used in Huangye Kiln glazes were probably from Yangtze province. The lead isotope data analysed by Cui et al. (2010) are plotted with the data in this study together in Figures 4.14a and 4.14b.

As seen in Figures 4.14a and 4.14b, the lead isotope data of Tang Sancai glaze samples analysed in this study are in accordance with those analysed by Cui et al. (2010). The lead isotope data of glaze samples from Huangpu Kiln and Huangye Kiln are very distinct from each other, which suggest that different ore sources were exploited by each kiln. Besides, the  $^{206}\text{Pb}/^{204}\text{Pb}$  ratios of the Huangpu kiln in this study are all lower than 17.8 and those of the Huangye kiln are all in the range of 17.8 and 18.3. Therefore, by this research, it can be suggested again that the lead ore used to make Tang Sancai glaze in the Huangpu Kiln collected from the Northern China province, while the Huangye Kiln potters probably selected the lead ore deposits from Yangtze province to produce Tang Sancai glaze. The reason for the distinct Pb isotopic ratios between these two geochemical regions is the differences of their complex tectonic setting (Zhu 2005). For example, the crust of the North China Block possesses the longest evolutionary history in China (2.5-3.5Ga) (Zhu 1995). Generally, in China, the higher ratios of  $^{208}\text{Pb}/^{206}\text{Pb}$  and

$^{206}\text{Pb}/^{204}\text{Pb}$  reflect the earlier time of formation of the lead ore sources (Peng et al. 1985).

The lead isotope data of glaze samples from the Huangye Kiln are distributed in a very narrow range. It suggests that one lead ore source or different ore sources with similar geochemical characteristics were used for Tang Sancai glaze making in Huangye Kiln. It means that the Huangye Kiln potters may have exploited the lead ore deposits from a narrow area. For Huangpu Kiln glaze samples, a possible mixing line of the lead isotope data can be seen in Figures 4.14a and 4.14b. Two possible reasons might explain this possible mixing line. Firstly, it might be caused by the variation within the same lead ore source; Secondly, more than one lead source with different Pb isotopic ratios might have been used for Huangpu Kiln glaze making. However, this is only tentative evidence of the lead sources mixing in Huangpu Kiln, because so far no useful lead isotope data of lead ore deposits from both Shaanxi and Henan Provinces where the Huangpu kiln and Huangye kiln locates have been published. Further research is necessary to provide more rigorous evidence.





**Figs 4.14a and 4.14b Lead isotopic ratios of Tang Sancai lead glazes from Huangpu Kiln (HPK) and Huangye Kiln (HYK) analysed in this study. The lead isotope ratios for Tang sancai lead glazes from these two kilns analysed by MC-ICP-MS by Cui et al. (2010) also are plotted here for comparison**

Although the exact lead ore source used to produce the glazes has not been determined, it is evident that the lead isotope ratios for lead ore sources used for glaze making in the Huangpu and Huangye kilns are very distinct from each other (see in Figures 4.13a and 4.13b). The Huangpu and Huangye kilns were the most important and productive Tang Sancai production centres in China. Therefore, it suggests that the lead isotope analysis of glazes could be a potentially provenancing tool for Tang Sancai wares unearthed from archaeological tombs and sites. The lead isotope ratios of two Tang Sancai glaze samples excavated from the NKZ Tang tomb and three samples unearthed from the WL Tang tomb of Xi'an City also were analysed and plotted in Figures 4.13a and 4.13b. As seen in Figures 4.13a and 4.13b, all five lead glaze samples are distributed within the Huangye kiln glaze group, suggesting that the Tang Sancai glazes excavated in the NKZ Tang tomb and the WL Tang tomb were made using the same lead ore source as that used in Huangye Kiln. When we take into account that the trace elemental composition of Tang Sancai lead glazes discussed in Section 4.4.1, this implication is supported. The Tang Sancai glazes made in Huangye Kiln and glazes excavated from the WL Tang tomb and NKZ Tang

tomb have similar contents of Sb, Sn and As, which are obviously lower than those of Huangpu Kiln glazes. Therefore, both the lead isotope and trace elements results in this study suggest that the Tang Sancai lead glazes unearthed from the WL and NKZ Tang tombs were made using the similar lead ore source as that used in Huangye Kiln glaze making.

The WL and NKZ Tang tombs were both located in Xi'an City. In fact, so far, most of the tombs containing Tang Sancai wares were found to distribute around two areas-Xi'an City in Shaanxi Province, where the capital of the Tang Dynasty was situated, and Luoyang City in Henan Province which served as the second capital during the Tang period. Besides, the Huangpu Kiln in Shaanxi province and Huangye Kiln in Henan province were two of the most important production centres of Tang Sancai wares supplying a large number of Tang Sancai wares not only for Xi'an and Luoyang cities but also for other places at home and abroad. Using the trace elements and lead isotope results discussed above, it can be inferred that all the Tang Sancai glaze samples found in WL and NKZ tombs were produced in the Huangye kiln and traded to Xi'an city rather than produced in the Huangpu Kiln in Shaanxi province near Xi'an. This deduction can be supported by previous studies by Miao and Lu (2001) and Lei (2007). They found that some shapes of Tang Sancai wares and Tang Sancai figures unearthed in tombs around Xi'an City can only be found in the Huangye Kiln rather than in the Huangpu Kiln. Besides, they also found that, for the Tang Sancai artefacts unearthed in the tombs around Xi'an City dating back to before the year AD705 when Empress Wu Zetian gave up the throne, the trace element compositions of their ceramic body samples are all similar with those of Tang Sancai body samples from Huangye Kiln rather than Huangpu Kiln. For the samples unearthed from the Xi'an tombs dated after the year of AD705, the trace element compositions of ceramic bodies of some Tang Sancai samples are similar with those from

the Huangpu Kiln, and the others are grouped within the trace element composition group of Huangye Kiln ceramic bodies. This suggests that some Huangye Kiln Tang Sancai artefacts were traded to Xi'an city. In this study, this trade also can be inferred by the lead sources used to make the Tang Sancai glazes. However, one should still keep in mind that it is highly possible that some more kilns in both Shaanxi and Henan provinces which produced Tang Sancai artefacts are still to be found. Thus another possibility is that the Tang Sancai samples found in WL and NKZ Tang tombs might have been produced in Henan Province kilns using the similar lead source as used in the Huangye Kiln.

According to excavation findings, the Tang Sancai production of the Huangye Kiln started from the early Tang period and was sustained during the whole Tang period (AD618-907), while the Huangpu kiln began to produce Tang Sancai artefacts from the Prospering Tang period (AD649-756), which is later than the Huangye Kiln. Besides, no evidence so far shows that the Tang Sancai made in Huangpu kiln in Shaanxi Province were ever traded to Luoyang City. However, as the discussion above, some evidence infers that the Tang Sancai made in Huangye kiln in Henan Province might be traded to Xi'an City. Specifically, it can be inferred by the type and decoration style, trace element compositions of body and lead isotope ratios of glazes of unearthed Tang Sancai wares and fragment. This might infer that during the early Tang period, the Huangye Kiln in Henan Province was the most important Tang Sancai production centre. After AD705 when Empress Wu Zetian gave up the throne, the political and economic centres shifted from Luoyang city to Xi'an city which led to the development of the Huangpu Kiln near Xi'an. The Huangpu Kiln then evolved gradually into another significant Tang Sancai production centre.

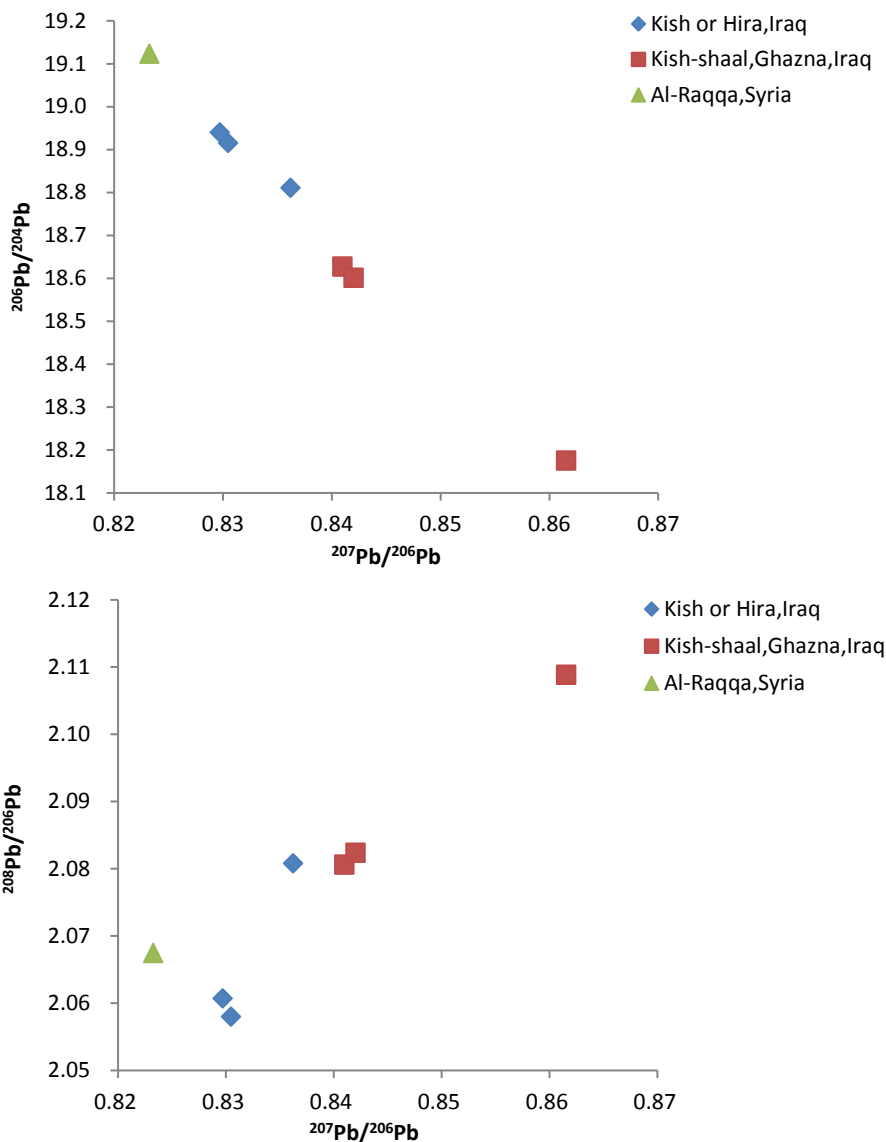
Based on the discussion above, the lead isotope analysis has proven a good way of

relating Tang Sancai glaze samples unearthed in tombs with the Tang Sancai production kilns, and it can be supported by the trace element analysis of glazes as a complementary method. Further lead isotope analysis of Tang Sancai glazes from more Tang Sancai kilns are necessary in order to provide more evidence of the trade of Tang Sancai artefacts.

## **4.5.2 Islamic splashed lead glazes from Syria and Iraq**

### **4.5.2.1 Results**

One lead glaze sample from Al-Raqqa in Syria, three lead glaze samples from Kish-shaal Ghazna site in Iraq and three samples from Kish or Hira in Iraq have been analysed in this study. The lead isotope values of these samples are shown on Table 4.4 and are plotted in  $^{207}\text{Pb}/^{206}\text{Pb}$  versus  $^{208}\text{Pb}/^{206}\text{Pb}$  and  $^{207}\text{Pb}/^{206}\text{Pb}$  versus  $^{206}\text{Pb}/^{204}\text{Pb}$  shown in Figures 4.15a and 4.15b. The only Syrian lead glaze sample (Syria-4) has a different ratio from the lead glazes from Iraq. The ratios of six Iraqi lead glaze samples are in a wide range which suggests that more than one lead source might have been used for them. To group the lead isotope ratios of these glaze samples as well as determine the possible origins of the lead sources used to produce them, the available lead isotopic data of lead ore deposit samples from different known locations have been selected to compare with the lead isotope ratios of the glazes in this study.



**Figs 4.15a and 4.15b Lead isotope ratios of Islamic lead glazes from Al-Raqqqa in Syria, Kish or Hira in Iraq and Kish-shaal Ghazna site in Iraq**

#### 4.5.2.2 Provenance discussion

To determine the lead sources used to produce the Islamic lead glazes, it is necessary to obtain the lead isotope data of ore deposits which are relevant to Islamic glaze production. According to some contemporary Islamic documents, several mines were referred to be utilised during the Islamic period. In about AD1154, al-Idrisi mentioned that lead from Yazd in central Iran was traded far and wide. Abu'l-Qasim wrote in about AD1300 that

lead is found in many places, especially in Kerman and Yazd in central Iran, in "Rum" (Rome or Byzantium, presumably in Anatolia), and in "the land of the Bulgars" (which was probably in the Volga area) (Mason et al. 1992). Besides, the operation of Tunisian lead mines during the 9th to 18th centuries AD also was recorded (Craig 1967). Furthermore, by archaeometallurgical evidence, lead–silver mines in south-west Spain were exploited from the Phoenician period to the Islamic period. Moreover, the Sardinian lead–silver mines were shown to have been utilised from the Late Bronze Age until the medieval period (Rothenberg and Blanco-Freijeiro 1981; Wolf et al. 2003). Besides, the lead–silver mines in the Taurus Mountains of southern Anatolia were exploited during the Bronze Age and again by the Hittites (Wolf et al. 2003). There is a significant Islamic town called Nigde located at the foothills of the Taurus Mountains, which shows the Islamic activities ever happened in the Taurus Mountains. Moreover, during the 11th–12th centuries AD, parts of Anatolia area (including the Taurus Mountains regions) were the war zone between the Seljuks and, first, the Byzantines, then the Armenians and then the Crusaders, which might lead to the trade among them. Thus it seems possible that the lead-silver mines in the Taurus Mountains were further exploited during the Islamic period (Wolf et al. 2003).

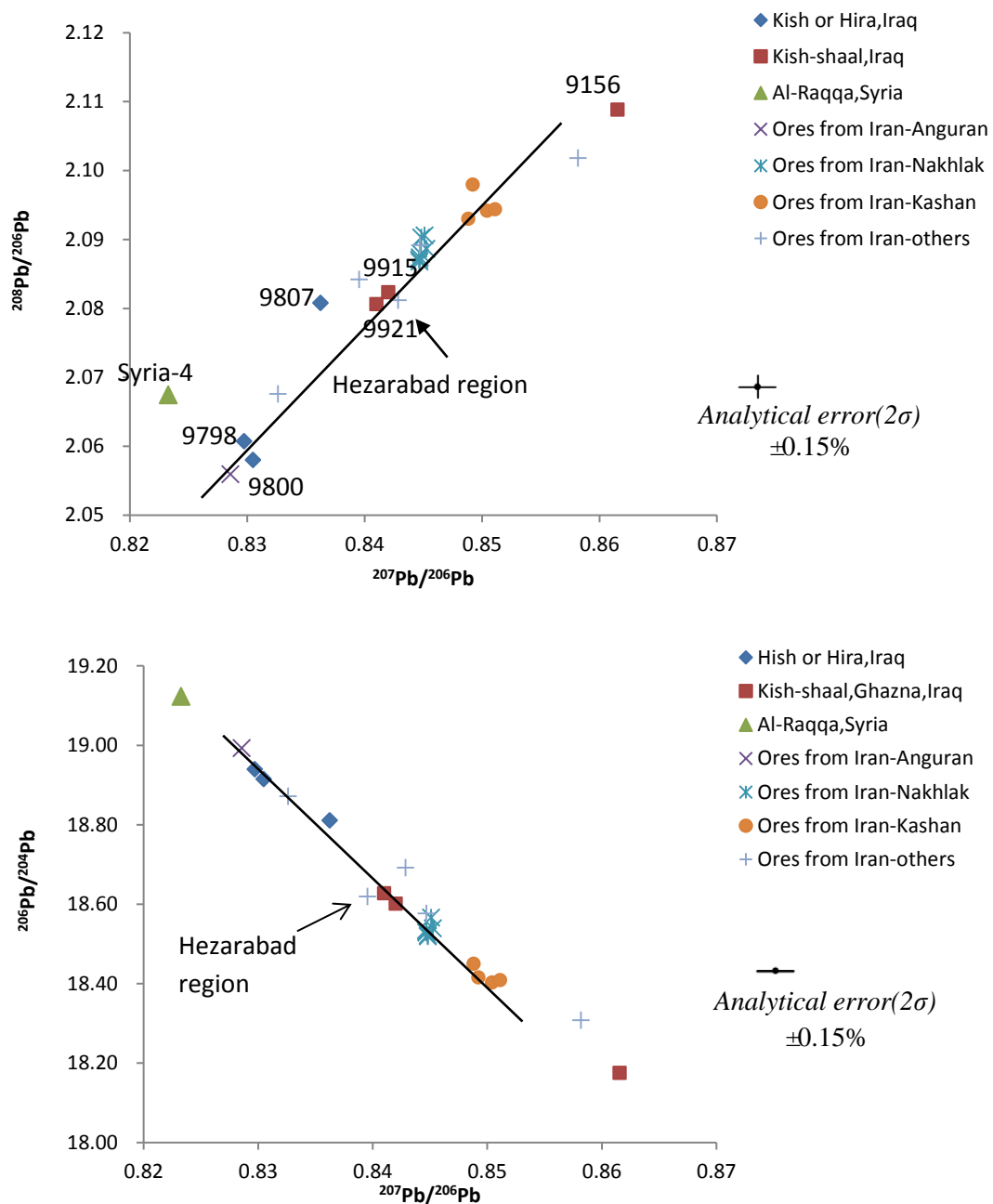
In this study, the available lead isotope data of ore deposits from the regions of central Iran, Anatolia, Tunisia, Southwest Spain and Sardinia mentioned above are selected for comparison with those of glaze samples. The lead isotope results of glaze samples in this study are plotted together with the available data ( $^{208}\text{Pb}/^{206}\text{Pb}$ ,  $^{207}\text{Pb}/^{206}\text{Pb}$  and  $^{206}\text{Pb}/^{204}\text{Pb}$ ) of lead ore sources mentioned above respectively are shown in Figures 4.16-4.20. In the plots, each glaze sample is compared with the ore deposit samples to determine the possible lead source for it. Specifically, if the relationship between the glaze sample and the ore samples of a particular region satisfies each of the following two conditions, the



ore deposit samples of this region might be suggested as the possible lead source to make the glaze: 1). The glaze sample falls within the range of all three lead isotopic data ( $^{208}\text{Pb}/^{206}\text{Pb}$ ,  $^{207}\text{Pb}/^{206}\text{Pb}$  and  $^{206}\text{Pb}/^{204}\text{Pb}$ ) of ore samples from a particular region; 2). The glaze sample is 'close enough' to the lead ore samples of a given area, and 'close enough' here means that the Euclidean distance for all three lead isotope data ( $^{208}\text{Pb}/^{206}\text{Pb}$ ,  $^{207}\text{Pb}/^{206}\text{Pb}$  and  $^{206}\text{Pb}/^{204}\text{Pb}$ ) of the glaze sample and ore sample are smaller than the lead isotope analytical error ( $2\sigma$ ) (Wolf et al. 2003). It needs to point that, the abundant lead ore deposit source of Islamic world make them convenient to use to make Islamic lead glazes and this have been demonstrated by some previous studies (Brill and Wampler 1967; Wolf et al. 2003). Besides, the lead metal also might be used to make Islamic lead glaze, because a large number of lead ingots were found representing the exploit of metal ingots and broken artefacts for recycling (Stargardt 2014). Therefore, the possibility that a mixture of lead sources or lead metal collected from more than one source was mixed and used to make glaze should always keep in mind during discussion below.

#### **A. the ore sources from Iran**

The lead isotope ratios of 18 lead ore samples from different regions of Iran listed by Stos-Gale (2001) were selected for comparison with those of Islamic glaze samples in this study. Specifically, seven lead ore deposit samples were from the Nakhlak area of central Iran, four galena samples were from the Kashan area of south-eastern Iran, one sample was from the Anguran region of north-western Iran and six galena samples were from other different parts of Iran. The lead isotope ratios and ore deposits information obtained from Stos-Gale (2001) are listed in Appendix I Table A12. The results of this study plotted together with data of lead sources from Iran, are shown in Figures 4.16a and 4.16b.



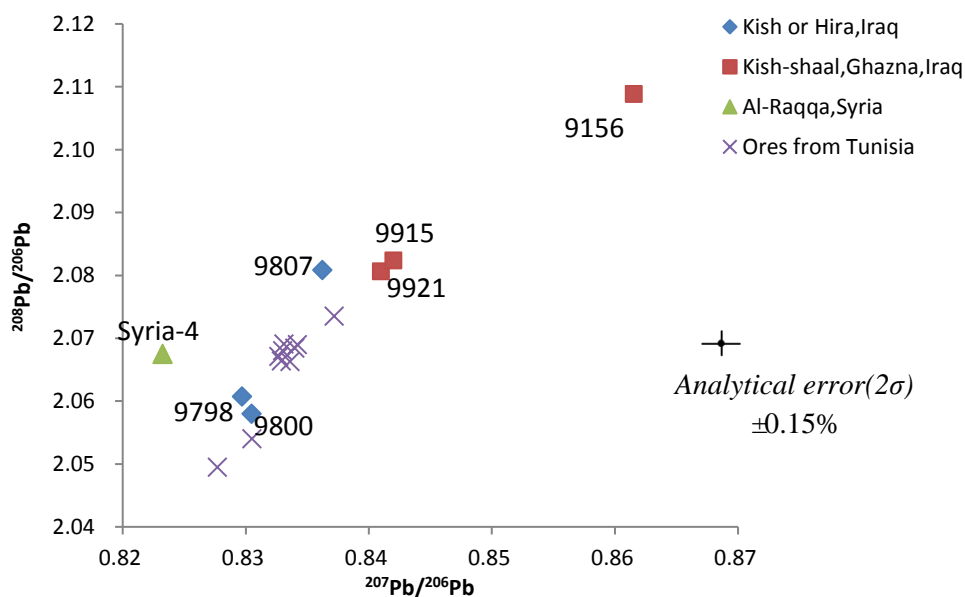
**Figures 4.16a and 4.16b Lead isotope ratios for lead glaze samples pottery from Syria and Iraq and lead ores from different regions of Iran**

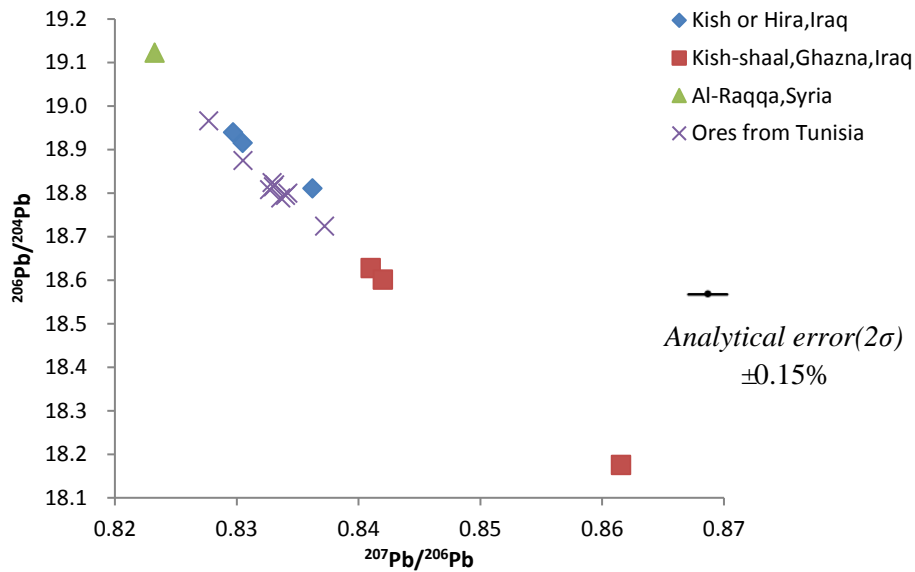
As shown in Figures 4.16a and 4.16b, no lead isotope ratios of the Iran ores are either close to or overlap with that of the Al-Raqqqa glaze sample (Syria-4), which suggests that the lead source used to make the Al-Raqqqa glaze sample was not Iran. With regards to the Iraqi glaze samples, the lead isotope ratio of the ore from the Hezarabad region of central Iran is ‘close enough’ to the two glaze samples (9915 and 9921) from Kish-shaal Ghazna

site of Iraq. It suggests that the ore from the Hezarabad region might be a possible ore source for these two glazes. No lead isotope ratio from a single region of Iran either overlaps with or is ‘close enough’ to samples 9798, 9800, 9807 and 9156. Nevertheless, if we consider the lead isotope ratios of all Iranian ores together, samples 9798 and 9800 fall into field which surround Iraqi lead glaze samples, suggesting the possibility that the mixing of lead from more than one source in Iran occurred in glaze production.

### B. the ore sources from Tunisia

The lead isotope ratios of 10 lead ore samples from Tunisia plotted by Wolf et al. (2003) were selected for comparison, which are listed in Appendix Table A13. The results of this study plotted together with data of lead sources from Tunisia, are shown in Figures 4.17a and 4.17b.





**Figures 4.17a and 4.17b Lead isotope ratios for lead glaze samples pottery from Syria and Iraq and lead ores from Tunisia**

As shown in Figures 4.17a and 4.17b, no lead isotope ratios of the Tunisian ores are either close to or overlap with those of Al-Raqqa glaze sample (Syria-4) and the three glaze samples (9915, 9921 and 9156) from Kish-shaal Ghazna site of Iraq. This means that the Tunisian ore deposits were not the lead source used to make these glaze samples. For the Kish or Hira site samples, the sample 9807 does not fall within the lead isotope ratio range of the Tunisian ores. Whereas, the lead isotope ratios of Tunisian ores overlap with the glaze samples 9798 and 9800, which suggests that Tunisian ore deposits might be the possible ore sources for these two glazes.

### **C. the ore sources from Anatolia**

For the Anatolian mines, the lead isotope ratios of 12 lead source samples from different regions of Anatolia are obtained from the Oxford Archaeological Lead Isotope Database (OXALID), which are available as Excel files on the OXALID website, at <http://oxalid.arch.ox.ac.uk>. Specifically, data for the following lead source samples were used: seven galena samples from the Elazig region of central eastern Anatolia; three

galena samples from the Giresun region of north-western Anatolia and two samples from the Malatya region of eastern Anatolia. Besides, the lead isotope ratios of 49 lead ore samples from ancient mining sites in the Central Taurus mountain area of southern Anatolia reported by Yener et al. (1991) also were selected. Because the  $^{206}\text{Pb}/^{204}\text{Pb}$  ratios of the Taurus mountain ores were not analysed by Yener et al. (1991), only the plot of  $^{207}\text{Pb}/^{206}\text{Pb}$  versus  $^{208}\text{Pb}/^{206}\text{Pb}$  is shown in Figure 4.18, and the Taurus 1A represents the galena samples from Kestel mine in the Niğde Massif region of Taurus, Taurus 1B represents the galena samples from Bolkardağ Valley region of Tarsus, the samples of 2A and 2B are from the Aladağ region of Tarsus. The lead isotope ratios and ore deposits information in details obtained from OXALID and Yener et al. (1991) are listed in Appendix I Table A14.

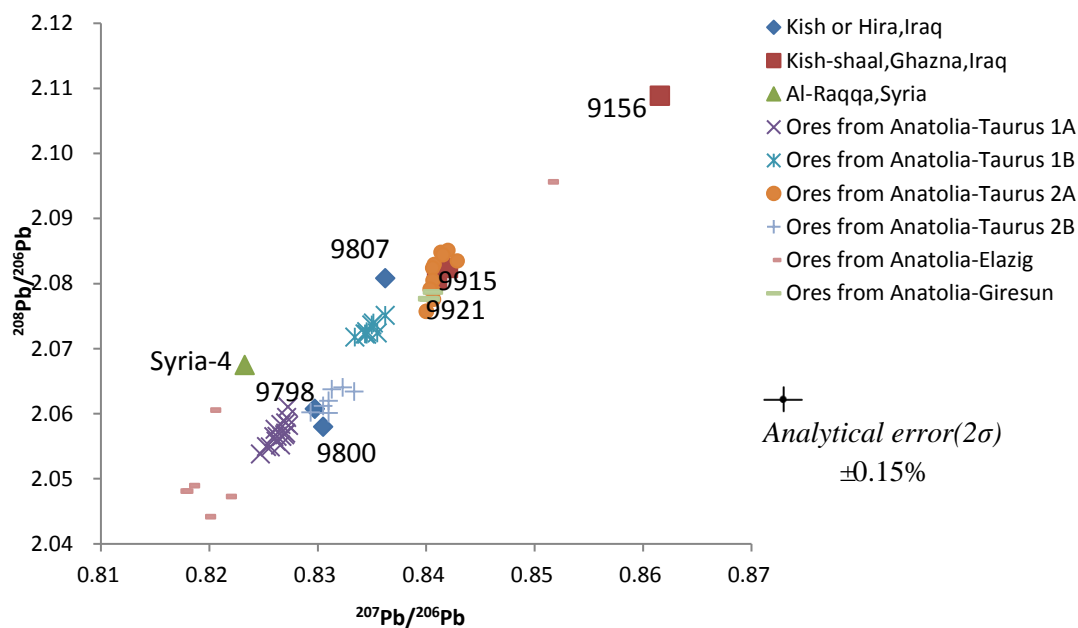


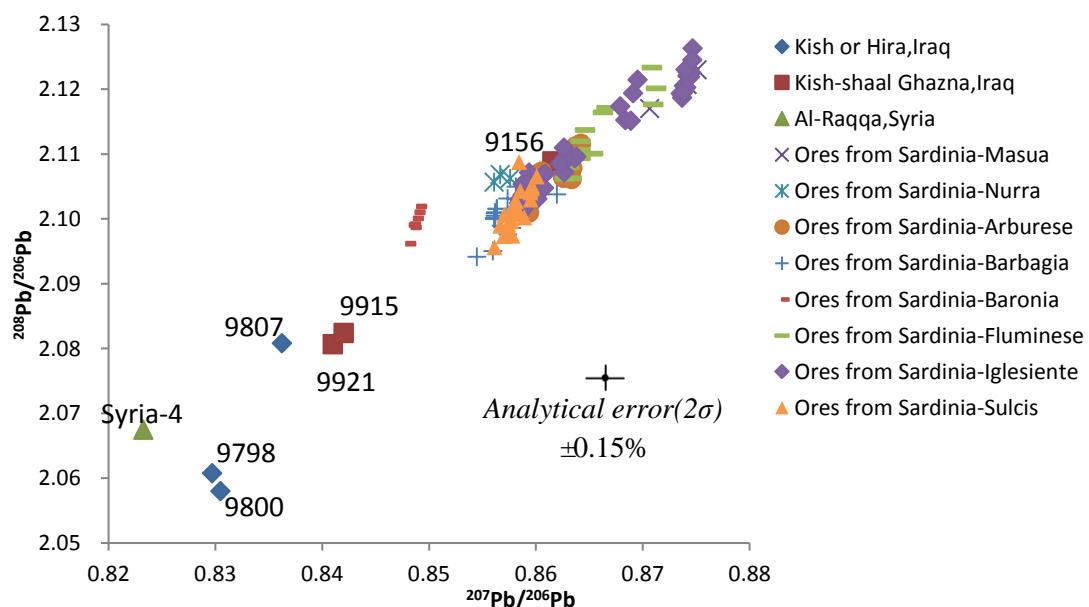
**Figure 4.18 Lead isotope ratios for lead glaze samples from Syria and Iraq and lead ores from different regions of Anatolia(Taurus 1A represents Kestel mine in the Niğde Massif region of Taurus; Taurus 1B stands for Bolkardağ Valley region of Taurus, Taurus 2A and 2B both represent the galena samples from the Aladağ region of Tarsus)**

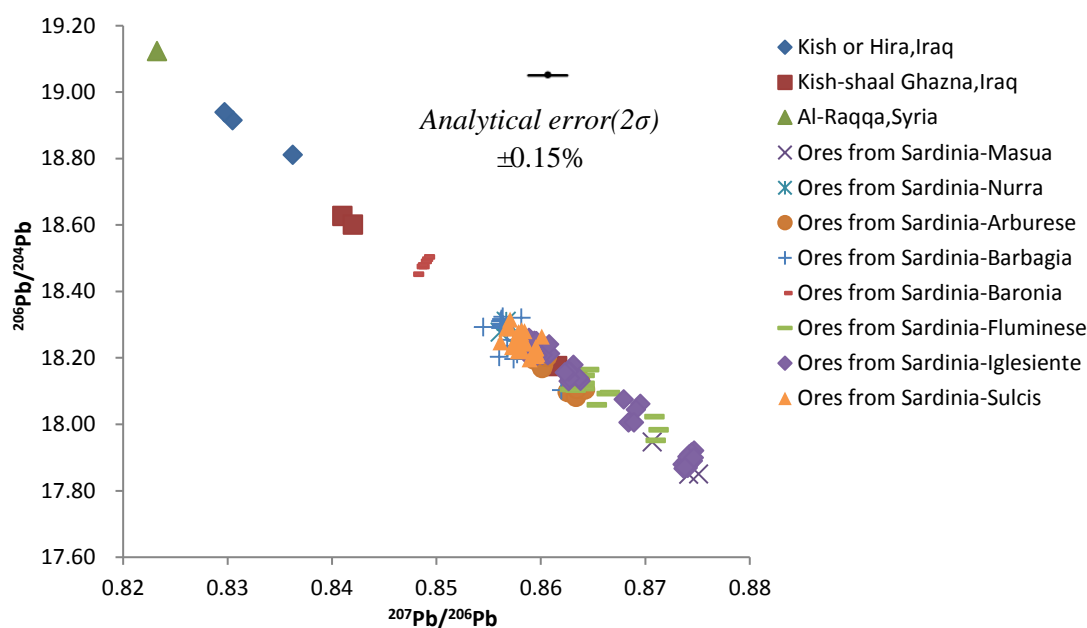
As shown in Figure 4.18, no lead isotope ratios of the Anatolia ores are either ‘close enough’ to or overlap with those of samples Syria-4, 9156 and 9807, which suggest that

the Anatolian ore deposits were not the lead source used to make these glaze samples. The samples of 9798 and 9800 fall within the lead isotope data range of the Taurus 2B ore samples, and samples 9915 and 9921 are closest to the Taurus 2A ore samples, which suggest that the ore deposits from the Aladağ region of Tarsus might be the possible ore sources for these four glazes.

#### D. the ore sources from Sardinia

For the Sardinian mines, the lead isotope ratios of 143 lead source samples from different regions of Sardinia are obtained from the Oxford Archaeological Lead Isotope Database (OXALID). Specifically, the lead deposit samples were collected from different mines from the Masua region of south-western Sardinia, Nurra region of north-western Sardinia, Baronia region of north-eastern Sardinia, Arburese region of central Sardinia as well as Barbagia, Fluminese, Iglesiasiente and Sulcis region of southern Sardinia. The lead isotope ratios and ore deposits information in details obtained from OXALID are listed in Appendix I Table A15. The results of this study plotted together with data of lead sources from Sardinia, are shown in Figures 4.19a and 4.19b.





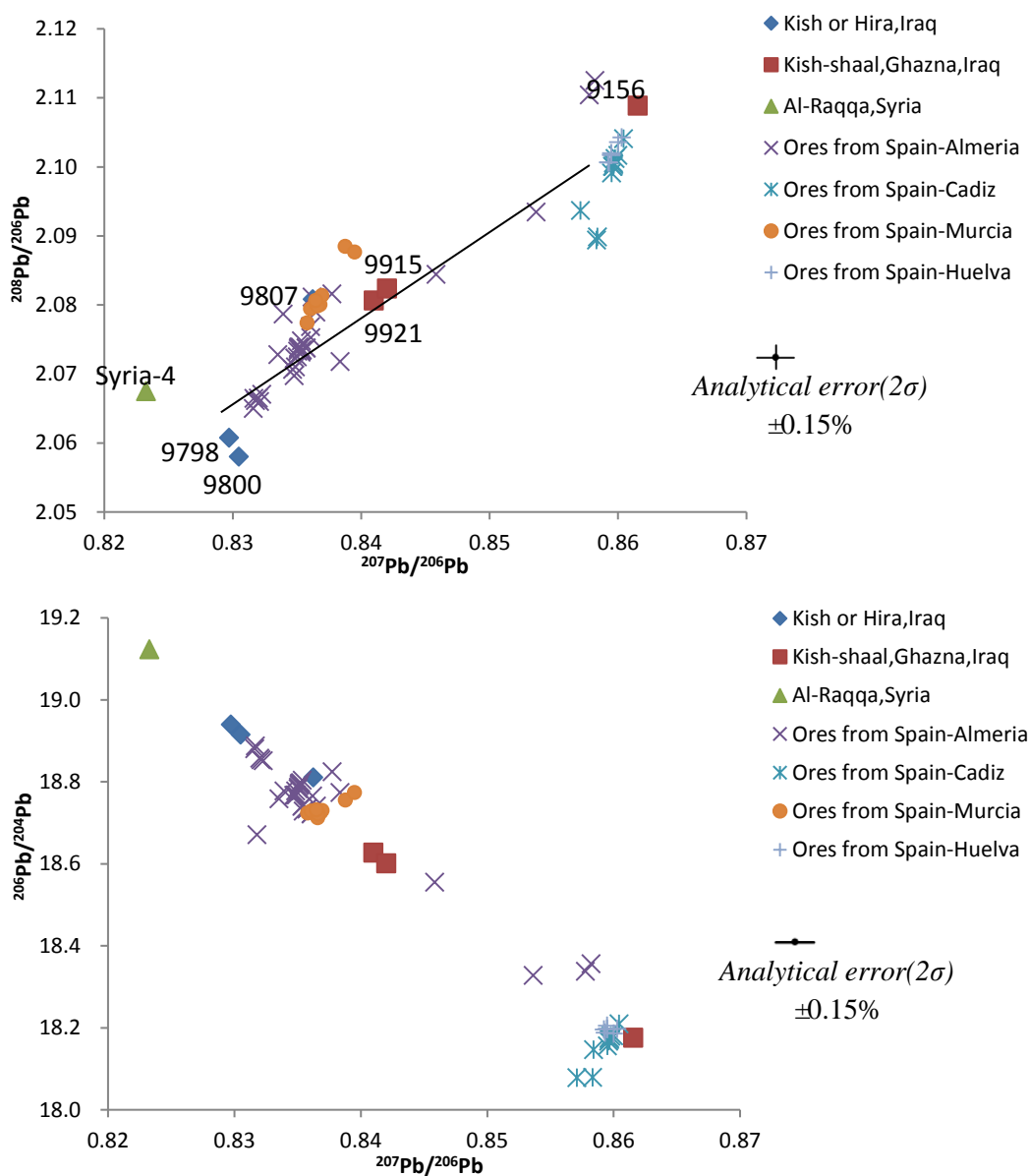
**Figures 4.19a and 4.19b Lead isotope ratios for lead glaze samples pottery from Syria and Iraq and lead ores from different regions of Sardinia**

As shown in Figures 4.19a and 4.19b, no lead isotope ratios of the Sardinian ores from different regions either are ‘close enough’ to or overlap with those of samples Syria-4, 9798, 9800, 9807, 9915 and 9921 which suggest that the Sardinian ore deposits were not the lead source used to make these glaze samples. Whereas, the lead isotope ratio for sample 9156 from Kish-shaal Ghazna site falls within those for ores from the mines in the Arburese region, Fluminese region and Lglesiente region. This suggests the lead source used to produce the sample 9156 have a possibility to import from the mine in these regions of Sardinia.

### **E. the ore sources from Spain**

For the Sardinian mines, the lead isotope ratios of 61 lead source samples from different regions of Sardinian are obtained from the Oxford Archaeological Lead Isotope Database (OXALID). Specifically, the lead deposit samples were collected from various mines from the Almeria region and Murcia region of south-eastern Spain, Cadiz region and

Huelva region of south-western Spain. The lead isotope ratios and ore deposits information in details obtained from OXALID are listed in Appendix I Table A16. The results of this study plotted together with data of lead sources from Spain, are shown in Figures 4.20a and 4.20b.



**Figures 4.20a and 4.20b Lead isotope ratios for lead glaze samples pottery from Syria and Iraq and lead ores from different regions of Spain**

As shown in Figures 4.20a and 4.20b, no lead isotope ratios of the Spanish ores from different regions are either ‘close enough’ to or overlap with those of samples Syria-4.



Although in the Figure 4.18b the lead isotope ratios of the ores from the Cadiz and Huela regions are 'close enough' to sample 9156, the  $^{208}\text{Pb}/^{206}\text{Pb}$  of the ores from the Cadiz and Huela regions seen in Figure 4.18a are not 'close enough' to 9156. These suggest that the Spanish ore deposits were not the lead source used to make the glaze samples of Syria-4 and 9156. Whereas, the lead isotope ratios for sample 9915 and 9921 from Kish-shaal Ghazna site fall within those of ores from the mines in the Almeria region, suggesting the Almeria region mines might be the lead source to make glaze sample 9915 and 9921. Similarly, the lead source used to produce the sample 9807 from Kish or Hira site might be from the mine in the Murcia region or Almeria region. Besides, the possibility that the mixing of lead from more than one sources of Spain used in the glaze production of sample 9915, 9921 and 9807 also is reasonable.

The isotopic compositions of lead ores depend on a combination of the geological age of the lead ore deposit and the geological region in which it was formed (Wolf et al. 2003). Therefore, the variation in the Pb isotopic compositions of lead ores is a function of its initial U, Th and Pb concentrations, the starting Pb isotopic composition, and the time-integrated growth of radiogenic Pb (Iñáñez et al. 2010). However, many lead ores in the Near East and the Mediterranean have been found to develop in similar geological regions and within a relatively narrow geological time (Wolf et al. 2003). This leads to the similarities and overlap of lead isotopic compositions between some different lead ore sources of these areas. Thus, in this study, one obstacle to a clear interpretation of lead source used in lead glaze is the overlapping lead isotopic signatures of ores from the Near East and the Mediterranean areas. Besides, the possibility that the mixture of lead from more than one mine used in glaze making is another reason which makes it hard to assign the lead source to specific mine. As a result, by the discussion above, more than one possible lead source has been suggested to the lead used to produce each glaze samples in

this study, which are listed in Table 4.5.

Sample No.	Date	Excavated	Possible ore sources
Syria-4	8th-9th Centuries	Al-Raqqa, Syria	None
9798 9800	8th-14th Centuries, maybe later than 10th Century	Hira or Kish, Iraq	Iran (Mixture of more than one lead ore deposits of Iran); Tunisia; Anatolia-Taurus-Aladağ
9807			Spain- Murcia or Almeria
9915 9921	10th-13th Centuries	Kish-shaal, Ghazna,Iraq	Iran-Hezarabad; Anatolia-Taurus-Aladağ; Spain-Almeria
9156			Sardinia

**Table 4.5 the possible ore deposit sources for the lead used to make glaze samples of Syria and Iraq in this study**

As it is seen in Table 4.5, even considering the possibility that a mixture of lead sources or lead metal collected from more than one source was mixed and used to make glaze, no possible ore deposits in this study can be found for the Al-Raqqa glaze. For the Iraqi glaze samples 9798, 9800, 9915 and 9921, the lead ore deposits both from Middle Eastern areas and Mediterranean area are possible sources of lead used for making them. Moreover, for samples of 9156 and 9807, the lead ore sources used in their glaze making were most probably obtained from remote Sardinian and Spain areas respectively. It may reflect the trade of lead deposits between different parts of Middle Eastern regions and Mediterranean area.

Three Iraqi glaze samples (9915, 9921 and 9156) were excavated from Kish-shaal Ghazna, the possible ore sources for them suggest that the glazes unearthed from the same archaeological site were made using lead obtained from different ore sources. This may be explained by two possibilities. First, these three samples were probably produced in

the same ceramic-making site using the lead from different lead ore sources. Secondly, glaze sample 9156 was made on the different ceramic-making site from samples 9915 and 9921. Furthermore, the possible lead source for glaze 9156 is from Sardinia, which is far away from the potential lead sources of glazes 9915 and 9921 (Iran, Anatolia or Spain). It seems unlikely that the potters within one ceramic production site selected the lead ore deposits from two places having such long distances from each other. Therefore, the latter possibility may be more reasonable. We may infer that the Iraqi glazed pottery wares unearthed from the same site might be imported from the different ceramic-making sites.

#### **4.5.3 The lead isotope comparison of Chinese Tang Sancai lead glazes and Islamic lead glazes of Syria and Iraq**

Figure 4.19 summarises the lead isotope results of some Chinese Tang Sancai glazes, Islamic lead glazes and ores from different regions of the Middle Eastern and Mediterranean areas. Although the ore deposits from different regions of Middle Eastern and Mediterranean areas spread out over a wide isotopic range, all of them fall in the lower range of isotopic values compared to the Chinese Tang Sancai lead glazes. It shows that lead isotope analysis of glazes is potentially distinguishing Chinese Tang Sancai lead glazes from lead glazes made in the Middle East.

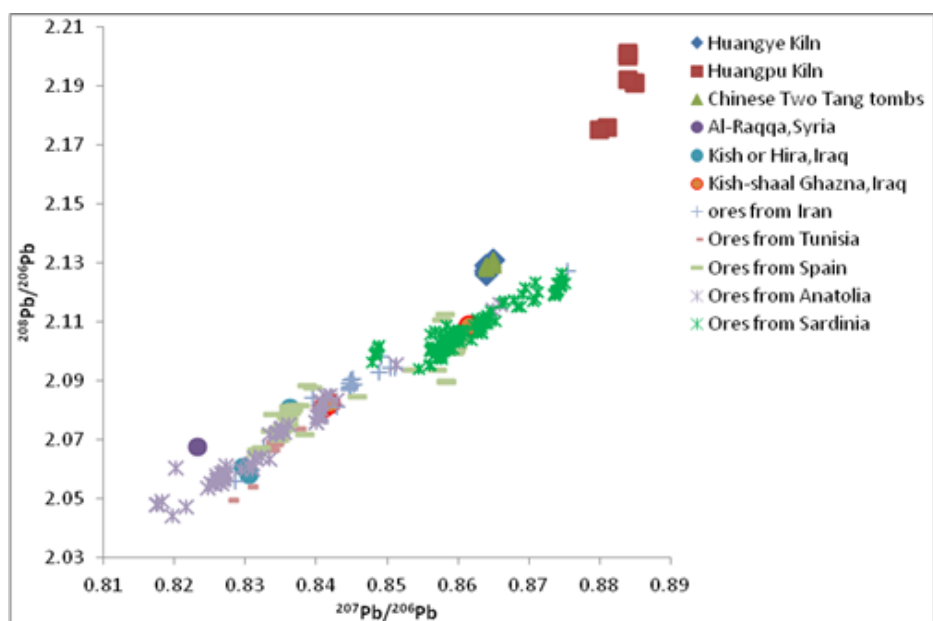


**Figure 4.19 Lead isotope ratios for Chinese and Islamic lead glazes and Iraq and lead ores from different regions of Middle Eastern and Mediterranean areas**

A number of imported Tang Sancai wares and their local imitations have been found in some Middle Eastern countries such as Egypt (Fustat), Iraq (Samarra) and Iran (Nishapur) (Lane 1947, 12; Needham 2004, 732-733; Watson 2004, 47). The distinction of lead isotope ratios between Chinese Tang Sancai lead glazes and lead ores from different regions of Middle Eastern and Mediterranean areas can be used to provenance the Tang Sancai wares unearthed in the Middle East sites. Besides, in this study, the distinction of Pb isotopic ratios of Tang Sancai glazes made in two important production kilns have been found, which might be used to identify the possible production centres in North China where the Chinese imported Tang Sancai excavated in the Middle East produced.

## 4.6 Conclusions

1. By discussing the major chemical compositions of glazes, it has been possible to infer the lead glazing technique for Chinese Tang Sancai lead glazes and Islamic splashed lead glazes from Syria and Iraq. For Chinese Tang Sancai glazes, the mixture of lead compound,

quartz/quartz sand and clay was applied. With regards to Islamic splashed lead glazes, the mixture of a lead compound plus quartz/quartz sand was applied and clay might be added into the glaze suspension sometimes.

2. The lead ore deposit used to produce Huangye Kiln glazes and Huangpu Kiln glazes can be distinguished using the chalcophile trace elements Sn and Sb which were mainly derived from the lead ore deposit. And the siliceous raw materials used to make Tang Sancai glazes in these two kilns can be probably distinguished by some lithophile trace elements –the Cr/La ratio, Zr/Ti ratio, Cs and Ba which were suggested to be mainly introduced from the siliceous raw materials. Besides, the trace element analysis has potential to associate Chinese Tang Sancai artefacts with their production kilns. With regards to Syrian and Iraqi splashed lead glazes, the trace elemental composition distinctions among them are less obvious. However, the trace elemental analysis may distinguish the splashed lead glazes made in China and the Middle East. The trace element analysis might be able to be used as a complementary method to distinguish the different sources of raw materials used in glaze making in some cases.

3. Lead isotope analysis has proven to potentially relate Chinese Tang Sancai glazes unearthed in archaeological sites of unknown origin with the Tang Sancai production kilns. By the sources of lead used to make Tang Sancai glazes, it can be inferred that some Tang Sancai artefacts unearthed in Xi'an City were made in Huangye Kiln and traded to Xi'an City.

4. Different ore sources were used to make the lead glazes in Syria and Iraq. Moreover, for the Iraqi glaze samples, the lead ore deposits both from the Middle Eastern and Mediterranean areas are possible sources of lead used for making them. The overlap of lead isotopic signatures among some different lead ore sources from the Middle Eastern

and Mediterranean areas make it impossible to associate the lead used in glaze making with a specific lead ore source. Moreover, in this case study, the lead used to produce two Iraqi glaze samples were most probably obtained from the remote Sardinian and Spain areas respectively. This may reflect the trade of lead deposits between the Middle Eastern regions and Mediterranean areas.

## **Chapter 5 The chemical and Sr isotopic analysis of Yaozhou celadon glaze from Northern China**

### **5.1 Introduction**

Yaozhou celadon ware is thought to be the best representative of Northern China greenware. The choice of raw materials used in Yaozhou celadon glaze production is relatively complicated and lacks detailed study because no historical record directly refers to the source of flux used. Chemical analyses of Yaozhou celadon glazes have been performed in recent decades, with some researchers suggesting that plant ash was used as the flux, because Yaozhou celadon glaze has relatively high contents of  $P_2O_5$  and  $K_2O$  (Guo and Li 1984; Ling et al. 2008; Zhu et al. 2011). Other researchers have suggested

that limestone may be a possible candidate for the flux used in Yaozhou celadon glaze due to its availability near to the Yaozhou kiln. Li and Guan (1979) and Li (1998, 260), for example, indicated a local Ordovician limestone called might have been suitable as a source of lime and flux in the glaze. Therefore, the question of which glaze raw materials were used by Yaozhou potters is still open. The probable flux used in Yaozhou celadon glazes are explored in the present chapter. Specifically, the chemical and Sr isotopic compositions of Yaozhou celadon glaze samples will be discussed so as to consider the following research objectives: firstly, identification of the raw materials and the glaze type of Yaozhou celadon glaze; secondly, identification of the changes of glaze recipes of Yaozhou celadon from the Tang period (AD618-907) to the Northern Song dynasty (AD960-1127); thirdly, the Sr isotopic composition pattern of Yaozhou celadon glaze will be determined.

## **5.2 Samples**

Twenty-one Yaozhou celadon glaze samples supplied by the Department of Cultural Heritage, Northwest University, China are included in this study to serve the research purpose of this chapter. Four of these samples (Tang-16a, Tang-20, Tang-BW3 and Tang-BW6) are dated to the Tang dynasty (AD618-907), nine of them (YZF-1, YZF-2, YZF-3, YZF-4, YZF-5, YZF-6, YZF-7, YZF-8 and YZF-9) are traced back to the Five Dynasties and Ten Kingdom periods (AD907-960, hereinafter referred to as FT dynasty). All these fragments of Yaozhou celadon glaze were excavated in the Xidajie-Bell Tower Area archaeological sites, located in the centre of Xi'an City (approximate 80 kilometres south of the Huangpu kiln sites). The remaining eight samples (NS-52, NS-53, NS-54, NS-55, NS-56, NS-57, NS-58 and NS-59) are dated to the Northern Song dynasty (AD960-1127) and were excavated in the Huangpu kiln sites. All the selected samples used in this study

have been identified as the products of Huangpu kiln sites, because they are found to have the typical characteristics of Huangpu kiln sites products in their glaze colour tone and decoration patterns. The pictures of all these samples are shown in Appendix II A-19.

## 5.3 Results

### 5.3.1 The major elemental compositions of Yaozhou celadon glaze

#### samples

By using the Cameca SX100 microprobe located in the Opening University, the major elemental compositions of Yaozhou celadon glaze samples were analysed following the methodology described in chapter three. The major elemental compositions of the Yaozhou celadon glaze samples tested are listed in Table 5.1.

Sample No	Date	SiO <sub>2</sub>	Al <sub>2</sub> O <sub>3</sub>	Na <sub>2</sub> O	K <sub>2</sub> O	CaO	MgO	FeO	TiO <sub>2</sub>	MnO	P <sub>2</sub> O <sub>5</sub>	Total
<b>Tang-16a</b>	Tang	56.89	13.24	0.31	1.84	19.68	2.43	2.23	0.32	0.11	1.04	98.09
<b>Tang-20</b>		58.37	13.29	0.26	1.59	18.98	2.41	2.30	0.32	0.10	1.03	98.65
<b>Tang-BW6</b>		58.60	11.55	0.13	1.64	20.50	1.99	2.66	0.27	0.04	1.26	98.64
<b>Tang-BW3</b>		63.12	12.50	0.30	1.88	16.90	1.87	1.66	0.26	0.08	0.60	99.17
<b>YZF-1</b>	FT dyansty	60.27	12.65	0.30	1.89	19.05	1.78	1.50	0.15	0.07	0.82	98.48
<b>YZF-2</b>		63.94	13.29	0.45	2.01	15.16	1.89	1.43	0.12	0.08	0.91	99.28
<b>YZF-3</b>		68.43	16.02	0.35	2.44	7.87	1.46	1.98	0.16	0.03	0.44	99.18
<b>YZF-4</b>		64.84	13.21	0.30	2.22	13.61	1.70	1.58	0.14	0.06	0.69	98.35
<b>YZF-5</b>		64.63	14.29	0.29	2.08	12.99	1.61	1.70	0.12	0.09	0.62	98.42
<b>YZF-6</b>		65.00	14.62	0.50	2.51	10.57	1.89	2.30	0.15	0.09	0.78	98.41
<b>YZF-7</b>		71.76	14.13	0.45	2.62	6.86	1.19	1.58	0.16	0.02	0.22	98.99



Sample No		SiO <sub>2</sub>	Al <sub>2</sub> O <sub>3</sub>	NaO	K <sub>2</sub> O	CaO	MgO	FeO	TiO <sub>2</sub>	MnO	P <sub>2</sub> O <sub>5</sub>	Total
YZF-8		66.57	15.77	0.36	2.25	10.21	1.25	1.60	0.17	0.04	0.33	98.55
YZF-9		59.54	16.41	1.00	2.26	11.13	2.02	4.23	0.45	0.08	0.08	97.20
NS-52	Northern Song	68.59	13.98	0.36	3.29	9.19	1.69	1.81	0.17	0.08	0.74	99.90
NS-53		67.21	12.62	0.63	3.01	10.78	1.84	1.85	0.17	0.05	0.67	98.83
NS-54		66.47	14.03	0.29	1.88	11.29	2.63	2.35	0.43	0.04	1.15	100.56
NS-55		71.31	13.88	0.22	3.55	5.59	1.81	2.80	0.45	0.04	0.74	100.39
NS-56		61.72	12.23	0.35	2.06	18.23	2.16	1.96	0.22	0.08	0.96	99.97
NS-57		64.15	13.47	0.63	3.15	11.31	2.74	2.40	0.27	0.06	1.26	99.44
NS-58		76.03	14.28	0.57	3.92	3.31	0.85	1.72	0.22	0.03	0.79	101.72
NS-59		65.91	14.00	0.33	2.36	12.27	1.59	1.65	0.10	0.06	0.62	98.89

**Table 5.1 the major chemical compositions of Yaozhou celadon glaze samples (wt.%)**

The SiO<sub>2</sub>+Al<sub>2</sub>O<sub>3</sub> contents of Tang celadon glaze samples range from 70.13 wt.% to 75.62 wt.%, while the SiO<sub>2</sub>+Al<sub>2</sub>O<sub>3</sub> contents of celadon glaze samples made in the FT dynasty and Northern Song dynasty range from 72.92 wt.% to 85.90 wt.% and from 73.95 wt.% to 90.31 wt.% respectively. The average content of SiO<sub>2</sub>+Al<sub>2</sub>O<sub>3</sub> of celadon glaze samples increases from 71.89 wt.% in the Tang dynasty to 81.23 wt.% in the Northern Song dynasty.

The increased SiO<sub>2</sub>+Al<sub>2</sub>O<sub>3</sub> contents (9.34 wt.% by average) from the Tang dynasty to Northern Song dynasty is mainly accompanied by the decreased CaO+MnO+MgO+P<sub>2</sub>O<sub>5</sub> contents (9.17 wt.% by average) during these three successive periods. Specifically, the combined content of CaO+ MnO+MgO+P<sub>2</sub>O<sub>5</sub> in Tang celadon samples ranges from 19.45 wt.% to 23.78 wt.% with an average of 22.25 wt.%, while for the glaze samples made in the FT dynasty and Northern Song dynasty, it ranges from 8.29 wt.% to 21.71 wt.% and

from 4.98 wt.% to 21.43 wt.% respectively. The average CaO+MnO+MgO+P<sub>2</sub>O<sub>5</sub> contents of celadon glaze samples decreased from 22.25 wt.% in the Tang dynasty to 13.08 wt.% in the Northern Song dynasty.

Sample No.	Date	MgO+CaO	Na <sub>2</sub> O+K <sub>2</sub> O	RO/RO+R <sub>2</sub> O
Tang-16a	Tang (AD618-907)	22.11	2.15	0.91
Tang-20		21.38	1.86	0.92
Tang-BW6		22.49	1.77	0.93
Tang-BW3		18.77	2.18	0.90
YZF-1	FT dynasty (AD907-960)	20.82	2.19	0.90
YZF-2		17.05	2.45	0.87
YZF-3		9.33	2.79	0.77
YZF-4		15.31	2.52	0.86
YZF-5		14.60	2.36	0.86
YZF-6		12.46	3.01	0.81
YZF-7		8.04	3.07	0.72
YZF-8		11.46	2.61	0.81
YZF-9		13.14	3.25	0.80
NS-52	Northern Song (AD960-1127)	10.88	3.65	0.75
NS-53		12.62	3.63	0.78
NS-54		13.91	2.17	0.86
NS-55		7.39	3.77	0.66
NS-56		20.39	2.41	0.89
NS-57		14.05	3.78	0.79
NS-58		4.16	4.49	0.48
NS-59		13.86	2.69	0.84

**Table 5.2 the glaze coefficient b of Yaozhou celadon glaze samples**

Following the glaze calculation method using the Seger Formula, as well as a series of deductions and statistics of chemical compositions of abundant Chinese glaze samples, Prof. Luo (1995) suggested ancient Chinese lime glazes could be categorised into three sub-groups by the ratio RO/ (RO+R<sub>2</sub>O) labelled as the glaze coefficient b: calcium glaze (b≥0.76), calcium- alkali glaze (0.76 < b≤0.50), and alkali-calcium glaze (b < 0.50). The

values of calculated glaze coefficient  $b$  of Yaozhou celadon glazes in this research are listed in Table 5.2 and provide the classification of Yaozhou celadon glazes. The results show that the  $b$  values for the Yaozhou celadon glazes in the Tang dynasty within the range of 0.90-0.93, which means that all these glazes are calcium glazes. With regards to the Yaozhou celadon glazes of the FT dynasty, almost all the glazes are of the calcium type too, with the range of  $b$  values from 0.77 to 0.90, only one glaze (YZF-7) from this period should be classified as a calcium- alkali glaze, with the  $b$  value of 0.72. Wang et al. (1999) analysed 26 Yaozhou celadon glazes of the FT dynasty. They found that half of the studied Yaozhou celadon glazes are calcium glaze, and half of them are calcium- alkali glaze. Regarding the glazes of the Northern Song dynasty, five out of eight glaze samples are calcium glazes with the range of  $b$  values from 0.78 to 0.89, and two in them (NS-55 and NS-52) are of the calcium- alkali glaze type with  $b$  values of 0.66 and 0.75 respectively. One glaze (NS-58) has the low  $b$  value of 0.48. This should be classified as an alkali-calcium glaze. It is inferred that, from the Tang dynasty to the Northern Song dynasty, the glaze recipes have a trend changing from ‘calcium glaze’ to ‘calcium-alkaline’ glaze.

### **5.3.2 The rare earth elemental compositions of Yaozhou celadon glaze samples**

Using laser ablation inductively coupled plasma mass spectrometry (LA-ICP-MS) located in the Analytical Geochemical Laboratories of British Geological Survey, the rare earth elemental (REE) compositions of Yaozhou celadon glaze samples were determined following the methodology described in chapter three. The rare earth elemental compositions of the tested samples are listed in Appendix I TableA5.

The chemically coherent behaviour of the REEs in geological materials has been extensively used as a tool for solving various geological and geochemical problems, including as reliable indicators of sources (Gao and Wedepohl 1995). REEs are lithophile elements. The Yaozhou celadon glazes are mainly comprised of two components: the siliceous raw material (glaze stone or local clay, or the mixture of them) and the lime-bearing flux. The strontium isotope compositions of Yaozhou glazes suggest that the flux used in Yaozhou glaze recipe was probably plant ash (see below). As mentioned above, based on the historical record dating to the Republican period (1912-1919 A.D.), 'Fuping stone' was used as siliceous raw material for making Yaozhou glaze. 'Fuping stone' is a calcareous clay rock deposited in Carboniferous-Permian strata, and analysis of 'Fuping stone' shows that it mainly composed of kaolinite and calcite (20%-25%), as well as a certain content of quartz (5%-10%) and feldspar (Li and Guan 1979; Li 1998, 260). The local clay used to make Yaozhou stoneware bodies is sedimentary clay deposited in Carboniferous-Permian strata, which consist largely of kaolinite and halloysite, as well as a certain content of quartz (5%-10%) and feldspar (Li 1998, 260). Therefore compared to Yaozhou body clay, 'Fuping stone' is not actually a different rock, but a shale compressed by the same local clay with Ordovician limestone and some other minerals. This infers that 'Fuping stone' may be an analogue of the body clay with a similar REE distribution curve. Therefore, in the REE distribution pattern discussion of this study, the siliceous raw material of Yaozhou celadon glaze is simplified to taken as one component, and the contents of REEs in glaze were introduced mainly by the siliceous raw material of glaze recipe. The siliceous raw material in the glaze, produced by different geological processes in different locations would have unique REE distribution patterns. In this study, we try to use the REEs to distinguish the sources of siliceous raw material used in the Yaozhou celadon glazes in different periods.

REEs are conventionally presented on a concentration versus atomic number diagram called as REE distribution pattern (Rollinson 1993, 135). In order to graphically compare the geochemical effect by REE distribution curves, the REEs concentrations are normalised to the chondritic reference value firstly to eliminate variation due to the higher abundances of REE with even atomic numbers (Evensen et al. 1978; Allen et al 1982; Li et al. 2005; Ma et al. 2012). In this research, the frequently used average compositions of the chondrite analysed by Boynton (1984) has been used as the normalising value and listed in Table 5.3.

REEs	La	Ce	Pr	Nd	Sm	Eu	Gd
Avg. chondrite	0.310	0.808	0.122	0.600	0.195	0.0735	0.259
REEs	Tb	Dy	Ho	Er	Tm	Yb	Lu
Avg. chondrite	0.0474	0.322	0.0718	0.210	0.0324	0.209	0.0322

**Table 5.3. The average chondrite compositions used for normalising the REE concentrations (concentrations in ppm) by Boynton (1984)**

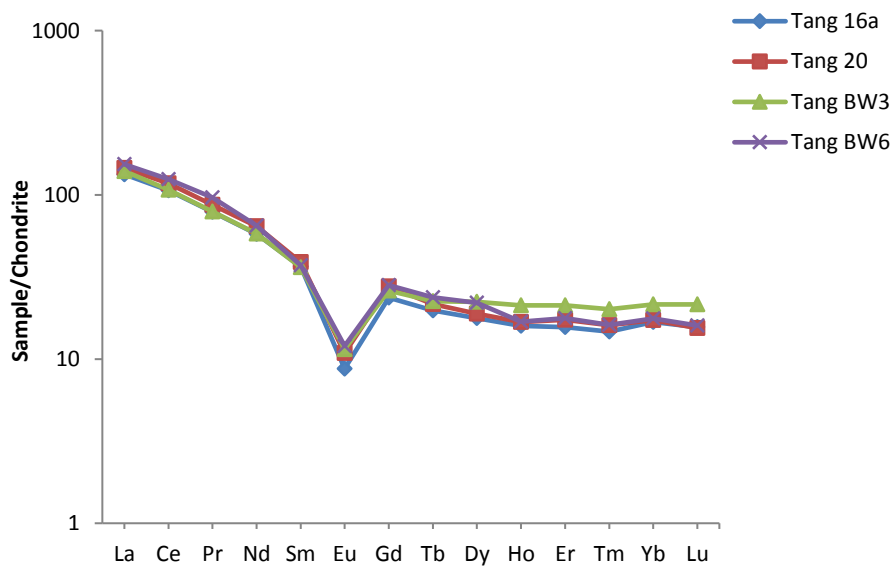


**Fig 5.1 REE distribution curves of Yaozhou celadon glaze samples in the Tang dynasty (AD618-907)**

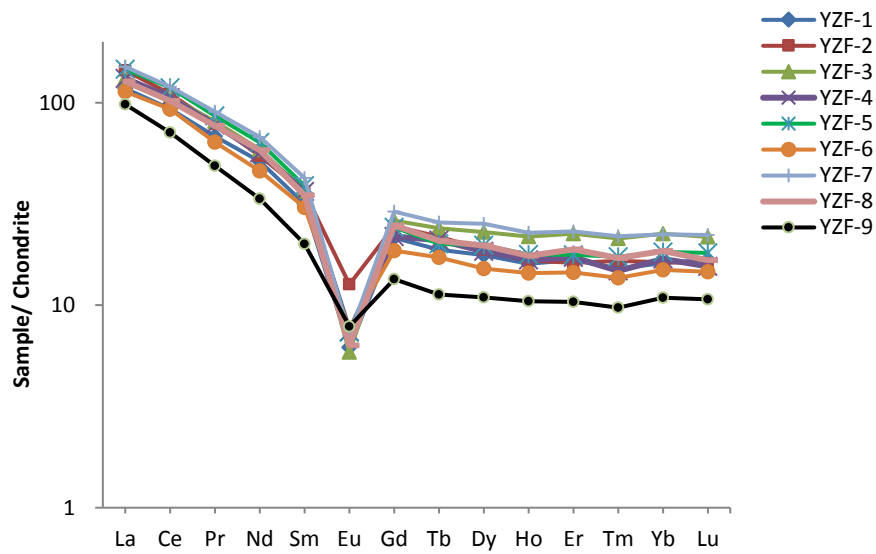


**Fig 5.2 REE distribution curves of Yaozhou celadon glaze samples in the FT dynasty (AD907-960)**

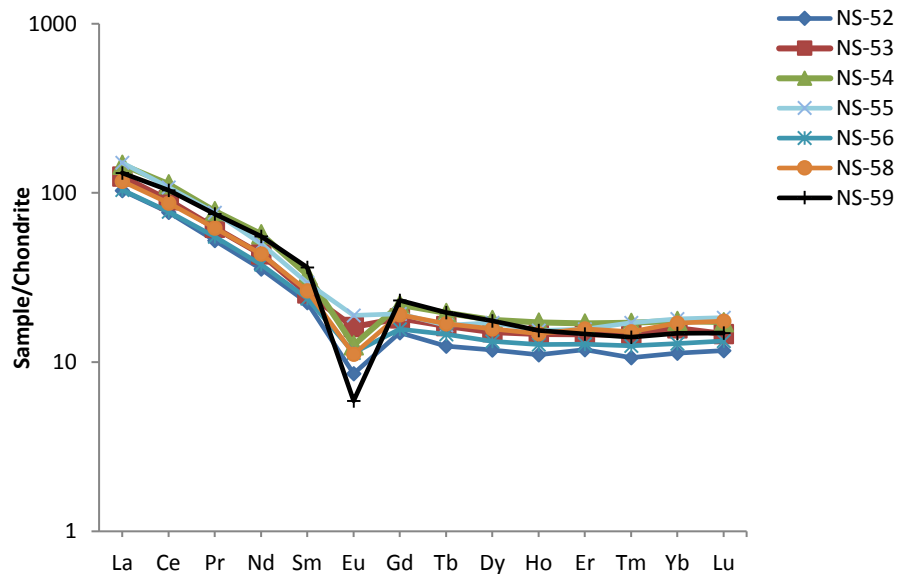


**Fig 5.3 REE distribution curves of Yaozhou celadon glaze samples in the Northern Song dynasty (AD960-1127)**

The REE distribution curves of Yaozhou kiln glaze samples in different periods are shown in Figures.5.1-5.3. In general, the curves for Yaozhou glaze samples of the three successive periods have similar patterns. Firstly, the absolute REE concentrations in all the Yaozhou glaze samples from the three successive periods are at the similar level of

generally between lg5 and lg200. Secondly, on the whole, no significant differences can be found in the decline from La to Sm as well as the decline from Gd to Lu in the glaze sample patterns of all three periods. The similarity of the REE distribution patterns suggests that similar geochemical sources of siliceous raw materials were probably used for Yaozhou glaze making.

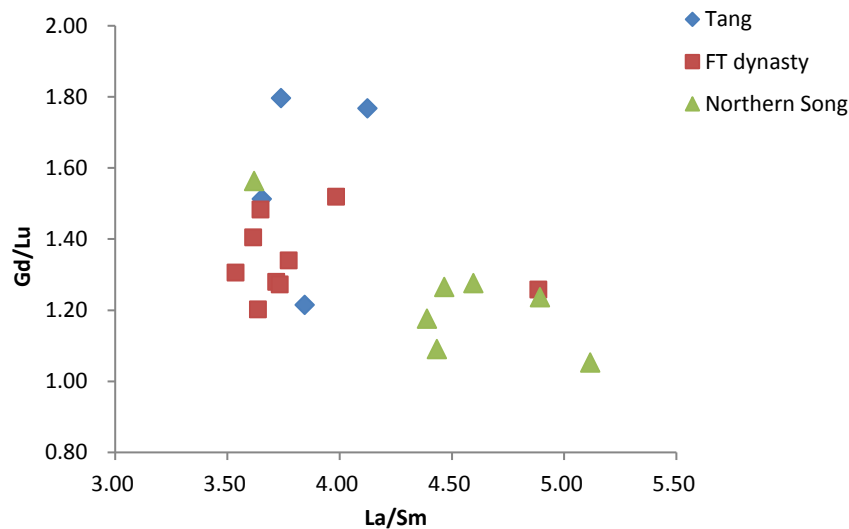


**Fig 5.4 Plot of La/Sm versus Gd/Lu of Yaozhou glaze samples**

Although sharing similar REE patterns in general, the slight differences in the REE distribution curves of Yaozhou glaze samples cannot be ignored. Firstly, the differences can be seen more clearly when plotted as  $(La/Sm)_N$  versus  $(Gd/Lu)_N$  as shown in Fig 5.4. The  $(La/Sm)_N$  ratio is used to present the degree of decline in the low REE (LREE) end, while the  $(Gd/Lu)_N$  ratio is used to show the decline degree at the high REE (HREE) end. It can be seen from Fig 5.4 that the majority of the Northern Song period glaze samples are distinct from the glaze samples in the Tang and FT dynasty due to the higher La/Sm ratios and lower Gd/Lu Ratios of Northern Song glaze samples. Besides, although the majority of glaze samples of the Tang dynasty and FT dynasty share similar REE patterns, the plotted Tang samples are scattered. These differences show that although the glaze stone used for the Yaozhou kiln from different periods probably has the same geological

source, it is highly likely that the potters collected the glaze stone raw materials from different locations.

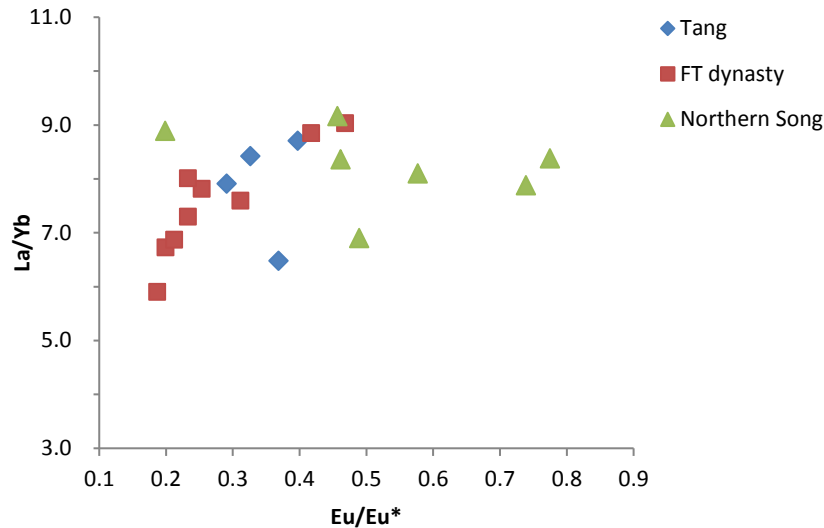


**Fig 5.5 Plot of Eu/Eu\* versus La/Yb of Yaozhou glaze samples**

Secondly, slight differences on the Eu anomalies of Yaozhou glaze samples can be seen in the REE distribution curves in Figures 5.1-5.3. The value of Eu/Eu\* is widely used as the parameter to display the degree of the Eu anomaly. The Eu\* is the interpolated value of Sm and Gd calculated by the following equation. The (Sm)<sub>N</sub> and (Gd)<sub>N</sub> in the equation are normalised values for Sm and Gd.

$$Eu^* = \frac{(Sm)_N + (Gd)_N}{2} \quad (5.1)$$

The value of La/Yb is used to represent the proportion of Light REEs (LREE) to Heavy REEs (HREE). The plot of Eu/Eu\* versus La/Yb is usually used to demonstrate the general characteristics of the REE distribution patterns. The Eu anomaly is a significant indicator that reflects the degree of weathering and alteration of the mineral composition and mineral decomposition from plagioclase/K-feldspar to mica/kaolinite and from amphibole to chlorite/smectite (Gao and Wedepohl 1995). In this study, when plotted as



Eu/Eu\* versus La/Yb as in Fig.5.5, the subtle differences in the REE distribution patterns between the Tang and FT dynasty glaze samples and the Northern Song glaze samples can be found. It can be seen in Fig.5.5, most Northern Song glaze samples have relatively higher Eu/Eu\* ratios than the samples of Tang and FT dynasty periods. It proves again that although the glaze stones used for the glaze making in Yaozhou kiln probably have a similar geological source, it is likely that the glaze stones from more than one location were selected by the potters.

### **5.3.3 The Sr isotopic compositions of Yaozhou celadon glaze samples**

#### **5.3.3.1 Samples**

Based on the chemical composition results of glazes, twelve representative Yaozhou celadon glaze samples were selected to do Sr isotope analysis on them. Four samples (Tang-BW3, Tang-BW6, Tang-16a and Tang-20) are dated to the Tang dynasty (AD618-907), four samples (YZF-2, YZF-3, YZF-4 and YZF-5) are dated to the Five dynasties and Ten Kingdoms (AD907-960) and five samples (NS-52, NS-53, NS-54, NS-55 and NS-59) are dated to the Northern Song dynasty (AD960-1127).

#### **5.3.3.2 Results**

The Thermo Finnegan Triton Thermal ionisation mass spectrometer (TIMS) located at NERC Isotope Geoscience Laboratory (NIGL) was used. The Sr isotope compositions of twelve Yaozhou celadon glaze samples were determined using the established method described in chapter three. The Sr isotopic compositions of Yaozhou celadon glaze samples are given in Table 5.4.

Sample No.	Date	Sr(ppm)	<sup>87</sup> Sr/ <sup>86</sup> Sr	1/(Sr ppm)
TangBW3	Tang dynasty (618-907AD)	487	0.714195	0.002053
TangBW6		1327	0.712897	0.000754
Tang16a		493	0.713721	0.002028
Tang20		1007	0.713546	0.000993
YZF-2	FT dynasty (907- 960AD)	582	0.714872	0.001718
YZF-3		318	0.714672	0.003145
YZF-4		474	0.713971	0.002111
YZF-5		270	0.715529	0.003704
NS-52	Northern Song dynasty (960-1127AD)	336	0.717883	0.002976
NS-53		515	0.714630	0.001942
NS-54		537	0.714948	0.001862
NS-59		402	0.714536	0.002488
NS-55	Northern Song dynasty (960- 1127AD)	1571 (analysed by TIMS)	0.716095	0.000637
		496 (analysed by LA-ICP-MS)		0.002016

**Table 5.4 the Sr isotopic compositions analysed by TIMS of Yaozhou celadon glaze samples**

During the sample pre-treatment, the weights of our glaze samples were 30.0-90.0 mg, except from one sample (sample number NS-55). Because the fragment of NS-55 sample was small and the glaze layer was hard to separate from its body entirely, only 8.0 mg weight of the glaze layer was removed from the ceramic body for Sr isotope analysis. The low weight of glaze sample for NS-55 has the possibility to cause the deviation of the analysed Sr content results. Therefore, before we discuss the result, we need to check whether the analysed Sr isotope composition result of sample NS-55 is reliable here.

The bulk of the Sr content in glass and glaze come from the lime-bearing portion of the raw material (Wedepohl and Baumann 2000, Ma et al. 2014). According to the REE distributions of Yaozhou celadon samples mentioned in Section 5.3.2, all these glaze

samples were probably made with glaze stone from a similar geochemical source, although the glaze stone might have been collected from more than one location. With regards to the fluxing agent, although the question of whether the 'Liaojiang stone' (limestone) or botanic ash was used still cannot be resolved clearly, what we can infer is that the similar raw materials might have been used as the flux in Yaozhou celadon. This means that the Sr isotopic composition of Yaozhou celadon in our research should derive from a similar lime-bearing portion of raw materials in the Yaozhou glaze samples. Therefore, in theory, the content of CaO and Sr should generally be positively correlated. Besides, the silica fraction (e.g. feldspar and mica) of siliceous raw materials has a minor Sr contribution to the final Sr isotope composition of glaze, which makes the correlation weaken to some extent. The plot of CaO (%) and Sr (ppm) is given in Fig.5.6. Excepting one outlier- sample NS-55 analysed by TIMS, all the glaze samples are found to have correlated values of the content of CaO (%) and Sr (ppm), although the correlation is not very strong due to the influence by the silica fraction of raw material. This suggests that due to the low sample weight of NS-55 mentioned above, an analytical error for its Sr concentration may be involved. In order to reconfirm this inference, the Sr concentration of glaze sample NS-55 analysed by LA-ICP-MS also present in Fig 5.6. The Sr concentration of sample NS-55 analysed by LA-ICP-MS is 496ppm, which is evidently different from that analysed by TIMS with the value of 1571ppm. Besides, the Sr concentration of NS-55 analysed by LA-ICP-MS falls on the correlation with some other samples. It can be inferred that the Sr concentration of sample NS-55 analysed by LA-ICP-MS is more reliable. Therefore, it is reasonable to use the value (496ppm) analysed by LA-ICP-MS (496ppm) instead of the value (1571ppm) analysed by TIMS as the Sr concentration of NS-55 in the following data discussion.

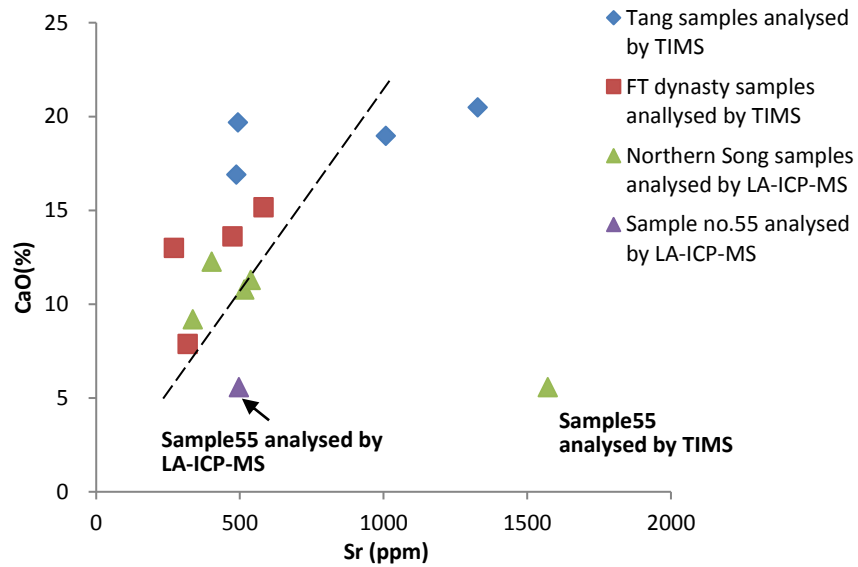


**Fig.5.6 Plot of Sr (ppm) versus CaO (%) of Yaozhou glaze samples**

The isotopic compositions of Yaozhou celadon glazes are listed in Table 5.4 and plotted as  $^{87}\text{Sr}/^{86}\text{Sr}$  versus  $1/(\text{Sr ppm})$  in Figure 5.7. The Sr concentrations of Yaozhou celadon extend across a wide range from 270ppm to 1327ppm and average 557 ppm. In the meanwhile, the  $^{87}\text{Sr}/^{86}\text{Sr}$  ratios of Yaozhou celadon glaze samples vary between 0.712897 and 0.717883 to the third decimal place.

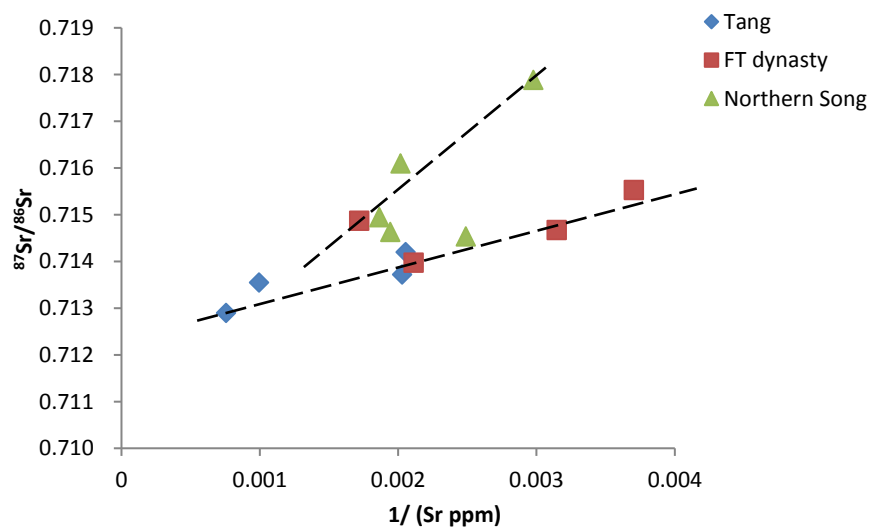


**Fig 5.7 Strontium isotope ratios plotted against  $1/(\text{Sr ppm})$  in Yaozhou celadon glaze samples**

According to the known geochemical theory (Dickin 2005 179), a straight line in a bi-plot of  $1/(Sr \text{ ppm})$  versus  $^{87}Sr/^{86}Sr$  means that the Sr isotopic compositions of samples were formed by the mixtures of two components of the samples in different proportions taking into account. As shown in Figure 5.7, two straight mixing lines can be plotted by all of the Yaozhou celadon glaze samples of the three successive periods. All four Tang period Yaozhou celadon glaze samples, most glaze samples of FT dynasty and one Northern Song glaze sample (NS-59) share the same straight mixing line. The Sr concentrations of these Tang and FT dynasty glaze-based samples extend across a wide range from 270ppm to 1327ppm and average 597ppm. The  $^{87}Sr/^{86}Sr$  ratios of these Yaozhou celadon glaze samples vary between 0.712897 and 0.715529. Four Northern Song Yaozhou celadon glaze samples and one FT dynasty glaze sample (YZF-2) are separated and fall onto another different mixing line. The Sr concentrations of these Northern Song glaze-based samples also extend in a wide range from 336ppm to 582ppm and average 493ppm. In the meantime, the  $^{87}Sr/^{86}Sr$  ratios of these glaze samples vary between 0.714630 and 0.717883.

## **5.4 Discussion**

### **5.4.1 The possible flux type used in Yaozhou celadon glaze based on major chemical compositions**

According to the calculated glaze coefficient  $b$  of Yaozhou celadon glaze mentioned in Section 5.3.1, Yaozhou celadon glaze can be generally categorised as calcium glaze. However, the question of whether Yaozhou celadon glazes were fluxed with limestone or plant ash as a source of CaO is still unresolved. In previous scientific studies, the combined contents of  $P_2O_5$  and MgO, and sometimes the content of MnO as well have

tended to be used as the indexes to identify whether a glaze was fluxed with limestone or plant ash. The high levels of these three oxides suggest botanic ash might be the dominant flux, conversely, limestone was more likely to have been the main fluxing agent (Wood 1999, 32). However, the boundary between the 'high' and 'low' value of these three indexes has not been determined clearly.

Our Yaozhou celadon glaze samples have  $P_2O_5+MgO+MnO$  contents ranging from 1.43 wt.% to 4.06 wt.% with an average of 2.78 wt.%. The Yaozhou celadon glaze samples from these three successive dynasties all contain a certain amount of phosphorus. Furthermore, as shown in Figure 5.8, the  $P_2O_5$  and CaO contents of Tang dynasty and FT dynasty glazes are mainly positively correlated. This suggests botanic ash was probably used as the flux in Yaozhou celadon glazes. The Tang dynasty glaze samples have higher contents of  $P_2O_5$  and CaO than those of the FT dynasty glaze samples, suggesting the higher proportion of flux might be used.

On the other hand, during the Northern Song dynasty, the CaO and  $P_2O_5$  contents in the glaze samples are not correlated. This suggests that, if botanic ash was used as a flux, it might not be the sole source of lime in the Northern Song Yaozhou celadon glazes. Other raw materials having calcium contents but low or negligible  $P_2O_5$  contents might have been used. This will be discussed further.

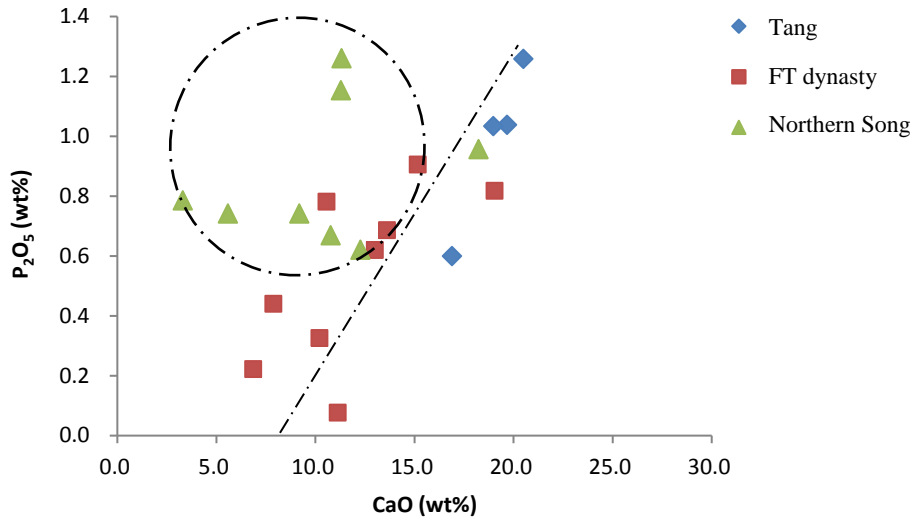


Fig.5.8 The plot of the contents of CaO versus P<sub>2</sub>O<sub>5</sub> (wt%)

#### 5.4.2 The changes in glaze recipes in Yaozhou celadon glaze in the three successive periods

An increase in SiO<sub>2</sub>+Al<sub>2</sub>O<sub>3</sub> contents (9.34 wt.% on average) and a decrease in CaO+MnO+MgO+P<sub>2</sub>O<sub>5</sub> contents (9.17 wt.% on average) in Yaozhou celadon glazes from the Tang dynasty to the Northern Song dynasty have been discerned. This trend could reflect a decrease in lime-bearing fluxing agent to glaze stone proportion in the glaze recipe over these three periods. Besides, the CaO to R<sub>2</sub>O (Na<sub>2</sub>O+K<sub>2</sub>O) ratios also show a decreasing trend from the Tang period to the Northern Song period as shown in Figure 5.9. These two trends actually contribute to the quality development of Yaozhou celadon wares. The typical Yaozhou celadon ware with incised and carved flower decoration reached its mature period in the Northern Song dynasty; the thickness of the glaze layer is a crucial factor in successfully carving the exquisite flower patterns. It is common knowledge that the lower proportion of CaO content, and increased content of K<sub>2</sub>O+Na<sub>2</sub>O can increase the range of melting temperatures during glaze making and enhance the viscosity of melting glaze. Thereby the glaze could be applied more thickly without

running when the wares were fired at the melting heat. Besides, the glaze recipe with a more siliceous raw material and less flux also is helpful to apply thicker glaze without running. By thses, the glaze with a uniform glaze layer and with a better fit to the celadon body could be obtained.

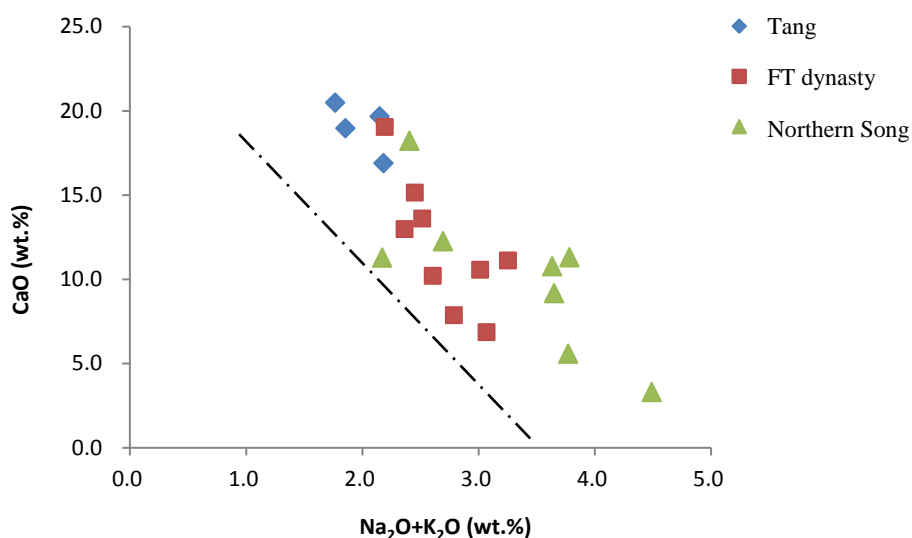


Fig.5.9 the plot of the contents of Na<sub>2</sub>O+K<sub>2</sub>O versus CaO (wt.%)

### 5.4.3 The clues from historical records and REE distribution curves of glaze stone used in Yaozhou celadon glazes

According to historical records, Fuping glaze stone which is a kind of Ordovician shale is the most likely siliceous raw material for Yaozhou celadon glaze making. The collection of Fuping glaze stone from the Mingyue Mountain area in Fuping county (around 30 kilometres away from where the Huangpu kiln is located) for making Yaozhou celadon wares is recorded in the book ‘The Great Gazetteer of Tongguan· Minguo’ 同官县志·民国志, which was compiled in 1944AD by Li Jinxi. Apart from Fuping stone, no other rock has so far been found in the local area which might be used as the major siliceous raw material for Yaozhou glaze making. Therefore, the Fuping glaze stone has been inferred as the possible porcelain stone used for making Yaozhou celadon from a



historical point of view.

Glaze stone is used as the high-siliceous raw material in the glaze. Therefore, the REE distribution curves of the Yaozhou celadon glaze samples should mainly reflect the geochemical characteristics of the glaze stones used. The similar REE distribution curves of Yaozhou celadon glaze samples in Tang, FT dynasty and Northern Song periods are shown in Figures 5.1-5.3. The similarity of the REE distribution patterns infers that, during the three successive periods, the glaze stone used for Yaozhou celadon glaze making probably had the same geochemical source.

However, the slight differences in the REE distribution curves of Yaozhou glaze samples cannot be ignored. The plot of La/Sm versus Gd/Lu and the plot of Eu/Eu\* versus La/Yb as shown in Fig.5.4 and Fig.5.5 both suggest that raw materials used in the majority of Northern Song period glaze samples could be distinguished from glaze samples of the Tang and FT dynasties. It could be inferred that, although glaze stones having the same geological source have been used, it is possible that the glaze stones were selected from more than one location. The potters in the early stage (Tang period and FT dynasty) of Yaozhou kiln seem mainly to have collected the glaze stones from the same location. However, the location from where the glaze stones were mainly collected in the Northern Song dynasty appears to be different.

Taken together, it hence infers that the same geochemical kind of glaze stone might be used as the siliceous raw material in the glaze recipes, and using historical information that Fuping glaze stone could be suggested as a highly likely candidate. However, more than one location of Fuping glaze stone seems to have been selected by the potters in different dynasties.

#### **5.4.4 The Sr isotopic composition pattern of Yaozhou celadon glaze and the suggested flux used in Yaozhou celadon glazes**

All the Yaozhou celadon glaze samples are plotted into two separated mixing lines as in the Figures 5.7. For each mixing line, it is shown that the Sr isotope composition of Yaozhou celadon glaze is controlled by the mixture of two components which varies by different proportions. A primary issue needs to be discussed here: which two components in the glaze recipe are the possible end members defining the Sr isotope composition. Related to this, the long-debated question of whether botanic ash or limestone was used as the fluxing agent in Yaozhou celadon glaze also might be resolved.

According to previous studies mentioned in Section 2.4.4 of Chapter 2, the Yaozhou celadon glaze recipes are mainly made up of two components-the high proportion of siliceous materials and a small amount of fluxing agent. The possible siliceous raw material is commonly thought to be the local glaze stone- 'Fuping glaze stone'. As for the fluxing agent, botanic ash, or limestone 'Liaojiang stone' could be the candidates. Therefore, in the case of Yaozhou celadon, the two components which form the mixing line of Sr isotopic composition are the glaze stone and the flux.

First of all, we can suggest that the limestone ('Liaojiang Stone') is one end member of the mixing line to be investigated with Sr isotope analysis.

According to historical records and previous studies, the proportion of porcelain stone used in high quality limestone glaze ranges between 70 and 95 wt.% and this conclusion is mainly on the basis of the study of South China limestone glazes (Zhou 1958, 14). For the Yaozhou celadon glaze, till now no research has mentioned on the proportion of glaze stone and fluxing agent because the flux of the Yaozhou celadon has not be determined in

depth. However, the analysis of Fuping stone shows that the rock is a kind of high quality glaze stone with only a small addition of calcium-rich flux would have been necessary to produce the celadon (Kerr and Wood 2004, 592). Therefore, we could infer reasonably that, if limestone is used as fluxing agent in the Yaozhou celadon glaze, the highest percentage of limestone in the Yaozhou celadon glaze recipe should range between 5 wt.% and 30 wt.%, and the glaze stone proportion in the glaze recipe should be 70 wt.%-95 wt.%.

As mentioned in Section 2.4.4 of Chapter 2, the local limestone ‘Liaojiang stone’ is Ordovician limestone distributed in Tongchuan City where the Yaozhou kiln sites are located. Although no limestone sample from this area is included in this study, according to previous geochemical studies, the rough Sr concentration value of limestone can be inferred. The Sr concentrations of more than 3000 worldwide Mesozoic and Paleozoic limestone samples were analysed and the average Sr concentration is 460ppm (Veizer 1978). Besides, three Ordovician limestone samples from Fuping County (around 20 kilometres away from where the ‘Liaojiang stone’ is located) were analysed by Wang et al. (2016). It showed that the Sr contents of these Ordovician limestone samples are 213.9ppm, 334.9ppm and 368.6ppm respectively with an average of 365.8ppm, which is a little lower than the average Sr content of worldwide Mesozoic and Paleozoic limestones (460ppm).

To calculate the possible maximum amount of Sr that limestone could contribute to the Yaozhou celadon glaze, it is reasonable to assume the limestone (‘Liaojiang stone’) has Sr content of 460ppm. An approximate range of Sr contents in glazes contributed by ‘Liaojiang Stone’ is  $5\text{-}30 \text{ wt.}\% \times 460 \text{ ppm}$ , 23-138 ppm. From Table 5.4, it can be seen that the Sr concentrations of Yaozhou celadon glazes have rather high levels of Sr

extending in the range from 270ppm to 1327 ppm. Therefore, it means that, the remaining 247-1189ppm of Sr must come from another raw material - 'glaze stone'.

However, this deduction is evidently unreasonable. Firstly, this result is incompatible with the mixing line of Sr isotopic compositions shown in Fig 5.7. Only on the precondition that the glaze samples have two end members containing comparable values of Sr, the Sr isotopic compositions of the glaze samples would display a two component mixing line as in Fig 5.7. On the basis of our hypothesis and deduction above, if limestone is the fluxing agent, the Sr content contribution from the two components would have too large a difference to form a mixing line. Furthermore, in Chinese calcium-glaze recipes, the flux is the necessary lime-bearing component that increases the content of CaO. Therefore it is impossible that the fluxing agent contributes such a low Sr content while the porcelain stone affords such a high Sr concentration. Therefore, conclusively, because limestone is proved to be incapable of providing a high enough Sr concentration in Yaozhou celadon glaze, the possibility that limestone as one end member of the Sr isotopic compositions mixing line can be excluded. It also means that the fluxing agent in the Yaozhou celadon glaze cannot be limestone. Actually, this conclusion is in agreement with a lot of previous research findings, which shows that limestone would not produce such a high concentration of Sr as found in calcium-bearing plant ash. For example, Freestone et al. (2003) found that Egypt limestone introduced a much lower Sr concentration in the glass of only c. 100-200 ppm.

Ruling out the possibility of limestone, the calcium-bearing botanic ash becomes the only possible fluxing agent of Yaozhou celadon glaze. It needs to be pointed out that, animal bone ash can be another possibility supplying high Sr content. However, no historical record mentioned that bone ash had been used in Chinese ceramic production. Besides,

the production of Yaozhou celadon wares was on a large scale, which suggests that it is hard to get enough animal bones for Yaozhou glaze production. Thus animal bone ash is excluded. The Sr compositions of Yaozhou celadon glazes (listed in Table 5.4) show that the Sr concentrations in Yaozhou celadon are high averaging 557 ppm with a large variation extending from 270ppm to 1327ppm. This Sr concentration characteristic of Yaozhou celadon is in accordance with the previous Sr studies of plant ash glass and glaze.

Freestone et al. (2003) and Henderson et al. (2005a) analysed plant ash glasses with a high content of Sr (c.400ppm average published by Freestone et al., 325-626 ppm published by Henderson et al.) were found. Henderson et al. (2009) reported the Sr contents of 30 plants sampled from Syria and one plant from Lebanon, the Sr concentrations of them extend across a wide range from 29ppm to 1070ppm. The only application of Sr isotopic analysis on the glazes (Ma et al. 2014 and 2016) found that the Sr isotopic characteristics of limestone glaze and ash glaze made in Southern China have large differences. Limestone glazes are characterised by low Sr concentrations (basically lower than 100 ppm), while the plant ash glaze is characterised by high Sr concentrations with a large variation (200-800 ppm and an average of around 400 ppm). The high-calcium plant ash could contain very high Sr concentrations of over c.1000 ppm (Ma et al. 2016). The reason for this is that, firstly  $\text{Sr}^{2+}$  replaces  $\text{Ca}^{2+}$  in minerals, and calcareous plants which are the calcium-bearing material and makes them has a certain amount of Sr. Secondly, a more concentrated Sr content would be in the plant ash than the calcareous plant itself because the ashing process burns out the organic materials in the vegetation (Freestone et al. 2003, Henderson et al. 2005a, Ma et al. 2014). The considerably wide range of Sr concentrations is common in plant ash glasses and glazes because the Sr concentrations of plant ashes vary according to a wide range of factors (Henderson et al.

2005a; Barkoudah and Henderson 2006). The Sr concentration depends upon the extent of ashing, the original water content of the plant, the geological source and composition of biologically available Sr (Henderson et al. 2005a, Barkoudah and Henderson 2006). On the basis of the discussion above, we could suggest that the calcium-bearing plant ash should be one end member of mixing line -the flux in the Yaozhou celadon glaze while the other end member influencing the mixing line should be the glaze stone.

#### **5.4.5 The possible contribution of glaze stone to the Sr isotopic composition and the characteristics of glaze stone**

As discussed in Section 5.4.4, glaze stone and calcium-bearing plant ash should be the two components controlling the Sr isotopic composition of Yaozhou celadon glaze. However which of them is the end member affording high Sr concentration, and which is the end member providing low Sr concentration needs further discussion.

According to previous studies of South China calcium glaze (Ma 2014 and Ma et al. 2014), the flux of calcium-bearing plant ash, used as the significant lime-bearing component in the glaze, has been proven to be the one dominating the Sr contribution of glaze. However, it is common knowledge that glaze stone used in North China Yaozhou celadon is largely different from that used in the glaze production in South China in terms of its mineralogy and chemistry. The porcelain stone used in South China is classified as an acid igneous rock with a very low calcium-bearing component, whereas the glaze stone used in Yaozhou celadon according to the historical record is a kind of Ordovician shale. Therefore, it is necessary to discuss whether it is possible for the glaze stone to have an adequate Sr concentration for it to be the end member with high Sr concentrations in Yaozhou celadon.

On the basis of the REEs discussion in Section 5.4.3, the glaze stone used in Yaohzhou celadon glazes of the Tang and FT periods has similar geological and geographical origins. Therefore the glaze stone used in Yaozhou celadon glaze of the Tang and FT periods should have a narrow range of both Sr isotopic signature and Sr concentration. According to previous research findings, on Chinese porcelain glazes, the glaze stone to flux ratio ranges between 4:1 and 3:2. The equations for the Sr contributions from the glaze stone and the flux in glaze samples in the extreme cases are as follows:

$$\text{Sr ppm}_{\text{glaze sample}} = 80\% \times \text{Sr ppm}_{\text{glaze stone}} + 20\% \times \text{Sr ppm}_{\text{flux}} \quad (5.2)$$

$$\text{Sr ppm}_{\text{glaze sample}} = 60\% \times \text{Sr ppm}_{\text{glaze stone}} + 40\% \times \text{Sr ppm}_{\text{flux}} \quad (5.3)$$

By these equations, we can estimate the maximum Sr concentration which the glaze stone could contribute to the glaze.

The Sr concentrations of analysed Yaozhou celadon glaze in this study extends from 270ppm to 1327ppm. If we assume that all of the Sr in an individual glaze with the lowest Sr concentration of 270ppm (sample YZF-5) is contributed by the glaze stone, and the lowest glaze stone to flux ratio of 3:2 is used in this glaze, then we could estimate that the maximum Sr concentration which the glaze stone could have is provided by the equation 5.3. By inserting the Sr concentration of sample YZF-5 (270 ppm) and the Sr concentration of flux (0 ppm based on assumption) in this equation, the Sr concentration of the glaze stone can be obtained as 450 ppm. Then because the highest glaze stone to flux ratio is 4:1, the maximum value of Sr concentration which the glaze stone could contribute to the glaze is  $80.\text{wt}\% \times 450\text{ppm} = 360\text{ppm}$ . This means that, even under this condition, the glaze stone only could contribute around 360ppm at most of Sr to the glaze sample. Compared to the Sr concentration of glaze samples Tang 20 (1007ppm) and Tang

BW6 (1327ppm), the estimated maximum Sr concentration of glaze stone would be still too low for the total Sr concentration in these glaze samples. Therefore, the possibility that the glaze stone is the end member with the high Sr concentration could be excluded. Hence it can be determined that the glaze stone should be the end member with a low Sr concentration while the calcium-bearing plant ash is the end member with a high Sr concentration.

As mentioned in Section 5.4.3, Fuping glaze stone has been inferred as the most likely glaze stone used for making Yaozhou celadon on the basis of historical evidence. Therefore since the glaze stone is the end member component with a low Sr concentration, it means that on the one hand the Sr concentration of glaze stone should be below c.270ppm theoretically, and on the other hand, the glaze stone should contain high enough Sr concentration (not too much below c.270ppm) to influence the total Sr concentration of Yaozhou glaze samples. The bulk of the Sr content in the glaze derived from the lime-bearing portion of the raw materials. Therefore, it seems that a certain proportion of lime-bearing minerals would have been included in the 'glaze stone' used in the Yaozhou celadon. A single chemical composition of Fuping glaze stone has been published by Li and Guan (1979), showing that it has a high CaO content (6.6 wt.%). 'Fuping glaze stone' is a kind of shale, which is mainly composed of kaolinite and calcite (20%-25%), a certain amount of quartz (5%-10%) and feldspar, a small amount of biotite, as well as some trace minerals, such as apatite, zircon and leucosene (Li and Guan 1979). The calcite, feldspar and biotite in the Fuping glaze stone are lime-bearing components and have the potential to contain a suitable Sr content as estimated above. Based on all this information, the historical record that the 'Fuping glaze stone' is the glaze stone used for making Yaozhou celadon glaze seems to make sense. This also could explain the unresolved question in 5.4.1, the identification of raw material in Yaozhou celadon glaze



recipe which has a calcium content and a lack of  $P_2O_5$ , all of which points to the use of 'Fuping glaze stone'.

#### **5.4.6 Possible explanations for the wide spread of $^{87}Sr/^{86}Sr$ signatures in Yaozhou celadon glaze**

As shown in Figure 5.7, the  $^{87}Sr/^{86}Sr$  signatures of Yaozhou glaze samples spread widely, and two separate mixing lines have been identified. Most Tang and FT dynasty period glaze samples share one straight mixing line, while most Northern Song period glaze samples are separated into another different mixing line. The low  $^{87}Sr/^{86}Sr$  ends of the two mixing lines basically share the same  $^{87}Sr/^{86}Sr$  signature. On the basis of what we discussed in Section 5.4.4, the calcium-bearing plant ash is the low  $^{87}Sr/^{86}Sr$  end member with a high Sr concentration. This suggests the  $^{87}Sr/^{86}Sr$  signatures of plant ashes used in Yaozhou celadon glazes of different periods might have been consistent. The  $^{87}Sr/^{86}Sr$  ratio of plant ash is mainly determined by the geological environment and the small-scale hydrology in which vegetation burnt for it grew (Evans et al. 2004, Henderson et al. 2005a). Thus, the plant ashes with similar source might be used for making Yaozhou celadon glazes of different periods.

As seen in Figure 5.7, the two separated mixing lines are formed because the  $^{87}Sr/^{86}Sr$  signatures of the high  $^{87}Sr/^{86}Sr$  end components-glaze stones are quite different. It suggests that the glaze stones used for making glazes on different mixing lines probably came from different sources. Normally the same kind of glaze made in a certain workshop within a short period should use the same source of glaze stone, and therefore the  $^{87}Sr/^{86}Sr$  signature of the glaze stones should be similar. The Tang period glaze samples, FT dynasty samples and Northern Song dynasty glaze samples in this study were

excavated from different archaeological sites and it is highly likely that they were made in different workshops of the Huangpu kiln complex. Based on our analysis, most Tang period and FT dynasty samples and one Northern Song sample might have been made using the glaze stones from the same source, whereas most Northern Song glaze samples and one FT dynasty samples might have been made using the glaze stone with a different source. It can be inferred that, in the Huangpu kiln complex, the different workshops might mainly use the glaze stone collected from a narrow area to produce glazes. However, the glaze stone collection centre shifted in the Northern Song dynasty.

According to the archaeological excavation of the Huangpu kiln complex, so far 84 workshops and 64 kiln sites have been found within the excavated areas of approximate 13000 square meters, suggesting that the workshops are densely distributed. Besides, some workshops exclusively carried out raw material preparation, ceramic moulding and glazing in the Huangpu kiln complex (Shaanxi Provincial Institute of Archaeology and Yaozhou Kiln Museum 1998). Therefore, it is reasonable to suggest that different workshops sometimes shared glaze stone from the same source. With regards to the deduction that the glaze stone collection centre might have been shifted in the Northern Song dynasty. This is in consistent with the REEs discussion in Section 5.4.3. In the Northern Song dynasty, the potters probably used the glaze stone collected from different location with that used in the Tang and FT dynasties. During the Northern Song dynasty, the production of Yaozhou celadon wares went into its golden age. The expansion of Yaozhou celadon production scale might lead to an increase in demand of raw material. Therefore, glaze stones from more than one location might be collected to sustain a large scale of production. It needs to be pointed out that, in future more samples collected from different workshops and periods need to be analysed so as to test this deduction.

### **5.4.7 The Sr isotopic composition as a method of comparing the glaze recipes**

Yaozhou celadon ware is the undoubted representative of Northern China greenware, and the greenware manufacture of South China is thought to be represented by the Yue greenware made in Yue kilns distributed across Zhejiang Province. Besides, archaeologists have reached a consensus that, in the late Tang period, the potters of Yaozhou kilns imitated the manufacturing techniques of Yue greenware mainly in firing techniques, decoration and moulding. However, whether the glaze recipe in Huangpu kiln also imitated that in Yue kiln is still not determined. In this section, the Sr isotopic compositions of Yaozhou celadon glaze and Yue ash glaze will be compared so as to investigate and compare their glaze recipes.

By historical records and chemical composition studies, Yue glazes have been proven to be ash glaze with a CaO content of around 15-20 wt.%. Ma et al. (2014) analysed the Sr isotopic composition pattern of eight Yue ash glaze samples, a pioneering work of Sr isotope analysis applied to Chinese glazes. A plot of Sr isotopic compositions of Yaozhou celadon glaze samples and Yue ash glaze samples (Ma et al. 2014) is given in Fig.5.10.

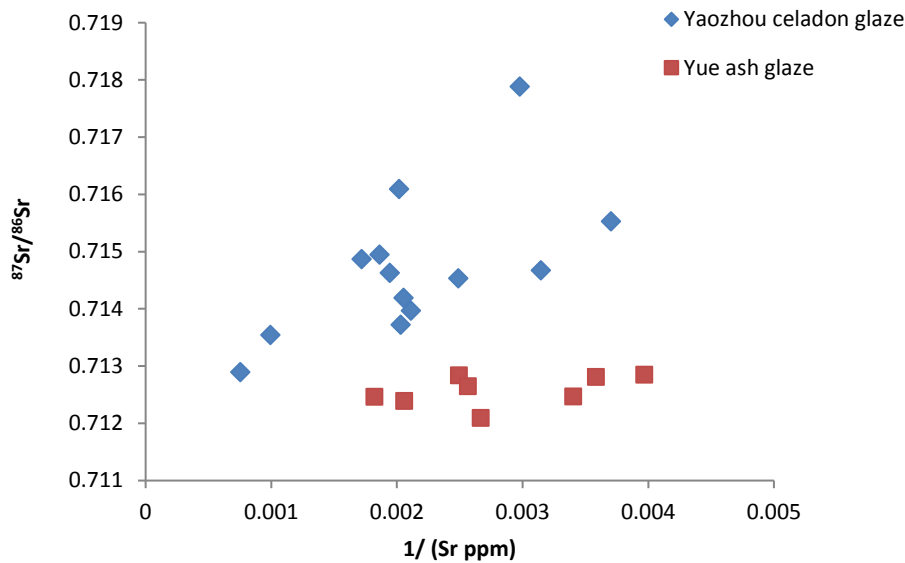


**Fig. 5.10 the plot of 1/ (Sr ppm) versus <sup>87</sup>Sr/<sup>86</sup>Sr of Yaozhou celadon glaze and Yue ash glaze**

In Fig.5.10, it is evident that, although both are plant ash glazes, the Sr isotopic composition patterns of Yaozhou celadon and Yue ash glaze are found to be different to some extent. The Sr contents of both Yaozhou celadon glazes and Yue ash glazes are at a high level with large variations. This has been shown to be the characteristics of plant ash glaze and glass. The differences of Sr isotope compositions between them are mainly reflected in two aspects. Firstly, the <sup>87</sup>Sr/<sup>86</sup>Sr signature of Yue ash glaze is characterised by a consistent <sup>87</sup>Sr/<sup>86</sup>Sr of around 0.712, whereas Yaozhou celadon glaze has higher <sup>87</sup>Sr/<sup>86</sup>Sr ratios with a wider range. Secondly, botanic ash dominates the Sr contribution of the Yue ash glaze, while, the Sr isotopic composition of Yaozhou celadon glaze is controlled by two components together-glaze stone and plant ash. All these distinctions between them might be the reflection of the different geological characteristics and origins of their siliceous raw materials.

The porcelain stone used in South China including Yue kilns can be broadly categorised as an acid igneous rock with a low calcium-bearing component, providing only 50-70ppm of Sr to the final Yue ash glaze (Ma et al. 2014). Wood et al. (2005) analysed the chemical

composition of some porcelain stone used in Yue kilns collected from Shanglinhu, showing that they had low CaO content. Besides, Ma (2014) analysed two porcelain stone samples from the Dehua Kiln also in South China. The results were CaO at 0.5 wt.% and 0.04 wt.%, and Sr concentrations are 130ppm and 73ppm. In contrast, the major raw material of Yaozhou celadon glaze-‘Fuping glaze stone’ contains 20-25 wt.% of calcite and a certain amount of feldspar and biotite; its CaO content can reach 6.6 wt.% (Li and Guan 1978). Therefore, being different from South China porcelain stone, the Fuping glaze stone could have the potential to provide a larger contribution to the Sr isotopic composition. And this might be the reason that different from the porcelain stone of South China, Fuping glaze stone controls the Sr isotopic composition of Yaozhou celadon glaze together with plant ash.

In Chinese glaze recipes, the fluxes are the lime-bearing component. As discussed above, Fuping glaze stone introduces relatively more of the lime-bearing component than the South China porcelain stone have. Therefore, compared to the Yue ash glaze, the theoretical lower flux to glaze stone proportion in the Northern Yaozhou celadon glaze recipe could satisfy the required lime content.

On the basis of archaeological findings, compared to the Yue ash glaze, the most significant improvement of Yaozhou celadon wares making is their thickened glaze allowing decoration with carved flower patterns. As discussed in Section 5.4.2, the lower flux to glaze stone ratios in the glaze recipe is beneficial in producing the typical Yaozhou celadon glaze with a thick glaze layer. Therefore, it suggests that while the potters in Yaozhou workshops imitated the glaze recipe of Yue ash glaze and used the calcium-bearing plant ash as flux, they found and utilised the strength of their local raw materials gradually over time, and finally produced Yaozhou style celadon wares.

## 5.5 Conclusions

1. The flux used for making Yaozhou celadon was calcium-bearing botanic ash. Fuping glaze stone was highly likely to have been used as the glaze stone for Yaozhou celadon glaze making, based on the evidence that the Fuping glaze stone has a certain content of calcium to contribute to the Sr isotopic composition mixing line.
2. The Sr isotopic composition pattern of Yaozhou plant ash glazes is a two component mixing line with a wide range of Sr contents. The calcium-bearing plant ash is the low  $^{87}\text{Sr}/^{86}\text{Sr}$  ratio end member with a high Sr content, while the glaze stone is the high  $^{87}\text{Sr}/^{86}\text{Sr}$  ratio end member with a low Sr content.
3. Two separated Sr isotopic composition mixing lines of Yaozhou celadon glazes are formed because the  $^{87}\text{Sr}/^{86}\text{Sr}$  signatures at the high  $^{87}\text{Sr}/^{86}\text{Sr}$  end components-glaze stones are quite different. It suggests that the glaze stones used for making glazes on different mixing lines probably came from different sources.
4. A decreasing botanic ash to glaze stone ratio in the Yaozhou glaze recipe from Tang period to Northern Song period has been identified. This chronological trend is actually beneficial to the quality improvement of Yaozhou celadon wares.
5. There is a major Sr isotopic contrast between Yaozhou celadon ash glaze and its South China counterpart-Yue ash glaze which reflects the different geochemical characteristics of their siliceous raw materials.

# **Chapter 6 A pilot study of the Sr isotopic composition of ceramic glazes from Al-Raqqa, Syria**

## **6.1 Introduction**

The pilot study of Northern Chinese Yaozhou celadon glaze has suggested that the Chinese glazes whether are fluxed with limestone or plant ash can be inferred by their Sr isotopic compositions. Different from Chinese glaze, Islamic alkaline glazes are usually fluxed with plant ash. Since no similar Sr isotope study of Islamic glaze has been done before, this small study focuses on identifying the siliceous raw material and flux used for making specific Islamic glazes. In this chapter, the Sr isotopic compositions of Al-Raqqa alkaline glazes from Northern Syria are determined as a pilot case study. So far both the siliceous raw material and flux used for making Al-Raqqa alkaline glazes have never been suggested clearly. Therefore, in this pilot study, the Sr isotopic compositions of Al-Raqqa alkaline glazes are used to discuss the Sr isotopic compositions pattern of Al-Raqqa alkaline glaze, and what kind of raw materials were used for making them.

## **6.2 The archaeology of Tell Zujaj and Tell Aswad in the Al-Raqqa industrial complex, northern Syria**

The eight glaze fragments used in this study were excavated from Tell Zujaj and Tell Aswad in Al-Raqqa, located in northern central Syria near the junction of the Euphrates River and its tributary the Balikh River. The industrial sites manufactured pottery (both glazed and unglazed) between c.800 and 1150AD and both primary and secondary glass in the 8th/9th, 11th and 12th centuries (Henderson et al. 2005). A brief history and

archaeological investigations of Al-Raqqa industrial complex have been introduced in Chapter 2. In this chapter, because the glaze samples excavated from Tell Zujaj and Tell Aswad are the major research subjects, a brief introduction of these two sites is presented below.

### **6.2.1 Introduction to Tell Zujaj**

The site of Tell Zujaj excavated between 1992 and 1996 found evidence for glass manufacture as well as glazed and unglazed pottery fragments. The Tell Zujaj site is located in the 'core' of the industrial area and is about 20×15m in size (Henderson 1999, 245).

A complete glass workshop having evidence for both glass making and glass working was discovered at Tell Zujaj. Three major phases of activity related to glass production were discovered and all date back to the late 8th to 9th century. The evidence for glass-working includes hundreds of Abbasid glass vessel fragments, some of which were distorted, pulls of glass, rods of glass, dribbles and drops of glass and a large number of raw glasses with different colours, glass moils (from glass blowing) and fragments of crucible (Henderson 1999, 246, Henderson et al 2005a). The glass-making evidence is in the form of raw glass blocks attached to tank furnace fragments and fragments of semi-vitrified frit; and the discovery of beehive-shaped three-chambered glass furnaces is evidence of glass working (Henderson et al. 2005a).

Pottery of the Abbasid period was found in large quantities in all three phases of the site, including Abbasid glazed wares, unglazed plain and stamp-decorated pottery. It is possible that pottery was made at Tell Zujaj. Although no pottery-making kiln was discovered at Tell Zujaj, kilns for making glazed wares were discovered at Abbasid Tell



Abu Ali in 2010. The middle phase of the glass workshop produced 'Abbasid pottery', but there was a much higher proportion of unglazed wares. A large number of melted furnace bricks were discovered connected to glass making and some of them had melted together (Henderson 1999, 246). Besides, a single sherd of Samarra lustreware dated to as early as AD 820 was found in the disturbed top surface of the surface layer, it is possible evidence for the production of such wares in Al-Raqqa itself (Henderson 1999, 246).

### **6.2.2 Introduction to Tell Aswad**

Tell Aswad is located at the northern edge of the Pleistocene Euphrates terrace, around one km to the east of Tell Zujaj.

The initial excavation of Tell Aswad was conducted by Professor Michael Meinecke between 1982 and 1993. The evidence for Abbasid pottery production was discovered, including a well-preserved pottery kiln, and a lot of industrial dump deposits (Henderson et al. 2005; Henderson 2013, 77).

From 1998, the large-scale investigation and excavation of the Tell Aswad were carried out under the direction of Professor Julian Henderson from the University of Nottingham. In total 14 incomplete kilns which belong to three contemporary kiln groups were identified. Some fragmentary structures were also identified, which could suggest the kiln construction, demolition and reconstruction. Besides, a large number of pottery sherds and wares were also discovered, including unglazed wheel-thrown vessels which account for around 90% of the total number of sherds so far, relief-moulded unglazed pottery and glazed earthenwares. This excavated evidence suggests that one or more of the pottery workshops dates back to late 8th and 9th centuries at Tell Aswad (Henderson et al. 2005a). That large-scaled pottery production developed at Tell Aswad can be explained for two

major reasons. Firstly, the inhabitants of the Al-Raqqa/ Al-Rafika cities created a demand for a large amount of simple but functional ceramic objects. Secondly, the geographical environment of the Al-Raqqa complex is highly suitable for pottery and glass production on a large scale because the Euphrates valley and the surrounding limestone steppe could provide plenty of glass and pottery making raw materials including clay, quartz, sand and plants (Henderson et al. 2005). Tell Aswad produced pottery of similar types and date to that found at Tell Zujaj (Henderson et al. 2005a).

## **6.3 Samples**

Eight turquoise monochrome glaze shards were supplied by Professor Julian Henderson. These are the so-called 'Raqqa ware'. Five of them (Syria-1, Syria-2, Syria-5, Syria-8, Syria-9) were excavated from Tell Zujaj and the rest (TA1043, TA357 and TA327) were unearthed from Tell Aswad. All these glaze samples are dated to the Early Islamic (8th–9th centuries AD) Abbasid Empire. The pictures of all these samples are shown in Appendix II A-20.

## **6.4 Results**

### **6.4.1 The major elemental composition of Al-Raqqa turquoise monochrome glaze samples**

Using the JEOL JXA-8200 electron microprobe located in Department of Archaeology, the University of Nottingham, major elemental compositions of Al-Raqqa glaze samples were determined following the methodology described in chapter three.

Sample No.	Excavated Locations	SiO <sub>2</sub>	Al <sub>2</sub> O <sub>3</sub>	Na <sub>2</sub> O	K <sub>2</sub> O	CaO	MgO	P <sub>2</sub> O <sub>5</sub>	CuO	FeO	MnO	TiO <sub>2</sub>
Syria-1	Tell Zujaj	67.03	5.20	11.03	3.74	7.13	2.53	0.19	1.28	1.13	0.04	0.12
syria-2		62.55	3.97	12.44	2.94	5.64	2.12	0.22	6.45	0.96	0.04	0.10
Syria-5		57.05	9.50	7.33	3.60	10.26	4.59	0.11	1.23	3.52	0.05	0.38
Syria-8		62.76	5.52	9.85	3.47	6.88	2.31	0.17	3.95	1.09	0.04	0.11
syria-9		65.50	2.44	15.63	1.79	7.19	3.20	0.22	1.71	0.67	0.03	0.06
TA1043	Tell Aswad	64.11	3.74	8.92	4.21	8.21	2.17	0.30	4.56	1.11	0.04	0.14
TA357		66.21	3.55	9.60	3.70	6.53	2.22	0.25	4.57	0.98	0.04	0.11
TA327		69.28	3.16	11.08	3.24	6.36	2.64	0.29	1.58	0.82	0.03	0.14

**Table 6.1 the major chemical compositions of ‘Raqqa ware’ glaze samples (wt.%)**

The major elemental compositions of turquoise monochrome glaze samples from Al-Raqqa sites are listed in Table 6.1. All eight turquoise monochrome glazes are characterised by having high amounts (average % Na<sub>2</sub>O = 10.74) of soda, as well as a certain amount of lime (average % CaO = 7.28) and a small amount of potash (average % K<sub>2</sub>O = 3.34). This suggests that all these samples can be classified into the alkaline-lime glaze group. According to previous studies, this kind of alkali glaze which was used for monochrome yellow, green or turquoise coloured glazes represents the earliest and long lasting tradition of glazing in Egypt and Mesopotamia, stretching from Bronze Age to the Islamic period. This glaze type became less popular in later Islamic ceramics, forming less than 1% of found glazed wares produced after the 9th Century (Henshaw 2010, 53). Because the lead-based glazes were extensively used throughout the Islamic and Byzantine worlds instead of alkali glaze (Tite et al. 1998).

The siliceous raw material and flux are the two basic components of alkaline glaze. The siliceous raw material is the main component of glaze and normally comes from using siliceous sand or crushed quartz (SiO<sub>2</sub>). Soda in this alkaline glaze group is the main fluxing agent which lowers the melting temperature of the siliceous raw material and

which may come from either plant ashes (or possibly natron). The plant ashes or natron normally used for the alkali are soluble in water, therefore, the alkaline glaze is typically created by pre-fritted silica (siliceous sand, or crushed quartz) with plant ashes or natron before preparing the glaze suspension (Hedges and Moorey 1975, 25; Tite et al. 1988, 253; Ziad 2002; Mason 2004, 174). Besides, a certain amount of clay may also be added into the glaze suspension (Tite et al. 1998). In this case, the contents of alumina in these alkali glazes range from 2.44 wt.% to 9.50 wt.% and average in 4.68 wt.%. Therefore, apart from the aluminium derived from silica sand used and (potentially) some diffusion from the body, it seems probable a small content of clay was added to the suspension together with silica (siliceous sand, or crushed quartz) to produce these alkali glazes. With regards to the soda fluxing agent, the levels of lime, potash, phosphorus and magnesia suggest that plant ashes were used. No significant differences in the chemical compositions of glaze samples were observed between the two sites- Tell Aswad and Tell Zujaj, suggesting that a stable glazing technology was used in the two ceramic production sites of Al-Raqqa complex sites. The glazes were all coloured by copper (cupric) oxide.

#### **6.4.2 The Sr isotopic composition of Al-Raqqa turquoise monochrome glaze samples**

Using a Thermo Finnegan Triton Thermal ionisation mass spectrometer located at NERC Isotope Geoscience Laboratory (NIGL), the Sr isotope compositions of five Al-Raqqa alkaline glaze samples were analysed using the established method described in Chapter three. Their Sr isotopic compositions are given in Table 6.2.

Sample No.	Excavated	Date	Sr ppm	<sup>87</sup> Sr/ <sup>86</sup> Sr
------------	-----------	------	--------	------------------------------------

	Locations			
Syria-1	Tell Zujaj	8th-9th Centuries AD	486	0.709340
Syria-5			662	0.709184
Syria-8			600	0.709271
TA327	Tell Aswad		699	0.709003
TA357			675	0.709198

**Table 6.2** the Sr isotopic compositions analysed by TIMS of Al-Raqqa glaze samples

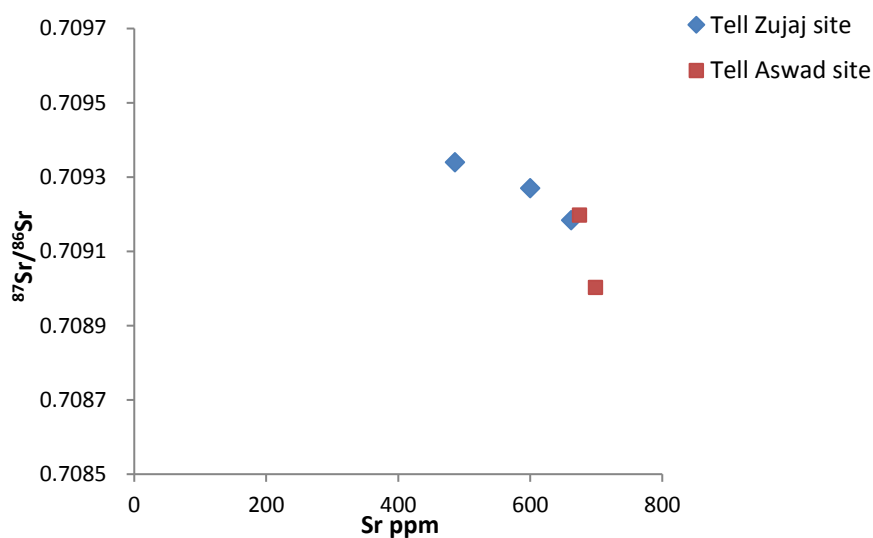


**Fig.6.1** Sr isotopic compositions of Al-Raqqa alkaline glaze samples

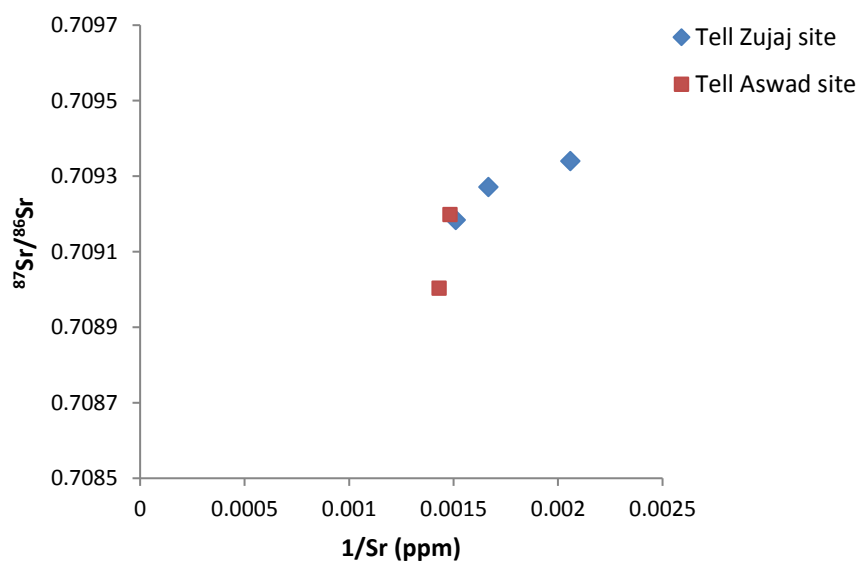


**Fig.6.2** the plot of 1/ (Sr ppm) against  $^{87}\text{Sr}/^{86}\text{Sr}$  of Al-Raqqa alkaline glaze samples

The Sr isotopic compositions of Al-Raqqa alkaline glaze samples are plotted as  $^{87}\text{Sr}/^{86}\text{Sr}$

against Sr ppm in Figure 6.1. The Al-Raqqa alkali glaze samples have relatively consistent Sr isotopic signature ( $^{87}\text{Sr}/^{86}\text{Sr}$ ) with a variation in the fourth decimal digit. With regards to their Sr contents, the relatively large variations ranging from 486 ppm to 699 ppm averages 624 ppm. All the five Al-Raqqa alkali glaze samples array on a straight line in the plot of  $1/(\text{Sr ppm})$  against  $^{87}\text{Sr}/^{86}\text{Sr}$  as shown in figure 6.2. A mixing line in a plot of  $1/(\text{Sr ppm})$  against  $^{87}\text{Sr}/^{86}\text{Sr}$  suggests that the individual glaze was formed from two or more components with different Sr isotope compositions, in differing proportions (Faure 1986). In the case of Al-Raqqa alkali glaze samples, the two components are the siliceous raw materials and the flux. The siliceous raw materials can also be a mixture of different subcomponents. But when dealing with the mixing line, it is simplified to two components for consideration, so we take the siliceous raw material as one component.

## **6.5 Discussion**

### **6.5.1 The Sr isotopic compositional pattern of Al-Raqqa alkaline glaze and the flux of Al-Raqqa alkaline glaze suggested by it**

As seen in Table 6.2 and Figure 6.2, all the five Al-Raqqa glaze samples plot on a straight mixing line, this suggests that their Sr isotopic compositions are controlled by two components in the glaze recipe with different Sr isotope ratios and concentrations. As mentioned in Chapter 3, because strontium generally substitutes for calcium, Sr isotopic compositions of ancient glass or glaze is mainly incorporated with the lime-bearing materials of glass or glaze recipes. K-bearing minerals, such as K-feldspar, micas, clay minerals and others can also influence the Sr isotopic composition of the glass or glaze batch to a small degree (Freestone et al. 2003; Degryse et al. 2006), for the reason that the strontium also can replace potassium in K-bearing silicate minerals. In Islamic alkali

glaze recipes, both the siliceous raw material and flux could be the lime-bearing component, which can occupy the high Sr concentration end of the mixing line. For a natron glaze recipe, the siliceous raw material is the lime-bearing component which might be either coastal sand (shell fragments) or inland sand (limestone-bearing inland sand) and clay, while in the plant ash glaze recipe, the flux-plant ash is likely to be the main lime-bearing component. In this section, an exclusion method is used to discuss which two glaze raw materials contribute to the Sr isotopic composition in this case. And by this, it can be investigated further whether botanic ash or natron was the probable flux used for making Al-Raqqa alkaline glazes.

Firstly, by the archaeological context of analysed glaze samples and their excavated sites, the possibility that coastal sand was used as the siliceous raw material to make the Al-Raqqa alkali glaze can basically be excluded. The Al-Raqqa industrial complex sites are believed to have manufactured pottery (both glazed and unglazed) between c.800 and 1150AD (Henderson et al. 2005). Tell Aswad was an Abbasid ceramic production site by the direct evidence of a well-preserved pottery kilns, and a large number of industrial dump deposits (Henderson et al. 2005; Henderson 2013, 77). Although no pottery-making kiln have been discovered in Tel Zujaj site, the large amount of excavated ceramic wares and fragments and some melted furnace bricks suggest that Tel Zujaj could possibly have been a pottery production site- or there was one nearby. Therefore, the five alkali glaze samples in this study were probably made in Al-Raqqa instead of being imported. The Al-Raqqa sites are distributed near the junction of the Euphrates River and its tributary the Balikh River, which is far away from the coast (the Al-Raqqa complex sites are around 280 km away from the nearest coast of the Mediterranean). A large amount of siliceous raw materials were required to sustain the large scale of production. Therefore, the potters would probably have used local or nearby silica-rich inland sands as the raw material

rather than the distant shell-bearing coastal sands. Besides, there is no historical evidence or previous studies that mention shell-bearing coastal sands being used in Islamic glaze production. Therefore, shell-bearing coastal sands are ruled out in this study. The following possible raw materials and recipes of Al-Raqqa alkali glaze making can be suggested: 1) a natron-fluxed glaze recipe with silica-rich inland sand and clay; 2) a plant ash-fluxed glaze recipe with quartz pebbles or sand and clay.

Whether natron might have been used as a flux in Al-Raqqa alkaline glaze should be discussed here taking the Sr isotopic evidence into account. Natron glazes have two main raw materials: natron and sand. Natron (trona) is a lime-deficient component of glaze and glass recipes with a relatively pure source of sodium carbonate. And natron has been proved to have a negligible contribution to the Sr content and Sr isotopic signatures of glass by Freestone et al. (2003). The silica-rich inland sand used might contain limestone and feldspar and is the only component of the glaze recipe which can contribute to the Sr concentration of the glaze. The average Sr concentration of limestone is 460 ppm (Wedepohl and Baumann 2000). Therefore, the average Sr concentration in inland sands which contains limestone must be less than 460ppm. The average Sr concentrations in sands and undifferentiated sandstone have been analysed by Wedepohl (1978) and are shown to range from 30ppm to 400ppm. Moreover, when natron is added as the flux in the glaze recipe, the percentage of sand in the glaze recipe cannot reach to 100%. Therefore, for the natron-fluxed glaze with limestone-bearing inland sand, the highest Sr concentration must be below 400ppm. However, all the Sr concentrations of the Al-Raqqa alkali glazes analysed in this study are higher than 400 ppm ranging from 486 ppm to 699 ppm and averaging in 624 ppm. Therefore, the possibility that natron was used as the flux and sand is the source of lime and Sr concentration is excluded. In any case, the import of natron from Egypt in large quantities would have been difficult; the use of local plant ash



is far more logical.

Having ruled out the possibility of a natron-fluxed glaze recipe, the use of calcium-bearing plant ashes is the only possible flux of Al-Raqqa alkaline glaze. The Al-Raqqa alkali glazes in this study have high Sr concentrations of averaging c.624 ppm, which is in accordance with the previous Sr concentration results for plant ash glass and glaze. In the Section 5.7.4 of Chapter 5, the high concentration of Sr in plant ashes has been discussed in detail- and how it can contribute to the high Sr concentrations that have been found in glasses and glazes. The plant ash-fluxed Yaozhou celadon glazes discussed in chapter 5 have Sr concentrations ranging from 270ppm to 1327ppm with an average of 557 ppm. The plant ash Chinese Yue glaze is also characterised by high Sr concentrations averaging around 400 ppm (Ma et al. 2016). Besides, plant ash glasses from Banias (in Israel) and Al-Raqqa (in Syria) also have high Sr concentrations ranging from around 300 ppm to 600 ppm and averaging around 400ppm (Freestone et al. 2003; Henderson et al. 2005a; Henderson et al. 2009). Therefore, on the basis of the discussion above, it could be suggested that the calcium-bearing plant ash might be one end member of a mixing line and used as the flux in the Al-Raqqa alkali glazes. The Sr isotope compositional pattern of Al-Raqqa alkali glazes confirm that the plant ash was used as the flux, which is suggested by the relatively high contents of K<sub>2</sub>O (3.34 wt.% in average) and MgO (2.72 wt.% in average) of these glazes.

## 6.5.2 The possible contribution of siliceous raw material to the Sr isotopic composition of Al-Raqqa alkali glaze and the characteristics of the siliceous raw material used

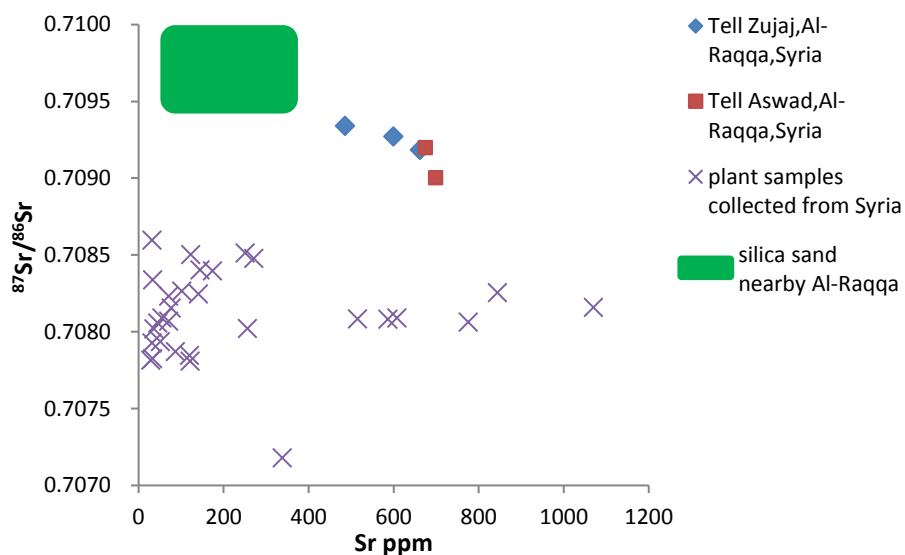


**Fig.6.3 Sr isotopic compositions of Al-Raqqa alkaline glaze samples and plant samples of Syria area. The ‘plant samples collected from Syria’ data are from Henderson et al. (2009)**

All five Al-Raqqa alkaline glaze samples are plotted on a straight line as shown in Figure 6.2. This suggests that their Sr isotope compositions are controlled by two components in the glaze recipe. One end member affords the high Sr concentration with the relatively lower  $^{87}\text{Sr}/^{86}\text{Sr}$  ratio below 0.70900; the other end member provides the low Sr concentration with the higher  $^{87}\text{Sr}/^{86}\text{Sr}$  ratio of above 0.70934. Plant ash has been suggested as one end member as discussed in Section 6.5.1. Besides, the plant ash used as a flux is the lime-bearing component in the plant ash recipe. Therefore, theoretically, plant ash used in Al-Raqqa alkali glazes must occupy the high Sr concentration end of the mixing line with the  $^{87}\text{Sr}/^{86}\text{Sr}$  ratios below 0.70900. This inference can be supported by the  $^{87}\text{Sr}/^{86}\text{Sr}$  ratios data of 30 plant samples collected from different areas of Syria. All the  $^{87}\text{Sr}/^{86}\text{Sr}$  ratios of 30 Syria plant samples analysed by Henderson et al. (2009) are below

0.70900 ranging from 0.70689 to 0.70860 (shown in Figure 6.3). Therefore, it is reasonable to suggest that the calcium-bearing plant ash might be the end member on the mixing line with high Sr concentrations and low  $^{87}\text{Sr}/^{86}\text{Sr}$  ratios.

Islamic plant ash glazes are composed of two main raw materials: plant ash and silica, the latter either quartz pebble or sand and clay. Plant ash has been proven to be the end member with a high Sr concentration and low  $^{87}\text{Sr}/^{86}\text{Sr}$  ratios on the mixing line. Therefore the siliceous raw material should be the one contributing the low Sr concentrations with high  $^{87}\text{Sr}/^{86}\text{Sr}$  ratios of above 0.70934. Both quartz pebbles and sands can be found in Syria near the site of Al-Raqqa. The quartz pebbles derived from the erosion of metamorphic terrains can be collected from the bed of the river Euphrates near Raqqa, and they may have been used in some Al-Raqqa plant ash glasses (Henderson et al. 2005a). With regards to the sand, fine-grained sandstone, clay, siltstone and gypsum assigned to the late Miocene age outcrop extensively in the east of Syria (Demir et al. 2007). Besides, the terrestrial sediments assigned to the Pliocene outcrop widely in eastern Syria around Deir ez-Zor (about 100km to the east of Al-Raqqa). The terrestrial sediments consist of sand and gravel with calcareous clay and gypsum interbeds (Demir et al. 2007). The sands can easily be obtained from these areas. The use of quartz pebbles or sands as the siliceous raw material in the Al-Raqqa alkali glaze needs to be discussed according to their Sr isotopic compositions.

Quartz pebbles are a lime-deficient component. Henderson et al. (2005) analysed two quartz pebbles collected from the bed of the river Euphrates near Al-Raqqa, finding that their Sr concentrations are low: 26 ppm and 0.26 ppm respectively. The low Sr concentrations suggest that if pebbles were used as the siliceous raw materials, it would have been too low to influence Sr concentrations in the final isotopic compositions of

glazes. This is incompatible with the analysed Sr isotopic compositions of Al-Raqqa alkali glazes. Therefore, the possibility that quartz pebbles were used as siliceous raw materials is basically excluded.

The only other source of siliceous raw material is inland silica sands which could contain a certain amount of Sr ranging from 30ppm to 400ppm depending on the amount of carbonate and silicate fractions within them (Wedepohl 1978). Thus silica sand has the potential to contribute to the mixing line of the Sr isotopic composition. However, to confirm that inland silica sands were used in Al-Raqqa alkali glazes, the  $^{87}\text{Sr}/^{86}\text{Sr}$  ratio also needs to be considered. The low Sr concentration end of the Al-Raqqa alkali glazes mixing line points to an  $^{87}\text{Sr}/^{86}\text{Sr}$  ratio above 0.70934, suggesting that the  $^{87}\text{Sr}/^{86}\text{Sr}$  ratio of silica sand used to making Al-Raqqa alkali glazes must have been above 0.70934.

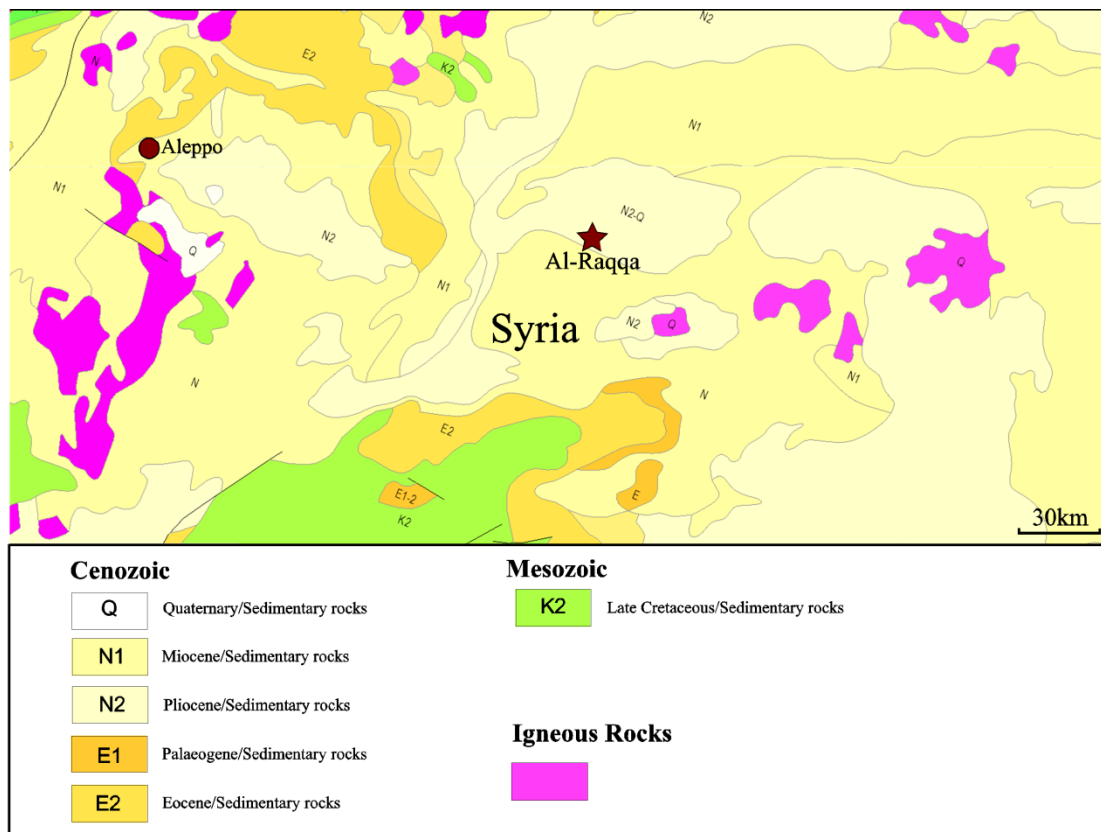


Figure 6.4 the geology around Al-Raqqa, Syria

According to the 1:1500000 geological map of Syria shown in Figure 6.4, the whole of

the area which includes the Al-Raqqa region is mainly formed by the Pliocene-Pleistocene sediments and Miocene sediments (both belong to the Cenozoic era) (Figure 6.4), therefore it is highly likely that the silica sands used to make the glazes were collected from these Cenozoic sediments. No Sr isotopic compositions of sands or sediments from this area have been analysed before. However, the Sr isotopic ratio range of the Cenozoic sediments of Al-Raqqa (Northern Syria) area can be estimated by that of Eastern Europe area, which it is also mainly formed by Cenozoic sediments. The  $^{87}\text{Sr}/^{86}\text{Sr}$  values of 179 natural mineral water samples from Cenozoic sediments in regions of Europe were analysed by Susanne et al. (2010), showing an  $^{87}\text{Sr}/^{86}\text{Sr}$  range of between 0.7090 and 0.7110 (0–2‰). Natural mineral water obtains its strontium isotopic content and characteristics from the processes of dissolution and re-precipitation from minerals in the soil and rock strata through which it percolates. Because no significant isotope fractionation occurs, it is assumed that in young natural mineral waters the strontium isotopic signature reflects that of the surface geology (Susanne et al. 2010). Therefore, Susanne et al. (2010) assume that  $^{87}\text{Sr}/^{86}\text{Sr}$  values of 0.7090 to 0.7110 (0–2‰) can reflect the  $^{87}\text{Sr}/^{86}\text{Sr}$  ratios of surface geology of these Cenozoic sedimentary units in Europe. Thereby, by the  $^{87}\text{Sr}/^{86}\text{Sr}$  values of Cenozoic sediments of Europe, the Sr isotopic ratio range of the Cenozoic sediments of this Syrian area can also be inferred as having a range of 0.7090 to 0.7110 (0–2‰). This proves that the  $^{87}\text{Sr}/^{86}\text{Sr}$  ratio of silica sand nearby Al-Raqqa (Northern Syria) area can satisfy the above deduction that the  $^{87}\text{Sr}/^{86}\text{Sr}$  ratio of siliceous raw material used for making Al-Raqqa alkali glazes must be above 0.70934. Therefore, both the Sr concentration and  $^{87}\text{Sr}/^{86}\text{Sr}$  ratio suggest that silica sand collected from the nearby Cenozoic sediments (either local or, less likely, imported from other locations of Syria) might be the source of the siliceous raw material used in Al-Raqqa alkali glazes.

On the basis of the discussion above, it can be suggested that it is highly possible that the Al-Raqqa alkali glazes were made by sand collected from the nearby Cenozoic sediments and fluxed with calcium-bearing plant ash. Besides, the Sr isotopic composition pattern of Al-Raqqa alkali glaze is mainly controlled by the Sr isotopic composition of calcium-bearing plant ash which contributes to the high Sr concentration and low  $^{87}\text{Sr}/^{86}\text{Sr}$  ratio, while the silica sand is the end member contributing to low Sr concentration with the high  $^{87}\text{Sr}/^{86}\text{Sr}$  ratio above 0.70934. Nevertheless only five Al-Raqqa glaze samples are included in this study as a pilot case study and further research on more Islamic glaze samples is necessary in order to provide more rigorous evidence of the Sr isotopic composition pattern of Al-Raqqa and other Islamic glazes.

### **6.5.3 The connection between the glass production and glazed ceramic production in Al-Raqqa**

The Sr isotopic compositions of Al-Raqqa plant ash glasses of 8th -9th Centuries AD analysed by Henderson et al. (2005a and 2009) are plotted together with those of Al-Raqqa plant ash glazes in this study in Fig.6.5 for comparison. By determining neodymium isotope compositions in the Raqqa glasses, it is clear that sands were used rather than quartz to make both raw furnace and vessel glasses (Henderson et al. 2009). Al-Raqqa plant ash glasses are believed to be made by plant ash and sand (Henderson et al. 2005a, 2009). In this study, the Al-Raqqa alkali glazes also have been suggested as being made from lime-bearing plant ash and sand. As can be seen in Figure 6.5, it is evident that different sources of silica used for making the Al-Raqqa glasses and glazes are reflected by their distinctive Sr isotopic composition patterns. The lime-bearing plant ash with high Sr concentrations dominates the Sr contribution in the plant ash glasses in Figure 6.5, whereas siliceous raw material (sand) makes a negligible contribution

(Henderson et al. 2005a). However, both plant ash and sand contribute to the mixing line of the Sr isotopic compositions of Al-Raqqa glazes. The local plant ashes are suggested as the flux used both in Al-Raqqa plant ash glasses and glazes and these have consistent  $^{87}\text{Sr}/^{86}\text{Sr}$  values. However, compared with the Sr isotopic compositions of glasses, both Sr concentrations and  $^{87}\text{Sr}/^{86}\text{Sr}$  ratios of glazes are elevated. As discussed above, for the Al-Raqqa plant ash glazes, although at present it is difficult to know where the sand derives from (local or other places in Syria), it is likely that the sand was obtained from nearby Cenozoic sediments. The possible Sr isotopic compositional range of this sand is shown in the low Sr concentration and high  $^{87}\text{Sr}/^{86}\text{Sr}$  ratio end of Figure 6.5, which contributes to the both the higher Sr concentrations and  $^{87}\text{Sr}/^{86}\text{Sr}$  ratios of glazes compared to those of glasses. Brems et al. (2013) analysed the Sr isotopic compositions of 77 beach sands from Spain, France and Italy. They found that the Sr isotopic composition of the sand is mainly contributed by the relatively unradiogenic Sr from the carbonates and the higher  $^{87}\text{Sr}/^{86}\text{Sr}$  ratios from the aluminosilicates. The radiogenic Sr in the silicate fraction of the sand, most probably in feldspar, and sometimes mica, can make the sand with higher  $^{87}\text{Sr}/^{86}\text{Sr}$  ratios above the modern value for seawater (Brems et al. 2013). The carbonate fraction of the sand supplies the main Sr concentration in the sand. Depending on the mineralogy and the amount of carbonate present (e.g. limestone grains) in the sand, the average Sr concentrations in sands and undifferentiated sandstones are in the range of 30-400 ppm (Wedepohl 1978). Therefore, in this study, compared to the source of sand used for Al-Raqqa plant ash glass production, the higher Sr concentration and  $^{87}\text{Sr}/^{86}\text{Sr}$  ratio of sand used to make glazes is probably due to the higher content of limestone grains and feldspar with radiogenic Sr. One Al-Raqqa glass (Raqqa-61) has higher  $^{87}\text{Sr}/^{86}\text{Sr}$  ratio than that of other Al-Raqqa plant ash glasses, whereas it is relatively similar to that of Al-Raqqa plant ash glazes. This suggests that the feldspar-rich continental sand with radiogenic Sr was

used. Nevertheless further research using Neodymium isotope analysis, for example, is necessary, in order to provide more information about the source of sand used for glaze production.

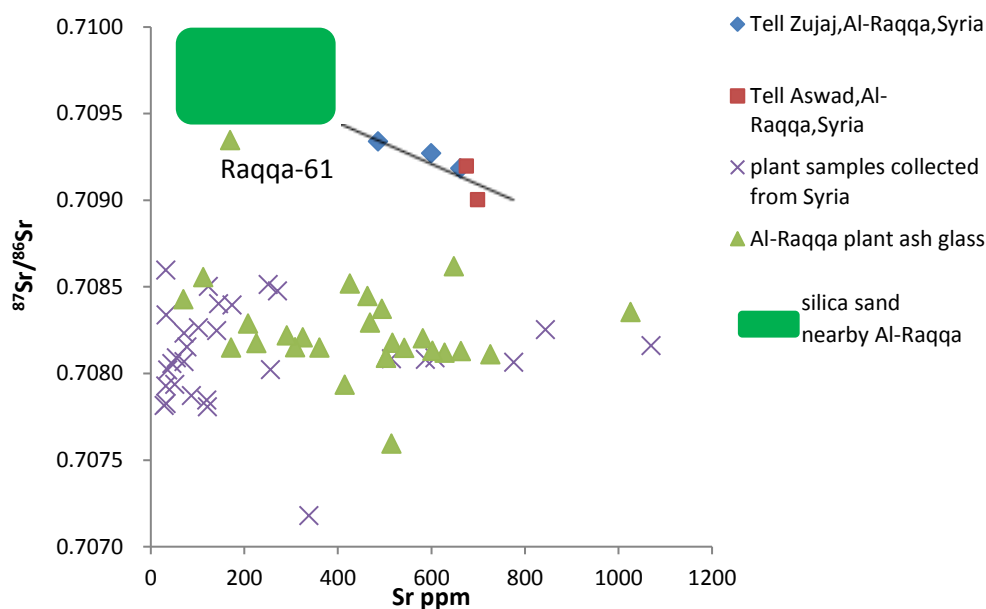


**Fig.6.5 Sr isotopic compositions of Al-Raqqa alkaline glaze samples, Al-Raqqa plant ash glass samples and plant samples of Syria area. The ‘Al-Raqqa plant ash glass’ data are from Henderson et al. (2005a and 2009) and the ‘plant samples collected from Syria’ data are from Henderson et al. (2009)**

In this study, it has been found that during the 8th-9th Centuries, the Al-Raqqa glass makers selected sand to produce both glass and glazes. However, the strontium isotope results are quite different. This suggests that although both glazed pottery and glass was made in Al-Raqqa during the 8th-9th Centuries, the developments in glass and glaze making largely followed their own courses according to different sources of sands with distinct isotopic characteristics.

Plant ash glass replaced natron glass in 9th Century Syria, which means that sand fluxed by natron are replaced by siliceous raw material (sand or quartz) fluxed with plant ash (Henderson et al. 2004). Sand usually contains feldspar, clay and mineral inclusions such



as plagioclases, pyroxenes and ilmenite. These inclusions in sand account for much of the impurities like alumina, iron and titanium in the final glass (Deer et al. 1966; Bezborodov 1975; Henderson 2000, 26-27; Henderson et al. 2004). Therefore, if quartz did replace sand as the silica source although there is very limited evidence for this, or sand with fewer impurities used as the silica source, it is a progressive ‘purification’ of the final glass (Henderson et al. 2004). The glaze is used to cover ceramic surfaces, which requires the expansion and contraction coefficient between the glaze and clay ceramic to be close. The alumina is a refractory material which is beneficial to help to match the glaze’s expansion and contraction coefficient to the clay ceramic body, thereby aiding a better glaze fit. Therefore, the sands with different geochemical characteristics and sources might be selected to produce glass and glaze separately. Given the limited number of samples in this study, it may be that other siliceous raw materials (crushed quartz) and sources were used to make Al-Raqqa plant ash glazes. Further studies of more Al-Raqqa glaze samples, especially those that can be proven to have been made in Al-Raqqa is necessary to place these results in a broader context.

## **6.6 Conclusions**

1. According to the discussions in this chapter, the flux used for making Al-Raqqa alkali glazes can be suggested as a calcium-bearing plant ash, and sand collected from the nearby Cenozoic sediments is highly likely to have been the siliceous raw material used for making for Al-Raqqa alkali glazes.

2. The Sr isotopic composition pattern of Al-Raqqa alkali glaze is a two-component mixing line in the high Sr content range. Calcium-bearing plant ash is one end member with high Sr concentrations and low  $^{87}\text{Sr}/^{86}\text{Sr}$  ratio, while the sand used is the end

member with low Sr concentration and high  $^{87}\text{Sr}/^{86}\text{Sr}$  ratio.

3. There is a major Sr isotopic composition difference between Al-Raqqa plant ash glaze and glasses, which reflects the different geochemical characteristics of their siliceous raw materials used- sand from two different sources were used for glaze and glass production.

## **Chapter 7 Conclusions and future work**

The results of this study have shown that it is possible to investigate the manufacturing techniques and provenance of different types of glazes by the application of chemical and isotopic analyses.

### **The application of chemical and lead isotopic analyses on lead glazes**

The chemical compositions of lead glazes can be used to discern possible raw materials and glazing techniques used to produce them, and specifically, whether a lead compound by itself or a mixture of lead oxide plus quartz/sand was used in glaze making and whether the clay was added. In the case study of this thesis, for Chinese Tang Sancai glazes, the mixture of lead oxide, quartz/quartz sand and clay was applied. With regards to Islamic splashed lead glazes, the mixture of a lead compound plus quartz/quartz sand was applied and clay might be added into the glaze suspension sometimes.

The trace element compositions and lead isotopic ratios of lead glazes potentially determine the origin of production centres of glazed ceramics with unknown origins. In this study, by comparing the selected chalcophile trace elements, lithophile trace elements and lead isotopic ratios of lead glazes, the Tang Sancai wares excavated from tombs with unknown origin can be associated with their probable production kilns.

By comparing the lead isotopic ratios of lead glazes and those of lead ore sources, the possible sources of lead used for making lead glazes can be suggested. However, in some cases, the overlap of lead isotopic signatures among some different lead ore sources make it impossible to associate the lead used in glaze making with a specific lead ore source.

For the Iraqi glaze samples, the lead ore deposits both from Middle Eastern areas and

Mediterranean areas are possible sources of lead used for making them. The overlap of lead isotopic signatures among some different lead ore sources make it impossible to decide definitely whether the lead derives from Middle Eastern areas or Mediterranean areas.

During the Tang dynasty (AD618-906), Tang imported glazed ceramics traded by Maritime Silk Route and their techniques have proven to stimulate the changes of early Islamic ceramic techniques to some extent. High lead glazed ceramic-Tang Sancai ware made in North China was one imported Chinese ceramic type which enlightens Islamic potters on applying multiple colours to a pottery's surface often in a semi-haphazard manner (Fleming et al. 1992). The high lead splashed wares made in the Middle East starting from around 8th century AD are thought to be influenced by imported Tang Sancai wares. A brief comparison work between Chinese Tang Sancai and Islamic high lead splashed wares has been conducted in this study. The similar glazing technique- the use of lead oxide plus quartz or sand were applied to both Chinese and Islamic lead glazes. Besides, the main difference in glaze recipes between them is that different colorants were used for brown-coloured glaze. For the Chinese Tang Sancai glaze, the iron oxide was used, while the iron oxide plus manganese together were used in Islamic lead glaze. Besides, all Chinese Tang Sancai glazes are transparent, while two Islamic splashed lead glaze samples in this study are found to be tin-opacified, which was used widely by Islamic potters since the second half of the 8th century AD. The application of lead-silica mixture in both the lead glaze production of China and the Middle East most probably occurred independently in each region. The Islamic splashed wares mainly attempt to simulate the appearance with multiple splashed colours of Chinese Tang Sancai based on their own lead glazing techniques. Besides, some imported Tang Sancai wares have been found in some Islamic countries such as Egypt, Iraq, Iran and Uzbekistan (Lane 1947, 12;

Needham 2004, 732-733; Watson 2004, 47). In this study, the distinct Pb isotopic ratios of Tang Sancai glazes made in two important production kilns have been found, which might be used to identify the possible production centres in North China where the Chinese imported Tang Sancai excavated in the Middle East produced.

### **Tang Sancai trade along the Maritime Silk Route**

Chinese Tang Sancai's influence on Islamic splashed lead glaze ware and the similarity of their glazing techniques discussed in the study reflect the mutual exchange and communication between Chinese ancient ceramics and Islamic ceramics along the land trade Silk Road, especially its watery counterpart-the Maritime Silk Route. Before the middle of 8th Century, the Silk Road dominated the international trade. In general, the Silk Road started in Chang'an (now called Xi'an) which was the capital of China in Tang Dynasty, passed through Dunhuang and Xijiang region, then tracked through Central Asia and finally descend west to Samarkand or south toward India (Hansen 2012). Silk, chemicals, spices, metals, saddles and leather products, glass, and paper were common trade goods (Hansen 2012). Only a little evidence was found to suggest that ceramic trade including Tang Sancai ware was conducted through the Silk Road during the Tang. The Tang Sancai fragments and wares unearthed in Amol county, Nishapur and Sha'al Ghazna, Kish in Iran (Wilkinson 1973, 54) showed the evidence of Tang Sancai trade by land Silk Road. From the middle of the 8th Century, the Maritime Silk Route started in China's southeast coast areas, tracked through South China Sea, then crossing over the Indian Ocean and Arabian Sea, finally arrived in Africa's east coast areas or crossing over the Red Sea and arrived in the Mediterranean countries became popular (Huang and Liu 2007, 38; Lewis 2009, 161). By this, porcelain became the major Chinese commodity trans-

shipped through India, because ceramics were too heavy and could be easily broken, which was possible only with the advent of sea trade (Lewis 2009,163). The Tang Sancai wares and fragments found in different places along 'Maritime Silk Route' have shown the evidences of exports of Tang Sancai. Specifically, 598 Tang sancai shards and wares were found in the Yang Zhou city in China (Li 2003, 69-70), which a principal port for imports and exports during the Tang dynasty; Tang Sancai wares and their local imitations were unearthed in Samara (Iraq) and in Fustat (Egypt) (Lane 1947, 12); the Tang sancai wares with high quality were found in Belitung cargo, a Tang cargo which sank on the western coast of Indonesia, in the western Java Sea (Guy 2001-2002, 17). Besides lead-glazed Tang Sancai, the trade of land Silk Road and Maritime Silk Rout also promoted the exchange of some other lead by-products. Forty-six different silver vessels served as medicine containers were found in Hejiacun in Xi'an city which combine different elements of Iranian and Chinese art in extraordinarily pleasing ways (Hansen 2012); There are 947 coins including both Sasanian and Arabo-Sasanian coins in the late 7th century were excavated in China (Hansen 2012); And there are a large number of lead ingots were found in the Belitung, Intan and Cirebon wrecks representing an significant trade from both India and China into Southeast Asia in metal ingots and broken artefacts for recycling, while at least 97 silver ingots from China were found from the Intan wreck (and 14 from the Cirebon wreck). They are a great rarity showing the history of taxation and currency inside China (Stargardt 2014). The Tang Sancai and other lead by-products mentioned above found along the land Silk Road and Maritime Silk Route reflected the cultural exchange and technology interaction between China and the West.

### **The application of Sr isotope analysis on lime and alkali glazes**

This project is the first time that Sr isotopic analysis has been used to study lime glazes from North China and alkaline glazes from the Middle East. It has revealed that the Sr isotope compositions can provide useful information on the characteristics of raw materials used for making the glazes and determine the glaze recipes of glazes from Northern China and the Middle East.

The Sr isotopic composition of Yaozhou celadon glaze is characterised by a two-component mixing line with large Sr concentration variation in high Sr concentration range. This Sr isotopic composition pattern suggests that the flux used for making Yaozhou celadon was calcium-bearing botanic ash and the glaze stone having a certain content of calcium to contribute to the Sr isotopic composition mixing line was used as the siliceous raw material. Sr isotopic analysis also is found to be a promising method to suggest the origins of the raw materials used in Yaozhou celadon glaze making. Two separated Sr isotopic composition mixing lines of Yaozhou celadon glazes are formed because the  $^{87}\text{Sr}/^{86}\text{Sr}$  signatures at the high  $^{87}\text{Sr}/^{86}\text{Sr}$  end components-glaze stones are quite different. It suggests that the glaze stones used for making glazes on different mixing lines probably came from different sources. By Sr isotopic analysis, it is the first time that the flux of Yaozhou celadon glaze and sources of glaze stone used in glaze making are identified in a more reliable method.

The comparison of Sr isotope compositions between Yaozhou celadon ash glaze and its South China counterpart-Yue ash glaze reflects that the same plant ash flux, and siliceous raw materials with different geochemical characteristics were used in their production. The early production of Yaozhou celadon ware during the Tang dynasty were initially influenced by Yue kiln mainly in firing techniques and developed gradually into their own characteristics by using their local raw materials. Specifically, the use of M-shaped sagger,

the glaze-coated foot and the 'bead-bearing firing method' of Yaozhou celadon production all were influenced by the Yue kiln firing technology (Wang and Eiji 2005). The most important technical advance of Yaozhou celadon comparing to the Yue style greenware was the largely thickened glaze (Guo and Li 1984). This improvement can be attributed to the used of suitable local glaze raw material, and the glazing technique that the wares were always applied in two layers of glaze slip before being fired.

The development, stagnation and decline of green stoneware of North and South China, like other Chinese ceramics, had their own courses with influences between each other on some degree which is mainly influenced by the shift of political centre, the available raw materials and the development of firing techniques (Kerr and Wood 2004, 50; Li 1998; 136). In specific, Yue wares started from the late Eastern Han dynasty (AD25-220) is the initiator and representative of South China green stoneware, while the earliest evidence of northern green stoneware were unearthed from tombs dated to the late Qi (AD550-577) to the early Sui (AD581-618) dynasties (Chen 1956; Feng 1958). During the following Tang Dynasty (AD618-907) and Five Dynasties (AD907-979), the production of green stoneware in North China went through their downturn stage, because the sedimentary clay widespread in North China was fully suitable as raw material used in the white porcelain production, which made it developed rapidly and finally dominated in the ceramic production of North China during this period. While green stonewares with high quality represented by Yue green stonewares flourished in South China (Li 1998, 136). During the following Northern Song dynasty (AD960-1127), with the political centre of authority was set up in Kaifeng in North China, green stonewares of North China represented by Yaozhou celadon stonewares finally ushered in their golden era (Zhuo 2008). However, after the Jurchen Jin-Northern Song war in AD1127, the Northern Song Empire lost the entire North China to the Jurchen Jin, the political centre of authority was



moved to South China and set up Southern Song Empire (AD1127-AD1279). The production centre of green stonewares was moved accordingly to South China again. The ceramics production of South China kept prosperous in the following dynasties, in contrast, the northern green stoneware including Yaozhou celadon wares has never actually recovered again (Zhuo 2008). The Yue green stonewares declined and was instead by the southern Longquan green stonewares during the Southern Song Empire, because the Longquan kiln improved the raw material recipe (Li and Ye 1989, 166), enhanced the firing temperature and reducing atmosphere (Li 1998, 137), which made Longquan wares had top quality.

Similar to Sr isotopic analysis on Yaozhou celadon glazes, the case study of the Al-Raqqa alkali glazes from Northern Syria reveals that Sr isotopic compositions is also a promising method to suggest the glaze recipes and characteristics of raw materials used in the production of glazes from the Middle East. The Sr isotopic composition pattern of Al-Raqqa alkali glaze is also a two-component mixing line in the high Sr content range. Based on the characteristics of Sr isotopic compositions, the flux used for making Al-Raqqa alkali glazes can be suggested as a calcium-bearing plant ash, and sand collected from the nearby Cenozoic sediments with a certain content of limestone grains and feldspar is highly likely to have been the siliceous raw material used.

### **Future work**

So far, in China, four kiln sites producing Tang Sancai ceramics have been discovered. In this case study, the distinct characteristics of trace element compositions and lead isotope ratios of the Huangye kiln and Huangpu kiln have been identified. In future work, the chemical and lead isotopic analyses could be carried out on the glazes of Tang Sancai ceramics made in the rest of the two production kilns- the Liqianfang kiln in the Shaanxi

Province and the Neiqiu kiln in the Hebei Province to see whether the Tang Sancai wares made in this four kilns can be distinguished by the trace elements Sb, Sn, Cr/La ratio, Zr/Ti ratio, Cs and Ba and lead isotope ratios of their glazes. By this, the Tang Sancai ceramics excavated in archaeological sites with unknown origin could be associated with the production centre. The transfer of manufacturing techniques and the trade of Tang Sancai in China can be discussed in detail. Besides, so far the lead sources used to make glazes of Tang Sancai wares could not be determined due to the lack of lead isotopic ratios of possible lead ore sources: these should be determined in future work. By this, the exploit and trade of lead ore sources can be discussed.

For the Islamic splashed lead glazes, the different sources of lead were found to make glaze excavated from the Kish-shaal Ghazna sites by the trace element compositions and lead isotopic ratios, which infer that the Iraqi glazed pottery wares unearthed from the the Kish-shaal Ghazna sites might be imported from the different ceramic-making sites (see discussion in Chapter 6). However, the limited glaze samples in this case study make it hard to identify the possible ceramic-making sites. In future work, some more glazed pottery excavated in Kish-shaal Ghazna sites need to analyse to provenance the origin of them, which is helpful to discuss the trade of Islamic lead glazed pottery. Besides, based on lead isotope ratios, we found that the lead used to produce two Iraqi glaze samples were probably obtained from the remote Sardinian and Spain areas respectively. Some more Iraqi lead glazed pottery is necessary to study in future to identify the trade of lead deposits between the Middle Eastern regions and Mediterranean areas.

Based on Sr isotope compositions of glazes, the possible flux used to make Yaozhou celadon glazes and Raqqa ware glazes have been suggested, which is plant ash. However, the Sr isotope composition only can give some limited information on the characteristic

of siliceous raw materials used in glaze making. In future work, further research like neodymium isotope analysis is necessary to study on Yaozhou celadon glazes and their possible siliceous raw material 'Fuping stone' or local clay to identify the source of siliceous raw material used in Yaozhou glaze production. For the Raqqa ware glazes, the neodymium isotopic compositions of Cenozoic sands collected near Al-Raqqa should be analysed to confirm the sources of sands used to make them.

## Bibliography

Albarède, F., Desaulty, A.M., and Blichert-toft, J. 2012. "A geological perspective on the use of Pb isotopes in Archaeometry." *Archaeometry* 54(5): 853–867.

Allen, R.O., Rogers, M.S., Mitchell, R.S., and Hoffman, M.A. 1982. "Geochemical approach to the understanding of ceramic technology in pre-dynastic Egypt." *Archaeometry* 24(2): 199-212.

Al-Hassan A.Y. 2009. An eighth century Arabic treatise on the colouring of glass: *Kitāb al-durra al-maknūna* (the book of the hidden pearl) of Jābir ibn Ḥayyān (c.721-c.815). *Arabic Sciences and Philosophy* 19: 121–156.

Al-Saa'd, Z. 2000. "Technology and provenance of a collection of Islamic copper-based objects as found by chemical and lead isotope analysis." *Archaeometry* 42(2): 385-397.

Al-Ziad, Z. 2002. "Chemical composition and manufacturing technology of a collection of various types of Islamic glazes excavated from Jordan." *Journal of Archaeological Science* 29:803–810.

Archaeological Institute of Neiqiu. 1987. "Investigation reports of Xing Kiln 邢窑遗址调查报告." *Cultural Relic 文物* (9): 1-3.

Atil, E. 1973. *Ceramics from the world of Islam*, Washington, D.C: Smithsonian Institution Washington.

Baker, J., Stos, S., and Waight, T. 2006. "Lead isotope analysis of archaeological metals by multiple-collector inductively coupled plasma mass spectrometry." *Archaeometry* 48(1): 45-56.

Barkoudah, Y., and Henderson, J. 2006. "Plant ashes from Syria and the manufacture of ancient glass: ethnographic and scientific aspects." *Journal of Glass Studies* 48: 297-321.

Barnes, I.L., Brill, R.H., Deal, E.C., and Piercy G.V. 1986. "Lead isotope studies of some of the finds from the Serce Liman Shipwreck." in *Proceedings of the 24th International Archaeometry Symposium*, edited by J. S. Olin and M. J. Blackman, Washington, D.C.: Smithsonian Institution Press: 1-12.

Bartle, E.K., and Watling, R.J. 2007. "Provenance Determination of Oriental Porcelain Using Laser Ablation-Inductively Coupled Plasma-Mass Spectrometry (LA-ICP-MS)." *Journal of Forensic Sciences* 52(2): 341-348.

Bishop, R.L., Rands, R.L., and Holley, G.R. 1982. "Ceramic compositional analysis in archaeological perspective." *Advances in Archaeological Method and Theory* 5: 275-330.

Borgia, I., Brunetti, B., Mariani, I., Sgamellotti, A., Cariati, F., Fermo, M., Mellini, M., Viti, C. and Padeletti, G. 2002. "Heterogeneous distribution of metal nanocrystals in glazes of historical pottery." *Applied Surface Science* 185: 206-216.

Borregaard, T. 2000. A scientific analysis of 8th-12th century Islamic glazed pottery from the industrial complex at Raqqa, Syria. Unpublished MSc dissertation. University of Nottingham.

Boynton, W.V. 1984. "Cosmochemistry of the rare earth elements: meteorite studies." *Rare earth element geochemistry*. 16 (7): 63-114.

Brems, D., Ganio, M., Latruwe, K., Balcaen, L., Carremans, M., Gimeno, D., Silvestri, A., Vanhaecke, F., Muchez, P., and Degryse, P. 2013. "Isotopes on the beach, part 1: Strontium isotope ratios as a provenance indicator from lime raw materials used in Roman glass making." *Archaeometry* 55(2): 214-234.

Brill, R.H. 1999. *Chemical Analyses of Early Glasses Volume 1*. New York: The Corning Museum of Glass: Corning.

Brill, R.H., Felker, D.C., Hirahata, H., and Joel, E.C. 1997. Lead Isotope Analyses of Some Chinese and Central Asian Pigments. *Conservation of Ancient Sites on the Silk Road*. Los Angeles: The Getty Conservation Institute: 369-378.

Brill, R.H., Wampler, J.M. 1965. "Isotope studies of ancient lead." *American Journal of Archaeology* 69: 165-166.

Brill, R.H., Wampler, J.M. 1967. "Isotope studies of ancient lead." *American Journal of Archaeology* 71: 63-77.

Brill, R.H., Yamasaki, K., Barnes, I.L., Rossman, K.J.R., and Diaz, M. 1979. "Lead isotopes in some Japanese and Chinese glasses." *Ars Orientalis* 11: 87-109.

Bulliet, R.W. 1992. "Pottery styles and social status in medieval Khurasan", edited by Knapp, A.B. *Archaeology, Annales and Ethnohistory*. Cambridge: Cambridge University Press: 75–82.

Capo, R. C., Stewart, B. W., and Chadwick, O. A. 1998. "Strontium isotopes as tracers of ecosystem processes: theory and methods." *Geoderma* 82(1): 197-225.

Carswell, J., 1998, *Iznik pottery*, London, British Museum Press.

Chen, W.L.陈万里. 1956. *The brief History of Chinese Green Stoneware 中国青瓷史略*. Shanghai: Shanghai People's Publishing House.

Cochrane, E.E., Neff, H. 2006. "Investigating compositional diversity among Fijian ceramics with laser ablation-inductively coupled plasma-mass spectrometry (LA-ICP-MS): implications for interaction studies on geologically similar islands". *Journal of Archaeological Science* 33: 378-390.

Craig, L. 1967. *Arab Tunisia. Guidebook to the geology and history of Tunisia*. Petroleum Exploration Society of Libya.

Cui, J.F., and Lei, Y. 2010. "Lead Isotope Analysis of Tang Sancai Pottery Glazes from Gongyi Kiln, Henan Province and Huangbao Kiln, Shaanxi Province." *Archaeometry* 52(4): 597-604

De Benedetto, G. E., Acquafredda, P., Masieri, M., Quarta, G., Sabbatini, L., Zambonin, P. G., Tite, M., and Walton, M. 2004. "Investigation of Roman lead glaze from Canosa: results of chemical analysis." *Archaeometry* 46: 615 –624.

Degryse, P., Henderson, J., Hodgins, G. 2009. "Isotopes in vitreous materials, a state-of-the-art and perspectives." In *Isotopes in vitreous materials*, edited by Degryse, P., Henderson, J., and Hodgins, G. Leuven: Leuven University Press.

Degryse, P., Shortland, A., Muynck, D.D., Heghe, L.V., Scott, R., Neyt, B., and Vanhaecke, F. 2010. "Considerations on the provenance determination of plant ash glasses using strontium isotopes." *Journal of Archaeological Science* 37(12):3129-3135.

De Laeter, J.R., Bohlke, J.K., Bievre, P.D., Hidaka, H., Peiser, H.S., Rosman, K.J.R., and Taylor, P.D.P. 2003. "Atomic weights of the elements: review." *Pure and Applied Chemistry* 75(6): 683-800.

Demir, T., Westaway, R., Bridgland, D., Pringle, M., Yurtmen, S., Beck, A., and Rowbotham, G. 2007. "Ar-Ar dating of late C enozoic basaltic volcanism in northern Syria: Implications for the history of incision by the River Euphrates and uplift of the northern Arabian Platform." *Tectonics* 26: 1-30.

Dickin, A.P. 2005. *Radiogenic Isotope Geology*: Cambridge University Press.

Dong, J.L., Zhao, W.J., Liu, G.D., Cheng, H.S., Liao, Y.M., and Zhang S.L. 2008. "Study of material distribution of Tang Sancai from Huangye Kiln 黄冶窑唐三彩原料产地的研究." *Nuclear Physics Review 原子核物理评论* 25(4): 380-384.

Duwe, S., and Neff, H. 2007. "Glaze and slip pigment analyses of Pueblo IV period ceramics from east-central Arizona using time of flight-laser ablation-inductively coupled plasma-mass spectrometry (TOF-LA-ICP-MS)." *Journal of Archaeological Science* (34): 403-414.

Evans, J., and Tatham, S. 2004. "Strontium isotope variation in a rural Anglo-Saxon population living on a clay carbonate terrain." *Geological Society* 232, 237-248.

Evensen, N.M., Hamilton, P.J., and O'Nions, R.K. 1978. "Rare-earth abundances in chondritic meteorites." *Geochimica et Cosmochimica Acta* 42: 1199-1212.

Fang, L.L. 2011. *Chinese ceramics*. Cambridge: the Cambridge University Press.

Faure, G. 1986. *Principles of isotope geology*. New Jersey: John Wiley & Sons, Inc.

Feng, X.M. 冯先铭. 1958. "The introduction to green stoneware of North China 略谈北方青瓷," *Palace Museum Journal 故宫博物院院刊*(1): 58-62.

Feng, X.M. 冯先铭. 1982. *History of Chinese Ceramic 中国陶瓷史*. Beijing: Cultural Relics Publishing House.

Feng, X.Q., Feng, S.L., Sha, Y., Jakšić, M. 2005. "Study on the provenance and elemental distribution in the glaze of Tang Sancai by proton microprobe." *Nuclear Instruments and Methods in Physics Research B* 231:553-556.

Fenn, T., Robertshaw, P., Wood, M., and Chesley, J. 2009. "Early Islamic commerce with sub-Saharan Africa: chemical and isotopic analyses of late 1st millennium A.D. glass beads from Igbo-Ukwu, Nigeria." In 2009 SAA Meetings, Atlanta, GA.

Field, H. 1929. The Field Museum-Oxford University expedition to Kish, Mesopotamia, 1923–1929. Chicago: Field Museum of Natural History 28: 25-32

Fleming, S. J., Hancock, R. G. V., Mason, R. B. and Scott, R. E. 1992. “Tang polychrome wares: an interaction with the Islamic West,” in Science and technology of ancient ceramics 2, Proceedings of the International Symposium. edited by Li J.Z. Shanghai: Shanghai Research Society of Science and Technology of Ancient Ceramics.

Freestone, I. C., Leslie, K. A., Thirlwall, M., Gorin-Rosen, Y. 2003. “Strontium isotopes in the investigation of early glass production: Byzantine and early Islamic glass from the Near East.” *Archaeometry* 45:19-32.

Gale, N.H., Stos-Gale, Z. 1982. “Bronze Age copper sources in the Mediterranean: a new approach.” *Science* 216: 11-18.

Gale, N.H., Stos-Gale, Z. 2000. “Lead isotope analyses applied to provenance studies.” in *Modern Analytical Methods in Art and Archaeology*, edited by Ciliberto E., and Spoto G. *Chemical Analyses Series* 155(17): 503-584.

Gao, S., and Wedepohl, K.H. 1995. “The negative Eu anomaly in Archean sedimentary rocks: Implications for decomposition, age and importance of their granitic sources.” *Earth and Planetary Science Letters* 133: 81-94.

Giussani, B., Monticelli, D., Rampazzi, L. 2009. “Role of laser ablation–inductively coupled plasma–mass spectrometry in cultural heritage research: A review.” *Analytica Chimica Acta* 635:6–21.

Gongyi city Institute of Cultural Relics. 2000. Excavations of the Tang Sancai Kiln at Huangye 黄冶唐三彩窑 Beijing: Science Press 北京: 科学出版社

Goldschmidt, V. M. 1937. “The principles of distribution of chemical elements in minerals and rocks” *Journal of the Chemical Society*: 655–673.

Gratuze, B., Blet-Lemarquand, M., Barrandon, J.N. 2001. “Mass spectrometry with laser sampling: A new tool to characterize archaeological materials.” *Journal of Radioanalytical and Nuclear Chemistry* 247(3): 645-656.

Gulson, B.L., 1986. *Lead Isotopes in Mineral Exploration*. Amsterdam: Elsevier.



Guo, Y.Y., Li, J.Z. 1984. "A study on Ru and Yaozhou green glazed wares of the Song dynasty 宋代汝, 耀州窑青瓷的研究." *Journal of The Chinese Ceramic Society 硅酸盐学报* 12 (02): 226- 235

Guy, J. 2001-2002 "Early Asian Ceramic trade and The Belitung (T'ang) Cargo," *Transactions of The Oriental Ceramic Society* 66: 13-27

Gyllensvärd, B., 1973. *Recent Finds of Chinese Ceramics at Fostat I. Stockholm: The Museum of Far Eastern Antiquities.*

Hansen, V., 2012. *The Silk Road. A new history.* Oxford: Oxford University Press.

Hao, W.T., Zheng, T.X., Li, Y.D., Zheng, J.M., Zhu, J., Glascock, M.D., and Wang, C.S. 2013. "Provenance study of Chinese proto-celadon in Western Han Dynasty." *Ceramics International* (39): 6325 – 6332.

Hedges, R. E. M., Moorey, P. R. S. 1975. "Pre-Islamic ceramic glazes at Kish and Nineveh in Iraq." *Archaeometry* 17(1): 25-43.

Hedges, R.E.M. 1976. "Pre-Islamic glazes in Mesopotamia- Nippur." *Archaeometry* 18: 209–213.

Henan provincial Institute of Cultural Relics and Archaeology, Cultural Relics Institute, Nara National Institute for Cultural Properties, Japan. 2005. *The new archaeological discovery at Huangye kiln site 黄冶窑考古新发现.* Zhengzhou: Elephant Press 郑州: 大象出版社.

Henderson, J. 1999. "Archaeological and Scientific Evidence for the Production of Early Islamic Glass in al-Raqqā, Syria." *The Journal of the Council for British Research in the Levant* 31:225-240.

Henderson, J. 2000. "Archaeological investigation of an Islamic Industrial Complex at Raqqā, Syria." *Damaszener Mitteilungen* 11: 243-265.

Henderson, J. 2013. *The science and archaeology of materials: an investigation of inorganic materials.* Oxford: Routledge.

Henderson, J., Challis, K., Gardner, A., O'Hara, S., and Priestnall, G. 2002. "The Raqqa Ancient Industry Project" *Antiquity* 76: 33-34.

Henderson, J., Evans, J.A., Sloane, H.J., Leng, M.J., and Doherty, C. 2005a. "The use of oxygen, strontium and lead isotopes to provenance ancient glasses in the Middle East." *Journal of Archaeological Science* 32: 665 -673.

Henderson, J., Challis, S., O'Hara, S., Mcloughlin, A., Gardner, A., and Priestnall, G. 2005b. "Experiment and innovation: Early Islamic industry at al-Raqqa, Syria." *Antiquity* 79: 130-145.

Henderson, J., Chenery, S., Kröger, J., and Faber, E.W. 2016. *Glass Provenance along the Silk Road: The Use of Trace Elements Analysis*, Chapter 2, edited by Gan, F.X., Li, Q.H. and Henderson, J. Recent advances in the scientific research on ancient glass and glaze. Series on archaeology and history of science in China 2. Singapore: World Scientific.

Henderson, J., Chenery, S., Faber, E., and Kroger, J. 2016. "The use of electron probe microanalysis and laser ablation-inductively coupled plasma-mass spectrometry for the investigation of 8th–14th century plant ash glasses from the Middle East." *Microchemical Journal* 128:134–152.

Henderson, J., Mcloughlin, S.D., Mcphail, D.S., 2004. "Radical changes in Islamic glass technology: evidence for conservatism and experimentation with new glass recipes from early and middle Islamic Raqqa, Syria." *Archaeometry* 46(3): 439-468.

Henderson, J., Tregear, M., and Wood, N. 1989. "The technology of sixteenth and seventeenth century Chinese CLOISONNÉ enamels." *Archaeometry* 31(2): 133-146.

Kennedy, H. 2004. *The Prophet and the Age of the Caliphates: The Islamic Near East from the 6th to the 11th Century (A History of the Near East)*. London: Pearson Education Limited.

Henshaw, C.M. 2010. *Early Islamic Ceramics and Glazes of Akhsiket, Uzbekistan*. Unpublished PhD thesis. University College London.

Huang, Q. Y., and Liu, X., 2007, the Role of Ceramics in the Cultural Communication among Ancient China and Broad 陶瓷在中外交流中的作用, *Chinese Ceramics 中国陶瓷*, 43(11): 38-40.

- Hill, D.V., Speakman, R.J., Glascock, M.D. 2004. "Chemical and Mineralogical Characterization of Sasanian and Early Islamic glazed ceramics from the Deh Luran Plain, Southwestern Iran." *Archaeometry* 46(4): 585- 605.
- Hirata, T., Hayano, Y., Ohno, T. 2003. "Improvements in precision of isotopic ratio measurements using laser ablation-multiplecollector-ICP-mass spectrometry: reduction of changes in measured isotopic ratios." *Journal of Analytical Atomic Spectrometry* (18): 1283-1288.
- Huntley, D.L., Spielmann, K.A., Habicht-Mauche, J.A. Herhahn, C.L., and Russell Flegal, A. 2007. "Local recipes or distant commodities? Lead isotope and chemical compositional analysis of glaze paints from the Salinas pueblos, New Mexico." *Journal of Archaeological Science* 34: 1135-1147.
- Hurst, D., Freestone, I. 1996. "Lead glazing technique from a medieval kiln site at Hanley Swan, Worcestershire." *Medieval Ceramics* 20, 13–18.
- Jenkins, M. 1983. "Islamic Pottery: A Brief History." *The Metropolitan Museum of Art Bulletin* 40(4): 1-52.
- Jia, C.H.贾成惠. Lei, Y.雷勇. Feng, S.L.冯松林. Feng, X.Q.冯向前. 2006. "Research on Tang Sancai of Xing Kiln 浅议邢窑唐三彩." *Study of Relics 文物春秋*(1): 8-11.
- Jiang, Q.Q. 2009. *Tang Sancai*. Unpublished PhD thesis. Oxford: University of Oxford.
- Jochum, K.P., Weis, U., Stoll, B., Kuzmin, D., Yang, Q., Raczek, I., Jacob, D.E., Stracke, A., Birbaum, K., Frick, D.A., Günther, D., and Enzweiler, J. 2011. "Determination of reference values for NIST SRM 610–617 glasses following ISO guidelines." *Geostandards and Geoanalytical Research* 35(4): 397–429.
- Kerr, R., and Wood, N. 2004. *Science and Civilisation in China, Vol. 5, Chemistry and Chemical Technology, Part XII: Ceramic Technology*. Cambridge: Cambridge University Press.
- Lane, A. 1947. *Early Islamic Pottery*. London: Faber and Faber.
- Lei, Y.雷勇. 2007. "Instrument neutron activation analysis of Tang Sancai ware and a study of its trajectory of development in the region of the capitals 唐三彩的仪器中子活化分析其在两京地区发展轨迹的研究." *Palace Museum Journal 故宫博物院院刊* 131(3): 86-127.

Lei, Y 雷勇., and Feng S.L.冯松林. 2002. "Study of the compositional differences among different kilns' Sancai of Tang Dynasty by SRXRF 不同产地唐三彩的 SRXRF 无损分析研究" *Nuclear Techniques 核技术* 25(10): 825-822.

Lei, Y., Feng, S.L., Feng, X.Q., Fan, D.Y., Xu, Q., Sha, Y., Cheng, L., Chai, Z.F., Jiang, J., Zhuo, Z.X., Zhang, S.L., and Liao, Y.M. 2005a. "Study on the compositional differences of Tang Sancai from different kilns by INAA." *Journal of Archaeological Science* (32): 183-191.

Lei, Y.雷勇, Feng, S.L.冯松林, Feng X.Q.冯向前, Guo H.T.郭洪涛. 2005b. "Analysis of SanCai glazed pottery clay excavated from Princess Ai tomb of Mausoleum Gong in Tang Dynasty 唐恭陵哀妃墓出土唐三彩的中子活化分析和产地研究." *Central Plain Relics 中原文物* (1): 81-86.

Leung, P. L., Luo, H. J. 2000. "A Study of Provenance and Dating of Ancient Chinese Porcelain by X-Ray Fluorescence Spectrometry, X-Ray Spectrometry." 29: 34-38.

Lewis, M.E., 2009. *China's Cosmopolitan Empire. The Tang Dynasty.* Cambridge, Mass: Harvard University Press.

Liang, B.L., Luo, H.J., Li, J.Z., and Stokes M.J. 1997. "Study on evolution process of the ancient Yaozhou porcelain 借助对应分析方法研究耀州古瓷的演变规律." *Journal of the Chinese Ceramic Society 硅酸盐学报* 25 (1):78-82.

Li, B.P., Alan, G., Zhao, J.X., Kenneth, D.C., Quan, K.S., Meng, Y.H., Ma, Z.L. 2005. "ICP-MS trace element analysis of Song dynasty porcelains from Ding, Jiexiu and Guantai kilns, north China." *Journal of Archaeological Science* 32: 251-259.

Li, G.X., and Zhao, W.J., 2002. "Fuzzy clustering analysis of the origin of the ancient Yaozhou porcelain body 古耀州瓷胎起源的模糊聚类分析." *Chinese Science Bulletin 科学通报* 47(23): 1747-1781.

Li, G.Z., and Guan, P.Y. 1979. "A Study on Yaozhou Celadon 耀州青瓷的研究." *Journal of The Chinese Ceramic Society 硅酸盐学报* 7(4): 360-369.

Li, G.Z., and Ye, H.M., 1989. "A study of the glaze of Longquan celadon 龙泉青瓷釉的研究." In *Studies of Longquan celadon 龙泉青瓷研究.* Beijing: Cultural Relic

Press.

Li J.X., 1944. The Great Gazetteer of Tongguan • Minguo 同官县志 • 民国志.  
Tongchuan: Office of Local Chronicles Compilation of Yintai district of Tongchuan city.

Li, J.Z. 1998. A History of Science of Technology in China- Volume of Ceramic 中国科学技术-陶瓷卷. Beijing: Science Press 北京: 科学出版社.

Li, Y.Q., 2003. 'The city of Zhangzhou during the Sui and Tang era 隋唐时代的扬州城.'  
Archaeology 考古 3: 9-18.

Li, R.W., Li, G.X., and Zhao, W.J. 2003. "Neutron activation analysis of colouring elements in ancient Yaozhou porcelain 古耀州瓷着色元素的中子活化分析." Journal of Beijing Normal University (Natural Science) 北京师范大学学报 (自然科学版) 39(2): 201-203.

Li Y., Zhang B., Cheng H., and Zheng J. 2015. "The Earliest Chinese Proto-Porcelain Excavated from Kiln Sites: An Elemental Analysis." PLoS ONE 10(11): 1-16.

Li, Z.Y. 李知宴. 1986. "Tang Sancai wares for Everyday Life 唐三彩生活用具." Cultural Relics 文物 (6): 1-6.

Ling, X., Jia, M.M., Wei, N., Yao, Z.Q., Sun, L.J. 2008. "The analysis of Porcelain from Yaozhou Kiln by EDXRF 耀州窑青瓷的能量色散 X 射线荧光光谱分析." Journal of Northwest of University(Natural Science Edition) 38(1): 57-62.

Luo, H.J., and Li, J.Z. 1998. "The definition of proto-porcelain 试论原始瓷的定义." Archaeology 考古 (7): 645-648.

Luo, H.J., Li, J.Z, and Gao, L.M. 1995. "The classification standard of Chinese lime glaze and its application 中国古瓷中钙系釉类型划分标准及其在瓷釉研究中的应用." Journal of the Chinese Ceramic Society 硅酸盐学报 (2): 50-53.

Ma, H.J. 2014. The exploration of strontium isotopic analysis applied to Chinese glazes. Unpublished PhD thesis. the University of Nottingham.

Ma, B., Liu, L., Feng, S.L., Xu, Q., and Feng, X.Q. 2014a. "Analysis of the elemental composition of Tang Sancai from the four major kilns in China using EDXRF." *Nuclear Instruments and Methods in Physics Research B* 319: 95–99.

Ma, H.J, Henderson, J., and Evans, J. 2014b. "The exploration of Sr isotopic analysis applied to Chinese glazes: part one." *Journal of Archaeological Science* 50: 551–558.

Ma, H.J, Henderson, J., and Evans, J. 2016. "The exploration of Sr isotopic analysis applied to Chinese glazes: part two." *Archaeometry* 58(1): 68– 80.

Ma, H.J., Zhu, J., Henderson J., Li, N.S. 2012. "Provenance of Zhangzhou export blue-and-white and its clay source." *Journal of Archaeological Science* 39: 1218-1226.

Matsumoto, K. 1991. "Preliminary report on the Excavations at Kish/Hursagkalama 1988–1989." *al-Rāfidān* 12:261-307.

Matsumoto, K., and Oguchi, O. 2002. "Excavations at Kish, 2000." *Al-Rāfidān* 23:1-16.

Matsumoto, K., Oguchi, O. 2004. "News from Kish: the 2001 Japanese work." *Al-Rāfidān* 25:1-8.

Mason, R.B., Keall, E.J. 1991. "The 'Abbāsīd Glazed Wares of Sīrāf and the Baṣra Connection: Petrographic Analysis." *Iran* 29: 51-66.

Mason, R.B., Farquhar, R.M., and Smith, P.E. 1992. "Lead isotope analysis of Islamic glazes: an exploratory study." *Muqarnas* 9: 67-71.

Mason, R.B., Tite, M.S. 1994. "The beginnings of Islamic stonepaste technology." *Archaeometry* 36: 77-91.

Mason, R.B. 1995. "New Looks at Old Pots: Results of Recent Multidisciplinary Studies of Glazed Ceramics from the Islamic World." *Muqarnas* 12: 1-10.

Mason, R.B. 1997. "Early medieval Iraq Lustre-painted and associated wares: Typology in a multidisciplinary" *Journal of the British Institute for the Study of Iraq* 59: 15-61.

Mason, R.B., Tite, M.S. 1997. "The beginnings of Tin-opacification of Pottery glazes." *Archaeometry*, 39(1): 41-58.

Mason, R.B., 2004. "Shine Like the Sun. Lustre-painted and Associated Pottery from the Medieval Middle East." In: *Bibliotheca Iranica: Islamic Art and Architecture Series*, vol. 12. Mazda Publishers, Inc., Costa Mesa, Canada.

McCarthy, B., Vandiver, P. B. and Gibson, M. 1995. Innovation and continuity in the technology of Southwest Asian monochrome blue glazes. *The ceramics cultural heritage: proceedings of the international symposium "The Ceramics Heritage" of the 8th CIMTEC-World Ceramics Congress and Forum on New Materials, Florence, Italy.*

McLennan, S.M. 1989. "Rare earth elements in sedimentary rocks: Influence of provenance and sedimentary processes." *Reviews in Mineralogy and Geochemistry* (21): 169–200.

Meinecke, M. 1991. Raqqa on the Euphrates: Recent Excavations at the Residence of Haruner-Rashid. *The Near East in Antiquity 2*, edited by Kerner S. Amman: Goethe-Institute: 17-32.

Miao, J.M.苗建民, Lu, S.L.陆寿麟. 2001. "The provenance study of Tang Sancai wares by INNA and major chemical analysis 中子活化分析和主成份分析对唐三彩产地问题的研究." *Southeast Culture 东南文化*. 149(9): 83-93.

Min, Y., Rehren, T., Zheng, J.M. 2011. "The earliest high-fired glazed ceramics in China: the composition of the proto-porcelain from Zhejiang during the Shang and Zhou periods (c. 1700–221 BC)." *Journal of Archaeological Science* 38 (9): 2352-2365.

Molera, J., Vendrell-Saz, M., Garcia-VallCs, M., and Pradell, T., 1997, "Technology and colour development of Hispano-Moresque lead-glazed pottery." *Archaeometry*39: 23-39.

Montgomery, J. 2002. Lead and Strontium Isotope Compositions of Human Dental Tissues as an Indicator of Ancient Exposure and Population Dynamics: The Application of Isotope Source-tracing Methods to Identify Migrants Among British Archaeological Burials and a Consideration of Ante-mortem Uptake, Tissue Stability and Post-mortem Diagenesis. Unpublished PhD thesis. University of Bradford.

Montgomery, J., Evans, J.A., and Neighbour, T. 2003. "Sr isotope evidence for population movement within the Hebridean Norse community of NW Scotland." *Journal of the Geological Society* 160(5): 649-653.

Montgomery, J., Evans, J.A., Powlesland, D., Roberts, C.A. 2005. "Continuity or colonization in Anglo-Saxon England? Isotope evidence for mobility, subsistence practice,

and status at West Heslerton.” *American Journal of Physical Anthropology* 126(2): 123-138.

Nara National Institute for Cultural Properties, Henan provincial Institute of Cultural Relics and Archaeology. 2011. “The lead isotope analysis on the glazes of ancient Chinese and Japanese lead glazed ceramics 关于古代日本及中国铅釉陶器釉药的铅同位素比值测定.” *Huaxia Archaeology 华夏考古*(2): 148-152.

Narasaki, S. 2000a. “The Establishment of Development of Glazed Pottery in Japan 施釉陶器在日本的确立和发展,” in *Huangye Kiln Tang Sancai 黄冶窑唐三彩*. Beijing: Science Press 北京: 科学出版社.

Narasaki, S. 2000b. *Tang Sancai excavated in Japan 日本出土的唐三彩, Huangye Kiln Tang Sancai 黄冶窑唐三彩*. Beijing: Science Press 北京: 科学出版社.

Needham, J. 2004. *Science and Civilisation in China*. Oxford: Cambridge University Press.

Neff, H. 2012. “Laser ablation ICP-MS in Archaeology,” in *Handbook of Mass Spectrometry*. New Jersey: John Wiley&Sons, Inc.: 829-843.

Oikonomou, A., Henderson, J., Gnade, M., Chenery, S., and Zacharias, N. 2016. “An archaeometric study of Hellenistic glass vessels: evidence for multiple sources.” *Archaeological and Anthropological Sciences*: 1-14.

Pace, M., Bianco, P.A., and Mirti, P. 2008. “The technology of production of Sasanian glazed pottery from Veh ARDAŠĪR (Centural Iraq).” *Archaeometry* 50(4): 591–605.

Paynter S., Okyar F., Wolf S., Tite M.S., and Tite M.S. 2004. “The production technology of Iznik pottery-a reassessment.” *Archaeometry* 46(3): 421-437.

Paynter, S., and Tite, M. S., 2001, “The evolution of glazing technologies in the ancient Near East and Egypt,” in *The social context of technological change: Egypt and the Near East 1650–1550 BC* (ed. A. J. Shortland), Oxford: Oxbow Books: 239–254.

Philip, D.C. 1984. *Cross-Cultural Trade in World History*. the Cambridge University Press.



Philon, H., 1980. *Early Islamic Ceramics*. Benaki Museum, Athens.

Pollard, A.M., Hatcher, H. 1994. "The Chemical Analysis of Oriental Ceramic Body Compositions: Part 1: Wares from North China." *Archaeometry* 36(1): 41-62.

Pradell, T., Molera, J., Smith, A.D., and Tite, M.S. 2008a. "The invention of lustre: Iraq 9th and 10th centuries AD." *Journal of Archaeological Science* 35: 1201-1215.

Pradell, T., Molera, J., Smith, A.D., and Tite M.S. 2008b. "Early Islamic lustre from Egypt, Syria and Iran (10th to 13th century AD)." *Journal of Archaeological Science* 35: 2649-2662.

Pradell T., Molera J., Smith A.D., Climent-Font A., and Tite M.S., 2008c. "Technology of Islamic lustre." *Journal of Cultural Heritage* 9: 123-128.

Priestman, S.M.N. 2011. "Opaque glazed ware: the definition, dating and distribution of a key Iraqi ceramic export in the Abbasid period." *British Institute of Persian Studies* 49: 89-113.

Rawson, J. 1984. "Song Silver and its Connexions with Ceramics." *Apollo* 269(120): 18-23.

Rawson, J., Tite, M., Hughes, M.J. 1989. "The export of Tang sancai wares: some recent research." *Transactions of the Oriental Ceramic Society* 52: 39-61.

Reitlinger, G. 1935. "Islamic Pottery from Kish." *Ars Islamica* 2(2): 198-218.

Resano, M., Garc ía-Ruiz, E., Vanhaecke, F. 2010. "Laser ablation-inductively coupled plasma-mass spectrometry in archaeometric research." *Mass Spectrometry Reviews* 29: 55-78

Resano, M., Pérez-Arategui, J., Garcia-Ruiz, F. 2005. "Laser ablation-inductively coupled plasma mass spectrometry for the fast and direct characterization of antique glazed ceramics." *Journal of Analytical Atomic Spectrometry* 20: 508-514.

Rice, D.T. 1932. The Oxford Excavation at Hira, 1931 *Antiquity* (6): 276-291.

Rice, D.T. 1934. The Oxford Excavation at Hira *Ars Islamica* (1):51-73.

- Robertson, J.D., Neff, H., Higgins, B. 2002. "Microanalysis of ceramics with PIXE and LA-ICP-MS." *Nuclear Instruments and Methods in Physics Research B* 189: 378-381.
- Rollinson, H.R. 1993. *Using Geochemical Data: Evaluation, Presentation, Interpretation*, Harlow, Essex, England: Longman Scientific & Technical.
- Rothenberg, B., Blanco-Freijeiro, A. 1981. *Studies in ancient mining and metallurgy in south-west Spain*. Institute for Archaeo-Metallurgical Studies. Institute of Archaeology. University College London.
- Sarre, F., 1925. *Del Ausgrabungen Von Samara, Zeiter Band, Die Keramik Von Samarra*, Berlin: Verlag Dietrich Reamer Ernst Vohsen.
- Schultze-Frentzel, U., Salge, H. 1975. "Glazes and decorating colours of Persian Islamic ceramics examined by X-radiography, and transparent Seljuq glazes examined by electron-probe microanalysis." *Kunst Des Orients* 10: 80-90.
- Shaanxi Provincial Institute of Archaeology. 1992. *Excavation of Tang kiln-site at Huangpu in Tongchuan, Shaanxi 唐代黄堡窑址*. Beijing: Cultural Relics Press.
- Shaanxi Provincial Institute of Archaeology. 1997. *Excavation of the Five dynasties period kiln-site at Huangpu in Tongchuan, Shaanxi 五代黄堡窑址*. Beijing: Cultural Relics Press.
- Shaanxi Provincial Institute of Archaeology, Yaozhou kiln Museum. 1998. *The Yaozhou kiln site of Song period 宋代耀州窑址*. Beijing: Cultural Relics Press.
- Shaanxi Provincial Institute of Archaeology. 2008. *Excavation of Tang kiln-site at Liqianfang in Chang'an Capital City, Shaanxi 唐长安醴泉坊三彩窑址*. Beijing: Cultural Relics Press.
- Shortland, A., Rogers, N., and Eremin, K. 2007. "Trace element discriminants between Egyptian and Mesopotamian Late Bronze Age glasses." *Journal of Archaeological Science* 34: 781-789.
- Silvestri, A., Molin, G., and Salviulo, G. 2008. "The coloured glass of Iulia Felix." *Journal of Archaeological Science* 35: 331-341.

Smith, D.T. 2006. Compositional analysis of early thirteenth century ceramic from Raqqa. Raqqa Revisited: Ceramics of Ayyubid Syria. New York: The Metropolitan Museum of Art.

Speakman, R.J., and Neff, H. 2002a. "Evaluation of painted pottery from the Mesa Verde region using laser ablation-inductively coupled plasma-mass spectrometry (LA-ICP-MS)." *American Antiquity* 67(1): 137-144.

Speakman, R.J., Neff, H., Glascock, M.A., and Higgins, B.J. 2002b. "Characterization of archaeological materials by laser ablation-inductively coupled plasma-mass spectrometry," in *Archaeological Chemistry: Materials, Methods, and Meaning*, edited by Jakes K.A. American Chemical Society: 48-63.

Stargardt J., 2014. 'Indian Ocean Trade in the Ninth and Tenth Centuries: Demand, Distance, and Profit.' *South Asian Studies* 30(1): 35-55

Stos-Gale, Z. A., Gale, N. H., Bass, G., Pulak, C., Galili, E., and Sharvit, J. 1998. "The copper and tin ingots of the Late Bronze Age Mediterranean: new scientific evidence," in *Proceedings of the Fourth International Conference on the Beginning of the Use on Metals and Alloys (BUMA-IV)*. The Japan Institute of Metals.

Stos-Gale, Z.A. 2001. "The impact of the natural sciences on studies of Hacksilber and early silver coinage," In: *Hacksilber to coinage: new insights into the monetary history of the Near East and Greece*. Numismatic Studies 24, edited by Balmuth M. New York: The American Numismatic Society: 53-76.

Sun, X.M. 孙新民. 2002. "Discovery and Research on Huangye Tang Sancai kiln site at Gongyi 巩义黄冶唐三彩窑址的发现与研究," in *Tang Sancai Wares of the Tang Dynasty from Huangye in Gongyi 巩义黄冶唐三彩*, edited by Henan Provincial Institute of Cultural Relics and Archaeology 河南省考古研究所. Henan: Elephant Press 河南: 大象出版社.

Susanne V., Gesine D., L., Susanne, R., Christophe R. Q., Gerhard, H., Malcolm, B., Christophe, B.P., Peter, D.I., Stefan, H., Jurian, H., Emmanuel, P., Marleen, V.B., and Henriette, U. 2010. "Strontium isotopic signatures of natural mineral waters, the reference to a simple geological map and its potential for authentication of food." *Food Chemistry* 118(4): 933-940.

Tite, M.S. 2008. "Ceramic Production, Provenance and Use-A Review." *Archaeometry* 50(2): 216 –231.

Tite, M.S. 2011. "The Technology of glazed Islamic ceramics using data collected by the late Alexander Kaczmarczyk." *Archaeometry* 52(2): 329-339.

Tite, M.S., Freestone, I.C., and Bimson, M.A. 1984. "Technological Study of Chinese Porcelain of the Yuan Dynasty." *Archaeometry* 26(2): 139-154.

Tite, M.S., Freestone, I., Mason, R., Molera, J., Vendrell-Saz, M. and Wood, N. 1998. "Lead glazes in antiquity-methods of production and reasons for use." *Archaeometry* 40:241-260.

Tite M.S., Wolf S., and Mason R.B. 2011. "The technological development of stonepaste ceramics from the Islamic Middle East." *Journal of Archaeological Science* 38: 570-580.

Tonghini, C., and Henderson, J. 1998. "An eleventh-century pottery production workshop at al-Raqqā." *The Journal of the Council for British Research in the Levant* 30(1): 113-127.

Tseng, Y.K., and Xu, B.Y. 2012. "An analysis of the gem-blue glaze of Ye Wang's Koji Pottery." *Archaeometry* 54(4): 643-663.

Turekian, K.K., and Kulp, J.L. 1956. "The geochemistry of strontium." *Geochimica et Cosmochimica Acta*. 10(5): 245-296.

Veizer, J. 1978. "Abundance of strontium in common sediments and sedimentary rocks," In: *Handbook of geochemistry II*, edited by Wedepohl K.H. Berlin Heidelberg: Springer.

Vendrell, M., Molera, J., and Tite, M.S. 2000. "Optical properties of tin-opacified glazes." *Archaeometry* 42(2): 325-340.

Waksman, S.Y., Bouquillon, A., Cantin, N., and Katona, I. 2007. "The first Byzantine 'Glazed White Wares' in the early medieval technological context," in *Archaeometric and archaeological approaches to ceramics*, edited by Waksman S.Y. BAR International Series 1691. Oxford.

Walton, M.S., and Tite, M.S. 2010. "Production technology of Roman lead-glazed pottery and its continuance into late antiquity" *Archaeometry* 52(5): 733-759.

Wang, F. 2000. *Yaozhou Porcelain 耀州窑陶瓷*. Xi'an: Shaanxi Science and Technology Press.

Wang F., Chen S, Sun H., 1999. "Research on Yaozhou celadon in the Five Dynasties Period 五代耀州窑青瓷研究," in Proceedings of the international symposium on science and technology of ancient ceramics 古陶瓷科学技术国际讨论会论文集, Shanghai: Shanghai Science and Technology Press: 55–62.

Wang, Q.C., Yan, Z., Ning, B., Shi, K., Liu, J.W., Li, B.Q., and Jin, C.G. 2016. "Characteristics and genesis of leopard limestone of the Ordovician Majiagou formation in Ordos Basin 鄂尔多斯盆地奥陶系马家沟组豹皮灰岩特征及其成因." *Journal of Palaeogeography 古地理学报* 18(1): 39-48.

Wang X.M., and Kato E., 2002. "Discussion on the production and development of Tang Sancai 试论唐三彩生产发展的轨迹," in Proceedings of the international symposium on science and technology of ancient ceramics 古陶瓷科学技术国际讨论会论文集, Shanghai: Shanghai Science and Technology Press: 410-417.

Wang X.M., and Kato E., 2005. "Development and evolvement of the cased-firing technology in Huangpu kiln- concurrently discussing the Relationship between the Huangpu kiln and the Yue kiln, Ru kiln as well as Korea celadon 黄堡窑装烧工艺的发展演变—兼谈黄堡窑与越窑、汝窑及高丽青瓷的关系," in Proceedings of the international symposium on science and technology of ancient ceramics 古陶瓷科学技术国际讨论会论文集. Shanghai: Shanghai Scientific and Technical Literature Publishing House: 199-209.

Watson, W. 1970. "On T'ang Soft Glazed Pottery," in *Pottery and Metalwork in T'ang China*. London : Percival David Foundation Colloquy.

Watson, O., 1985. *Persian Lustre Ware*. The Faber Monographs on Pottery and Porcelain. Faber and Faber, London.

Watson, O. 2014. *Ceramics from Islamic Lands*. London: Thames&Hudson.

Watson, O., 2015. Chinese-Iranian Relations xi. Mutual Influence of Chinese and Persian Ceramics, *Encyclopædia Iranica*, online edition, available at <http://www.iranicaonline.org/articles/chinese-iranian-xi> (accessed on 20 May 2015).

Wedepohl, K.H., 1978. *Handbook of Geochemistry Vol. II/4 Elements Kr (36) to Ba (56)*. Berlin: Springer-Verlag.

Wedepohl, K. H., and A. Baumann. 2000. "The use of marine molluscan shells for Roman glass and local raw glass production in the Eifel area (Western Germany)." *Naturwissenschaften* 87(3): 129-132.

Weeks, L. et al., 2009. "Lead isotope analyses of Bronze Age copper-base artefacts from the site of al-Midamman, Yemen: towards the identification of an indigenous metal production and exchange system in the Southern Red Sea region." *Archaeometry* 51(4): 576-597.

Wilkinson C.K., 1973. *Nishapur: Pottery of the Early Islamic Period*, the Metropolitan Museum of Art, New York.

Wolf, S., Stos, S., Mason, R., and Tite, M.S., 2003. "Lead isotope analyses of Islamic pottery glazes from Fustat, Egypt." *Archaeometry* 45: 405-420.

Wood, N. 2011. *Chinese glazes: Their origins, chemistry, and recreation*. Philadelphia : University of Pennsylvania Press.

Wood, N., Tite, M.S., Doherty, C., and Gilmour, B. 2007. "A technological examination of 9-10th century AD Abbasid blue-and-white ware from Iraq, and its comparison with 8th century AD Chinese blue-and-white sancai ware." *Archaeometry* 49 (4): 665–684.

Wood, N., Doherty, C., and Owen, M.R. 2009. "A technological study of Iraqi imitations of Chinese Changsha wares and Chinese Sancai wares found at Samarra," in *Science and Technology of ancient ceramics 古陶瓷科学技术* Shanghai: Shanghai Scientific and Technical Literature Publishing House: 154-180.

Wood, N., Doherty, C., and Rastelli, S., 2005. 'Some aspects of Yue ware production at Shanglinhu in the Late Tang dynasty.' in *Science and Technology of ancient ceramics 古陶瓷科学技术* Shanghai: Shanghai Scientific and Technical Literature Publishing House: 185-198.

Wu, J.M.吴军明, Wu, J.吴隽, Zheng, N.Z.郑乃章, Li Q.J.李其江, Zhang M.L.张茂林, Deng Z.Q.邓泽群. 2010. "A Comparative Study of "Jiaohuang" and Tang Tricolor Yellow Glazes 唐三彩黄釉与娇黄釉的比较研究." *China Ceramics 中国陶瓷* 46(9): 21-27.

- Xiao, X.Q.肖新琦. 2007. the comparing study of Tang Sancai earthenwares in Shaanxi and Henan Province 陕西, 河南地区出土唐三彩的比较研究. Jilin University 吉林大学.
- Xue, D.X. 2005. "The development of Yaozhou celadon 耀州窑青瓷的发展及延续," in the International Academic Symposium Corpus of Yaozhou Kiln 中国耀州窑国际学术讨论会文集. Xi'an: Sanqin Press.
- Yang, D.W.杨大伟. 2007. The application of Nuclear technology and database in the study of porcelain of Yaozhou Kiln 核技术和数据库技术在古耀州瓷研究中的应用, University of Zhengzhou 郑州大学.
- Yang, D.W., Ji, Y., and Li, R.W. 2010. "Non-destructive discrimination of Ancient Yaozhou Porcelain from different times 不同时期古耀州瓷的无损鉴别研究." Journal of Ceramics 陶瓷学报 31(2): 190-194.
- Yang, Y.杨勇, Ji, Y.冀勇, Li, G.X.李国霞, Zhao, W.J.赵维娟, Sun, H.W.孙洪巍, Gao, Z.Y.高正耀., Guo, M.郭敏, and Xie, J.Z.谢建忠. 2008. "Study on the Finger print Elements of Tang Tricolor Pottery of Huangye Kiln and Yaozhou Kiln by Multivariate Statistical Analysis 黄冶窑和耀州窑唐三彩指纹元素的多元统计分析." Journal of Xinyang Normal University, 信阳师范学院学报:自然科学版 21(2): 121-190.
- Yang, Z.T., Zhuo, Z.X., and Du, B.R. 1991. "Microstructure study on the Yaozhou celadon wares and the development of celadon manufacture techniques 耀州窑历代青瓷微结构研究及其古代制瓷工艺技术发展讨论." Journal of Xi'an Institute of Geological Science 中国地质科学院西安地质矿产研究所所刊 32: 99-100.
- Yaozhou kiln Museum, Shaanxi Provincial Institute of Archaeology and Tongchuan Archaeological Institute. 2004. Yaozhou kiln site at Lidipo and Shangdian. Xi'an: Sanqin Press.
- Yener, K.A., Sayre, E.V., Ozbal, H., Joel, E.C., Barnes, I.L., and Brill, R.H. 1991. "Stable lead isotope studies of Central Taurus ore sources and related artifacts from Eastern Mediterranean Chalcolithic and Bronze Age sites." Journal of Archaeological Science 18(5): 541-77.
- Ye, Z.M.叶喆民. 1989. The History of Chinese Ceramics 中国陶瓷史纲要. Beijing: Light Industry Press.

Yin, M., Rehren, T., and Zheng, J. 2011. "The earliest high-fired glazed ceramics in China: the composition of the proto-porcelain from Zhejiang during the Shang and Zhou periods (c. 1700-221 BC)." *Journal of Archaeological Science* 38: 2352-2365.

Yu, F.W. 余扶危, and Zhang J. 张剑. 1994. "Introduction of Tang Sancai 唐三彩概况." *Cultural Relics of Central China 中原文物* (1): 4-11.

Zhang, B., and Gao, Z.Y. 2002. "NAA and Mössbauer Study on the Coloration Mechanism of Yaozhou Celadon in Ancient China." *Hyperfine Interactions* 142: 593-599.

Zhang, F.K. 张福康, and Zhang, Z.G. 张志刚. 1980. "Low-temperature coloured glazes of successive dynasties in ancient China 中国历代低温色釉的研究." *Journal of the Chinese Ceramic Society 硅酸盐学报* 8(1): 9-19.

Zhang, F.K. 张福康, and Zhang, Z.G. 张志刚. 1983. "Study on Chinese low-fired coloured glazes and overglazes in past dynasties 中国历代低温色釉和釉上彩的研究." *Collection of essays on Chinese ancient ceramics 中国古陶瓷论文集*. Beijing: Cultural Relics Publishing House.

Zhang, F.K. 张福康. 2000. *The science of Chinese ancient ceramics 中国古代陶瓷科学*. Shanghai: Shanghai People's Fine Arts Publishing House 上海: 上海人民艺术出版社.

Zhang, Z.G., Li, J.Z., and Zhuo, Z.X. 1995. *Study on celadon technology of Yaozhou kiln in successive dynasties, Science and Technology of Ancient Ceramics-International Symposium*. Beijing: Science Press.

Zhou, R. 1958. *The research of Jingdezhen ceramics 景德镇瓷器的研究*. Beijing: Science Press.

Zhu, B.Q. 1995. "The mapping of geochemical provinces in China based on Pb isotopes." *Journal of Geochemical Exploration* 55: 171-181.

Zhu, B.Q. 2001. *Geochemical province and geochemical discordance*. Beijing: Scientific Press.

Zhuo, Z.X. 2008. "Development and Identification of Green Porcelain of Yaozhou Kiln 青釉耀瓷的考古发现与鉴定." *Collection 收藏* 189: 36-39.



Zhu, T.Q., Zhu, M.M., Li, W.R., M, Z.W., and Yi, X.B. 2010. “The elemental characteristics of celadon glaze from Xicun Klin and Yaozhou kiln in Song dynasty 宋代西村窑与耀州窑青瓷胎釉化学组成特征”. *Rock and mineral analysis 岩矿测试* 29(3): 291-295.

Zhu, T.Q., Sun, W.D., Wang, H.M. 2012. “Study on the provenance of Xicun Qingbai wares from the Northern Song dynasty of China.” *Archaeometry* 54: 475-488.

## **APPENDIX I Data tables**

Table A1 the major chemical compositions of turquoise monochrome glaze samples from Al-Raqqa sites

Table A2 the major chemical compositions of Yaozhou celadon glaze samples

Table A3 the major chemical compositions of Tang Sancai lead glaze samples

Table A4 the major chemical compositions of Islamic lead glaze samples

Table A5 the REEs compositions of Yaozhou celadon glaze samples

Table A6 the trace elemental compositions of Tang Sancai lead glaze samples

Table A7 the trace elemental compositions of Islamic lead glaze samples

Table A8 Body and adjusted glaze compositions for Tang Sancai sherds produced in Huangpu kiln, normalised to 100%

Table A9 Body and glaze compositions for Tang Sancai sherds produced in Huangye kiln, normalised to 100% (analysed by Dong et al. 2008)

Table A10 the body compositions for Islamic high lead glaze sherds collected from Hira and Nineveh of Iraq, normalised to 100% (analysed by Kaczmarczyk, the University of Oxford)

Table A11 the adjusted glaze compositions for Islamic high lead glaze sherds collected from Syria (Al-Raqqa) and Iraq (Kish-shaal Ghazna)

Table A12 Lead isotope ratios for lead ore deposits from different regions of Iran (Stos-Gale 2001)

Table A13 Lead isotope ratios for lead ore deposits from different regions of Tunisia (Wolf 2003)

Table A14 Lead isotope ratios for lead ore deposits from different regions of Anatolia (OXALID and Yener et al. 1991)

Table A15 Lead isotope ratios for lead ore deposits from different regions of Sardinia (OXALID)

Table A16 Lead isotope ratios for lead ore deposits from different regions of Spain (OXALID)

Sample No.	SiO <sub>2</sub>	Al <sub>2</sub> O <sub>3</sub>	Na <sub>2</sub> O	K <sub>2</sub> O	CaO	MgO	P <sub>2</sub> O <sub>5</sub>	CuO	FeO	MnO	TiO <sub>2</sub>
Syria-1-1	68.34	3.94	9.18	3.52	8.19	2.62	0.18	1.25	0.15	0.08	0.12
Syria-1-2	66.09	5.55	11.91	3.90	6.47	2.70	0.18	1.27	0.10	0.12	0.15
Syria-1-3	66.66	6.09	11.99	3.80	6.72	2.26	0.21	1.31	0.08	0.13	0.09
<b>Syria-1 Mean</b>	<b>67.03</b>	<b>5.20</b>	<b>11.03</b>	<b>3.74</b>	<b>7.13</b>	<b>2.53</b>	<b>0.19</b>	<b>1.28</b>	<b>1.13</b>	<b>0.04</b>	<b>0.12</b>
Syria-2-1	62.04	4.00	12.59	2.90	5.63	2.12	0.22	6.37	0.98	0.05	0.10
Syria-2-2	62.23	4.02	12.43	2.93	5.90	2.26	0.22	6.30	1.01	0.05	0.10
Syria-2-3	63.38	3.90	12.31	2.98	5.40	1.98	0.21	6.68	0.88	0.04	0.11
<b>Syria-2 Mean</b>	<b>62.55</b>	<b>3.97</b>	<b>12.44</b>	<b>2.94</b>	<b>5.64</b>	<b>2.12</b>	<b>0.22</b>	<b>6.45</b>	<b>0.96</b>	<b>0.04</b>	<b>0.10</b>
Syria-5-1	58.34	7.80	7.58	3.03	9.93	5.70	0.13	1.43	3.17	0.04	0.30
Syria-5-2	55.34	10.65	8.45	3.75	8.57	3.94	0.15	1.38	4.12	0.09	0.47
Syria-5-3	57.46	10.04	5.97	4.01	12.27	4.14	0.05	0.89	3.28	0.11	0.38
<b>Syria-5 Mean</b>	<b>57.05</b>	<b>9.50</b>	<b>7.33</b>	<b>3.60</b>	<b>10.26</b>	<b>4.59</b>	<b>0.11</b>	<b>1.23</b>	<b>3.52</b>	<b>0.05</b>	<b>0.38</b>
Syria-8-1	62.62	5.42	9.98	3.44	6.79	2.32	0.19	4.03	1.11	0.04	0.10
Syria-8-2	63.43	5.78	9.67	3.48	6.97	2.26	0.12	3.81	1.08	0.03	0.10
Syria-8-3	62.24	5.35	9.94	3.48	6.88	2.36	0.20	4.01	1.09	0.04	0.12
<b>Syria-8 Mean</b>	<b>62.76</b>	<b>5.52</b>	<b>9.85</b>	<b>3.47</b>	<b>6.88</b>	<b>2.31</b>	<b>0.17</b>	<b>3.95</b>	<b>1.09</b>	<b>0.04</b>	<b>0.11</b>
Syria-9-1	65.51	2.41	15.73	1.78	7.18	3.22	0.23	1.78	0.67	0.03	0.08
Syria-9-2	65.31	2.48	15.68	1.80	7.11	3.21	0.22	1.69	0.67	0.02	0.05
Syria-9-3	65.68	2.42	15.48	1.79	7.27	3.16	0.21	1.67	0.66	0.03	0.07
<b>Syria-9 Mean</b>	<b>65.50</b>	<b>2.44</b>	<b>15.63</b>	<b>1.79</b>	<b>7.19</b>	<b>3.20</b>	<b>0.22</b>	<b>1.71</b>	<b>0.67</b>	<b>0.03</b>	<b>0.06</b>
TA1043-1	63.94	3.82	8.89	4.18	8.33	2.28	0.29	4.62	1.11	0.01	0.17
TA1043-2	64.26	3.62	8.89	4.15	8.30	2.17	0.33	4.62	1.06	0.04	0.15
TA1043-3	64.12	3.77	8.99	4.30	8.00	2.06	0.29	4.45	1.17	0.07	0.09
<b>TA1043 Mean</b>	<b>64.11</b>	<b>3.74</b>	<b>8.92</b>	<b>4.21</b>	<b>8.21</b>	<b>2.17</b>	<b>0.30</b>	<b>4.56</b>	<b>1.11</b>	<b>0.04</b>	<b>0.14</b>
TA357-1	66.63	3.73	9.58	3.70	6.57	2.19	0.21	4.24	1.08	0.04	0.16
TA357-2	65.85	3.53	9.60	3.68	6.64	2.34	0.18	4.33	0.98	0.04	0.14
TA357-3	65.59	3.33	9.77	3.68	6.97	2.37	0.23	4.58	0.98	0.01	0.11
TA357-4	67.28	3.21	9.50	3.67	6.59	2.17	0.22	4.60	0.87	0.04	0.10
TA357-5	67.33	3.40	9.44	3.76	6.35	2.23	0.26	4.36	0.90	0.04	0.10
TA357-6	64.46	3.36	9.79	3.59	7.19	2.29	0.26	4.98	1.03	0.08	0.11
TA357-7	65.82	3.68	9.62	3.72	6.32	2.10	0.28	4.92	0.97	0.05	0.10
TA357-8	66.68	4.16	9.53	3.81	5.57	2.06	0.34	4.57	1.04	0.03	0.09
<b>TA357 Mean</b>	<b>66.21</b>	<b>3.55</b>	<b>9.60</b>	<b>3.70</b>	<b>6.53</b>	<b>2.22</b>	<b>0.25</b>	<b>4.57</b>	<b>0.98</b>	<b>0.04</b>	<b>0.11</b>
TA327-1	69.85	3.28	10.92	3.39	5.88	2.65	0.36	1.50	0.80	0.01	0.16
TA327-2	69.23	3.46	11.26	3.28	6.02	2.49	0.36	1.49	0.84	0.04	0.11
TA327-3	69.40	3.01	11.13	3.19	6.64	2.69	0.24	1.59	0.91	0.01	0.14
TA327-4	68.70	2.73	11.21	3.19	6.83	2.73	0.24	1.71	0.89	0.00	0.14
TA327-5	69.23	3.30	10.90	3.15	6.45	2.65	0.26	1.63	0.68	0.09	0.17
<b>TA327 Mean</b>	<b>69.28</b>	<b>3.16</b>	<b>11.08</b>	<b>3.24</b>	<b>6.36</b>	<b>2.64</b>	<b>0.29</b>	<b>1.58</b>	<b>0.82</b>	<b>0.03</b>	<b>0.14</b>

**A1 the major chemical compositions of turquoise monochrome glaze samples from Al-Raqqa sites (Unit: wt.%)**

Sample Number	SiO <sub>2</sub>	Al <sub>2</sub> O <sub>3</sub>	Na <sub>2</sub> O	K <sub>2</sub> O	CaO	MgO	FeO	TiO <sub>2</sub>	MnO	P <sub>2</sub> O <sub>5</sub>
Tang16a-1	57.33	13.07	0.31	1.87	19.58	2.34	2.03	0.29	0.11	1.01
Tang16a-2	57.43	13.48	0.37	1.73	19.51	2.41	2.35	0.50	0.06	0.90
Tang16a-3	56.63	13.34	0.30	1.88	19.71	2.43	2.39	0.29	0.07	1.04
Tang16a-4	56.65	13.14	0.31	1.90	19.67	2.45	2.31	0.30	0.13	0.98
Tang16a-5	56.42	13.16	0.27	1.81	19.92	2.51	2.07	0.24	0.16	1.26
<b>Tang16a Mean</b>	<b>56.89</b>	<b>13.24</b>	<b>0.31</b>	<b>1.84</b>	<b>19.68</b>	<b>2.43</b>	<b>2.23</b>	<b>0.32</b>	<b>0.11</b>	<b>1.04</b>

Tang20-1	57.79	13.80	0.29	1.55	18.91	2.26	2.16	0.35	0.10	0.80
Tang20-2	57.61	13.37	0.27	1.57	19.29	2.30	2.28	0.26	0.10	1.18
Tang20-3	58.66	13.06	0.25	1.57	19.28	2.52	2.39	0.32	0.12	1.21
Tang20-4	59.03	13.22	0.27	1.71	18.58	2.34	2.36	0.36	0.09	0.94
Tang20-5	58.76	12.98	0.24	1.56	18.82	2.62	2.31	0.32	0.08	1.04
<b>Tang20 Mean</b>	<b>58.37</b>	<b>13.29</b>	<b>0.26</b>	<b>1.59</b>	<b>18.98</b>	<b>2.41</b>	<b>2.30</b>	<b>0.32</b>	<b>0.10</b>	<b>1.03</b>
TangBW6-1	58.88	12.23	0.15	1.55	20.34	1.97	1.99	0.25	0.02	1.45
TangBW6-2	58.14	11.86	0.13	1.62	20.26	1.58	2.45	0.25	0.06	1.38
TangBW6-3	59.07	11.39	0.15	1.60	20.00	2.36	2.46	0.29	0.02	0.96
TangBW6-4	57.07	11.22	0.11	1.59	21.00	2.02	3.00	0.26	0.08	1.50
TangBW6-5	58.52	11.35	0.14	1.52	21.00	1.98	2.98	0.30	0.04	1.42
TangBW6-6	58.37	11.32	0.11	1.53	21.00	2.14	2.98	0.30	0.04	1.15
TangBW6-7	60.59	11.63	0.16	2.21	18.23	2.15	2.42	0.23	0.03	0.94
TangBW6-8	58.30	11.36	0.12	1.57	21.32	1.67	3.05	0.26	0.03	1.25
TangBW6-9	58.44	11.59	0.09	1.54	21.31	2.05	2.60	0.31	0.02	1.28
<b>TangBW6 Mean</b>	<b>58.60</b>	<b>11.55</b>	<b>0.13</b>	<b>1.64</b>	<b>20.50</b>	<b>1.99</b>	<b>2.66</b>	<b>0.27</b>	<b>0.04</b>	<b>1.26</b>
TangBW3-1	62.95	12.40	0.30	1.90	16.77	1.90	1.62	0.21	0.08	0.67
TangBW3-2	64.12	12.37	0.32	2.00	16.47	1.81	1.60	0.17	0.06	0.41
TangBW3-3	63.36	12.66	0.33	1.90	16.82	1.81	1.71	0.34	0.07	0.65
TangBW3-4	61.94	12.61	0.28	1.69	17.55	1.96	1.66	0.34	0.11	0.72
TangBW3-5	63.25	12.45	0.29	1.91	16.89	1.87	1.72	0.26	0.07	0.55
<b>TangBW3 Mean</b>	<b>63.12</b>	<b>12.50</b>	<b>0.30</b>	<b>1.88</b>	<b>16.90</b>	<b>1.87</b>	<b>1.66</b>	<b>0.26</b>	<b>0.08</b>	<b>0.60</b>
YZF-1-1	60.42	12.77	0.29	1.89	18.88	1.70	1.43	0.12	0.06	0.80
YZF-1-2	60.68	12.67	0.31	1.91	18.90	1.82	1.51	0.15	0.08	0.83
YZF-1-3	59.91	12.61	0.32	1.75	19.75	1.82	1.56	0.19	0.09	0.83
YZF-1-4	61.29	12.51	0.30	2.06	18.23	1.63	1.49	0.12	0.07	0.56
YZF-1-5	59.04	12.70	0.30	1.84	19.47	1.91	1.51	0.15	0.07	1.07
<b>YZF-1 Mean</b>	<b>60.27</b>	<b>12.65</b>	<b>0.30</b>	<b>1.89</b>	<b>19.05</b>	<b>1.78</b>	<b>1.50</b>	<b>0.15</b>	<b>0.07</b>	<b>0.82</b>
YZF-2-1	62.79	14.37	0.46	1.65	15.81	1.96	1.45	0.12	0.06	0.90
YZF-2-2	65.51	12.99	0.40	2.55	14.03	1.68	1.29	0.09	0.07	0.77
YZF-2-3	62.94	12.80	0.43	1.82	16.26	2.20	1.66	0.15	0.10	0.98
YZF-2-4	64.58	13.65	0.51	2.16	14.07	1.58	1.30	0.11	0.10	0.93
YZF-2-5	63.87	12.65	0.44	1.85	15.62	2.03	1.44	0.14	0.09	0.95
<b>YZF-2 Mean</b>	<b>63.94</b>	<b>13.29</b>	<b>0.45</b>	<b>2.01</b>	<b>15.16</b>	<b>1.89</b>	<b>1.43</b>	<b>0.12</b>	<b>0.08</b>	<b>0.91</b>
YZF-3-1	71.31	15.05	0.33	2.74	6.22	1.30	1.83	0.36	0.02	0.54
YZF-3-2	68.21	15.99	0.37	2.60	7.52	1.54	2.28	0.13	0.04	0.40
YZF-3-3	68.19	15.47	0.35	2.36	7.94	1.73	2.17	0.17	0.02	0.67
YZF-3-4	69.03	15.42	0.37	2.55	7.88	1.58	2.06	0.09	0.03	0.27
YZF-3-5	65.41	18.17	0.34	1.93	9.81	1.15	1.56	0.06	0.04	0.32
<b>YZF-3 Mean</b>	<b>68.43</b>	<b>16.02</b>	<b>0.35</b>	<b>2.44</b>	<b>7.87</b>	<b>1.46</b>	<b>1.98</b>	<b>0.16</b>	<b>0.03</b>	<b>0.44</b>
YZF-4-1	63.88	14.24	0.32	2.10	14.06	1.69	1.39	0.14	0.05	0.87
YZF-4-2	63.95	12.71	0.25	2.32	14.73	1.83	1.50	0.15	0.10	0.84
YZF-4-3	67.64	11.91	0.30	2.07	12.41	1.64	1.50	0.16	0.05	0.61
YZF-4-4	64.47	13.63	0.31	2.28	13.41	1.61	1.71	0.13	0.09	0.48
YZF-4-5	64.26	13.57	0.30	2.33	13.44	1.75	1.80	0.13	0.01	0.63
<b>YZF-4 Mean</b>	<b>64.84</b>	<b>13.21</b>	<b>0.30</b>	<b>2.22</b>	<b>13.61</b>	<b>1.70</b>	<b>1.58</b>	<b>0.14</b>	<b>0.06</b>	<b>0.69</b>

YZF-5-1	65.37	14.02	0.29	2.17	12.47	1.55	1.59	0.12	0.09	0.52
YZF-5-2	64.35	14.20	0.27	2.06	13.09	1.58	1.71	0.13	0.07	0.53
YZF-5-3	64.79	14.28	0.32	1.89	13.17	1.69	1.75	0.11	0.08	0.61
YZF-5-4	64.37	14.58	0.26	2.11	13.34	1.56	1.69	0.10	0.07	0.67
YZF-5-5	64.28	14.37	0.30	2.15	12.89	1.66	1.74	0.16	0.13	0.77
<b>YZF-5 Mean</b>	<b>64.63</b>	<b>14.29</b>	<b>0.29</b>	<b>2.08</b>	<b>12.99</b>	<b>1.61</b>	<b>1.70</b>	<b>0.12</b>	<b>0.09</b>	<b>0.62</b>
YZF-6-1	66.43	13.49	0.44	2.75	9.79	1.92	2.33	0.21	0.11	0.50
YZF-6-2	64.82	13.42	0.54	2.38	10.65	2.22	2.68	0.15	0.10	0.93
YZF-6-3	65.24	13.56	0.48	2.86	10.08	2.17	2.59	0.14	0.10	0.90
YZF-6-4	62.96	18.35	0.50	2.02	11.73	1.32	1.63	0.12	0.05	0.36
YZF-6-5	65.57	14.28	0.55	2.55	10.58	1.83	2.26	0.15	0.09	1.22
<b>YZF-6 Mean</b>	<b>65.00</b>	<b>14.62</b>	<b>0.50</b>	<b>2.51</b>	<b>10.57</b>	<b>1.89</b>	<b>2.30</b>	<b>0.15</b>	<b>0.09</b>	<b>0.78</b>
YZF-7-1	70.51	14.41	0.43	2.50	7.34	1.28	1.64	0.13	0.02	0.39
YZF-7-2	72.80	13.75	0.45	2.72	6.66	1.14	1.39	0.14	0.00	0.14
YZF-7-3	71.49	14.24	0.46	2.63	6.92	1.15	1.68	0.13	0.04	0.17
YZF-7-4	72.36	13.98	0.45	2.64	6.59	1.11	1.57	0.20	0.02	0.11
YZF-7-5	71.65	14.29	0.46	2.61	6.77	1.25	1.63	0.22	0.04	0.30
<b>YZF-7 Mean</b>	<b>71.76</b>	<b>14.13</b>	<b>0.45</b>	<b>2.62</b>	<b>6.86</b>	<b>1.19</b>	<b>1.58</b>	<b>0.16</b>	<b>0.02</b>	<b>0.22</b>
YZF-8-1	66.54	15.39	0.37	2.37	9.95	1.30	1.64	0.20	0.03	0.24
YZF-8-2	66.43	15.41	0.33	2.32	10.24	1.37	1.81	0.17	0.04	0.37
YZF-8-3	65.65	17.62	0.39	1.96	10.86	1.06	1.32	0.22	0.04	0.27
YZF-8-4	66.20	15.53	0.40	2.03	10.61	1.44	1.78	0.14	0.07	0.35
YZF-8-5	68.01	14.91	0.30	2.57	9.40	1.08	1.45	0.13	0.03	0.40
<b>YZF-8 Mean</b>	<b>66.57</b>	<b>15.77</b>	<b>0.36</b>	<b>2.25</b>	<b>10.21</b>	<b>1.25</b>	<b>1.60</b>	<b>0.17</b>	<b>0.04</b>	<b>0.33</b>
YZF-9-1	59.91	14.55	0.94	2.33	10.99	2.52	4.95	0.44	0.09	0.12
YZF-9-2	59.17	18.26	1.06	2.19	11.27	1.51	3.51	0.45	0.06	0.04
<b>YZF-9 Mean</b>	<b>59.54</b>	<b>16.41</b>	<b>1.00</b>	<b>2.26</b>	<b>11.13</b>	<b>2.02</b>	<b>4.23</b>	<b>0.45</b>	<b>0.08</b>	<b>0.08</b>
NS-52-1	69.13	13.72	0.35	3.14	9.42	1.74	1.67	0.19	0.08	0.83
NS-52-2	68.05	14.23	0.37	3.45	8.95	1.64	1.95	0.16	0.08	0.66
<b>NS-52 Mean</b>	<b>68.59</b>	<b>13.98</b>	<b>0.36</b>	<b>3.29</b>	<b>9.19</b>	<b>1.69</b>	<b>1.81</b>	<b>0.17</b>	<b>0.08</b>	<b>0.74</b>
NS-53-1	66.95	12.45	0.62	3.13	10.40	1.76	1.73	0.14	0.07	0.69
NS-53-2	67.48	12.78	0.64	2.88	11.15	1.92	1.97	0.20	0.04	0.65
<b>NS-53 Mean</b>	<b>67.21</b>	<b>12.62</b>	<b>0.63</b>	<b>3.01</b>	<b>10.78</b>	<b>1.84</b>	<b>1.85</b>	<b>0.17</b>	<b>0.05</b>	<b>0.67</b>
NS-54-1	66.36	14.21	0.32	1.95	10.90	2.60	2.30	0.42	0.04	1.31
NS-54-2	66.57	13.85	0.26	1.82	11.68	2.65	2.41	0.45	0.05	1.00
<b>NS-54 Mean</b>	<b>66.47</b>	<b>14.03</b>	<b>0.29</b>	<b>1.88</b>	<b>11.29</b>	<b>2.63</b>	<b>2.35</b>	<b>0.43</b>	<b>0.04</b>	<b>1.15</b>
NS-55-1	71.75	13.85	0.22	3.63	5.33	1.83	2.82	0.43	0.07	0.62
NS-55-2	70.87	13.91	0.23	3.46	5.84	1.79	2.78	0.46	0.01	0.87
<b>NS-55 Mean</b>	<b>71.31</b>	<b>13.88</b>	<b>0.22</b>	<b>3.55</b>	<b>5.59</b>	<b>1.81</b>	<b>2.80</b>	<b>0.45</b>	<b>0.04</b>	<b>0.74</b>
NS-56-1	60.30	12.46	0.37	2.29	17.51	1.89	1.97	0.22	0.09	1.04
NS-56-2	63.12	12.40	0.36	2.19	18.07	2.15	1.95	0.20	0.07	0.94
NS-56-3	61.67	12.02	0.31	1.86	18.65	2.25	2.03	0.22	0.09	0.81
NS-56-4	61.79	12.05	0.34	1.90	18.70	2.35	1.91	0.25	0.08	1.03
<b>NS-56 Mean</b>	<b>61.72</b>	<b>12.23</b>	<b>0.35</b>	<b>2.06</b>	<b>18.23</b>	<b>2.16</b>	<b>1.96</b>	<b>0.22</b>	<b>0.08</b>	<b>0.96</b>
NS-57-1	64.28	13.38	0.64	3.20	11.00	2.86	2.48	0.23	0.05	1.43
NS-57-2	64.02	13.55	0.63	3.10	11.62	2.62	2.32	0.30	0.07	1.09

<b>NS-57 Mean</b>	<b>64.15</b>	<b>13.47</b>	<b>0.63</b>	<b>3.15</b>	<b>11.31</b>	<b>2.74</b>	<b>2.40</b>	<b>0.27</b>	<b>0.06</b>	<b>1.26</b>
NS-58-1	77.16	13.75	0.56	4.08	2.96	0.72	1.66	0.24	0.03	0.52
NS-58-2	74.90	14.81	0.58	3.76	3.67	0.98	1.78	0.20	0.03	1.06
<b>NS-58 Mean</b>	<b>76.03</b>	<b>14.28</b>	<b>0.57</b>	<b>3.92</b>	<b>3.31</b>	<b>0.85</b>	<b>1.72</b>	<b>0.22</b>	<b>0.03</b>	<b>0.79</b>
NS-59-1	66.95	13.90	0.35	2.38	12.32	1.55	1.56	0.06	0.05	0.84
NS-59-2	66.71	14.08	0.35	2.45	11.74	1.64	1.67	0.09	0.05	0.52
NS-59-3	64.78	14.11	0.33	2.27	12.64	1.61	1.78	0.13	0.08	0.67
NS-59-4	65.20	13.89	0.32	2.34	12.38	1.57	1.59	0.11	0.07	0.45
<b>NS-59 Mean</b>	<b>65.91</b>	<b>14.00</b>	<b>0.33</b>	<b>2.36</b>	<b>12.27</b>	<b>1.59</b>	<b>1.65</b>	<b>0.10</b>	<b>0.06</b>	<b>0.62</b>

**A2 the major chemical compositions of Yaozhou celadon glaze samples  
(Unit: wt.%)**

Sample No.	Glaze colour	PbO	SiO <sub>2</sub>	Al <sub>2</sub> O <sub>3</sub>	Na <sub>2</sub> O	K <sub>2</sub> O	CaO	MgO	CuO	FeO	TiO <sub>2</sub>	SnO <sub>2</sub>
HYK-1-1	green	49.41	34.95	6.97	0.26	0.51	0.65	0.12	1.92	0.37	0.11	b.d.
HYK-1-2		50.95	34.58	5.36	0.18	0.43	0.66	0.16	2.18	0.40	0.11	b.d.
<b>HYK-1 Mean</b>		<b>50.18</b>	<b>34.77</b>	<b>6.17</b>	<b>0.22</b>	<b>0.47</b>	<b>0.65</b>	<b>0.14</b>	<b>2.05</b>	<b>0.39</b>	<b>0.11</b>	<b>b.d.</b>
HYK-1-1	white	51.14	36.31	6.50	0.20	0.50	0.45	0.13	0.11	0.26	0.10	b.d.
HYK-1-2		50.60	37.33	6.23	0.16	0.46	0.52	0.18	0.12	0.29	0.10	b.d.
<b>HYK-1 Mean</b>		<b>50.87</b>	<b>36.82</b>	<b>6.37</b>	<b>0.18</b>	<b>0.48</b>	<b>0.48</b>	<b>0.15</b>	<b>0.12</b>	<b>0.28</b>	<b>0.10</b>	<b>b.d.</b>
HYK-2-1	white	54.97	31.95	6.05	0.17	0.33	1.27	0.12	0.14	0.30	0.03	b.d.
HYK-2-2		55.32	33.06	4.83	0.17	0.29	1.19	0.12	0.13	0.33	0.03	b.d.
HYK-2-3		55.79	32.15	5.17	0.18	0.30	1.15	0.12	0.13	0.34	0.02	b.d.
<b>HYK-2 Mean</b>		<b>55.36</b>	<b>32.39</b>	<b>5.35</b>	<b>0.17</b>	<b>0.31</b>	<b>1.20</b>	<b>0.12</b>	<b>0.13</b>	<b>0.32</b>	<b>0.03</b>	<b>b.d.</b>
HYK-2-1	green	49.32	30.07	8.53	0.27	0.55	1.94	0.31	2.78	1.95	0.25	b.d.
HYK-2-2		50.63	29.64	7.70	0.28	0.42	1.95	0.33	2.63	2.06	0.22	b.d.
HYK-2-3		50.47	30.54	6.98	0.29	0.46	1.97	0.36	2.78	1.82	0.25	b.d.
<b>HYK-2 Mean</b>		<b>50.14</b>	<b>30.08</b>	<b>7.74</b>	<b>0.28</b>	<b>0.48</b>	<b>1.95</b>	<b>0.33</b>	<b>2.73</b>	<b>1.94</b>	<b>0.24</b>	<b>b.d.</b>
HYK-2-1	brown	52.52	27.83	7.91	0.32	0.52	2.08	0.46	0.40	2.89	0.24	b.d.
HYK-2-2		52.92	27.67	7.48	0.36	0.52	2.09	0.44	0.39	3.21	0.25	b.d.
HYK-2-3		53.43	27.93	7.82	0.36	0.53	2.08	0.47	0.39	2.91	0.20	b.d.
<b>HYK-2 Mean</b>		<b>52.96</b>	<b>27.81</b>	<b>7.74</b>	<b>0.35</b>	<b>0.53</b>	<b>2.08</b>	<b>0.46</b>	<b>0.39</b>	<b>3.00</b>	<b>0.23</b>	<b>b.d.</b>
HYK-5-1	green	50.70	35.01	5.24	0.28	0.38	1.50	0.14	2.26	0.35	0.13	b.d.
HYK-5-2		50.11	35.32	5.60	0.19	0.51	1.44	0.15	2.12	0.34	0.18	b.d.
HYK-5-3		51.34	35.33	5.35	0.21	0.43	1.17	0.08	2.24	0.35	0.14	b.d.
<b>HYK-5 Mean</b>		<b>50.72</b>	<b>35.89</b>	<b>5.40</b>	<b>0.23</b>	<b>0.44</b>	<b>1.37</b>	<b>0.13</b>	<b>2.21</b>	<b>0.35</b>	<b>0.15</b>	<b>b.d.</b>
HYK-5-1	white	48.24	35.63	7.22	0.26	0.68	1.66	0.15	1.14	0.30	0.17	b.d.
HYK-5-2		43.83	40.83	9.39	0.35	1.22	0.92	0.19	0.64	0.31	0.22	b.d.
HYK-5-3		42.94	39.25	9.69	0.42	1.54	0.83	0.13	0.39	0.29	0.20	b.d.
<b>HYK-5 Mean</b>		<b>45.00</b>	<b>38.57</b>	<b>8.77</b>	<b>0.34</b>	<b>1.15</b>	<b>1.14</b>	<b>0.16</b>	<b>0.72</b>	<b>0.30</b>	<b>0.20</b>	<b>b.d.</b>
HYK-7-1	brown	56.38	33.43	3.05	0.10	0.35	1.00	0.20	0.69	3.35	0.07	b.d.
HYK-7-2		54.67	31.81	3.33	0.16	0.38	0.97	0.15	0.67	3.35	0.03	b.d.
HYK-7-3		53.87	32.22	3.38	0.16	0.34	1.01	0.21	0.70	3.55	0.02	b.d.
<b>HYK-7 Mean</b>		<b>54.97</b>	<b>32.49</b>	<b>3.25</b>	<b>0.14</b>	<b>0.36</b>	<b>0.99</b>	<b>0.19</b>	<b>0.69</b>	<b>3.42</b>	<b>0.04</b>	<b>b.d.</b>
HYK-7-1	green and brown mix	52.34	33.12	5.41	0.19	0.46	1.14	0.23	1.22	2.89	0.13	b.d.
HYK-7-2		53.09	32.55	5.16	0.22	0.44	1.18	0.26	1.06	2.60	0.09	b.d.
HYK-7-3		52.07	33.81	4.25	0.21	0.44	1.03	0.23	1.35	2.40	0.16	b.d.
<b>HYK-7 Mean</b>		<b>52.50</b>	<b>33.16</b>	<b>4.94</b>	<b>0.21</b>	<b>0.44</b>	<b>1.12</b>	<b>0.24</b>	<b>1.21</b>	<b>2.63</b>	<b>0.13</b>	<b>b.d.</b>
HYK-8-1	brown	54.99	28.78	6.03	0.17	0.38	2.08	0.43	0.50	2.71	0.17	b.d.
HYK-8-2		53.71	27.93	6.36	0.26	0.39	1.99	0.40	0.45	2.92	0.14	b.d.
<b>HYK-8 Mean</b>		<b>54.35</b>	<b>28.36</b>	<b>6.20</b>	<b>0.21</b>	<b>0.38</b>	<b>2.04</b>	<b>0.42</b>	<b>0.48</b>	<b>2.82</b>	<b>0.16</b>	<b>b.d.</b>

HYK-8-1	green	50.35	32.44	7.24	0.30	0.40	1.31	0.26	3.09	0.79	0.23	b.d.
HYK-8-2		50.71	30.03	6.86	0.23	0.43	1.41	0.25	3.02	0.95	0.17	b.d.
<b>HYK-8 Mean</b>		<b>50.53</b>	<b>30.24</b>	<b>7.05</b>	<b>0.26</b>	<b>0.42</b>	<b>1.36</b>	<b>0.26</b>	<b>3.06</b>	<b>0.87</b>	<b>0.20</b>	<b>b.d.</b>
HYK-8-1	white	57.05	32.71	5.09	0.13	0.25	0.51	0.07	0.12	0.24	0.02	b.d.
HYK-8-2		53.03	35.87	5.25	0.13	0.29	0.61	0.09	0.13	0.31	0.03	b.d.
HYK-8-3		55.34	34.04	5.47	0.15	0.26	0.59	0.10	0.13	0.29	0.03	b.d.
<b>HYK-8 Mean</b>	<b>55.14</b>	<b>34.21</b>	<b>5.27</b>	<b>0.14</b>	<b>0.27</b>	<b>0.57</b>	<b>0.09</b>	<b>0.13</b>	<b>0.28</b>	<b>0.03</b>	<b>b.d.</b>	
HYK-9-1	dark brown	52.93	29.53	7.67	0.27	0.47	1.98	0.32	1.01	1.77	0.16	b.d.
HYK-9-2		54.98	27.84	7.72	0.28	0.52	2.01	0.28	1.11	1.89	0.18	b.d.
HYK-9-3		49.89	31.42	7.86	0.31	0.51	1.93	0.31	1.07	1.81	0.19	b.d.
<b>HYK-9 Mean</b>	<b>52.60</b>	<b>29.60</b>	<b>7.75</b>	<b>0.29</b>	<b>0.50</b>	<b>1.97</b>	<b>0.30</b>	<b>1.06</b>	<b>1.82</b>	<b>0.18</b>	<b>b.d.</b>	
HYK-10-1	brown	57.14	31.38	5.99	0.17	0.61	0.90	0.26	0.65	1.13	0.32	0.01
HYK-10-2		58.00	30.76	5.90	0.18	0.51	1.01	0.16	0.74	1.04	0.30	0.05
<b>HYK-10 Mean</b>		<b>57.57</b>	<b>31.07</b>	<b>5.94</b>	<b>0.18</b>	<b>0.56</b>	<b>0.95</b>	<b>0.21</b>	<b>0.69</b>	<b>1.09</b>	<b>0.31</b>	<b>0.03</b>
HYK-10-1	white and yellow	61.70	32.18	3.63	0.03	0.38	0.19	0.11	0.00	0.26	0.11	b.d.
HYK-10-2		61.46	32.46	3.33	0.03	0.32	0.21	0.16	0.02	0.23	0.16	b.d.
<b>HYK-10 Mean</b>		<b>61.58</b>	<b>32.32</b>	<b>3.48</b>	<b>0.03</b>	<b>0.35</b>	<b>0.20</b>	<b>0.13</b>	<b>0.01</b>	<b>0.24</b>	<b>0.13</b>	<b>b.d.</b>
HYK-11-1	brown	40.24	42.44	9.58	0.27	0.85	1.88	0.57	0.54	2.54	0.39	0.18
HYK-11-2		39.83	41.85	10.07	0.22	0.77	1.96	0.45	0.46	2.63	0.34	0.02
<b>HYK-11 Mean</b>		<b>40.03</b>	<b>42.15</b>	<b>9.82</b>	<b>0.24</b>	<b>0.81</b>	<b>1.92</b>	<b>0.51</b>	<b>0.50</b>	<b>2.59</b>	<b>0.37</b>	<b>0.10</b>
HYK-11-1	green	40.69	40.42	7.88	0.20	0.60	2.49	0.54	2.41	1.08	0.34	b.d.
HYK-11-2		41.06	39.14	9.04	0.24	0.65	2.23	0.60	2.37	0.96	0.35	b.d.
<b>HYK-11 Mean</b>		<b>40.88</b>	<b>39.78</b>	<b>8.46</b>	<b>0.22</b>	<b>0.63</b>	<b>2.36</b>	<b>0.57</b>	<b>2.39</b>	<b>1.02</b>	<b>0.34</b>	<b>b.d.</b>
HYK-13-1	green and yellow mix	51.43	33.93	3.41	0.15	0.35	1.28	0.27	1.70	2.23	0.10	b.d.
HYK-13-2		50.51	33.99	4.75	0.23	0.36	1.21	0.23	1.67	2.04	0.10	b.d.
HYK-13-3		50.37	33.59	4.30	0.17	0.38	1.22	0.25	1.72	2.02	0.12	b.d.
<b>HYK-13 Mean</b>	<b>50.77</b>	<b>33.84</b>	<b>4.15</b>	<b>0.18</b>	<b>0.36</b>	<b>1.24</b>	<b>0.25</b>	<b>1.70</b>	<b>2.10</b>	<b>0.11</b>	<b>b.d.</b>	
HYK-13-1	brown	49.07	34.08	5.57	0.24	0.51	1.59	0.26	0.23	3.52	0.14	b.d.
HYK-13-2		48.66	33.89	5.71	0.24	0.49	1.64	0.28	0.21	3.54	0.17	b.d.
HYK-13-3		48.45	33.63	5.95	0.27	0.50	1.68	0.27	0.21	3.55	0.11	b.d.
<b>HYK-13 Mean</b>	<b>48.73</b>	<b>33.87</b>	<b>5.74</b>	<b>0.25</b>	<b>0.50</b>	<b>1.64</b>	<b>0.27</b>	<b>0.22</b>	<b>3.54</b>	<b>0.14</b>	<b>b.d.</b>	
HYK-18-1	brown	49.66	35.81	2.92	0.10	0.21	0.43	0.17	0.07	5.66	0.07	b.d.
HYK-18-2		48.84	36.79	3.69	0.12	0.24	0.49	0.15	0.05	5.15	0.12	b.d.
HYK-18-3		50.65	36.65	3.39	0.12	0.24	0.47	0.12	0.07	5.25	0.05	b.d.
<b>HYK-18 Mean</b>	<b>49.72</b>	<b>36.42</b>	<b>3.33</b>	<b>0.11</b>	<b>0.23</b>	<b>0.46</b>	<b>0.15</b>	<b>0.06</b>	<b>5.35</b>	<b>0.08</b>	<b>b.d.</b>	
HYK-18-1	dark green	47.26	35.59	7.04	0.26	0.37	0.45	0.31	3.35	0.61	0.19	b.d.
HYK-18-2		47.82	35.34	7.24	0.25	0.38	0.44	0.36	3.30	0.61	0.15	b.d.
HYK-18-3		48.62	35.44	6.35	0.14	0.34	0.47	0.30	3.65	0.66	0.14	b.d.
<b>HYK-18 Mean</b>	<b>47.90</b>	<b>35.46</b>	<b>6.88</b>	<b>0.22</b>	<b>0.36</b>	<b>0.45</b>	<b>0.33</b>	<b>3.43</b>	<b>0.63</b>	<b>0.16</b>	<b>b.d.</b>	
HPK-1-1	brown	44.94	37.32	8.07	0.13	0.52	1.02	0.34	0.49	1.65	0.32	0.09
HPK-1-2		44.33	37.58	9.10	0.14	0.55	1.01	0.32	0.46	1.54	0.42	0.06
<b>HPK-1 Mean</b>		<b>44.64</b>	<b>37.45</b>	<b>8.59</b>	<b>0.14</b>	<b>0.53</b>	<b>1.01</b>	<b>0.33</b>	<b>0.47</b>	<b>1.60</b>	<b>0.37</b>	<b>0.08</b>
HPK-1-1	green	44.88	36.16	8.38	0.21	0.54	1.38	0.28	1.36	0.82	0.29	0.21
HPK-1-2		45.71	36.20	7.80	0.25	0.50	1.49	0.29	1.40	0.92	0.23	0.27
HPK-1-3		46.34	35.29	6.95	0.12	0.45	1.44	0.33	1.62	0.91	0.31	0.36
<b>HPK-1 Mean</b>	<b>45.64</b>	<b>35.88</b>	<b>7.71</b>	<b>0.19</b>	<b>0.50</b>	<b>1.44</b>	<b>0.30</b>	<b>1.46</b>	<b>0.88</b>	<b>0.28</b>	<b>0.28</b>	
HPK-2-1	yellow and green mix	40.61	40.39	9.25	0.19	0.53	0.43	0.29	0.76	1.86	0.36	0.11
HPK-2-2		40.95	42.10	7.61	0.12	0.47	0.39	0.31	0.81	2.25	0.33	0.18
HPK-2-3		40.71	42.38	7.83	0.21	0.47	0.37	0.31	0.79	2.08	0.33	0.14
<b>HPK-2 Mean</b>	<b>40.76</b>	<b>41.62</b>	<b>8.23</b>	<b>0.17</b>	<b>0.49</b>	<b>0.40</b>	<b>0.30</b>	<b>0.78</b>	<b>2.06</b>	<b>0.34</b>	<b>0.14</b>	
HPK-2-1	green	37.44	42.39	10.39	0.21	0.71	0.45	0.30	1.37	1.23	0.39	0.34

HPK-2-2		40.50	40.73	9.10	0.16	0.50	0.44	0.32	1.63	1.27	0.48	0.36
HPK-2-3		41.35	40.33	9.21	0.18	0.49	0.43	0.32	1.60	1.26	0.46	0.33
<b>HPK-2 Mean</b>		<b>39.76</b>	<b>41.15</b>	<b>9.57</b>	<b>0.18</b>	<b>0.57</b>	<b>0.44</b>	<b>0.31</b>	<b>1.53</b>	<b>1.25</b>	<b>0.44</b>	<b>0.35</b>
HPK-3-1	brown	36.37	41.50	10.38	0.16	0.83	0.34	0.42	0.15	4.32	0.50	b.d.
HPK-3-2		36.42	41.33	10.31	0.17	0.87	0.33	0.44	0.14	4.09	0.49	b.d.
HPK-3-3		36.55	42.21	10.38	0.14	0.84	0.38	0.47	0.17	4.17	0.48	b.d.
<b>HPK-3 Mean</b>		<b>36.45</b>	<b>41.68</b>	<b>10.36</b>	<b>0.16</b>	<b>0.85</b>	<b>0.35</b>	<b>0.44</b>	<b>0.15</b>	<b>4.19</b>	<b>0.49</b>	<b>b.d.</b>
HPK-4-1	brown	60.79	29.25	3.66	0.03	0.17	0.18	0.20	0.08	4.06	0.24	0.01
HPK-4-2		61.55	29.49	4.38	0.04	0.25	0.18	0.07	0.15	3.49	0.20	0.13
<b>HPK-4 Mean</b>		<b>61.17</b>	<b>29.37</b>	<b>4.02</b>	<b>0.03</b>	<b>0.21</b>	<b>0.18</b>	<b>0.13</b>	<b>0.11</b>	<b>3.78</b>	<b>0.22</b>	<b>0.07</b>
HPK-5-1	green	54.48	35.45	6.16	0.07	0.36	0.33	0.27	1.23	0.83	0.40	0.22
HPK-5-2		55.32	34.13	7.40	0.09	0.36	0.34	0.22	1.12	0.90	0.42	0.12
HPK-5-3		50.98	36.17	6.80	0.11	0.43	1.05	0.45	1.94	0.94	0.44	0.39
HPK-5-4		50.70	34.84	7.01	0.09	0.39	1.02	0.41	2.02	0.92	0.37	0.38
<b>HPK-5 Mean</b>		<b>52.87</b>	<b>35.15</b>	<b>6.85</b>	<b>0.09</b>	<b>0.38</b>	<b>0.68</b>	<b>0.34</b>	<b>1.57</b>	<b>0.90</b>	<b>0.41</b>	<b>0.28</b>
HPK-5-1	brown	53.87	33.86	5.72	0.05	0.31	0.30	0.21	0.38	4.41	0.31	0.10
HPK-5-2		54.26	33.04	5.67	0.04	0.32	0.31	0.27	0.33	4.33	0.41	0.00
HPK-5-3		53.64	35.02	6.62	0.04	0.40	0.30	0.28	0.17	4.19	0.38	0.00
HPK-5-4		53.52	34.70	6.73	0.07	0.34	0.29	0.20	0.09	4.01	0.39	0.06
<b>HPK-5 Mean</b>		<b>53.82</b>	<b>34.15</b>	<b>6.18</b>	<b>0.05</b>	<b>0.34</b>	<b>0.30</b>	<b>0.24</b>	<b>0.24</b>	<b>4.23</b>	<b>0.37</b>	<b>0.04</b>
HPK-6-1	green	45.37	39.85	6.02	0.10	0.39	0.33	0.31	2.45	0.79	0.30	b.d.
HPK-6-2		46.21	40.18	5.08	0.11	0.37	0.30	0.40	2.65	0.82	0.27	b.d.
<b>HPK-6 Mean</b>		<b>45.79</b>	<b>40.02</b>	<b>5.55</b>	<b>0.10</b>	<b>0.38</b>	<b>0.32</b>	<b>0.36</b>	<b>2.55</b>	<b>0.80</b>	<b>0.29</b>	<b>b.d.</b>
HPK-7-1	green	44.68	40.30	4.70	0.16	0.64	1.11	0.31	1.93	0.69	0.18	b.d.
HPK-7-2		45.42	39.72	4.46	0.16	0.58	1.15	0.37	1.95	0.77	0.28	b.d.
HPK-7-3		45.32	39.90	3.67	0.13	0.51	1.28	0.44	2.16	0.81	0.19	b.d.
<b>HPK-7 Mean</b>		<b>45.14</b>	<b>39.97</b>	<b>4.28</b>	<b>0.15</b>	<b>0.58</b>	<b>1.18</b>	<b>0.37</b>	<b>2.01</b>	<b>0.76</b>	<b>0.22</b>	<b>b.d.</b>
HPK-8-1	green	48.64	38.49	5.20	0.08	0.29	0.32	0.17	2.89	0.34	0.11	b.d.
HPK-8-2		48.64	38.03	4.53	0.09	0.25	0.38	0.19	3.15	0.34	0.18	b.d.
HPK-8-3		49.71	37.62	5.38	0.10	0.28	0.39	0.19	3.04	0.34	0.11	b.d.
<b>HPK-8 Mean</b>		<b>49.00</b>	<b>38.05</b>	<b>5.04</b>	<b>0.09</b>	<b>0.27</b>	<b>0.36</b>	<b>0.18</b>	<b>3.03</b>	<b>0.34</b>	<b>0.13</b>	<b>b.d.</b>
HPK-9-1	brown	50.28	35.98	6.21	0.06	0.57	0.55	0.35	0.13	3.67	0.26	0.05
HPK-9-2		50.07	35.69	6.49	0.10	0.58	0.55	0.37	0.09	3.34	0.28	0.07
<b>HPK-9 Mean</b>		<b>50.18</b>	<b>35.83</b>	<b>6.35</b>	<b>0.08</b>	<b>0.57</b>	<b>0.55</b>	<b>0.36</b>	<b>0.11</b>	<b>3.51</b>	<b>0.27</b>	<b>0.06</b>
HPK-10-1	green and brown mix	47.11	37.19	6.29	0.15	0.83	0.28	0.28	2.45	1.44	0.32	0.49
HPK-10-2		47.26	37.66	6.26	0.16	0.80	0.23	0.27	2.62	1.32	0.28	0.48
<b>HPK-10 Mean</b>		<b>47.19</b>	<b>37.42</b>	<b>6.27</b>	<b>0.16</b>	<b>0.81</b>	<b>0.25</b>	<b>0.28</b>	<b>2.53</b>	<b>1.38</b>	<b>0.30</b>	<b>0.49</b>
NKZ-1-1	green	46.32	35.89	7.50	0.26	0.62	0.93	0.37	3.59	0.50	0.20	b.d.
NKZ-1-2		45.89	35.75	7.91	0.20	0.61	0.90	0.38	3.53	0.52	0.36	b.d.
NKZ-1-3		45.34	35.69	6.81	0.12	0.53	0.88	0.38	3.98	0.56	0.19	b.d.
<b>NKZ-1 Mean</b>		<b>45.85</b>	<b>35.78</b>	<b>7.41</b>	<b>0.19</b>	<b>0.59</b>	<b>0.90</b>	<b>0.38</b>	<b>3.70</b>	<b>0.53</b>	<b>0.25</b>	<b>b.d.</b>
NKZ-1-1	dark brown	51.29	33.09	5.68	0.18	0.55	0.99	0.26	0.78	3.66	0.11	b.d.
NKZ-1-2		50.43	33.81	6.70	0.22	0.62	0.96	0.27	1.02	2.84	0.30	b.d.
NKZ-1-3		49.44	33.26	5.93	0.24	0.52	0.96	0.26	1.47	2.85	0.14	b.d.
<b>NKZ-1 Mean</b>		<b>50.39</b>	<b>33.39</b>	<b>6.10</b>	<b>0.21</b>	<b>0.56</b>	<b>0.97</b>	<b>0.26</b>	<b>1.09</b>	<b>3.12</b>	<b>0.18</b>	<b>b.d.</b>
NKZ-2-1	green	51.40	32.87	6.39	0.20	0.64	0.76	0.23	3.72	2.53	0.31	b.d.
NKZ-2-2		51.11	32.94	6.38	0.19	0.63	0.67	0.31	3.66	2.50	0.33	b.d.
<b>NKZ-2 Mean</b>		<b>51.26</b>	<b>32.91</b>	<b>6.39</b>	<b>0.19</b>	<b>0.63</b>	<b>0.71</b>	<b>0.27</b>	<b>3.69</b>	<b>2.52</b>	<b>0.32</b>	<b>b.d.</b>
NKZ-2-1	dark	53.39	31.88	6.01	0.16	0.53	0.93	0.17	1.01	3.99	0.24	0.00



NKZ-2-2	brown	54.08	32.33	6.20	0.18	0.58	0.86	0.19	1.08	3.84	0.27	0.15
NKZ-2-3		54.52	31.61	5.50	0.15	0.52	0.89	0.23	1.25	3.63	0.24	0.12
NKZ-2-4		54.08	32.16	5.45	0.14	0.49	0.87	0.28	1.41	3.66	0.21	0.06
<b>NKZ-2 Mean</b>		<b>54.02</b>	<b>32.00</b>	<b>5.79</b>	<b>0.16</b>	<b>0.53</b>	<b>0.89</b>	<b>0.22</b>	<b>1.19</b>	<b>3.78</b>	<b>0.24</b>	<b>0.08</b>
NKZ-3-1	green and yellow mix	58.53	29.29	5.58	0.17	0.67	1.22	0.17	0.98	2.82	0.27	b.d.
NKZ-3-2		58.37	29.12	5.67	0.18	0.78	1.26	0.21	0.91	2.86	0.24	b.d.
<b>NKZ-3 Mean</b>		<b>58.45</b>	<b>29.20</b>	<b>5.62</b>	<b>0.18</b>	<b>0.72</b>	<b>1.24</b>	<b>0.19</b>	<b>0.95</b>	<b>2.84</b>	<b>0.26</b>	<b>b.d.</b>
NKZ-4-1	brown	64.97	25.14	4.14	0.05	0.25	1.20	0.14	0.10	3.43	0.15	0.03
NKZ-4-2		63.71	25.66	5.26	0.06	0.30	1.27	0.13	0.10	3.04	0.20	0.07
<b>NKZ-4 Mean</b>		<b>64.34</b>	<b>25.40</b>	<b>4.70</b>	<b>0.06</b>	<b>0.27</b>	<b>1.24</b>	<b>0.14</b>	<b>0.10</b>	<b>3.24</b>	<b>0.18</b>	<b>0.05</b>
WL-1-1	dark green	59.68	26.64	5.78	0.10	0.59	0.97	0.64	1.36	1.13	0.32	b.d.
WL-1-2		58.08	26.06	5.41	0.10	0.55	2.06	0.62	1.26	1.13	0.30	b.d.
<b>WL-1 Mean</b>		<b>59.88</b>	<b>26.35</b>	<b>5.59</b>	<b>0.10</b>	<b>0.57</b>	<b>1.51</b>	<b>0.63</b>	<b>1.31</b>	<b>1.13</b>	<b>0.31</b>	<b>b.d.</b>
WL-2-1	brown	61.42	29.42	4.47	0.09	0.47	0.26	0.14	0.06	2.29	0.19	b.d.
WL-2-2		60.33	30.13	4.29	0.09	0.51	0.28	0.13	0.05	2.17	0.23	b.d.
<b>WL-2 Mean</b>		<b>60.87</b>	<b>29.77</b>	<b>4.38</b>	<b>0.09</b>	<b>0.49</b>	<b>0.27</b>	<b>0.13</b>	<b>0.06</b>	<b>2.23</b>	<b>0.21</b>	<b>b.d.</b>
WL-3-1	green	61.84	28.00	4.84	0.10	0.31	0.44	0.29	1.23	0.44	0.24	b.d.
WL-3-2		60.72	27.73	5.48	0.13	0.36	0.41	0.19	1.21	0.42	0.16	b.d.
<b>WL-3 Mean</b>		<b>61.28</b>	<b>27.87</b>	<b>5.16</b>	<b>0.11</b>	<b>0.33</b>	<b>0.42</b>	<b>0.24</b>	<b>1.22</b>	<b>0.43</b>	<b>0.20</b>	<b>b.d.</b>
WL-4-1	brown	47.02	35.22	7.69	0.20	0.68	0.41	0.28	0.21	3.82	0.21	b.d.
WL-4-2		46.97	36.73	8.48	0.20	0.77	0.41	0.29	0.17	3.29	0.21	b.d.
<b>WL-4 Mean</b>		<b>47.00</b>	<b>35.98</b>	<b>8.09</b>	<b>0.20</b>	<b>0.73</b>	<b>0.41</b>	<b>0.28</b>	<b>0.19</b>	<b>3.56</b>	<b>0.21</b>	<b>b.d.</b>
WL-4-1	white	43.28	40.51	8.44	0.20	0.78	0.49	0.33	0.12	0.39	0.25	b.d.
WL-4-2		43.09	42.98	7.95	0.16	0.81	0.49	0.37	0.09	0.38	0.29	b.d.
WL-4-3		42.86	40.99	8.46	0.18	0.82	0.54	0.32	0.07	0.40	0.24	b.d.
<b>WL-4 Mean</b>		<b>43.08</b>	<b>41.49</b>	<b>8.28</b>	<b>0.18</b>	<b>0.80</b>	<b>0.50</b>	<b>0.34</b>	<b>0.09</b>	<b>0.39</b>	<b>0.26</b>	<b>b.d.</b>

Table A3 the major chemical compositions of Tang Sancai lead glaze samples (Unit: wt.%)

Sample No.	SiO <sub>2</sub>	Al <sub>2</sub> O <sub>3</sub>	PbO	Na <sub>2</sub> O	K <sub>2</sub> O	CaO	MgO	CuO	FeO	Sb <sub>2</sub> O <sub>5</sub>	MnO	SnO <sub>2</sub>	TiO <sub>2</sub>	ZnO
<b>Al-Raqqa, Syria, 8th-9th Centuries AD</b>														
Syria-4 green-1	35.40	1.06	53.76	0.30	0.40	2.10	0.45	2.55	0.75	0.03	0.07	b.d.	0.03	0.92
Syria-4 green-2	36.28	1.30	50.31	0.35	0.41	3.03	1.08	2.01	0.98	0.03	0.11	b.d.	0.02	0.79
Syria-4 green-3	38.69	3.32	45.65	0.46	1.31	2.30	0.54	1.73	0.85	0.08	0.09	b.d.	0.04	0.60
<b>Syria-4 green Mean</b>	<b>36.79</b>	<b>1.89</b>	<b>49.91</b>	<b>0.37</b>	<b>0.71</b>	<b>2.48</b>	<b>0.69</b>	<b>2.10</b>	<b>0.86</b>	<b>0.05</b>	<b>0.09</b>	<b>b.d.</b>	<b>0.03</b>	<b>0.77</b>
Syria-7 green-1	37.98	1.03	50.02	0.70	0.33	2.15	0.48	3.31	0.12	b.d.	0.71	0.55	0.04	0.01
Syria-7 green-2	34.79	1.14	54.31	0.74	0.35	2.35	0.52	3.72	0.15	b.d.	0.77	0.59	0.05	0.01
<b>Syria-7 green Mean</b>	<b>36.38</b>	<b>1.08</b>	<b>52.16</b>	<b>0.72</b>	<b>0.34</b>	<b>2.25</b>	<b>0.50</b>	<b>3.51</b>	<b>0.13</b>	<b>b.d.</b>	<b>0.74</b>	<b>0.57</b>	<b>0.05</b>	<b>0.01</b>
<b>Kish-shaal Ghazna, Iraq, 10th-13th Centuries AD</b>														
9913 white-1	38.38	2.04	53.47	0.62	0.89	1.59	1.37	0.07	0.53	0.05	0.06	0.01	0.20	0.02
9913 white-2	41.72	4.92	40.42	0.93	1.59	4.45	2.84	0.04	0.49	0.04	0.01	0.04	0.30	0.06

<b>9913 white Mean</b>	<b>40.05</b>	<b>3.48</b>	<b>46.95</b>	<b>0.78</b>	<b>1.24</b>	<b>3.02</b>	<b>2.10</b>	<b>0.05</b>	<b>0.51</b>	<b>0.05</b>	<b>0.03</b>	<b>0.03</b>	<b>0.25</b>	<b>0.04</b>
9393 yellow-1	33.59	2.58	56.12	0.57	1.27	1.65	0.59	0.05	1.79	0.03	0.02	b.d.	0.03	0.02
9393 yellow-2	33.44	4.06	54.63	0.59	1.37	1.60	0.40	0.01	1.87	0.03	0.04	b.d.	0.10	0.03
<b>9393 yellow Mean</b>	<b>33.51</b>	<b>3.32</b>	<b>55.37</b>	<b>0.58</b>	<b>1.32</b>	<b>1.62</b>	<b>0.50</b>	<b>0.03</b>	<b>1.83</b>	<b>0.03</b>	<b>0.03</b>	<b>b.d.</b>	<b>0.07</b>	<b>0.02</b>
9393 green-1	36.70	3.00	51.49	0.63	1.14	1.86	0.44	2.82	0.85	b.d.	0.06	0.05	0.10	0.21
9393 green-2	37.38	4.09	51.01	0.66	1.35	1.39	0.42	2.02	0.70	b.d.	0.06	0.02	0.16	0.25
<b>9393 green Mean</b>	<b>37.04</b>	<b>3.55</b>	<b>51.25</b>	<b>0.65</b>	<b>1.24</b>	<b>1.62</b>	<b>0.43</b>	<b>2.42</b>	<b>0.78</b>	<b>b.d.</b>	<b>0.06</b>	<b>0.03</b>	<b>0.13</b>	<b>0.23</b>
9921 yellow-1	37.48	0.65	53.49	1.06	1.74	1.45	0.44	0.16	1.51	b.d.	0.04	0.09	0.00	0.03
9921 yellow-2	36.90	0.84	54.26	1.07	1.71	1.35	0.44	0.10	1.37	b.d.	0.01	0.21	0.07	0.00
<b>9921 yellow Mean</b>	<b>37.19</b>	<b>0.75</b>	<b>53.88</b>	<b>1.07</b>	<b>1.72</b>	<b>1.40</b>	<b>0.44</b>	<b>0.13</b>	<b>1.44</b>	<b>b.d.</b>	<b>0.03</b>	<b>0.15</b>	<b>0.04</b>	<b>0.01</b>
9921 green-1	34.79	0.94	55.63	0.90	1.46	1.51	0.42	1.47	0.61	0.09	0.03	0.12	0.09	0.27
9921 green-2	35.26	1.45	54.14	1.07	1.58	1.43	0.38	1.60	0.56	0.07	0.03	0.23	0.10	0.21
<b>9921 green Mean</b>	<b>35.03</b>	<b>1.19</b>	<b>54.89</b>	<b>0.99</b>	<b>1.52</b>	<b>1.47</b>	<b>0.40</b>	<b>1.54</b>	<b>0.59</b>	<b>0.08</b>	<b>0.03</b>	<b>0.18</b>	<b>0.09</b>	<b>0.24</b>
9921 black-1	31.37	1.05	57.48	0.59	0.65	1.82	0.53	0.81	1.54	b.d.	1.03	0.19	0.05	0.62
9921 black-2	32.10	1.21	56.62	0.64	0.73	1.79	0.49	0.86	1.41	b.d.	1.02	0.21	0.14	0.69
<b>9921 black Mean</b>	<b>31.73</b>	<b>1.13</b>	<b>57.05</b>	<b>0.62</b>	<b>0.69</b>	<b>1.80</b>	<b>0.51</b>	<b>0.83</b>	<b>1.47</b>	<b>b.d.</b>	<b>1.02</b>	<b>0.20</b>	<b>0.10</b>	<b>0.66</b>
9156 yellow-1	30.32	1.92	58.30	0.78	0.89	1.57	0.34	0.17	4.63	b.d.	0.01	0.01	0.20	0.03
9156 yellow-2	32.99	4.15	54.40	1.12	1.33	1.48	0.36	0.14	3.07	b.d.	0.01	0.03	0.12	0.04
<b>9156 yellow Mean</b>	<b>31.65</b>	<b>3.04</b>	<b>56.35</b>	<b>0.95</b>	<b>1.11</b>	<b>1.53</b>	<b>0.35</b>	<b>0.16</b>	<b>3.85</b>	<b>b.d.</b>	<b>0.01</b>	<b>0.02</b>	<b>0.16</b>	<b>0.04</b>
9156 green-1	34.09	1.67	58.17	0.71	0.88	1.62	0.52	1.51	0.56	b.d.	0.02	0.07	0.03	0.19
9156 green-2	33.76	1.95	57.54	0.75	0.94	1.70	0.42	1.51	0.54	b.d.	0.04	0.06	0.07	0.24
<b>9156 green Mean</b>	<b>33.92</b>	<b>1.81</b>	<b>57.85</b>	<b>0.73</b>	<b>0.91</b>	<b>1.66</b>	<b>0.47</b>	<b>1.51</b>	<b>0.55</b>	<b>b.d.</b>	<b>0.03</b>	<b>0.07</b>	<b>0.05</b>	<b>0.21</b>
9156 white-1	34.48	0.96	60.04	0.59	0.63	1.69	0.52	0.04	0.66	0.01	0.07	0.07	0.09	0.02
9156 white-2	34.44	0.94	59.87	0.53	0.61	1.79	0.57	0.00	0.66	0.08	0.11	0.14	0.06	0.04
<b>9156 white Mean</b>	<b>34.46</b>	<b>0.95</b>	<b>59.95</b>	<b>0.56</b>	<b>0.62</b>	<b>1.74</b>	<b>0.55</b>	<b>0.02</b>	<b>0.66</b>	<b>0.04</b>	<b>0.09</b>	<b>0.10</b>	<b>0.07</b>	<b>0.03</b>
9161 green-1	29.14	1.84	64.14	0.09	0.12	1.03	0.25	1.05	0.37	b.d.	0.01	1.49	0.11	0.13

9161 green-2	29.45	0.89	64.55	0.10	0.11	1.08	0.22	1.42	0.48	b.d.	0.01	1.18	0.14	0.17
<b>9161 green Mean</b>	<b>29.29</b>	<b>1.36</b>	<b>64.35</b>	<b>0.09</b>	<b>0.12</b>	<b>1.06</b>	<b>0.23</b>	<b>1.24</b>	<b>0.43</b>	<b>b.d.</b>	<b>0.01</b>	<b>1.33</b>	<b>0.12</b>	<b>0.15</b>
9161 white-1	26.74	0.90	68.61	0.00	0.07	0.93	0.28	0.16	0.36	b.d.	0.32	1.10	0.11	0.03
9161 white-2	27.24	0.88	68.32	0.02	0.06	0.88	0.27	0.14	0.33	b.d.	0.31	1.08	0.11	0.04
<b>9161 white Mean</b>	<b>26.99</b>	<b>0.89</b>	<b>68.46</b>	<b>0.01</b>	<b>0.06</b>	<b>0.90</b>	<b>0.28</b>	<b>0.15</b>	<b>0.35</b>	<b>b.d.</b>	<b>0.31</b>	<b>1.09</b>	<b>0.11</b>	<b>0.03</b>
9147 yellow-1	24.81	2.14	64.62	0.15	0.21	1.42	0.32	0.34	2.81	0.04	0.01	0.04	0.17	0.04
9147 yellow-2	24.84	2.36	64.96	0.14	0.22	1.32	0.34	0.36	3.01	0.01	0.01	0.04	0.13	0.03
<b>9147 yellow Mean</b>	<b>24.82</b>	<b>2.25</b>	<b>64.79</b>	<b>0.15</b>	<b>0.21</b>	<b>1.37</b>	<b>0.33</b>	<b>0.35</b>	<b>2.90</b>	<b>0.03</b>	<b>0.01</b>	<b>0.04</b>	<b>0.15</b>	<b>0.04</b>
9147 green-1	25.21	2.40	65.02	0.11	0.19	1.38	0.37	1.07	2.55	b.d.	0.01	0.06	0.14	0.12
9147 green-2	24.44	2.13	65.50	0.12	0.16	1.36	0.37	1.11	2.60	b.d.	0.03	0.00	0.07	0.09
<b>9147 green Mean</b>	<b>24.83</b>	<b>2.27</b>	<b>65.26</b>	<b>0.12</b>	<b>0.17</b>	<b>1.37</b>	<b>0.37</b>	<b>1.09</b>	<b>2.58</b>	<b>b.d.</b>	<b>0.02</b>	<b>0.03</b>	<b>0.10</b>	<b>0.10</b>
9159 brown-1	28.81	2.85	59.85	0.57	0.70	1.85	0.56	0.15	2.83	b.d.	1.14	0.29	0.13	0.11
9159 brown-2	28.79	3.10	59.92	0.61	0.75	1.83	0.60	0.19	2.68	b.d.	1.11	0.13	0.18	0.00
<b>9159 brown Mean</b>	<b>28.80</b>	<b>2.98</b>	<b>59.88</b>	<b>0.59</b>	<b>0.72</b>	<b>1.84</b>	<b>0.58</b>	<b>0.17</b>	<b>2.75</b>	<b>b.d.</b>	<b>1.13</b>	<b>0.21</b>	<b>0.16</b>	<b>0.05</b>
9159 white-1	32.91	2.84	59.09	0.74	1.08	1.40	0.41	0.08	0.60	0.17	0.05	0.20	0.16	0.06
9159 white-2	32.99	2.81	58.60	0.80	1.06	1.41	0.48	0.02	0.63	0.05	0.06	0.25	0.16	0.06
<b>9159 white Mean</b>	<b>32.95</b>	<b>2.83</b>	<b>58.84</b>	<b>0.77</b>	<b>1.07</b>	<b>1.41</b>	<b>0.44</b>	<b>0.05</b>	<b>0.62</b>	<b>0.11</b>	<b>0.05</b>	<b>0.23</b>	<b>0.16</b>	<b>0.06</b>
9159 yellow-1	30.76	4.67	56.16	0.97	1.18	0.98	0.32	0.14	4.32	b.d.	0.01	0.22	0.19	0.03
9159 yellow-2	30.06	4.87	56.78	1.07	1.22	0.98	0.27	0.21	3.85	b.d.	0.01	0.08	0.19	0.00
<b>9159 yellow Mean</b>	<b>30.41</b>	<b>4.77</b>	<b>56.47</b>	<b>1.02</b>	<b>1.20</b>	<b>0.98</b>	<b>0.30</b>	<b>0.18</b>	<b>4.08</b>	<b>b.d.</b>	<b>0.01</b>	<b>0.15</b>	<b>0.19</b>	<b>0.01</b>
9915 white-1	33.37	3.94	57.40	0.56	1.06	1.45	0.37	0.09	0.46	b.d.	0.01	0.40	0.07	0.00
9915 white-2	34.07	3.94	56.34	0.60	1.13	1.60	0.38	0.05	0.61	b.d.	0.01	0.29	0.19	0.04
<b>9915 white Mean</b>	<b>33.72</b>	<b>3.94</b>	<b>56.87</b>	<b>0.58</b>	<b>1.10</b>	<b>1.52</b>	<b>0.37</b>	<b>0.07</b>	<b>0.53</b>	<b>b.d.</b>	<b>0.01</b>	<b>0.34</b>	<b>0.13</b>	<b>0.02</b>
9915 brown-1	31.20	4.57	54.61	0.46	0.80	2.81	0.59	0.11	2.64	0.04	1.04	0.29	0.31	0.05
9915 brown-2	34.72	4.66	45.06	0.49	0.75	3.06	2.85	0.15	3.66	0.01	1.00	0.39	0.26	0.05
<b>9915 brown Mean</b>	<b>32.96</b>	<b>4.61</b>	<b>49.83</b>	<b>0.48</b>	<b>0.78</b>	<b>2.93</b>	<b>1.72</b>	<b>0.13</b>	<b>3.15</b>	<b>0.02</b>	<b>1.02</b>	<b>0.34</b>	<b>0.28</b>	<b>0.05</b>

9915 green-1	43.42	3.85	39.32	1.40	3.31	2.46	0.50	1.86	0.71	b.d.	0.02	0.49	0.19	0.78
9915 green-2	42.78	3.96	39.47	1.48	3.42	2.51	0.53	1.93	0.75	b.d.	0.02	0.30	0.14	0.73
<b>9915 green Mean</b>	<b>43.10</b>	<b>3.91</b>	<b>39.40</b>	<b>1.44</b>	<b>3.36</b>	<b>2.48</b>	<b>0.51</b>	<b>1.89</b>	<b>0.73</b>	<b>b.d.</b>	<b>0.02</b>	<b>0.39</b>	<b>0.16</b>	<b>0.76</b>
9162 brown-1	30.26	2.41	59.61	1.16	1.24	1.40	0.48	0.36	0.75	0.18	1.57	0.01	0.14	0.00
9162 brown-2	28.73	1.93	60.13	0.99	1.04	1.50	0.45	0.61	0.73	0.19	2.78	0.00	0.23	0.00
<b>9162 brown Mean</b>	<b>29.50</b>	<b>2.17</b>	<b>59.87</b>	<b>1.07</b>	<b>1.14</b>	<b>1.45</b>	<b>0.46</b>	<b>0.48</b>	<b>0.74</b>	<b>0.18</b>	<b>2.18</b>	<b>0.01</b>	<b>0.19</b>	<b>0.00</b>
9162 green-1	29.43	2.37	60.28	1.17	1.11	1.61	0.45	1.45	0.86	0.26	0.02	0.02	0.30	0.16
9162 green-2	29.73	2.37	60.02	1.18	1.16	1.64	0.54	1.51	0.84	0.16	0.01	0.11	0.19	0.16
<b>9162 green Mean</b>	<b>29.58</b>	<b>2.37</b>	<b>60.15</b>	<b>1.17</b>	<b>1.14</b>	<b>1.62</b>	<b>0.49</b>	<b>1.48</b>	<b>0.85</b>	<b>0.21</b>	<b>0.02</b>	<b>0.06</b>	<b>0.24</b>	<b>0.16</b>
9160 green-1	29.23	3.42	57.65	0.80	0.99	2.48	0.80	0.93	1.32	b.d.	0.11	0.32	0.18	0.26
9160 green-2	28.71	2.93	58.24	0.71	0.87	2.27	0.78	1.09	1.39	b.d.	0.13	0.46	0.17	0.14
<b>9160 green Mean</b>	<b>28.97</b>	<b>3.18</b>	<b>57.94</b>	<b>0.76</b>	<b>0.93</b>	<b>2.37</b>	<b>0.79</b>	<b>1.01</b>	<b>1.35</b>	<b>b.d.</b>	<b>0.12</b>	<b>0.39</b>	<b>0.18</b>	<b>0.20</b>
9160 brown-1	32.98	4.64	49.69	1.30	1.85	2.24	0.82	0.30	3.95	b.d.	1.05	0.36	0.33	0.08
9160 brown-2	33.08	4.76	47.72	1.33	1.96	2.81	0.79	0.35	3.87	b.d.	1.07	0.37	0.24	0.05
<b>9160 brown Mean</b>	<b>33.03</b>	<b>4.70</b>	<b>48.71</b>	<b>1.32</b>	<b>1.90</b>	<b>2.53</b>	<b>0.81</b>	<b>0.32</b>	<b>3.91</b>	<b>b.d.</b>	<b>1.06</b>	<b>0.37</b>	<b>0.28</b>	<b>0.06</b>

#### Kish or Hira, 8th-14th Centuries, maybe later than 10th Century

9312 green-1	27.46	1.00	65.41	0.42	0.49	1.36	0.23	1.54	0.63	b.d.	0.03	b.d.	0.03	0.33
9312 green-2	26.94	0.99	64.53	0.40	0.45	1.43	0.24	1.52	0.67	b.d.	0.01	b.d.	0.05	0.31
<b>9312 green Mean</b>	<b>27.20</b>	<b>0.99</b>	<b>64.97</b>	<b>0.41</b>	<b>0.47</b>	<b>1.39</b>	<b>0.23</b>	<b>1.53</b>	<b>0.65</b>	<b>b.d.</b>	<b>0.02</b>	<b>b.d.</b>	<b>0.04</b>	<b>0.32</b>
9309 yellow-1	27.61	1.80	61.71	0.35	0.40	1.51	0.48	0.13	3.25	b.d.	0.01	0.38	0.07	0.10
9309 yellow-2	27.08	1.45	62.72	0.36	0.36	1.52	0.44	0.12	3.37	b.d.	0.05	0.47	0.05	0.07
<b>9309 yellow Mean</b>	<b>27.35</b>	<b>1.62</b>	<b>62.21</b>	<b>0.36</b>	<b>0.38</b>	<b>1.51</b>	<b>0.46</b>	<b>0.12</b>	<b>3.31</b>	<b>b.d.</b>	<b>0.03</b>	<b>0.42</b>	<b>0.06</b>	<b>0.08</b>
9309 green-1	29.58	4.09	55.49	0.19	0.39	1.05	0.24	3.95	0.40	0.01	0.02	0.05	0.15	0.66
9309 green-2	29.80	4.35	55.85	0.21	0.38	1.02	0.21	3.86	0.45	0.05	0.04	0.04	0.18	0.70
<b>9309 green Mean</b>	<b>29.69</b>	<b>4.22</b>	<b>55.67</b>	<b>0.20</b>	<b>0.38</b>	<b>1.04</b>	<b>0.23</b>	<b>3.90</b>	<b>0.43</b>	<b>0.03</b>	<b>0.03</b>	<b>0.05</b>	<b>0.17</b>	<b>0.68</b>
9308 brown-1	28.13	2.00	63.58	0.46	0.50	1.06	0.23	0.06	2.00	0.01	1.57	b.d.	0.17	0.00

9308 brown-2	28.49	2.44	62.16	0.49	0.57	1.06	0.12	0.04	1.90	0.05	1.54	b.d.	0.07	0.02
<b>9308 brown Mean</b>	<b>28.31</b>	<b>2.22</b>	<b>62.87</b>	<b>0.47</b>	<b>0.54</b>	<b>1.06</b>	<b>0.17</b>	<b>0.05</b>	<b>1.95</b>	<b>0.03</b>	<b>1.55</b>	<b>b.d.</b>	<b>0.12</b>	<b>0.01</b>
9308 yellow-1	30.18	2.83	61.80	0.63	0.81	1.02	0.24	0.04	1.24	b.d.	0.07	b.d.	0.14	0.05
9308 yellow-2	27.07	2.09	65.27	0.52	0.59	0.94	0.20	0.03	1.20	b.d.	0.00	b.d.	0.13	0.07
<b>9308 yellow Mean</b>	<b>28.63</b>	<b>2.46</b>	<b>63.54</b>	<b>0.58</b>	<b>0.70</b>	<b>0.98</b>	<b>0.22</b>	<b>0.03</b>	<b>1.22</b>	<b>b.d.</b>	<b>0.03</b>	<b>b.d.</b>	<b>0.13</b>	<b>0.06</b>
9808 green-1	30.49	2.69	60.64	0.78	0.95	1.16	0.24	1.90	0.50	0.02	0.01	0.02	0.11	0.37
9808 green-2	29.99	2.74	60.05	0.84	0.98	1.13	0.23	1.82	0.31	0.01	0.01	0.05	0.15	0.39
<b>9808 green Mean</b>	<b>30.24</b>	<b>2.71</b>	<b>60.35</b>	<b>0.81</b>	<b>0.96</b>	<b>1.15</b>	<b>0.24</b>	<b>1.86</b>	<b>0.40</b>	<b>0.02</b>	<b>0.01</b>	<b>0.03</b>	<b>0.13</b>	<b>0.38</b>
9798 green-1	39.04	1.16	46.08	2.16	1.55	2.55	0.88	2.58	0.70	b.d.	0.08	0.33	0.07	0.38
9798 green-2	41.52	1.04	43.32	2.07	1.47	3.68	1.78	2.50	0.60	b.d.	0.12	0.30	0.08	0.38
<b>9798 green Mean</b>	<b>40.28</b>	<b>1.10</b>	<b>44.70</b>	<b>2.11</b>	<b>1.51</b>	<b>3.11</b>	<b>1.33</b>	<b>2.54</b>	<b>0.65</b>	<b>b.d.</b>	<b>0.10</b>	<b>0.31</b>	<b>0.08</b>	<b>0.38</b>
9800 green-1	35.48	0.97	52.39	2.15	0.99	2.39	0.88	1.43	0.74	b.d.	0.19	1.67	0.12	0.19
9800 green-2	36.34	1.28	51.24	2.22	1.04	2.46	0.97	1.22	0.63	b.d.	0.23	1.12	0.09	0.18
9800 green-3	35.85	0.84	50.67	2.10	1.03	2.33	1.11	1.15	0.58	b.d.	0.15	3.02	0.03	0.15
9800 green-4	36.02	0.96	51.37	2.04	1.00	2.29	1.05	1.48	0.75	b.d.	0.17	1.46	0.08	0.13
<b>9800 green Mean</b>	<b>35.91</b>	<b>1.13</b>	<b>51.82</b>	<b>2.18</b>	<b>1.02</b>	<b>2.43</b>	<b>0.92</b>	<b>1.32</b>	<b>0.69</b>	<b>b.d.</b>	<b>0.21</b>	<b>1.39</b>	<b>0.11</b>	<b>0.19</b>
9800 brown-1	32.83	1.00	52.88	1.41	0.80	2.22	0.80	0.75	0.71	b.d.	2.25	1.07	0.10	0.07
9800 brown-2	34.01	1.01	51.17	1.43	0.77	2.17	0.69	0.75	0.73	b.d.	2.52	2.62	0.09	0.08
<b>9800 brown Mean</b>	<b>33.42</b>	<b>1.00</b>	<b>52.02</b>	<b>1.42</b>	<b>0.78</b>	<b>2.19</b>	<b>0.75</b>	<b>0.75</b>	<b>0.72</b>	<b>b.d.</b>	<b>2.39</b>	<b>1.85</b>	<b>0.10</b>	<b>0.08</b>
9807 green-1	27.68	2.14	59.89	0.77	0.86	1.67	0.44	3.50	0.59	0.15	0.00	0.02	0.14	0.58
9807 green-2	28.57	1.92	60.08	0.75	0.82	1.66	0.50	3.66	0.56	0.20	0.02	0.06	0.08	0.52
<b>9807 green Mean</b>	<b>28.12</b>	<b>2.03</b>	<b>59.98</b>	<b>0.76</b>	<b>0.84</b>	<b>1.66</b>	<b>0.47</b>	<b>3.58</b>	<b>0.57</b>	<b>0.18</b>	<b>0.01</b>	<b>0.04</b>	<b>0.11</b>	<b>0.55</b>

**Table A4 the major chemical compositions of Islamic lead glaze samples (Unit: wt.%)**

<b>Sample No.</b>	<b>La</b>	<b>Ce</b>	<b>Pr</b>	<b>Nd</b>	<b>Sm</b>	<b>Eu</b>	<b>Gd</b>	<b>Tb</b>	<b>Dy</b>	<b>Ho</b>	<b>Er</b>	<b>Tm</b>	<b>Yb</b>	<b>Lu</b>
Tang 16a-1	38.78	81.17	9.14	32.08	6.89	0.64	6.01	0.90	5.56	1.10	3.01	0.43	3.53	0.49
Tang 16a-2	41.86	87.29	9.87	35.67	7.34	0.67	6.41	0.91	5.72	1.17	3.38	0.49	3.48	0.50
Tang 16a-3	43.25	88.67	9.74	36.20	7.10	0.62	5.93	0.97	5.88	1.16	3.45	0.51	3.54	0.52
<b>Tang 16a Mean</b>	<b>41.30</b>	<b>85.71</b>	<b>9.58</b>	<b>34.65</b>	<b>7.11</b>	<b>0.64</b>	<b>6.12</b>	<b>0.93</b>	<b>5.72</b>	<b>1.14</b>	<b>3.28</b>	<b>0.48</b>	<b>3.52</b>	<b>0.50</b>

Tang 20-1	46.94	99.74	11.10	40.11	8.27	0.82	7.89	1.08	6.66	1.28	4.16	0.54	3.84	0.53
Tang 20-2	45.49	95.02	10.96	39.05	7.07	0.93	7.10	1.01	6.44	1.24	3.54	0.57	3.90	0.53
Tang 20-3	42.71	89.10	9.69	36.54	7.40	0.64	6.55	0.95	5.13	1.09	3.24	0.44	3.07	0.43
<b>Tang 20 Mean</b>	<b>45.04</b>	<b>94.62</b>	<b>10.59</b>	<b>38.57</b>	<b>7.58</b>	<b>0.80</b>	<b>7.18</b>	<b>1.01</b>	<b>6.08</b>	<b>1.21</b>	<b>3.65</b>	<b>0.52</b>	<b>3.61</b>	<b>0.50</b>
Tang BW3-1	39.01	79.44	8.76	31.34	6.02	0.77	6.46	1.07	7.64	1.66	4.93	0.69	4.74	0.77
Tang BW3-2	43.32	87.23	9.77	35.44	7.38	0.86	6.58	1.07	7.38	1.48	4.48	0.66	4.54	0.66
Tang BW3-3	47.33	93.40	10.36	37.80	7.82	0.99	7.23	1.03	6.49	1.43	3.97	0.60	4.21	0.65
<b>Tang BW3 Mean</b>	<b>43.22</b>	<b>86.69</b>	<b>9.63</b>	<b>34.86</b>	<b>7.07</b>	<b>0.84</b>	<b>6.76</b>	<b>1.06</b>	<b>7.17</b>	<b>1.52</b>	<b>4.46</b>	<b>0.65</b>	<b>4.50</b>	<b>0.69</b>
Tang BW6-1	47.92	95.39	11.72	38.30	7.71	0.88	7.92	1.16	7.34	1.32	3.98	0.59	3.87	0.56
Tang BW6-2	49.59	109.45	13.29	41.29	7.50	0.91	7.62	1.15	7.73	1.23	3.90	0.53	3.82	0.53
Tang BW6-3	45.12	96.13	10.30	37.12	6.53	0.85	6.38	1.04	6.16	1.08	3.30	0.45	3.35	0.45
<b>Tang BW6 Mean</b>	<b>47.54</b>	<b>100.32</b>	<b>11.77</b>	<b>38.90</b>	<b>7.25</b>	<b>0.88</b>	<b>7.31</b>	<b>1.12</b>	<b>7.08</b>	<b>1.21</b>	<b>3.72</b>	<b>0.52</b>	<b>3.68</b>	<b>0.51</b>
YZF-1-1	38.60	79.37	8.64	31.98	6.59	0.46	6.06	0.96	5.86	1.26	3.63	0.48	3.68	0.53
YZF-1-2	36.88	76.22	8.42	31.56	5.64	0.38	5.24	0.92	5.38	1.10	3.61	0.46	3.32	0.52
YZF-1-3	33.92	70.92	7.90	28.88	6.28	0.52	5.41	0.77	5.86	1.08	3.32	0.54	3.10	0.58
<b>YZF-1 Mean</b>	<b>36.47</b>	<b>75.50</b>	<b>8.32</b>	<b>30.81</b>	<b>6.17</b>	<b>0.45</b>	<b>5.57</b>	<b>0.88</b>	<b>5.70</b>	<b>1.15</b>	<b>3.52</b>	<b>0.49</b>	<b>3.37</b>	<b>0.54</b>
YZF-2-1	48.50	99.67	10.40	36.59	8.03	0.73	7.39	1.11	6.49	1.30	3.49	0.55	3.80	0.51
YZF-2-2	48.06	93.93	10.88	37.50	7.66	0.95	6.38	1.04	6.56	1.20	3.78	0.55	3.46	0.58
YZF-2-3	35.79	75.03	7.50	24.21	5.53	1.12	5.28	0.94	5.12	1.07	2.95	0.50	2.98	0.47
<b>YZF-2 Mean</b>	<b>44.78</b>	<b>89.54</b>	<b>9.59</b>	<b>32.77</b>	<b>7.07</b>	<b>0.93</b>	<b>6.35</b>	<b>1.03</b>	<b>6.06</b>	<b>1.19</b>	<b>3.41</b>	<b>0.54</b>	<b>3.41</b>	<b>0.52</b>
YZF-3-1	34.95	73.30	8.91	31.89	6.46	0.43	5.67	0.93	6.73	1.47	3.76	0.57	3.91	0.61
YZF-3-2	41.83	89.12	10.15	34.74	6.91	0.42	6.85	1.10	7.88	1.49	5.18	0.77	5.00	0.78
YZF-3-3	46.92	96.70	10.52	39.14	8.03	0.44	7.82	1.35	7.58	1.75	5.24	0.74	5.21	0.72
<b>YZF-3 Mean</b>	<b>41.24</b>	<b>86.37</b>	<b>9.86</b>	<b>35.25</b>	<b>7.13</b>	<b>0.43</b>	<b>6.78</b>	<b>1.13</b>	<b>7.40</b>	<b>1.57</b>	<b>4.73</b>	<b>0.69</b>	<b>4.71</b>	<b>0.70</b>
YZF-4-1	36.44	77.55	8.29	29.18	7.04	0.44	5.18	0.95	5.66	1.14	3.66	0.46	3.58	0.47
YZF-4-2	40.12	82.06	9.21	34.23	6.05	0.64	5.18	0.90	5.66	1.12	3.26	0.43	3.08	0.48
YZF-4-3	46.26	97.25	10.94	38.74	8.29	0.55	6.62	1.11	6.49	1.34	3.93	0.55	3.93	0.55
<b>YZF-4 Mean</b>	<b>40.94</b>	<b>85.62</b>	<b>9.48</b>	<b>34.05</b>	<b>7.12</b>	<b>0.54</b>	<b>5.66</b>	<b>0.99</b>	<b>5.94</b>	<b>1.20</b>	<b>3.62</b>	<b>0.48</b>	<b>3.53</b>	<b>0.50</b>
YZF-5-1	53.02	115.12	12.48	45.17	8.79	0.50	7.16	1.11	6.86	1.42	3.65	0.59	3.81	0.59
YZF-5-2	43.90	93.46	10.51	38.28	7.25	0.56	5.50	0.93	6.47	1.27	4.08	0.57	3.81	0.55
YZF-5-3	39.56	79.13	8.55	31.06	6.71	0.56	6.19	0.79	5.77	1.13	3.43	0.53	3.87	0.61
<b>YZF-5 Mean</b>	<b>45.49</b>	<b>95.90</b>	<b>10.51</b>	<b>38.17</b>	<b>7.58</b>	<b>0.54</b>	<b>6.28</b>	<b>0.94</b>	<b>6.37</b>	<b>1.28</b>	<b>3.72</b>	<b>0.56</b>	<b>3.83</b>	<b>0.58</b>
YZF-6-1	29.47	66.21	6.62	22.90	5.02	0.49	4.45	0.70	4.51	1.00	2.78	0.43	3.05	0.46
YZF-6-2	35.96	77.12	7.71	27.44	6.16	0.54	5.26	0.86	5.02	1.10	3.36	0.41	3.01	0.47
YZF-6-3	40.15	82.14	9.03	32.49	6.61	0.65	4.72	0.87	5.11	1.00	3.02	0.49	3.32	0.48
<b>YZF-6 Mean</b>	<b>35.19</b>	<b>75.16</b>	<b>7.79</b>	<b>27.61</b>	<b>5.93</b>	<b>0.56</b>	<b>4.81</b>	<b>0.81</b>	<b>4.88</b>	<b>1.03</b>	<b>3.05</b>	<b>0.44</b>	<b>3.12</b>	<b>0.47</b>
YZF-7-1	55.32	108.66	12.65	48.00	9.50	0.54	8.86	1.40	9.04	1.90	5.54	0.84	5.74	0.80
YZF-7-2	46.26	94.98	10.53	39.02	7.98	0.54	7.21	1.12	7.72	1.60	4.57	0.60	4.36	0.68
YZF-7-3	38.35	86.69	9.89	35.03	7.41	0.49	6.43	1.09	7.60	1.40	4.46	0.68	3.92	0.66
<b>YZF-7 Mean</b>	<b>46.64</b>	<b>96.78</b>	<b>11.03</b>	<b>40.68</b>	<b>8.30</b>	<b>0.52</b>	<b>7.50</b>	<b>1.21</b>	<b>8.12</b>	<b>1.63</b>	<b>4.86</b>	<b>0.71</b>	<b>4.68</b>	<b>0.71</b>
YZF-8-1	37.47	76.44	8.59	32.12	5.60	0.45	5.54	0.86	5.54	1.05	4.05	0.51	3.86	0.45
YZF-8-2	35.67	72.79	8.42	29.94	6.26	0.49	5.57	0.85	6.01	1.23	3.42	0.54	3.42	0.50
YZF-8-3	45.44	98.13	11.17	42.89	8.59	0.46	8.12	1.22	7.47	1.51	4.42	0.62	4.36	0.66
<b>YZF-8 Mean</b>	<b>39.52</b>	<b>82.45</b>	<b>9.39</b>	<b>34.98</b>	<b>6.82</b>	<b>0.47</b>	<b>6.41</b>	<b>0.98</b>	<b>6.34</b>	<b>1.26</b>	<b>3.96</b>	<b>0.56</b>	<b>3.88</b>	<b>0.54</b>
YZF-9-1	32.84	61.20	6.24	20.64	4.14	0.61	3.68	0.55	3.66	0.77	2.26	0.33	2.38	0.37
YZF-9-2	31.35	59.90	6.35	21.71	3.89	0.62	3.55	0.61	3.54	0.78	2.45	0.35	2.71	0.39
YZF-9-3	27.16	51.43	5.28	17.97	3.73	0.50	3.21	0.44	3.37	0.70	1.83	0.26	1.73	0.27

<b>YZF-9 Mean</b>	<b>30.45</b>	<b>57.51</b>	<b>5.96</b>	<b>20.11</b>	<b>3.92</b>	<b>0.58</b>	<b>3.48</b>	<b>0.53</b>	<b>3.52</b>	<b>0.75</b>	<b>2.18</b>	<b>0.31</b>	<b>2.27</b>	<b>0.34</b>
NS-52-1	31.40	62.00	6.49	21.90	4.89	0.53	4.32	0.58	3.74	0.84	2.50	0.34	2.13	0.40
NS-52-2	32.10	61.10	6.08	20.26	4.11	0.58	3.48	0.53	3.89	0.72	2.41	0.37	2.30	0.37
NS-52-3	32.72	62.80	6.58	21.70	4.17	0.78	3.82	0.64	3.75	0.82	2.57	0.33	2.65	0.37
<b>NS-52 Mean</b>	<b>32.07</b>	<b>61.97</b>	<b>6.38</b>	<b>21.29</b>	<b>4.39</b>	<b>0.63</b>	<b>3.87</b>	<b>0.58</b>	<b>3.79</b>	<b>0.79</b>	<b>2.49</b>	<b>0.35</b>	<b>2.36</b>	<b>0.38</b>
NS-53-1	41.90	78.40	8.01	28.00	5.41	1.30	4.37	0.81	4.87	1.02	3.25	0.48	3.38	0.52
NS-53-2	39.30	73.10	7.63	25.10	4.67	1.16	4.76	0.75	4.86	1.09	2.91	0.47	3.02	0.45
NS-53-3	35.07	68.40	7.15	25.00	4.87	1.10	4.97	0.75	4.81	1.04	3.05	0.46	3.55	0.44
<b>NS-53 Mean</b>	<b>38.76</b>	<b>73.30</b>	<b>7.60</b>	<b>26.03</b>	<b>4.98</b>	<b>1.19</b>	<b>4.70</b>	<b>0.77</b>	<b>4.85</b>	<b>1.05</b>	<b>3.07</b>	<b>0.47</b>	<b>3.32</b>	<b>0.47</b>
NS-54-1	45.70	93.40	9.87	35.60	6.52	0.97	5.93	0.97	5.60	1.28	3.71	0.55	3.74	0.61
NS-54-2	45.53	89.60	9.40	34.00	6.75	0.92	5.61	0.87	5.80	1.21	3.50	0.52	3.49	0.51
NS-54-3	45.33	90.50	9.33	33.30	5.96	0.89	5.40	0.92	5.76	1.20	3.46	0.59	3.78	0.54
<b>NS-54 Mean</b>	<b>45.52</b>	<b>91.17</b>	<b>9.53</b>	<b>34.30</b>	<b>6.41</b>	<b>0.93</b>	<b>5.65</b>	<b>0.92</b>	<b>5.72</b>	<b>1.23</b>	<b>3.56</b>	<b>0.55</b>	<b>3.67</b>	<b>0.56</b>
NS-55-1	45.01	83.80	9.10	29.60	5.56	1.43	4.74	0.75	5.54	1.12	3.04	0.44	3.79	0.66
NS-55-2	46.57	86.50	8.98	28.60	5.21	1.22	4.45	0.67	4.72	0.96	3.08	0.55	3.45	0.54
NS-55-3	48.90	90.90	9.90	32.10	6.50	1.52	5.81	0.91	6.25	1.23	3.75	0.68	4.06	0.57
<b>NS-55 Mean</b>	<b>46.83</b>	<b>87.07</b>	<b>9.33</b>	<b>30.10</b>	<b>5.76</b>	<b>1.39</b>	<b>5.00</b>	<b>0.78</b>	<b>5.50</b>	<b>1.10</b>	<b>3.29</b>	<b>0.55</b>	<b>3.77</b>	<b>0.59</b>
NS-56-1	32.35	62.79	6.87	22.44	4.73	0.99	4.10	0.71	4.22	0.91	2.64	0.40	2.55	0.41
NS-56-2	33.38	63.21	6.70	23.38	4.58	0.84	4.21	0.69	4.45	0.87	2.80	0.44	3.01	0.45
NS-56-3	31.23	61.52	6.59	22.07	4.58	0.68	3.86	0.66	4.13	0.95	2.59	0.38	2.51	0.43
<b>NS-56 Mean</b>	<b>32.32</b>	<b>62.51</b>	<b>6.72</b>	<b>22.63</b>	<b>4.63</b>	<b>0.84</b>	<b>4.05</b>	<b>0.69</b>	<b>4.27</b>	<b>0.91</b>	<b>2.68</b>	<b>0.41</b>	<b>2.69</b>	<b>0.43</b>
NS-58-1	36.61	72.42	7.55	26.60	5.33	0.79	4.68	0.81	4.84	0.95	3.11	0.43	3.36	0.54
NS-58-2	35.16	65.64	7.25	24.50	5.00	0.92	4.63	0.82	5.56	1.06	3.26	0.43	3.63	0.58
NS-58-3	37.31	72.88	7.88	27.30	5.14	0.74	5.50	0.75	4.77	1.16	3.55	0.60	3.67	0.57
<b>NS-58 Mean</b>	<b>36.36</b>	<b>70.31</b>	<b>7.56</b>	<b>26.13</b>	<b>5.16</b>	<b>0.82</b>	<b>4.94</b>	<b>0.79</b>	<b>5.06</b>	<b>1.06</b>	<b>3.31</b>	<b>0.49</b>	<b>3.55</b>	<b>0.56</b>
NS-59-1	35.94	76.67	7.95	29.41	6.26	0.42	5.66	0.87	5.05	0.94	2.61	0.39	2.60	0.44
NS-59-2	35.20	73.31	7.90	28.66	6.03	0.40	5.38	0.79	5.23	1.08	2.89	0.48	2.95	0.49
NS-59-3	50.97	101.78	11.64	41.89	8.93	0.49	7.01	1.10	6.64	1.30	3.74	0.49	3.72	0.50
<b>NS-59 Mean</b>	<b>40.70</b>	<b>83.92</b>	<b>9.16</b>	<b>33.32</b>	<b>7.07</b>	<b>0.43</b>	<b>6.02</b>	<b>0.92</b>	<b>5.64</b>	<b>1.10</b>	<b>3.08</b>	<b>0.46</b>	<b>3.09</b>	<b>0.48</b>

**A5 the REEs compositions of Yaozhou celadon glaze samples (Unit: ppm)**

Sample No.	Glaze colour	Li	B	Ti	V	Cr	Co	Ni	Zn	As
HYK-1	green	199.30	33.60	1571.00	32.30	16.49	2.74	11.94	250.80	55.93
HYK-5	green	121.15	45.29	1531.71	34.15	16.59	1.10	11.91	563.02	30.28
HYK-7	brown	96.20	40.67	1078.23	26.37	16.02	5.43	12.24	60.20	21.94
HYK-8	brown	151.27	53.59	975.85	27.49	12.21	9.59	13.93	22.80	23.56
HYK-9	dark brown	93.61	41.78	919.90	21.52	13.22	7.01	14.35	66.68	27.22
HYK-10	brown	87.56	72.34	1429.19	29.91	19.23	2.34	9.70	75.82	33.29
HYK-11	brown	331.67	49.20	2443.00	43.87	19.28	4.65	15.21	84.73	9.24
HYK-11	green	304.40	40.07	1961.67	46.84	19.19	2.66	14.76	88.50	4.77
HYK-13	green and yellow mix	108.27	53.97	1504.67	29.20	14.48	5.62	11.72	27.97	17.64

HYK-18	green	252.44	35.90	1965.09	33.40	16.33	2.37	10.55	238.29	63.58
HPK-1	brown	183.80	63.67	2540.67	32.89	21.97	2.75	19.41	43.03	75.10
HPK-2	green	258.97	79.77	3102.67	43.73	23.13	4.27	22.92	33.83	75.43
HPK-2	brown	192.53	84.37	2550.67	39.42	21.68	4.74	21.56	33.13	76.50
HPK-3	brown	154.90	98.20	3728.33	72.67	39.62	6.59	31.00	174.9	109.14
HPK-4	brown	68.77	51.90	1286.67	26.90	15.14	4.81	20.09	41.20	72.13
HPK-5	brown	143.77	76.33	2208.33	37.82	24.01	4.17	24.13	71.50	122.36
HPK-5	green	164.07	58.07	2156.00	32.95	20.26	1.45	19.88	39.10	89.41
HPK-6	green	183.07	54.63	2201.33	27.31	21.49	2.33	20.39	36.57	112.43
HPK-8	green	131.47	42.97	1371.67	27.92	26.42	1.90	12.12	382.73	138.97
HPK-9	brown	212.20	65.80	1925.00	116.06	26.72	5.91	22.15	44.93	115.91
NKZ-1	green	132.73	40.47	1687.67	72.67	24.25	2.36	11.20	255.27	27.59
NKZ-1	dark brown	132.70	41.10	1434.67	33.54	19.40	5.49	10.97	199.13	19.12
NKZ-2	dark brown	88.69	37.12	1526.57	35.28	15.93	5.24	9.52	660.12	8.10
NKZ-2	green	102.76	35.03	1565.68	35.89	17.73	4.24	7.21	630.89	11.78
NKZ-3	green and yellow mix	285.83	127.77	3504.33	78.53	42.28	17.11	28.47	345.00	21.10
NKZ-4	brown	320.70	177.90	4079.00	97.87	48.09	24.37	43.52	96.90	77.30
WL-1	green	332.70	53.43	2119.00	52.99	17.45	6.25	29.71	102.00	20.36
WL-2	brown	263.03	49.00	1188.67	36.35	16.83	3.00	21.44	43.90	74.70
WL-3	green	262.58	36.73	1288.45	32.65	18.79	34.84	19.59	75.91	63.83
WL-4	white	411.10	65.80	2644.33	59.53	14.65	5.88	32.40	67.37	22.76
<b>Sample No.</b>	<b>Glaze colour</b>	<b>Rb</b>	<b>Sr</b>	<b>Y</b>	<b>Zr</b>	<b>Nb</b>	<b>Sn</b>	<b>Sb</b>	<b>Cs</b>	<b>Ba</b>
HYK-1	green	13.63	41.63	13.54	73.13	7.15	16.33	8.76	0.86	117.87
HYK-5	green	13.71	47.16	7.17	48.32	5.68	4.29	4.47	0.80	109.44
HYK-7	brown	17.11	40.69	7.97	48.90	4.20	4.55	4.23	0.98	254.32
HYK-8	brown	9.88	39.47	12.72	63.02	4.75	18.23	4.61	0.55	103.19
HYK-9	dark brown	10.43	32.41	9.24	43.46	3.39	6.67	5.09	0.60	142.92
HYK-10	brown	17.43	44.68	6.87	58.49	5.40	4.18	4.6	0.96	211.76
HYK-11	brown	16.65	103.33	10.87	101.33	10.25	6.17	5.15	1.06	384.00



HYK-11	green	17.17	126.53	9.87	87.33	8.57	5.72	5.18	1.06	316.33
HYK-13	green and yellow mix	17.23	45.18	9.74	46.37	6.34	3.42	4.01	1.09	250.37
HYK-18	green	13.78	43.99	11.94	76.97	7.04	18.3	6.76	0.87	119.50
HPK-1	brown	15.63	93.03	19.79	149.07	11.75	1225.77	419.13	2.39	84.43
HPK-2	green	17.55	56.47	14.13	168.17	13.37	3642	796.33	2.33	62.07
HPK-2	brown	16.27	48.57	13.90	113.43	11.64	530.2	863.00	2.18	65.60
HPK-3	brown	33.53	64.26	22.04	172.10	16.40	158.93	461.57	4.57	96.90
HPK-4	brown	7.49	31.22	12.21	48.93	5.47	117.7	723.53	0.79	49.43
HPK-5	brown	11.76	58.54	15.71	90.53	9.21	524.57	617.87	1.50	56.12
HPK-5	green	11.66	41.10	13.76	90.00	8.86	1876.67	579.83	1.53	44.04
HPK-6	green	15.21	102.30	15.86	143.47	9.77	3760	412.1	2.01	84.13
HPK-8	green	13.44	31.17	9.18	75.20	6.48	119.83	1221.00	1.91	54.38
HPK-9	brown	25.19	96.18	16.65	101.07	9.44	319.3	316.97	3.33	83.11
NKZ-1	green	18.46	31.53	10.33	82.03	7.17	11.7	4.51	1.40	95.93
NKZ-1	dark brown	15.34	35.05	10.80	60.77	5.88	7.2	4.09	1.09	95.33
NKZ-2	dark brown	22.71	40.38	10.27	81.25	6.43	6.54	3.04	1.43	131.25
NKZ-2	green	24.81	39.41	8.99	80.47	6.86	8.94	2.82	1.30	137.57
NKZ-3	green and yellow mix	42.33	98.93	26.47	173.33	14.61	14.86	10.31	1.45	235.23
NKZ-4	brown	36.35	128.57	34.73	187.30	17.35	19.88	13.83	1.30	310.55
WL-1	green	26.26	121.33	17.88	112.70	8.74	20.8	20.75	1.15	110.87
WL-2	brown	14.44	74.33	9.36	55.23	6.55	17.56	11.22	1.58	57.57
WL-3	green	12.85	66.09	11.15	67.21	5.42	61.41	14.52	1.24	140.64
WL-4	white	29.51	135.03	21.43	143.17	10.82	37.37	23.14	1.06	165.07
<b>Sample No.</b>	<b>Glaze colour</b>	<b>La</b>	<b>Ce</b>	<b>Pr</b>	<b>Nd</b>	<b>Sm</b>	<b>Eu</b>	<b>Gd</b>	<b>Tb</b>	<b>Dy</b>
HYK-1	green	24.23	39.93	5.03	18.01	3.36	0.58	2.61	0.38	2.56
HYK-5	green	23.99	43.88	4.41	13.70	1.76	0.26	1.33	0.18	1.22
HYK-7	green and brown mix	18.47	49.62	3.57	12.05	1.97	0.34	1.73	0.25	1.52
HYK-8	brown	17.59	81.39	4.30	16.74	3.72	0.63	3.51	0.48	2.65
HYK-9	dark brown	13.52	50.94	3.02	11.06	2.13	0.40	2.12	0.29	1.84
HYK-10	brown	21.06	41.59	4.08	14.28	2.13	0.32	1.43	0.20	1.26
HYK-11	brown	27.74	56.33	5.62	19.54	3.36	0.58	2.38	0.31	2.05

HYK-11	green	25.18	46.61	4.81	16.75	2.62	0.51	1.95	0.28	1.84
HYK-13	green and yellow mix	19.38	47.68	3.81	12.42	1.99	0.35	1.66	0.27	1.83
HYK-18	green	22.47	37.67	4.70	17.29	2.98	0.53	2.44	0.36	2.23
HPK-1	brown	25.84	39.80	5.63	21.05	3.97	0.75	3.92	0.60	4.07
HPK-2	green	25.66	45.22	5.35	18.23	3.24	0.63	2.93	0.46	2.89
HPK-2	brown	22.04	39.36	4.69	16.60	3.20	0.60	2.81	0.45	2.88
HPK-3	brown	31.31	53.95	6.74	23.81	4.68	0.81	4.08	0.65	4.16
HPK-4	brown	13.23	20.10	2.80	10.52	2.00	0.37	2.20	0.33	2.13
HPK-5	brown	24.97	41.18	5.42	18.77	3.28	0.57	2.77	0.45	2.86
HPK-5	green	21.41	33.84	4.26	14.92	2.55	0.45	2.32	0.39	2.58
HPK-6	green	21.61	34.08	4.79	17.67	3.37	0.62	3.10	0.48	3.01
HPK-8	green	15.03	19.79	2.73	9.84	1.63	0.34	1.50	0.24	1.67
HPK-9	brown	26.13	60.48	6.46	23.98	3.99	0.66	3.44	0.45	2.88
NKZ-1	green	25.87	43.39	4.66	15.02	2.08	0.34	1.65	0.26	1.70
NKZ-1	dark brown	23.07	50.83	4.54	16.15	2.53	0.40	2.14	0.31	2.03
NKZ-2	dark brown	23.94	44.73	4.47	15.08	2.37	0.38	1.99	0.29	1.91
NKZ-2	green	24.23	43.60	4.47	14.49	2.00	0.31	1.56	0.22	1.54
NKZ-3	green and yellow mix	55.24	129.20	11.10	38.30	6.48	1.04	5.40	0.84	5.14
NKZ-4	brown	72.71	175.85	14.53	52.01	8.85	1.46	7.64	1.16	7.01
WL-1	green	26.59	60.04	6.53	24.44	4.36	0.81	3.83	0.56	3.28
WL-2	brown	24.49	34.24	3.66	13.78	2.34	0.46	2.03	0.30	1.77
WL-3	green	23.97	36.26	3.84	14.59	2.87	0.51	2.42	0.33	2.04
WL-4	white	25.48	72.60	7.75	29.12	5.27	0.93	4.44	0.62	3.97
<b>Sample No.</b>	<b>Glaze colour</b>	<b>Ho</b>	<b>Er</b>	<b>Tm</b>	<b>Yb</b>	<b>Lu</b>	<b>Hf</b>	<b>Th</b>	<b>U</b>	
HYK-1	green	0.55	1.75	0.27	1.87	0.30	2.22	9.40	4.42	
HYK-5	green	0.29	0.89	0.15	0.93	0.12	1.37	5.86	1.52	
HYK-7	green and brown mix	0.31	0.89	0.13	0.96	0.12	1.45	4.34	1.32	
HYK-8	brown	0.50	1.44	0.21	1.35	0.18	1.76	6.70	2.02	
HYK-9	dark brown	0.36	1.03	0.15	0.98	0.15	1.15	2.85	1.28	
HYK-10	brown	0.28	0.87	0.11	0.84	0.11	1.82	5.87	1.44	
HYK-11	brown	0.42	1.22	0.19	1.34	0.18	3.21	9.09	3.05	
HYK-11	green	0.37	1.14	0.15	1.09	0.15	2.70	8.86	2.99	
HYK-13	green and yellow mix	0.38	1.17	0.16	1.13	0.17	1.45	4.64	1.42	
HYK-18	green	0.48	1.48	0.22	1.66	0.24	2.24	9.09	3.59	
HPK-1	brown	0.80	2.39	0.33	2.24	0.34	4.53	9.25	2.37	
HPK-2	green	0.60	1.88	0.29	2.05	0.31	4.86	10.51	2.78	
HPK-2	brown	0.57	1.72	0.24	1.76	0.27	3.39	9.58	2.75	
HPK-3	brown	0.84	2.57	0.36	2.55	0.39	5.06	12.99	3.40	
HPK-4	brown	0.44	1.29	0.17	1.18	0.18	1.52	4.45	1.39	
HPK-5	brown	0.60	1.88	0.27	1.77	0.28	2.63	7.99	2.29	
HPK-5	green	0.55	1.69	0.25	1.73	0.24	2.79	8.31	1.97	
HPK-6	green	0.59	1.81	0.27	1.76	0.26	4.31	8.04	2.10	
HPK-7	green	0.37	1.17	0.18	1.15	0.17	1.55	4.83	1.54	
HPK-8	green	0.35	1.23	0.17	1.19	0.17	2.42	8.09	1.88	
HPK-9	brown	0.60	1.72	0.26	1.69	0.26	3.11	11.69	2.88	

NKZ-1	green	0.36	1.16	0.18	1.17	0.17	2.52	7.17	4.36
NKZ-1	dark brown	0.41	1.31	0.18	1.24	0.18	1.84	6.01	2.99
NKZ-2	dark brown	0.40	1.22	0.17	1.28	0.19	2.48	6.87	2.41
NKZ-2	green	0.33	1.06	0.16	1.06	0.17	2.36	6.78	3.16
NKZ-3	green and yellow mix	1.06	3.35	0.49	3.34	0.47	5.42	15.15	5.26
NKZ-4	brown	1.45	4.37	0.60	4.17	0.58	5.52	20.25	5.19
WL-1	green	0.67	1.95	0.28	1.80	0.29	3.47	10.64	3.36
WL-2	brown	0.34	1.05	0.14	0.96	0.14	1.77	6.07	1.99
WL-3	green	0.43	1.28	0.19	1.21	0.17	1.97	6.09	2.33
WL-4	white	0.83	2.46	0.35	2.31	0.34	4.48	13.43	3.91

**Table A6 the trace elemental compositions of Tang Sacnai lead glaze samples (Unit: ppm)**

Sample No.	Glaze colour	Li	B	Ti	V	Cr	Co	Ni	Zn	As
<b>Al-Raqqa, Syria, 8th-9th</b>										
Syria-4	green	17.95	15.12	872.21	23.87	52.86	15.49	90.67	7642.67	7935.00
Syria-7	green	21.79	12.58	709.68	18.14	15.87	10.15	31.98	1085.09	7392.71
<b>Kish or Hira, 8th-14th Centuries, maybe later than 10th Century</b>										
9798	green	40.90	21.87	808.33	18.08	17.88	9.10	57.50	5006.67	4690.00
9800	brown	22.39	15.73	525.73	25.85	18.31	6.27	62.47	1264.60	2868.33
9800	green	29.14	19.20	471.93	13.91	23.78	5.91	62.87	1867.67	3335.33
9807	green	37.34	39.00	804.00	114.69	36.11	9.49	72.07	6816.67	1709.67
9808	green	52.45	30.13	1317.96	26.38	25.05	13.10	45.69	8255.07	406.15
9308	brown	137.73	25.67	1674.00	44.10	48.01	24.96	338.07	8282.06	2816.27
9309	yellow	49.27	24.13	465.67	34.39	20.49	7.06	76.87	861.33	3378.67
9309	green	95.33	18.33	958.67	22.48	19.93	25.94	279.20	7755.00	4139.00
9312	green	32.28	12.40	419.40	10.27	13.88	8.73	84.47	3167.67	764.63
<b>Kish-shaal Ghazna, Iraq, 10th-13th Centuries AD</b>										
9161	green	45.40	11.16	476.67	11.16	11.06	1.99	18.37	582.93	694.63
9161	white	37.31	10.13	380.93	8.92	14.11	1.51	14.43	521.27	562.87
9162	green	56.82	14.85	1220.04	21.86	37.22	6.73	41.58	1485.59	1369.02
9162	brown	41.72	16.38	1040.83	30.55	29.85	6.80	25.31	143.43	1113.60
9159	brown	57.57	16.18	842.33	31.13	38.96	7.50	38.67	207.60	140.20
9159	yellow	60.43	17.82	1026.33	23.22	25.49	3.05	24.47	187.00	98.53
9160	green	51.03	20.47	961.67	22.03	42.24	6.21	50.40	1777.67	222.27
9921	brown	82.07	33.70	1373.00	36.33	49.93	6.96	46.23	420.67	163.77
9915	brown	41.70	24.40	994.86	35.64	45.71	9.25	66.29	186.32	78.33
9915	white	53.16	21.46	847.28	23.46	35.62	3.55	26.77	228.77	57.19
9156	green	107.95	40.39	1002.65	31.60	29.73	12.50	99.35	7649.99	34.91
Sample No.	Glaze colour	Rb	Sr	Y	Zr	Nb	Sn	Sb	Cs	Ba
<b>Al-Raqqa, Syria, 8th-9th</b>										
Syria-4	green	13.84	150.91	5.12	43.59	2.37	155.84	534.67	0.53	59.70
Syria-7	green	10.26	126.93	2.99	48.25	2.50	8013.09	735.86	0.53	68.54
<b>Kish or Hira, 8th-14th Centuries, maybe later than 10th Century</b>										
9798	green	63.87	147.87	2.71	22.16	3.90	3160.00	151.60	2.21	87.23
9800	brown	18.29	149.13	2.54	16.50	1.66	16500.00	271.57	0.84	95.33
9800	green	29.54	145.10	2.43	16.98	1.99	15663.33	260.97	0.74	85.17
9807	green	25.34	171.37	4.61	21.28	2.50	559.67	1207.67	1.48	32.91
9808	green	72.62	130.70	5.00	60.65	3.75	331.42	55.06	4.01	68.50
9308	brown	72.77	129.20	6.91	43.31	4.84	1106.97	0.31	2.93	126.93

9309	yellow	7.99	94.00	2.53	13.16	1.50	3978.67	239.23	0.43	78.37
9309	green	9.93	53.71	5.25	31.98	3.04	109.70	270.57	0.66	89.23
9312	green	15.81	71.28	2.41	12.07	1.24	107.82	656.80	0.81	333.00
<b>Kish-shaal Ghazna, Iraq, 10th-13th Centuries AD</b>										
9161	green	3.23	66.79	3.13	15.34	1.52	19476.67	288.80	0.22	45.61
9161	white	1.50	48.74	1.99	7.49	1.09	19706.67	269.67	0.11	40.24
9162	green	43.99	65.36	4.20	35.29	3.25	60.06	1946.86	3.31	151.78
9162	brown	43.77	115.13	5.17	36.02	3.26	28.71	1770.14	3.49	146.95
9159	brown	24.42	87.43	5.68	24.21	2.56	1380.67	45.63	1.89	86.47
9159	yellow	54.16	56.46	6.34	28.19	3.09	1477.00	35.34	2.66	95.42
9160	green	27.70	126.53	5.37	29.44	2.90	2858.33	85.03	1.10	77.97
9921	brown	74.80	126.20	8.94	40.57	4.10	3467.00	72.73	3.60	60.32
9915	brown	14.87	253.23	6.27	27.60	3.05	2206.64	82.48	1.57	66.74
9915	white	36.36	86.38	5.13	24.58	2.58	2137.91	90.17	1.56	54.95
9156	green	80.47	117.25	5.71	34.03	3.03	3532.80	149.45	3.29	105.81
<b>Sample No.</b>	<b>Glaze colour</b>	<b>La</b>	<b>Ce</b>	<b>Pr</b>	<b>Nd</b>	<b>Sm</b>	<b>Eu</b>	<b>Gd</b>	<b>Tb</b>	<b>Dy</b>
<b>Al-Raqqa, Syria, 8th-9th</b>										
Syria-4	green	6.19	12.56	1.46	5.69	1.20	0.29	1.12	0.16	0.97
Syria-7	green	4.80	9.68	1.05	3.82	0.73	0.15	0.73	0.10	0.51
<b>Kish or Hira, 8th-14th Centuries, maybe later than 10th Century</b>										
9798	green	3.92	8.10	0.93	3.39	0.62	0.15	0.60	0.08	0.57
9800	brown	2.61	5.35	0.62	2.49	0.60	0.18	0.59	0.08	0.55
9800	green	2.34	4.96	0.58	2.26	0.55	0.14	0.51	0.08	0.43
9807	green	5.67	13.25	1.65	6.75	1.42	0.29	1.15	0.16	1.03
9808	green	4.40	8.95	1.02	3.85	0.88	0.19	0.87	0.13	0.89
9308	brown	7.82	15.93	1.84	6.76	1.45	0.34	1.37	0.22	1.21
9309	yellow	2.50	5.03	0.60	2.43	0.54	0.13	0.48	0.07	0.46
9309	green	5.39	15.25	1.57	6.96	1.42	0.28	1.19	0.17	1.06
9312	green	3.69	6.61	0.75	2.79	0.53	0.18	0.49	0.08	0.50
<b>Kish-shaal Ghazna, Iraq, 10th-13th Centuries AD</b>										
9161	green	3.98	7.79	0.93	3.56	0.75	0.15	0.67	0.10	0.59
9161	white	2.45	5.11	0.61	2.40	0.45	0.11	0.40	0.07	0.39
9162	green	4.57	8.53	0.93	3.48	0.71	0.17	0.72	0.11	0.75
9162	brown	4.17	7.64	0.84	3.20	0.63	0.23	0.65	0.13	0.80
9159	brown	5.94	13.40	1.69	6.66	1.53	0.32	1.27	0.18	1.12
9159	yellow	6.80	15.16	1.89	7.80	1.55	0.33	1.37	0.21	1.22
9160	green	6.02	12.48	1.54	6.39	1.34	0.30	1.24	0.16	1.05
9921	brown	9.91	21.22	2.70	11.54	2.22	0.51	2.08	0.28	1.81
9915	brown	5.49	11.97	1.39	5.48	1.22	0.29	1.25	0.19	1.16
9915	white	4.92	18.08	2.13	7.94	1.44	0.28	1.13	0.15	0.92
9156	green	5.16	11.25	1.37	5.38	1.24	0.27	1.22	0.16	1.03
<b>Sample No.</b>	<b>Glaze colour</b>	<b>Ho</b>	<b>Er</b>	<b>Tm</b>	<b>Yb</b>	<b>Lu</b>	<b>Hf</b>	<b>Th</b>	<b>U</b>	
<b>Al-Raqqa, Syria, 8th-9th</b>										
Syria-4	green	0.20	0.51	0.07	0.55	0.07	1.17	1.49	0.58	
Syria-7	green	0.11	0.29	0.05	0.33	0.04	1.30	1.80	0.48	
<b>Kish or Hira, 8th-14th Centuries, maybe later than 10th Century</b>										
9798	green	0.10	0.27	0.04	0.30	0.04	0.66	1.65	0.43	
9800	brown	0.10	0.27	0.04	0.23	0.04	0.47	0.85	0.40	
9800	green	0.09	0.25	0.03	0.22	0.03	0.52	0.67	0.31	
9807	green	0.20	0.52	0.07	0.51	0.07	0.61	2.36	0.62	

9808	green	0.18	0.56	0.09	0.63	0.09	7.00	1.27	0.85
9308	brown	0.25	0.78	0.13	0.71	0.11	1.32	4.12	0.73
9309	yellow	0.10	0.29	0.04	0.26	0.04	0.37	1.18	0.34
9309	green	0.22	0.62	0.09	0.62	0.09	0.95	3.94	0.57
9312	green	0.09	0.28	0.04	0.26	0.04	0.38	1.18	0.27

**Kish-shaal Ghazna, Iraq, 10th-13th Centuries AD**

9161	green	0.12	0.34	0.05	0.33	0.05	0.44	1.79	0.32
9161	white	0.09	0.21	0.03	0.20	0.03	0.21	0.85	0.19
9162	green	0.15	0.44	0.07	0.49	0.07	0.97	2.57	0.45
9162	brown	0.17	0.52	0.07	0.53	0.08	1.14	2.87	0.61
9159	brown	0.23	0.66	0.08	0.60	0.08	0.69	2.91	0.83
9159	yellow	0.24	0.72	0.10	0.72	0.11	0.87	3.68	0.59
9160	green	0.21	0.60	0.08	0.56	0.08	0.98	3.18	0.48
9921	brown	0.33	1.00	0.14	0.89	0.12	1.24	5.08	0.77
9915	brown	0.23	0.70	0.09	0.58	0.09	0.82	2.06	0.56
9915	white	0.18	0.60	0.09	0.54	0.10	0.73	2.95	0.51
9156	green	0.19	0.60	0.08	0.70	0.10	0.96	3.37	0.59

**Table A7 the trace elemental compositions of Islamic lead glaze samples (Unit: ppm)**

Sample No.	Date	SiO <sub>2</sub>	Al <sub>2</sub> O <sub>3</sub>	Na <sub>2</sub> O	K <sub>2</sub> O	CaO	MgO	FeO	TiO <sub>2</sub>	Removed PbO	Removed CuO
<b>Body</b>											
HPK-1	7th-9th	64.43	28.42	1.58	0.89	1.34	0.97	1.29	1.08		
HPK-2	7th-9th	60.11	32.22	0.82	2.16	0.92	1.74	0.76	1.27		
HPK-3	7th-9th	62.05	30.21	0.54	2.55	1.23	1.18	1.33	0.91		
HPK-4	7th-9th	65.26	27.43	2.03	0.96	0.76	1.67	1.07	0.82		
HPK-5	7th-9th	63.76	29.85	1.19	1.17	1.19	1.08	0.79	0.97		
HPK-6	7th-9th	61.17	31.59	1.33	1.08	1.29	1.42	1.2	0.92		
<b>Glaze</b>											
HPK-1 brown	7th-9th	74.88	17.17	0.28	1.07	2.02	0.66	3.19	0.74	44.64	0.47
HPK-2 green	7th-9th	76.33	17.75	0.33	1.05	0.82	0.58	2.32	0.82	39.76	1.53
HPK-3 brown	7th-9th	71.22	17.70	0.27	1.45	0.60	0.76	7.17	0.84	36.45	0.15
HPK-4brown	7th-9th	77.41	10.60	0.08	0.56	0.48	0.35	9.95	0.57	61.17	0.11
HPK-5 brown	7th-9th	74.45	13.48	0.11	0.75	0.65	0.52	9.23	0.82	53.82	0.24
HPK-6 green	7th-9th	83.70	11.61	0.21	0.79	0.66	0.75	1.68	0.60	45.79	2.55

**Table A8 Body and adjusted glaze compositions for Tang Sancai sherds produced in Huangpu kiln, normalised to 100%**

Sample No.	Date	NaO	MgO	Al <sub>2</sub> O <sub>3</sub>	SiO <sub>2</sub>	K <sub>2</sub> O	CaO	TiO <sub>2</sub>	FeO
<b>Body</b>									
HY01B	8th-9th	0.00	1.03	29.48	64.41	2.00	0.63	0.95	1.49
HY02B	8th-9th	0.21	1.39	33.09	61.12	2.20	0.34	1.03	0.82
HY04B	8th-9th	0.65	1.68	30.56	61.63	2.16	1.37	1.01	1.60
HY06B	8th-9th	0.42	1.42	30.45	62.34	2.39	1.00	1.11	1.30
HY08B	8th-9th	1.66	1.88	32.75	60.27	2.10	0.75	0.93	1.32
HY09B	8th-9th	1.44	1.57	31.01	62.81	1.87	0.57	0.98	1.19
HY10B	8th-9th	0.77	1.62	30.26	63.44	1.75	0.50	1.03	1.40
HY11B	8th-9th	0.85	1.66	30.69	63.37	1.79	0.39	0.93	1.16
HY12B	8th-9th	0.47	1.45	30.59	64.07	1.81	0.33	1.10	0.65
HY13B	8th-9th	0.09	0.95	31.25	62.37	1.95	1.31	0.96	1.21

HY15B	8th–9th	1.14	1.24	29.76	63.43	2.20	0.56	1.10	1.71		
HY16B	8th–9th	0.94	1.03	30.39	63.40	2.00	0.58	1.12	1.48		
HY17B	8th–9th	0.00	0.89	29.70	64.47	1.91	0.58	0.97	1.47		
HY18B	8th–9th	0.80	1.17	30.32	63.71	1.74	0.57	1.10	1.38		
HY23B	8th–9th	0.00	0.72	31.49	61.47	2.46	1.19	1.04	1.64		
HY26B	8th–9th	0.72	1.44	30.51	63.23	1.92	0.55	0.84	1.52		
HY27B	8th–9th	2.30	2.11	31.77	59.59	2.98	1.29	1.00	1.28		
HY29B	8th–9th	0.94	1.80	28.66	62.81	3.02	1.44	1.11	1.16		
Sample No.	Date	NaO	MgO	Al <sub>2</sub> O <sub>3</sub>	SiO <sub>2</sub>	K <sub>2</sub> O	CaO	TiO <sub>2</sub>	FeO	Removed PbO	Removed CuO
Glaze											
HY01white	8th–9th	0.15	1.08	6.17	85.75	1.66	3.75	0.25	1.19	31.69	0.06
HY01brown	8th–9th	0.38	3.67	20.82	60.62	1.51	2.02	0.62	10.36	41.6	0.06
HY01green	8th–9th	1.42	4.22	22.80	66.39	0.51	1.36	0.70	2.60	44.37	4.15
HY02white	8th–9th	0.73	1.53	7.05	88.48	1.04	0.66	0.19	0.32	31.33	0.13
HY02green	8th–9th	0.43	3.61	26.24	63.82	2.53	1.46	0.82	1.09	41.21	5.36
HY04white	8th–9th	0.99	1.74	7.80	86.56	0.52	1.73	0.21	0.46	28.19	0.02
HY04brown	8th–9th	1.00	4.40	20.02	61.39	0.86	3.37	0.71	8.25	47.67	0.09
HY04blue	8th–9th	0.13	2.71	12.95	78.76	1.27	1.82	0.40	1.97	37.4	0.41
HY06brown	8th–9th	0.33	4.96	21.97	61.63	0.83	2.66	0.75	6.87	47.98	0.04
HY06green	8th–9th	0.15	3.42	19.33	70.66	1.11	3.04	0.55	1.74	47.41	4.95
HY08blue	8th–9th	0.66	4.96	19.12	71.32	0.47	1.52	0.30	1.67	50.62	0.43
HY09blue	8th–9th	0.00	5.35	22.92	68.75	0.54	0.72	0.50	1.22	52.88	0.46
HY10blue	8th–9th	0.00	5.54	22.41	69.08	0.16	0.83	0.47	1.51	54.48	0.41
HY11green	8th–9th	0.00	4.43	22.88	64.26	0.74	5.33	0.72	1.63	45.06	3.91
HY12green	8th–9th	1.39	5.03	21.80	67.73	1.11	1.15	0.68	1.11	47.04	6.07
HY15black	8th–9th	1.60	4.61	18.38	67.19	0.82	3.71	0.76	2.93	43.11	6.6
HY16yellow	8th–9th	0.00	2.05	18.39	69.00	1.45	1.48	0.73	6.91	33.68	1.83
HY17brown	8th–9th	0.16	1.04	14.04	66.48	12.32	3.58	0.70	1.68	16.72	2.38
HY18brown	8th–9th	1.38	1.96	16.64	74.85	1.94	1.33	0.59	1.30	33.22	2.89
HY23yellow	8th–9th	0.00	2.18	17.97	69.15	0.73	1.91	0.68	7.39	47.95	0.06
HY23blue	8th–9th	2.24	3.65	13.98	75.92	0.33	1.20	0.54	2.15	50.96	0.15
HY26brown	8th–9th	0.00	2.23	18.19	69.24	1.69	2.15	0.69	5.81	41.54	0.07
HY27yellow	8th–9th	0.00	5.31	22.52	63.00	0.66	3.04	0.66	4.80	53.2	0.12
HY27green	8th–9th	4.85	3.74	13.88	66.44	4.28	3.94	0.51	2.37	44.92	1.79
HY29yellow	8th–9th	0.96	3.91	19.75	68.04	0.86	1.31	0.55	4.63	41.76	0.07

**Table A9 Body and glaze compositions for Tang Sancai sherds produced in Huangye kiln, normalised to 100% (analysed by Dong et al. 2008)**

Sample No	Glaze Colour	Excavated Place	SiO <sub>2</sub>	Al <sub>2</sub> O <sub>3</sub>	CaO	MgO	Na <sub>2</sub> O	K <sub>2</sub> O	FeO	TiO <sub>2</sub>	MnO <sub>2</sub>
9037	Green	Hira, Iraq	57.87	11.00	14.50	5.60	2.10	2.15	6.00	0.68	0.10
9038	Green		54.86	12.50	14.50	6.80	1.20	2.10	7.20	0.73	0.11
9044	Green		55.46	12.80	15.00	5.85	1.05	1.80	7.20	0.73	0.11
9051	Green		56.01	12.50	13.00	6.80	1.10	2.60	7.10	0.78	0.11
9053	Green		58.12	12.00	13.00	6.00	1.20	2.40	6.40	0.78	0.10
9067	Green		57.37	11.50	13.70	6.50	1.35	2.15	6.50	0.73	0.20
9364	Transparent	Nineveh, Iraq	58.69	11.00	14.00	5.50	0.94	2.50	6.50	0.78	0.10
9365	Green		56.68	11.50	14.00	5.90	0.84	3.50	6.70	0.78	0.10

9367	Transparent		55.30	12.20	14.00	6.50	0.86	3.00	7.20	0.84	0.10
9368	Transparent		56.30	12.00	13.00	7.20	1.07	2.75	6.80	0.78	0.10
9368	Yellow		56.30	12.00	13.00	7.20	1.07	2.75	6.80	0.78	0.10
9369	Transparent		53.29	12.50	15.00	7.20	0.76	2.70	7.60	0.84	0.11
9373	Green		56.44	12.70	13.00	6.30	0.78	2.50	7.40	0.78	0.10
9374	Green		53.26	13.00	15.00	7.30	0.94	2.30	7.20	0.90	0.10
9375	Green		54.49	14.00	12.00	6.80	1.00	2.80	7.90	0.90	0.11
9376	Green		57.10	11.80	14.00	6.30	0.92	2.15	6.90	0.73	0.10
9377	Green		56.78	13.00	12.50	6.20	1.07	2.30	7.20	0.84	0.11
9378	Green		56.05	12.20	14.00	6.50	0.96	2.15	7.20	0.84	0.10
9379	Green		57.60	11.30	14.00	6.50	0.92	1.90	6.90	0.78	0.10
9380	Transparent		55.65	13.70	13.00	6.30	1.00	2.20	7.20	0.84	0.11
9382	Green		55.97	11.70	14.00	7.20	0.90	2.20	7.20	0.73	0.10
9382	Green		55.97	11.70	14.00	7.20	0.90	2.20	7.20	0.73	0.10

**Table A10 the body compositions for Islamic high lead glaze sherds collected from Hira and Nineveh of Iraq, normalised to 100% (analysed by Kaczmarczyk, the University of Oxford)**

Sample No.	SiO <sub>2</sub>	Al <sub>2</sub> O <sub>3</sub>	Na <sub>2</sub> O	K <sub>2</sub> O	CaO	MgO	FeO	MnO	TiO <sub>2</sub>	Removed PbO	Removed CuO
<b>Al-Raqqa, Syria, 8th-9th Centuries AD</b>											
Syria-4 green	83.80	4.31	0.84	1.61	5.64	1.58	1.96	0.20	0.07	49.91	2.10
Syria-7 green	86.21	2.56	1.71	0.81	5.33	1.19	0.32	1.75	0.12	52.16	3.51
<b>Kish-shaal Ghazna, Iraq, 10th-13th Centuries AD</b>											
9913 white	77.83	6.76	1.51	2.41	5.87	4.09	0.99	0.06	0.48	46.95	0.05
9393 yellow	78.36	7.75	1.35	3.08	3.79	1.16	4.27	0.07	0.15	55.37	0.03
9393 green	81.43	7.80	1.42	2.73	3.57	0.94	1.70	0.12	0.28	51.25	2.42
9921 yellow	84.40	1.69	2.42	3.91	3.17	1.00	3.26	0.07	0.08	53.88	0.13
9921 green	84.81	2.89	2.39	3.68	3.55	0.97	1.42	0.07	0.23	54.89	1.54
9921 black	81.20	2.89	1.57	1.77	4.62	1.31	3.77	2.62	0.25	57.05	0.83
9156 yellow	74.22	7.12	2.22	2.61	3.58	0.82	9.03	0.02	0.38	56.35	0.16
9156 green	84.54	4.51	1.81	2.26	4.14	1.17	1.37	0.07	0.12	57.85	1.51
9156 white	86.82	2.40	1.41	1.56	4.37	1.37	1.66	0.22	0.18	59.95	0.02
9161 green	89.55	4.16	0.29	0.36	3.23	0.71	1.30	0.03	0.37	64.35	1.24
9161 white	90.26	2.97	0.03	0.21	3.02	0.93	1.15	1.05	0.36	68.46	0.15
9147 yellow	77.10	7.00	0.45	0.64	4.26	1.03	9.02	0.03	0.46	64.79	0.35
9147 green	77.99	7.12	0.37	0.55	4.31	1.17	8.10	0.07	0.32	65.26	1.09
9159 brown	72.83	7.53	1.50	1.82	4.64	1.47	6.97	2.85	0.39	59.88	0.17
9159 white	81.77	7.01	1.91	2.66	3.49	1.10	1.53	0.13	0.41	58.84	0.05
9159 yellow	70.79	11.10	2.37	2.80	2.28	0.69	9.50	0.02	0.44	56.47	0.18
9915 white	80.46	9.40	1.39	2.62	3.64	0.89	1.28	0.02	0.31	56.87	0.07
9915 brown	68.76	9.62	1.00	1.62	6.12	3.59	6.57	2.13	0.59	49.83	0.13
9915 green	77.36	7.02	2.58	6.04	4.45	0.92	1.31	0.04	0.29	39.40	1.89
9162 brown	75.84	5.57	2.76	2.93	3.72	1.19	1.90	5.60	0.49	59.87	0.48
9162 green	78.92	6.32	3.13	3.04	4.33	1.32	2.27	0.03	0.65	60.15	1.48
9160 green	74.96	8.22	1.96	2.41	6.14	2.04	3.50	0.31	0.45	57.94	1.01
9160 brown	66.68	9.48	2.66	3.84	5.10	1.63	7.89	2.14	0.57	48.71	0.32
<b>Kish or Hira, 8th-14th Centuries, maybe later than 10th Century</b>											
9312 green	86.63	3.16	1.30	1.50	4.43	0.74	2.06	0.06	0.11	64.97	1.53
9309 yellow	77.99	4.62	1.01	1.08	4.31	1.30	9.44	0.08	0.16	62.21	0.12
9309 green	81.62	11.60	0.55	1.06	2.85	0.62	1.17	0.08	0.46	55.67	3.90
9308 brown	77.80	6.10	1.30	1.48	2.91	0.48	5.35	4.27	0.32	62.87	0.05

9308 yellow	81.92	7.05	1.65	2.00	2.80	0.63	3.49	0.09	0.37	63.54	0.03
9308 green	82.51	7.40	2.20	2.63	3.13	0.64	1.10	0.03	0.36	60.35	1.86
9798 green	80.13	2.19	4.20	3.00	6.19	2.64	1.30	0.20	0.15	44.70	2.54
9800 green	80.54	2.53	4.90	2.28	5.44	2.07	1.54	0.47	0.24	51.82	1.32
9800 brown	78.14	2.35	3.33	1.83	5.12	1.74	1.68	5.58	0.22	52.02	0.75
9807 green	81.33	5.87	2.21	2.43	4.81	1.35	1.66	0.03	0.31	59.98	3.58

**Table A11 the adjusted glaze compositions for Islamic high lead glaze sherds collected from Syria (Al-Raqqa) and Iraq (Kish-shaal Ghazna) analysed in this study, normalised to 100%**

Sample No.	Region	Mine/Site	Type	$^{208}\text{Pb}/^{206}\text{Pb}$	$^{207}\text{Pb}/^{206}\text{Pb}$	$^{206}\text{Pb}/^{204}\text{Pb}$
Pb-823	Anguran , North-western Iran	Anguran	Sulphide	2.05595	0.82854	18.993
PI2	Nakhlak , Central Iran	Nakhlak	Pb slag	2.08709	0.84463	18.535
PI1b	ditto	ditto	ditto	2.0868	0.84466	18.529
PI1a	ditto	ditto	ditto	2.08739	0.84468	18.532
Pb-833	ditto	Fortress of Nakhlak	Pb slag/litharge	2.08792	0.84479	18.522
Pb-834	ditto	ditto	Galena	2.0903	0.8448	18.519
Pb-832	ditto	ditto	Cerussite	2.09061	0.84509	18.566
Pb-835	ditto	ditto	Litharge	2.08864	0.84525	18.539
Pb-824	Kashan, South-eastern Iran	Lakan, Arak-Kashan	Galena	2.093	0.8488	18.45
Pb-825	ditto	Ahangaran, Arak-Kashan	ditto	2.098	0.8492	18.416
Pb-827	ditto	Darreh Noghre Siler valley, Arak-Kashan	ditto	2.0942	0.8504	18.403
Pb-826	ditto	Hosseinabad, Arak-Kashan	ditto	2.0944	0.8511	18.409
Pb-820	Larassam, near Teheran, Northern Iran	Larassam	ditto	2.0676	0.83261	18.872
Pb-112	Isfahan, Central Iran	Khaneh Sormeh	ditto	2.0842	0.83952	18.619
Pb-821	Tofresh, Central Iran	Hezarabad, North-west of Arak	ditto	2.08119	0.84284	18.692
PI3	Biabanak Rural, Isfahan, Central Iran	Farrokhi	Pb slag	2.08916	0.84468	18.577
PI 27	Zarkan Rural, Isfahan, Central Iran	Muteh	ditto	2.1018	0.85817	18.308

**Table A12 Lead isotope ratios for lead ore deposits from different regions of Iran (Stos-Gale 2001)**

Sample number	Region	Type	$^{208}\text{Pb}/^{206}\text{Pb}$	$^{207}\text{Pb}/^{206}\text{Pb}$	$^{206}\text{Pb}/^{204}\text{Pb}$
A	Tunisia	Lead ore	2.0495	0.8277	18.966
B	ditto	ditto	2.054	0.8305	18.875
C	ditto	ditto	2.0691	0.8331	18.819
D	ditto	ditto	2.068	0.833	18.815
E	ditto	ditto	2.0671	0.8327	18.808
F	ditto	ditto	2.0664	0.8329	18.824
G	ditto	ditto	2.0663	0.8336	18.789
H	ditto	ditto	2.0684	0.834	18.795
I	ditto	ditto	2.069	0.8342	18.8
J	ditto	ditto	2.0735	0.8372	18.724



**Table A13 Lead isotope ratios for lead ore deposits from different regions of Tunisia  
(Wolf 2003)**

Sample No.	Region	Mine/Deposit	Type	$^{208}\text{Pb}/^{206}\text{Pb}$	$^{207}\text{Pb}/^{206}\text{Pb}$	$^{206}\text{Pb}/^{204}\text{Pb}$
BIL 8	Elazig,Central east Anatolia	Billurdere(Pb)	Galena	2.04896	0.81821	19.204
BIL 5	ditto	Billurdere(Pb)	Galena	2.04809	0.81742	19.220
BIL 6	ditto	Billurdere(Pb)	Galena	2.06057	0.82016	19.323
BIL 7	ditto	Billurdere(Pb)	Galena	2.04809	0.81757	19.218
HAL 11	ditto	Halimustafa(Pb/Zn)	Sphalerite	2.09563	0.85131	18.362
TUR 19 keb	ditto	Keban(Pb, Cu, Ag)	Galena	2.04417	0.81968	19.122
KEB 1	ditto	Keban(Pb, Cu, Ag)	Galena	2.04727	0.82161	19.051
SEB 2	Giresun,North-western Anatolia	Sebinkarahisar(Zn, Pb)	Galena	2.07868	0.84062	18.628
SEB 3	ditto	Sebinkarahisar(Zn, Pb)	Galena	2.07765	0.84018	18.632
SEB 4	ditto	Sebinkarahisar(Zn, Pb)	Galena	2.07762	0.84033	18.629
GOR 9	Malatya,Eastern Anatolia	Gorgu(Pb)	Galena	2.11394	0.86500	18.102
GOR 10	ditto	Gorgu(Pb)	Galena	2.11581	0.86588	18.120
AOB152	Niğde Massif region of Taurus(Taurus 1A)	Central Taurus Mountains	lead ore or slag	2.0594	0.82712	0.052632
AON078	ditto	ditto	ditto	2.05578	0.82615	0.052601
AON103	ditto	ditto	ditto	2.05836	0.82658	0.052583
AON106	ditto	ditto	ditto	2.05495	0.82525	0.05272
AON109	ditto	ditto	ditto	2.05762	0.82605	0.052767
AON119	ditto	ditto	ditto	2.05487	0.82562	0.05263
AON125	ditto	ditto	ditto	2.0582	0.82729	0.052666
AON129	ditto	ditto	ditto	2.05652	0.82623	0.052801
AON134	ditto	ditto	ditto	2.06105	0.82723	0.052673
AON135	ditto	ditto	ditto	2.05645	0.82593	0.052568
AON137	ditto	ditto	ditto	2.0538	0.82471	0.052578
AON141	ditto	ditto	ditto	2.05674	0.82694	0.052668
ASN040	ditto	ditto	ditto	2.05699	0.82703	0.052583
ASN041	ditto	ditto	ditto	2.0565	0.82669	0.052601
ASN042	ditto	ditto	ditto	2.05519	0.82657	0.052706
ASN046	ditto	ditto	ditto	2.05857	0.82702	0.052708
AONI16	Bolkardağ valley region of Tarsus(Taurus 1B)	ditto	ditto	2.07179	0.83342	0.053137
AON159	ditto	ditto	ditto	2.07364	0.83496	0.053225
AON399	ditto	ditto	ditto	2.07224	0.83435	0.053218
AON428	ditto	ditto	ditto	2.0722	0.83449	0.053238
AON429	ditto	ditto	ditto	2.07511	0.8362	0.053275
AON463	ditto	ditto	ditto	2.07242	0.83547	0.053263
AON466	ditto	ditto	ditto	2.0726	0.8345	0.053253
ASN459	ditto	ditto	ditto	2.07394	0.83511	0.053322
AON157	Aladağ region of Tarsus(Taurus 2A)	ditto	ditto	2.07759	0.84066	0.053432

AON455	ditto	ditto	ditto	2.08295	0.84073	0.053489
AON456	ditto	ditto	ditto	2.07569	0.83999	0.053551
AON461	ditto	ditto	ditto	2.08346	0.84285	0.053657
CevrimB1	ditto	ditto	ditto	2.08239	0.84057	0.053393
CevrimB7	ditto	ditto	ditto	2.07575	0.84003	0.053234
CevrimB12	ditto	ditto	ditto	2.08045	0.8406	0.053525
CevrimB14	ditto	ditto	ditto	2.0788	0.84068	0.053462
CevrimB16	ditto	ditto	ditto	2.07913	0.84036	0.053464
CevrimB17	ditto	ditto	ditto	2.08478	0.84135	0.053419
CevrimB18	ditto	ditto	ditto	2.0851	0.84199	0.05349
CevrimB26	ditto	ditto	ditto	2.08441	0.84153	0.053356
AON419	Aladağ region of Tarsus(Taurus 2B)	ditto	ditto	2.06339	0.83334	0.05283
AON442	ditto	ditto	ditto	2.06019	0.82932	0.052753
AMN434	ditto	ditto	ditto	2.06196	0.831	0.052824
ASN434	ditto	ditto	ditto	2.06117	0.83048	0.05286
CevrimB22	ditto	ditto	ditto	2.06405	0.83229	0.052888
CevrimB24	ditto	ditto	ditto	2.06011	0.83098	0.052637
CevrimB30	ditto	ditto	ditto	2.06373	0.83129	0.052754

**Table A14 Lead isotope ratios for lead ore deposits from different regions of Anatolia (OXALID and Yener et al. 1991)**

Sample No.	Region	Mine/Deposit	Type	$^{208}\text{Pb}/^{206}\text{Pb}$	$^{207}\text{Pb}/^{206}\text{Pb}$	$^{206}\text{Pb}/^{204}\text{Pb}$
ACQ1	Masua region, South-western Sardinia	Acquaresi (CA)	Galena, calamine, malachite	2.12074	0.87416	17.850
ACQ2	ditto	ditto	Galena, sphalerite	2.12297	0.87509	17.851
ACQ3	ditto	ditto	Galena, calamine, malachite	2.11701	0.87065	17.947
ARG1 (AM1)	Nurra region, North-western of Sardinia	Argentiera, Nurra (SS)	Galena, sphalerite	2.10683	0.85667	18.310
ARG2	ditto	ditto	Galena, sphalerite	2.10564	0.85609	18.278
BM 52016	ditto	ditto	Tetrahedrite	2.10624	0.85758	18.233
MM 1004A	Arburese region, Central Sardinia	Monte Mannu, Villacidro, (CA)	Galena, Sphal, Cassiterite, Chalcopyrite	2.10095	0.85937	18.195
MM 1004B	ditto	ditto	ditto	2.10411	0.85978	18.232
MM 1004F	ditto	ditto	ditto	2.10560	0.86013	18.235
MM 1004G	ditto	ditto	ditto	2.10557	0.85991	18.223
MCA1	ditto	ditto	Galena, Sphalerite, Cerussite, (Azurite)	2.10525	0.85922	18.205
MV	ditto	ditto	ditto	2.10551	0.86020	18.179
MTE1	ditto	ditto	ditto	2.10698	0.86028	18.208

MPI1	ditto	ditto	ditto	2.10539	0.86011	18.170
MSA1	ditto	ditto	ditto	2.10730	0.86057	18.203
MSN1	ditto	ditto	ditto	2.11118	0.86373	18.136
MSN1/repeat	ditto	ditto	ditto	2.10634	0.86257	18.097
MSN2	ditto	ditto	ditto	2.10613	0.86335	18.083
MSN3	ditto	ditto	ditto	2.10698	0.86028	18.208
MSN3/repeat	ditto	ditto	ditto	2.11160	0.86422	18.105
MGAS1	ditto	ditto	ditto	2.10783	0.86341	18.107
FR 1011A	Barbagia region,Southern Sardinia	Funtana Raminosa (NU)	Galena, Chalcopyrite, Sphalerite	2.09895	0.85676	18.254
FR 1011B	ditto	ditto	ditto	2.09758	0.85737	18.197
FRM	ditto	ditto	Galena, Chalcopyrite	2.10325	0.85870	18.214
SARD 10	ditto	ditto	ditto	2.10378	0.86196	18.103
SARD 40a	ditto	ditto	Galena, Sphalerite	2.09861	0.85773	18.212
SARD 41ca	ditto	ditto	Galena, Chalcopyrite	2.09502	0.85599	18.203
SARD 41d	ditto	ditto	Malachite, Azurite, Galena	2.10004	0.85808	18.225
SARD 43	ditto	ditto	ditto	2.10179	0.85814	18.244
SARD 49a	ditto	ditto	Galena, Sphalerite	2.09413	0.85448	18.293
SARD 50a	ditto	ditto	Pyrite, Chalcopyrite, Galena	2.10017	0.85732	18.236
SARD 9	ditto	ditto	Chalcopyrite, Pyrite, Galena	2.10355	0.85919	18.243
PS 1013A/95	ditto	ditto	Galena, Spahlerite	2.10086	0.85619	18.303
PS 1013D	ditto	ditto	ditto	2.10012	0.85611	18.290
PS 1013E	ditto	ditto	ditto	2.10007	0.85619	18.296
PS 1013F	ditto	ditto	ditto	2.10154	0.85637	18.300
PS 1013G	ditto	ditto	ditto	2.10156	0.85635	18.324
PS 1013H/87	ditto	ditto	ditto	2.10498	0.85813	18.321
PS 1013H/95	ditto	ditto	ditto	2.10312	0.85734	18.270
PS 1013I	ditto	ditto	ditto	2.10046	0.85618	18.312
PS 1013J	ditto	ditto	ditto	2.09997	0.85613	18.310
PS 1013K	ditto	ditto	ditto	2.10099	0.85622	18.317
CB 1007A	Baronia region,North-eastern Sardinia	Canale Barisone, Torpe, (NU)	Galena, Chalcopyrite	2.09616	0.84785	18.452
CB 1007B	ditto	ditto	ditto	2.09869	0.84837	18.475
CB 1007C	ditto	ditto	ditto	2.09902	0.84818	18.475
CB 1007D	ditto	ditto	ditto	2.09916	0.84832	18.480
CB 1007E	ditto	ditto	ditto	2.10099	0.84872	18.497
CB 1007F	ditto	ditto	ditto	2.10392	0.85944	18.248
CB 1007G	ditto	ditto	ditto	2.10528	0.85984	18.253
CB 1007H	ditto	ditto	ditto	2.10005	0.84858	18.491
CB 1007I	ditto	ditto	ditto	2.10191	0.84888	18.504

PSO 100/88	Fluminese region,Southern Sardinia	Perda s'Oliu, (CA)	Galena, Chalcopyrite	2.10894	0.86284	18.136
PSO 100/94	ditto	ditto	ditto	2.11370	0.86460	18.165
PSO 101	ditto	ditto	ditto	2.10799	0.86311	18.124
PSO 1014	ditto	ditto	Galena	2.11063	0.86419	18.108
PSO 1014A	ditto	ditto	ditto	2.10618	0.86276	18.105
PSO 1015	ditto	ditto	Galena, Chalcopyrite	2.11640	0.86630	18.093
PSO 1015A/84	ditto	ditto	ditto	2.11005	0.86536	18.059
PSO 1015A/94	ditto	ditto	ditto	2.11710	0.86660	18.095
PSO 1016A/84	ditto	ditto	Galena	2.10625	0.86334	18.103
PSO 1016A/94	ditto	ditto	ditto	2.11196	0.86418	18.148
PSO 102	ditto	ditto	ditto	2.10937	0.86418	18.123
SZF1	ditto	ditto	Galena, Baryte	2.12335	0.87086	18.023
SZU 100	ditto	ditto	ditto	2.12011	0.87126	17.984
SZU 101	ditto	ditto	ditto	2.11767	0.87098	17.952
CA 1017A	Iglesiente region,Southern Sardinia	Carreras, Iglesias, (CA)	Galena	2.11931	0.87357	17.880
CAR1	ditto	ditto	ditto	2.12050	0.87387	17.889
COR1	ditto	ditto	Galena, Pyrite, Sphalerite, Siderite	2.12269	0.87421	17.909
COR2	ditto	ditto	ditto	2.12304	0.87436	17.898
COR3	ditto	ditto	ditto	2.12630	0.87468	17.921
FES1/86	ditto	ditto	ditto	2.11009	0.86312	18.179
FES1/94	ditto	ditto	ditto	2.10534	0.85877	18.233
FS1/87	ditto	ditto	ditto	2.10092	0.85854	18.214
FS1/94	ditto	ditto	ditto	2.10246	0.85843	18.229
FS12/87	ditto	ditto	ditto	2.10961	0.86379	18.131
FS12/94	ditto	ditto	ditto	2.10715	0.85937	18.252
FS13	ditto	ditto	ditto	2.10366	0.85875	18.251
FS14/87	ditto	ditto	ditto	2.10256	0.85886	18.231
FS14/94	ditto	ditto	ditto	2.10412	0.86014	18.224
FS15/87	ditto	ditto	ditto	2.10297	0.85845	18.252
FS15/94	ditto	ditto	ditto	2.10438	0.85898	18.252
FS16	ditto	ditto	ditto	2.10326	0.85896	18.255
FS18	ditto	ditto	ditto	2.10360	0.85896	18.241
FS20/87	ditto	ditto	ditto	2.10155	0.85886	18.260
FS20/94	ditto	ditto	ditto	2.10382	0.85907	18.232
FS3	ditto	ditto	ditto	2.10678	0.86066	18.208
FS4	ditto	ditto	ditto	2.10717	0.86265	18.130
FS5/87	ditto	ditto	ditto	2.10898	0.86279	18.158
FS5/94	ditto	ditto	ditto	2.10696	0.86086	18.213
FS6/87	ditto	ditto	ditto	2.10388	0.85930	18.216
FS6/94	ditto	ditto	ditto	2.10384	0.85923	18.224

FS8	ditto	ditto	ditto	2.10308	0.86013	18.209
FS9/87	ditto	ditto	ditto	2.10477	0.86078	18.241
FS9/94	ditto	ditto	ditto	2.10575	0.85955	18.250
FSAC/87	ditto	ditto	ditto	2.10936	0.86364	18.140
FSAC/94	ditto	ditto	ditto	2.10430	0.85964	18.207
MAL1	ditto	Malacalzetta Nuovo, (CA)	Galena	2.11736	0.86791	18.075
MAL2	ditto	ditto	ditto	2.12148	0.86953	18.062
MAL2/94	ditto	ditto	ditto	2.11936	0.86910	18.044
BMMP	ditto	Monteponi, Iglesias, (CA)	Galena, Baryte, Cerussite	2.12188	0.87442	17.915
MNP1	ditto	ditto	ditto	2.12225	0.87424	17.885
MNP2	ditto	ditto	ditto	2.12255	0.87455	17.890
NIE 100	ditto	Nieddoris, (CA)	Galena, Sphalerite, Siderite	2.11523	0.86837	18.006
NIE 101	ditto	ditto	ditto	2.10944	0.86278	18.139
NIE 102	ditto	ditto	ditto	2.11098	0.86264	18.159
NIED1	ditto	ditto	ditto	2.10853	0.86228	18.156
SARD 52A	ditto	S. Giovanni, Iglesias, (CA)	Galena, Spahlerite	2.12306	0.87434	17.895
SGV5	ditto	ditto	ditto	2.12304	0.87401	17.903
SGV3A	ditto	ditto	ditto	2.12025	0.87406	17.869
SGV3B	ditto	ditto	ditto	2.12451	0.87465	17.900
SGV4	ditto	ditto	ditto	2.11870	0.87367	17.867
SGV1	ditto	ditto	ditto	2.11512	0.86890	18.006
SGV2	ditto	ditto	ditto	2.11947	0.87377	17.870
IL 1019A	Sulcis region, Southern Sardinia	Is Luas, Giba, (CA)	Galena, Sphalerite, Pyrite, Chalcopyrite	2.10023	0.85892	18.196
IL 1019B	ditto	ditto	ditto	2.10297	0.85950	18.232
IL 1019C	ditto	ditto	ditto	2.10484	0.85959	18.206
IL 1019D	ditto	ditto	ditto	2.10477	0.85956	18.229
IL 1019E	ditto	ditto	ditto	2.10443	0.85949	18.227
IL 1019H	ditto	ditto	ditto	2.10510	0.85964	18.211
IL 1019I	ditto	ditto	ditto	2.10657	0.86007	18.264
IL 1019J	ditto	ditto	ditto	2.10406	0.85947	18.205
IL 1019K	ditto	ditto	ditto	2.10482	0.85963	18.213
R 1000A	ditto	Rosas, Nuxis, (CA)	Galena, Malachite	2.10075	0.85769	18.245
R 1000B	ditto	ditto	ditto	2.10434	0.85856	18.243
R 1000C	ditto	ditto	ditto	2.09861	0.85738	18.237
R 1000D	ditto	ditto	ditto	2.09963	0.85769	18.247
R 1000E	ditto	ditto	ditto	2.10240	0.85799	18.259
R 1000F	ditto	ditto	ditto	2.09914	0.85740	18.246
R 1000I	ditto	ditto	ditto	2.10060	0.85705	18.315
R 1000J	ditto	ditto	ditto	2.10272	0.85814	18.283
R 1000M	ditto	ditto	ditto	2.10182	0.85801	18.277
R 1000P	ditto	ditto	ditto	2.10163	0.85785	18.277
R 1000Q	ditto	ditto	ditto	2.10170	0.85788	18.278

SM 1001A	ditto	Sa Marchesa, Nuxis, (CA)	Galena, Sphalerite, Chalcopyrite	2.09738	0.85779	18.220
SM 1001B	ditto	ditto	ditto	2.09564	0.85613	18.247
SM 1001C	ditto	ditto	Galena	2.09737	0.85698	18.290
SM 1001D	ditto	ditto	Galena, Sphalerite, Chalcopyrite	2.10101	0.85822	18.221
SM 1001G	ditto	ditto	ditto	2.09894	0.85667	18.288
TRB1/84	ditto	Truba Niedda, Nuxis, (CA)	Galena, Sphalerite, Pyrite (some Chalcopyrite)	2.09804	0.85724	18.232
TRB1/86	ditto	ditto	Galena, Sphalerite, Pyrite, Chalcopyrite	2.10014	0.85767	18.250
TRB5	ditto	ditto	Galena, Sphalerite, Pyrite (some Chalcopyrite)	2.10203	0.85812	18.273
TRB6	ditto	ditto	ditto	2.10138	0.85803	18.270
TRB7	ditto	ditto	ditto	2.10878	0.85843	18.281

**Table A15 Lead isotope ratios for lead ore deposits from different regions of Sardinia (OXALID)**

Sample No.	Region	Deposit	Type	<sup>208</sup> Pb/ <sup>206</sup> Pb	<sup>207</sup> Pb/ <sup>206</sup> Pb	<sup>206</sup> Pb/ <sup>204</sup> Pb
SP6A	Almeria region, South-eastern Spain	Sierra del Cabo de Gata	Galena, Pyrite, Sphal., Chalcopyrite	2.07376	0.83572	18.734
SP12	ditto	ditto	Galena, (Ag, Cerussite)	2.07066	0.83467	18.767
SP13	ditto	ditto	ditto	2.07390	0.83524	18.798
SP15	ditto	ditto	ditto	2.06976	0.83479	18.768
SP16	ditto	ditto	ditto	2.07330	0.83506	18.787
SP17A	ditto	ditto	ditto	2.07230	0.83483	18.778
SP17B	ditto	ditto	ditto	2.07480	0.83535	18.804
SP18	ditto	ditto	ditto	2.07102	0.83487	18.768
SP19A	ditto	ditto	ditto	2.07247	0.83504	18.783
SP19B	ditto	ditto	ditto	2.07368	0.83510	18.794
SP19C	ditto	ditto	ditto	2.07380	0.83514	18.792
SP19D	ditto	ditto	ditto	2.07388	0.83515	18.797
SP38	ditto	ditto	Galena, Grey copper sulphides	2.06705	0.83227	18.852
SP40	ditto	ditto	ditto	2.06651	0.83198	18.858
SP41	ditto	ditto	ditto	2.06601	0.83210	18.854
SP44	ditto	ditto	ditto	2.06644	0.83164	18.888
SP1A	ditto	ditto	Galena	2.07180	0.83835	18.774
SP2	ditto	ditto	Galena, Pyrite, Sphal., Chalcopyrite	2.07526	0.83608	18.723
SP3A	ditto	ditto	ditto	2.07347	0.83543	18.729
SP4A	ditto	ditto	ditto	2.07316	0.83532	18.740
SP6A	ditto	ditto	ditto	2.07376	0.83572	18.734
SP7A	ditto	ditto	ditto	2.07339	0.83538	18.742
SP23	ditto	ditto	Galena, Malachite, Chalcocite	2.08441	0.84583	18.555
SP25	ditto	ditto	ditto	2.06501	0.83159	18.881

SP26	ditto	ditto	ditto	2.06614	0.83177	18.671
SP33	ditto	ditto	ditto	2.09344	0.85361	18.328
ALH1/295	ditto	Sierra Alhamila	Galena with Ag, siderite, baryte	2.11253	0.85819	18.356
ALH1/67	ditto	ditto	ditto	2.11042	0.85776	18.338
ALM2/64	ditto	ditto	Galena in shist, siderite, chalcopryrite.	2.08162	0.83772	18.825
SP53	ditto	ditto	Galena	2.08114	0.83617	18.766
ALM1/294	ditto	Sierra Almagrera north	Galena and baryte	2.07894	0.83648	18.741
ALM1/60	ditto	ditto	ditto	2.07686	0.83606	18.722
B3/269	ditto	Sierra de Bedar	Galena	2.07868	0.83392	18.778
B3/61	ditto	ditto	ditto	2.07279	0.83350	18.759
JDA	Murcia region, South-eastern Spain	Cartagena	ditto	2.08847	0.83875	18.756
HALLIDA Y 1	ditto	ditto	ditto	2.08765	0.83949	18.774
SP58A	ditto	Mazarron	ditto	2.08006	0.83679	18.725
SP58B	ditto	ditto	ditto	2.07742	0.83578	18.724
SP60A	ditto	ditto	ditto	2.07948	0.83606	18.729
SP60B	ditto	ditto	ditto	2.08002	0.83657	18.713
SP61A	ditto	ditto	ditto	2.08137	0.83693	18.730
SP61B	ditto	ditto	ditto	2.07989	0.83659	18.722
SP61C	ditto	ditto	ditto	2.08064	0.83646	18.732
TDB/10	Cadiz region, South-western Spain	Torre Dona Blanca	Fragment of litharge	2.10122	0.85977	18.180
TDB/11	ditto	ditto	ditto	2.08939	0.85832	18.079
TDB/12	ditto	ditto	ditto	2.10407	0.86042	18.210
TDB/14	ditto	ditto	ditto	2.08987	0.85840	18.147
TDB/15	ditto	ditto	ditto	2.09367	0.85708	18.079
TDB/16	ditto	ditto	ditto	2.09912	0.85949	18.156
TDB/18	ditto	ditto	ditto	2.10034	0.85968	18.171
TDB/19	ditto	ditto	ditto	2.10007	0.85958	18.167
TDB/20	ditto	ditto	ditto	2.10009	0.85963	18.174
TDB/7	ditto	ditto	ditto	2.10169	0.85998	18.181
TDB/10	ditto	ditto	ditto	2.10059	0.85964	18.175
RTI	Huelva region, South-western Spain	Minas de Rio Tinto	Galena	2.10200	0.85948	18.205
RTm	ditto	ditto	ditto	2.10426	0.86028	18.197
RTn	ditto	ditto	ditto	2.10065	0.85923	18.196
RTo	ditto	ditto	ditto	2.10356	0.86000	18.186
RTq	ditto	ditto	ditto	2.10172	0.85948	18.198
RTr	ditto	ditto	ditto	2.10174	0.85948	18.197
RTs	ditto	ditto	ditto	2.10060	0.85929	18.188

**Table A16 Lead isotope ratios for lead ore deposits from different regions of Spain (OXALID)**

## APPENDIX II The photos of samples

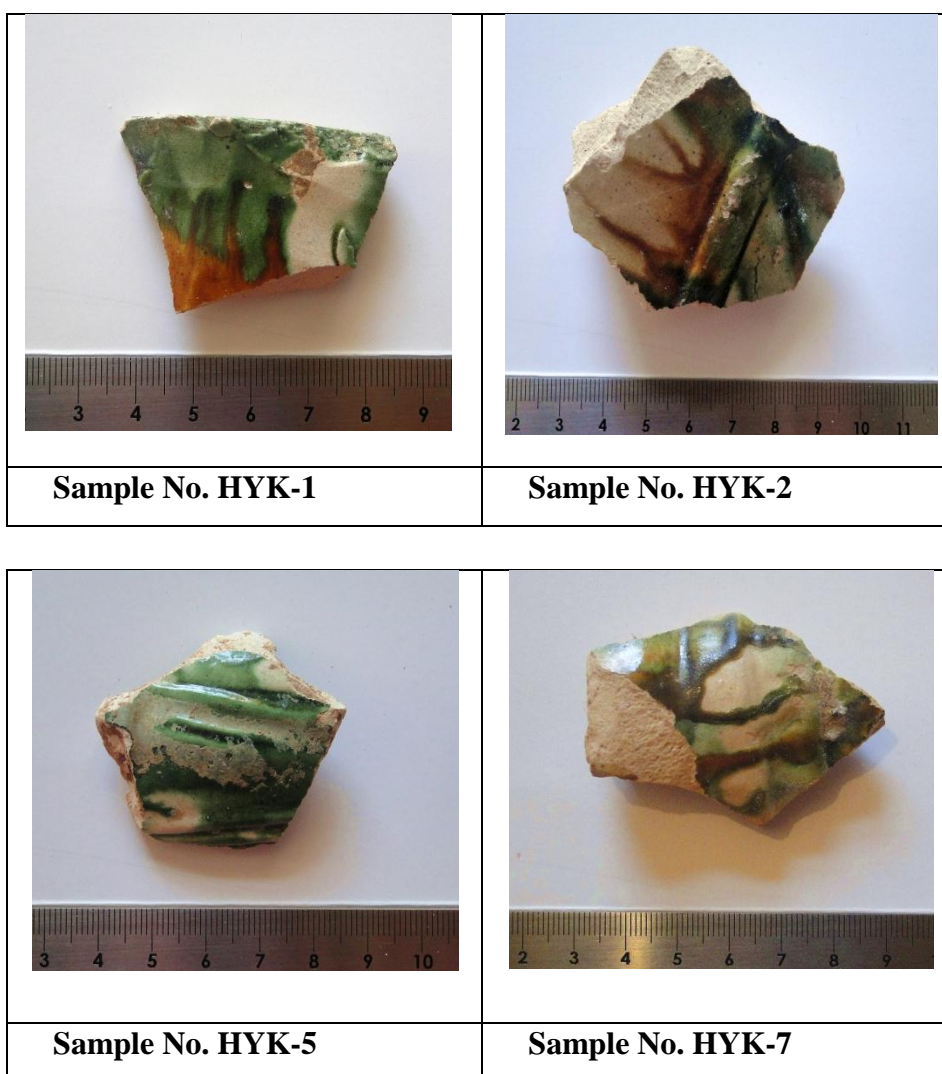
A-17 the photos of 'Chinese Tang Sancai' samples

A-18 the photos of Islamic lead glaze samples from Al-Raqqah in Syria and Hira or Kish in Iraq

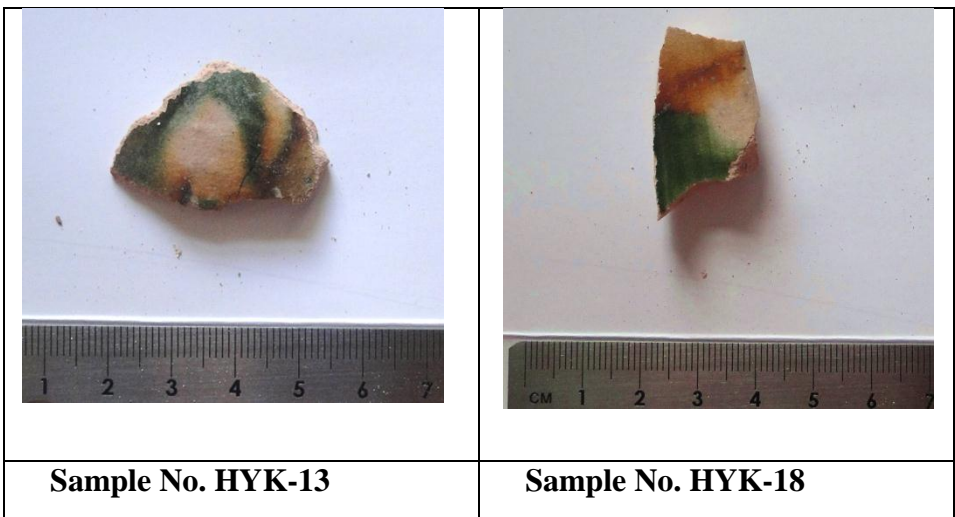
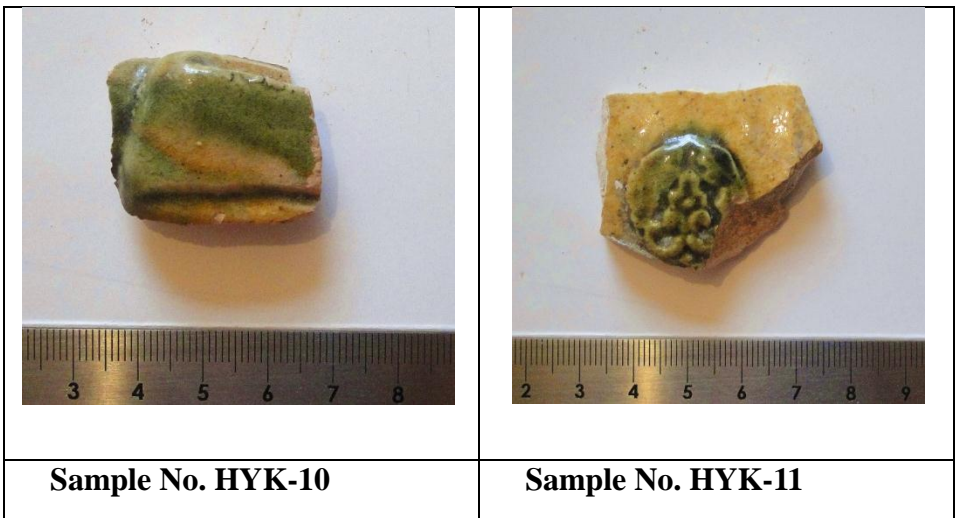
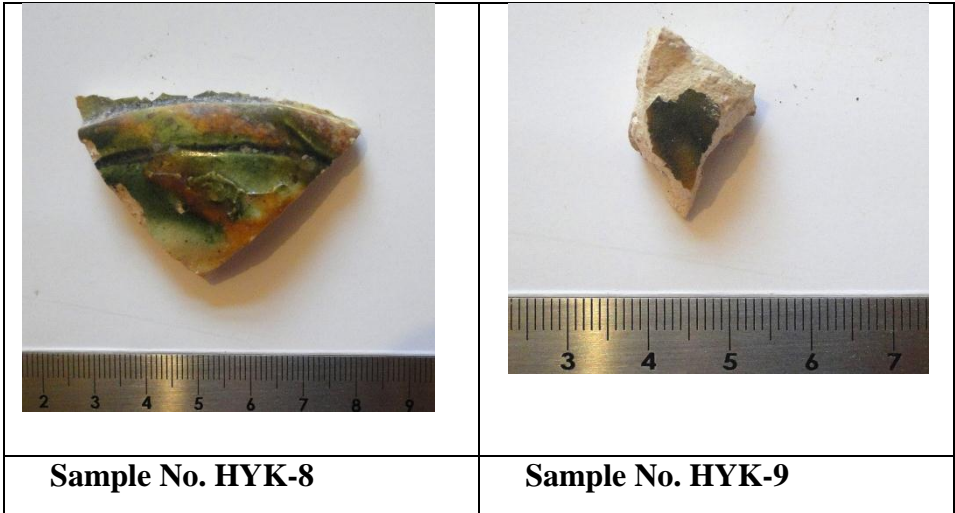
A-19 the photos of 'Yaozhou celadon glaze' samples

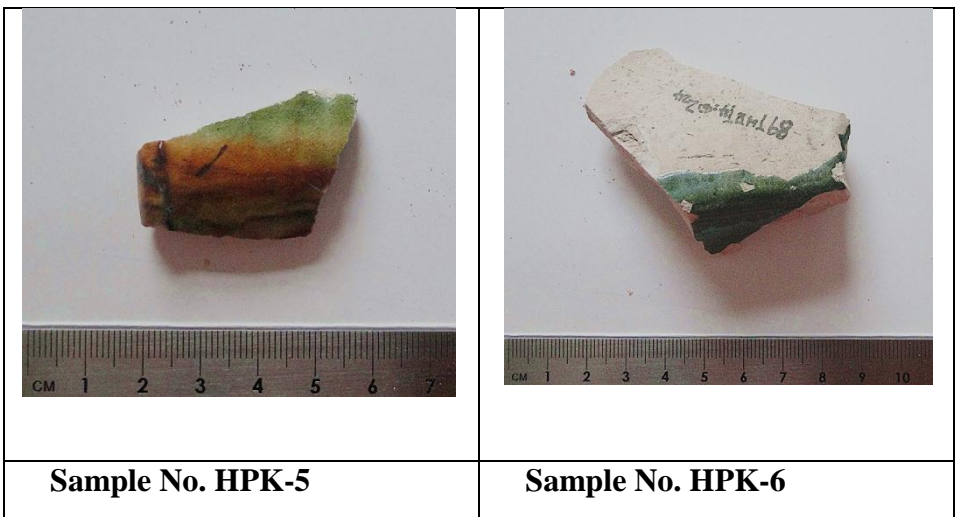
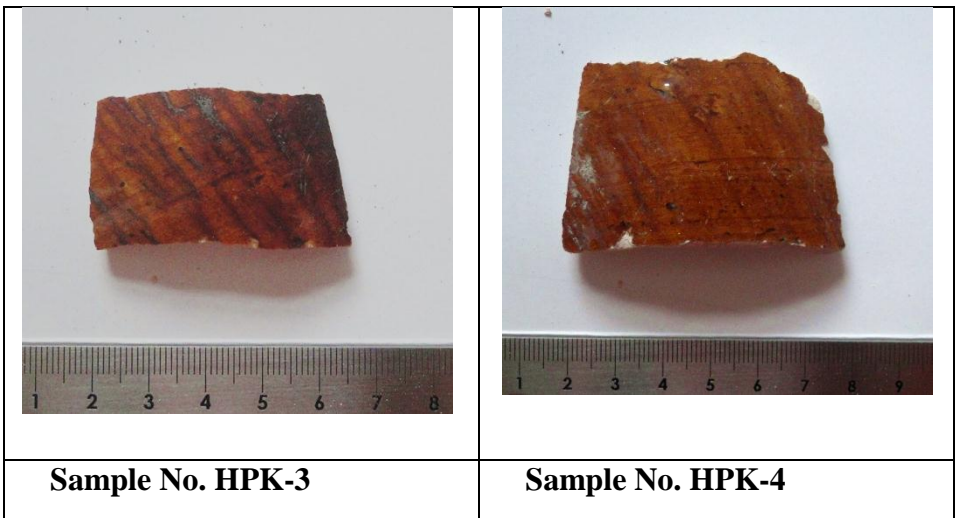
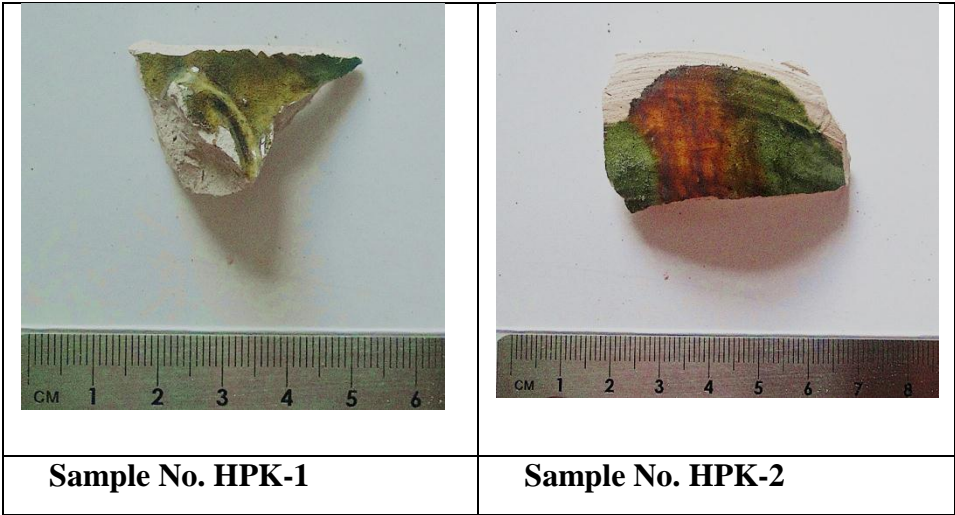
A-20 the photos of 'Raqqah ware' samples

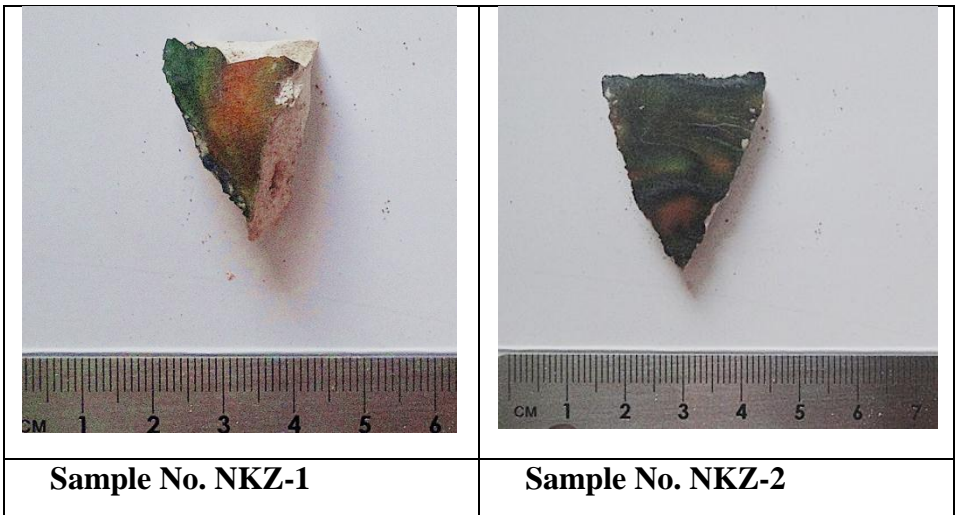
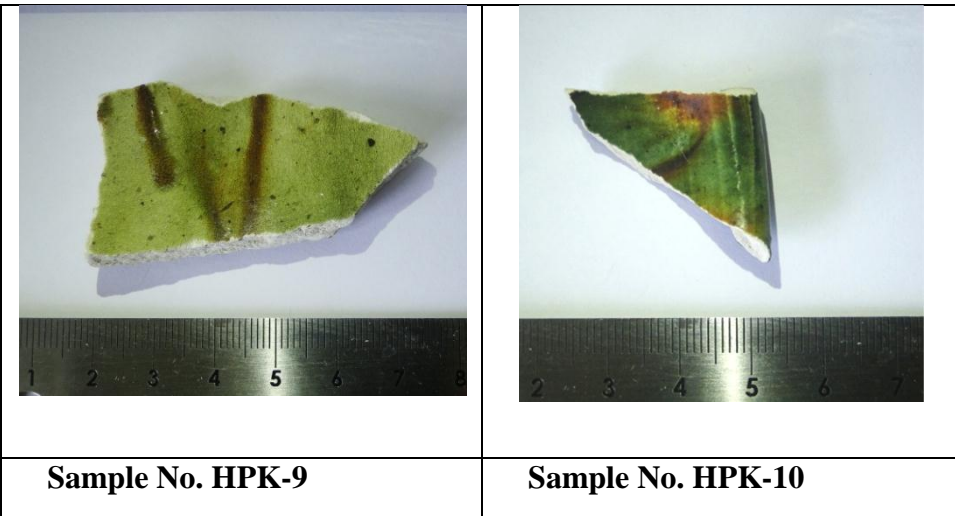
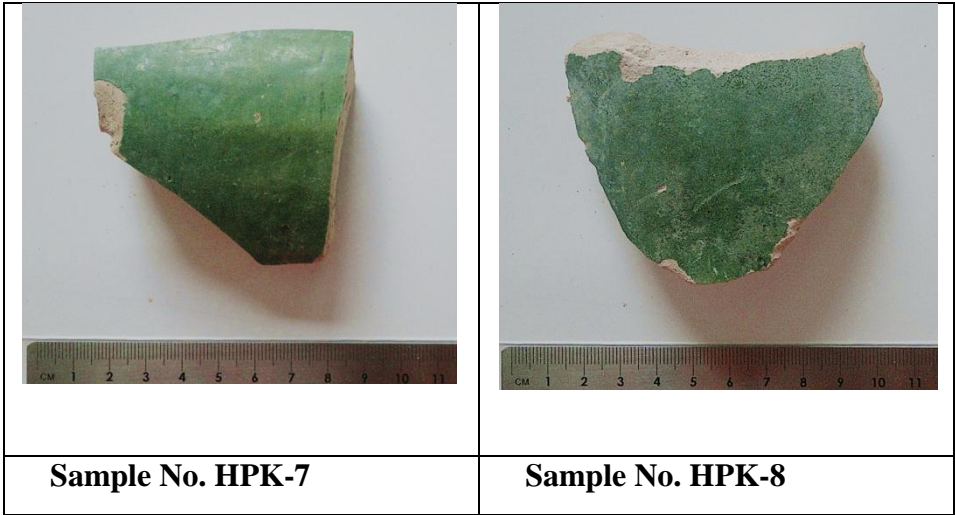
### A-17 the photos of 'Chinese Tang Sancai' samples



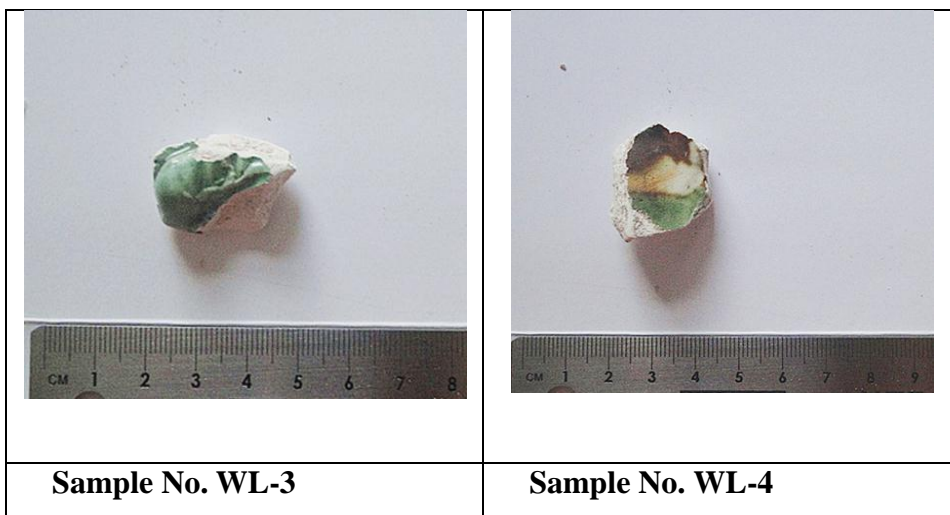
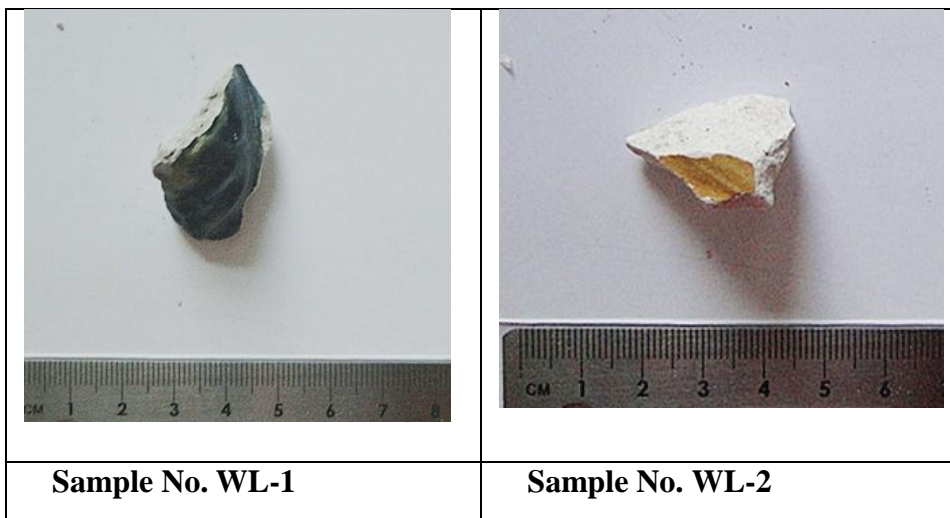
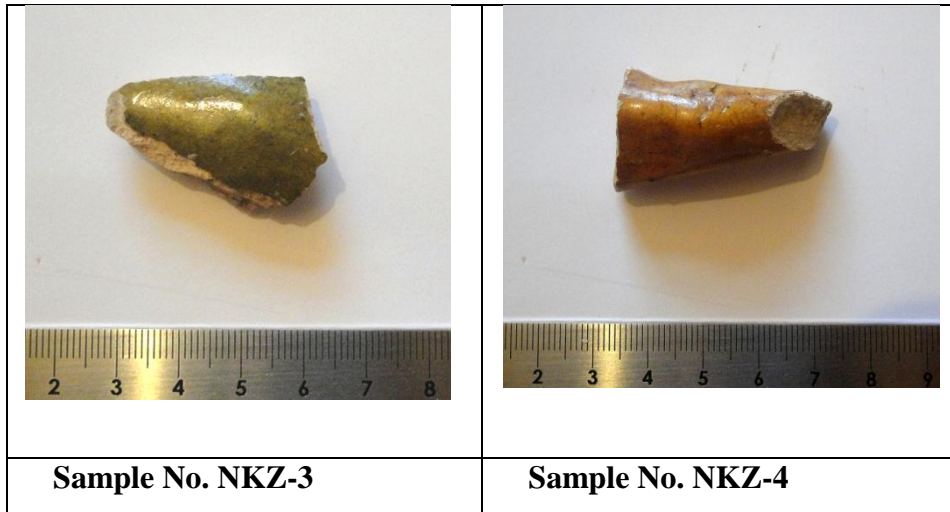


















**A-18 the photos of Islamic lead glaze samples from Al-Raqqa in Syria**

and Hira or Kish in Iraq

	
<b>Sample No. Syria-4</b>	<b>Sample No. Syria-7</b>

	
<b>Sample No. 9913</b>	<b>Sample No. 9393</b>

	
<b>Sample No. 9921</b>	<b>Sample No. 9921</b>



**Sample No. 9156**



**Sample No. 9156**



**Sample No. 9161**



**Sample No. 9161**



**Sample No. 9147**



**Sample No. 9162**





**Sample No. 9159**



**Sample No. 9159**



**Sample No. 9915**



**Sample No. 9915**



**Sample No. 9160**



**Sample No. 9160**



**Sample No. 9312**



**Sample No. 9312**



**Sample No. 9309**



**Sample No. 9309**

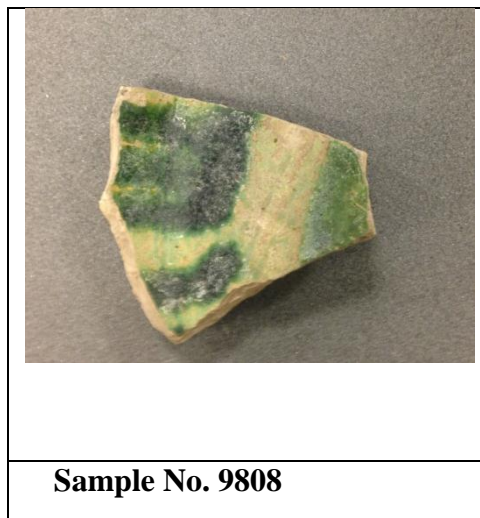
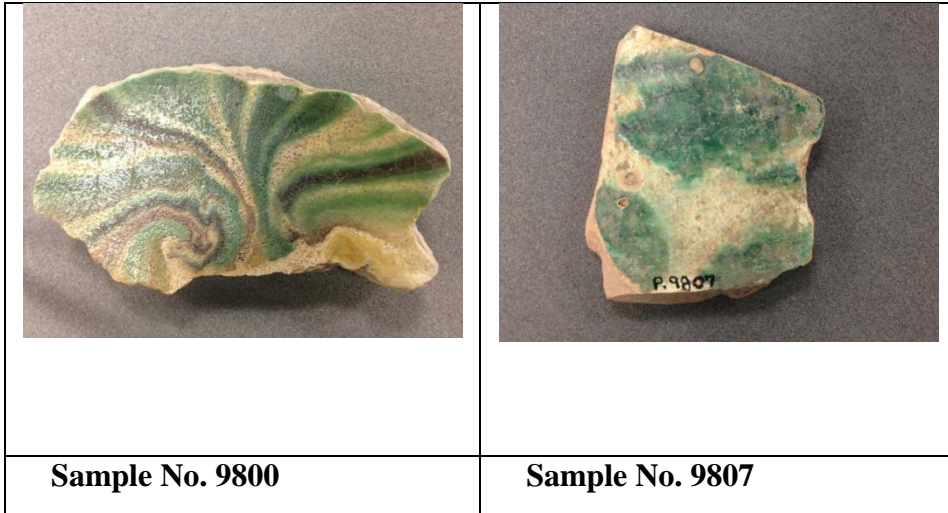


**Sample No. 9308**

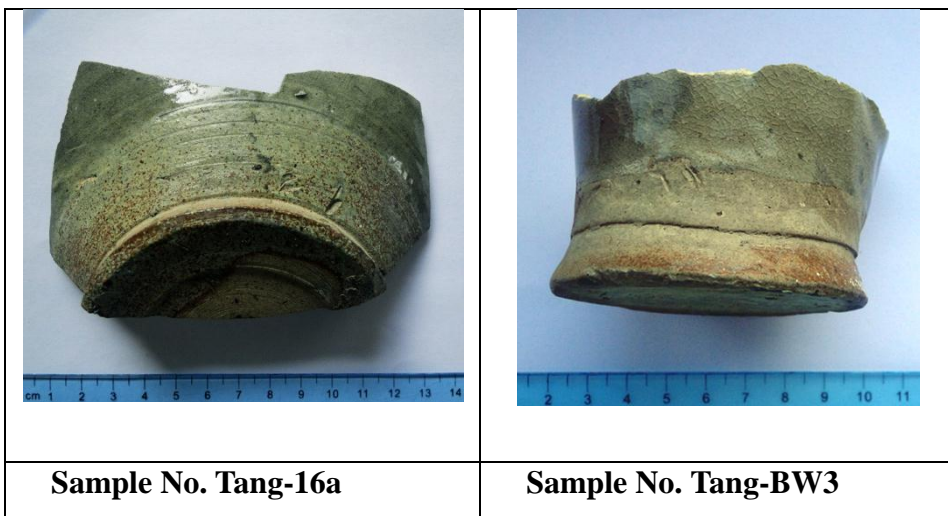


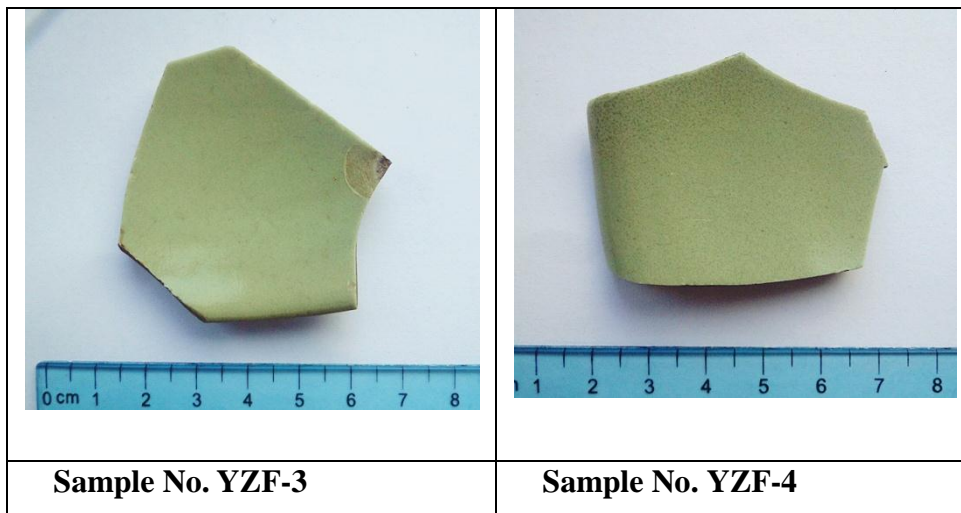
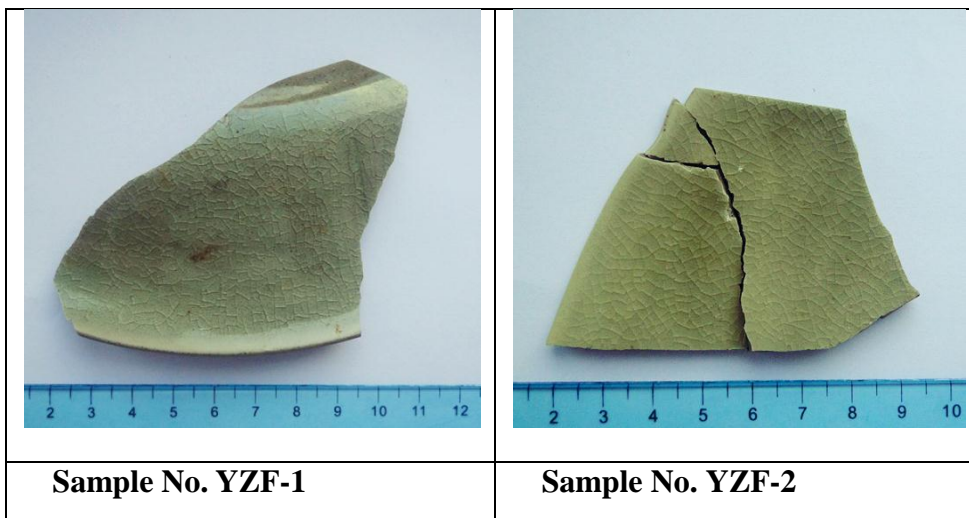
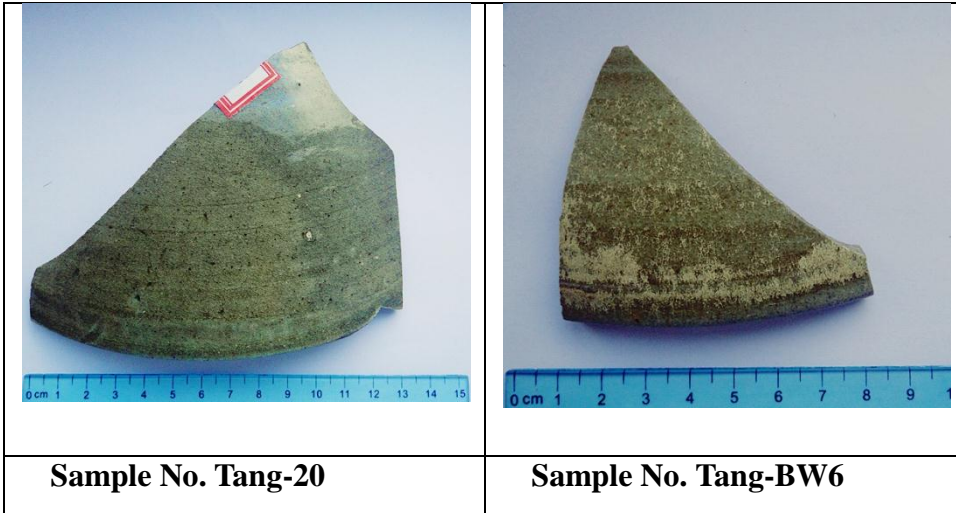
**Sample No. 9798**





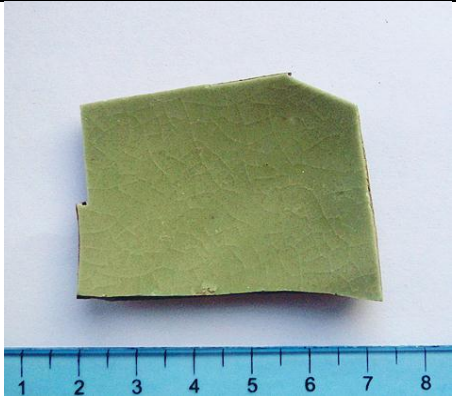
**A-19 the photos of 'Yaozhou celadon glaze' samples**







**Sample No. YZF-5**



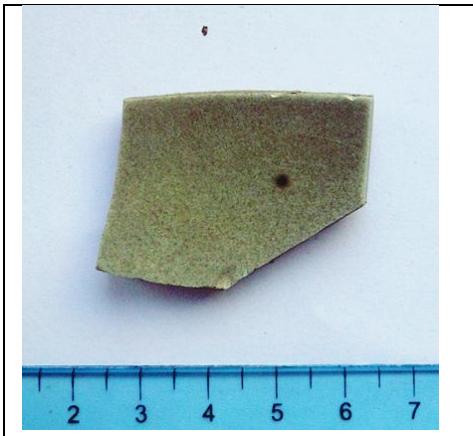
**Sample No. YZF-6**



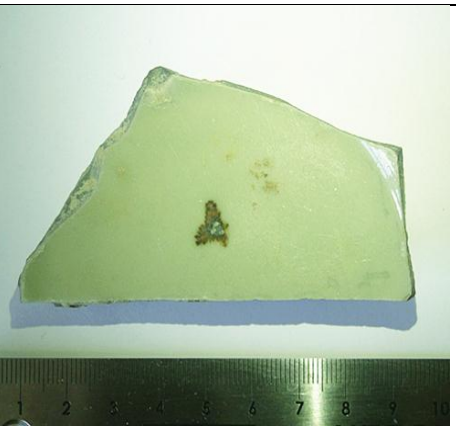
**Sample No. YZF-7**



**Sample No. YZF-7**

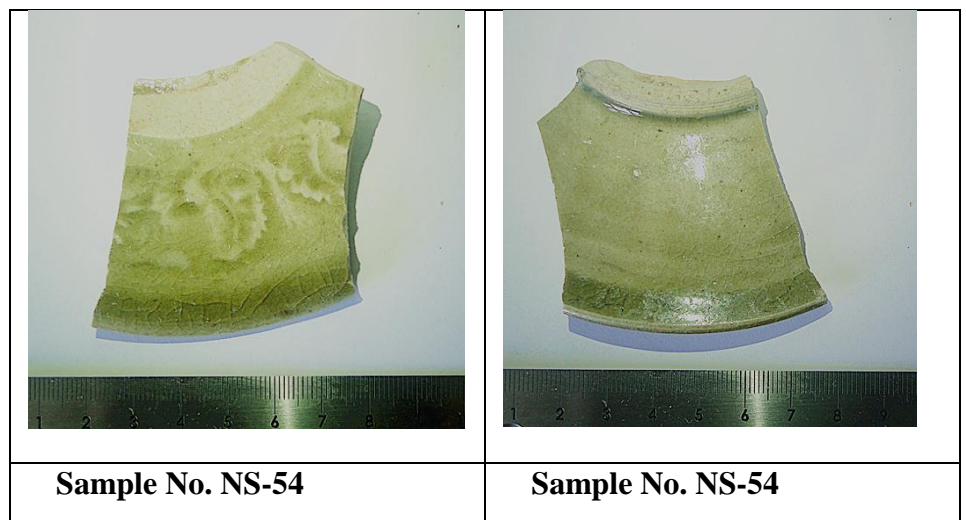
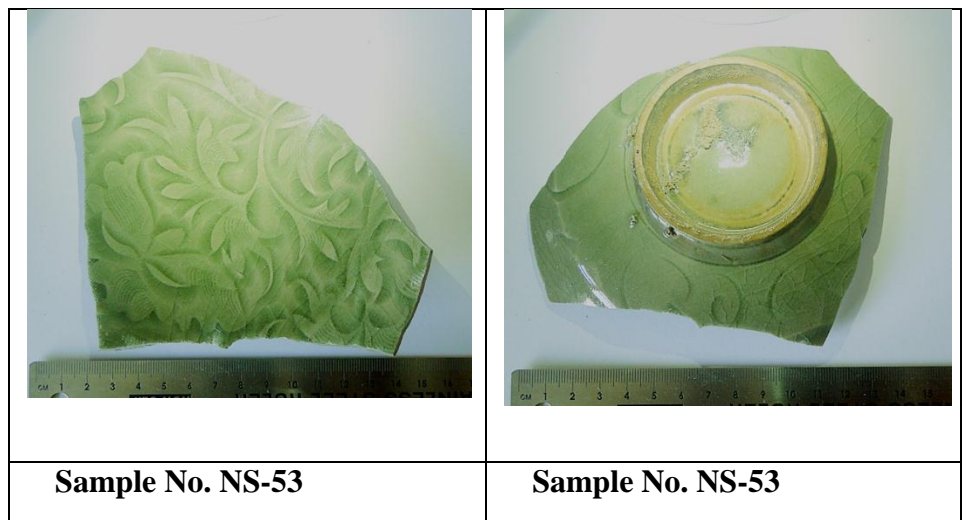
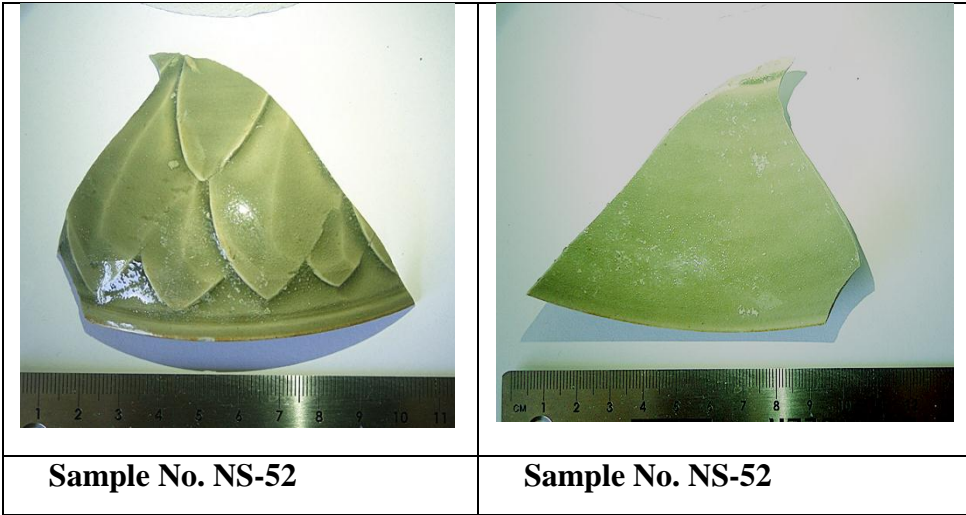


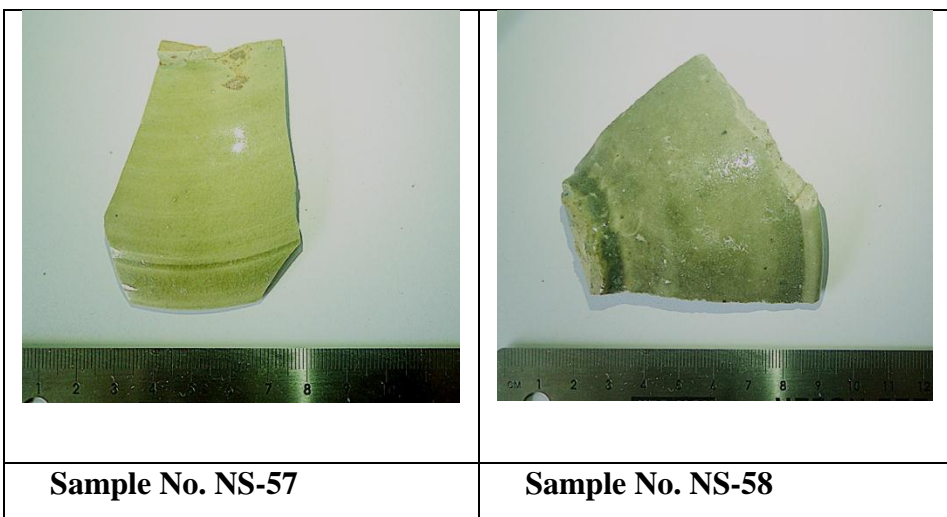
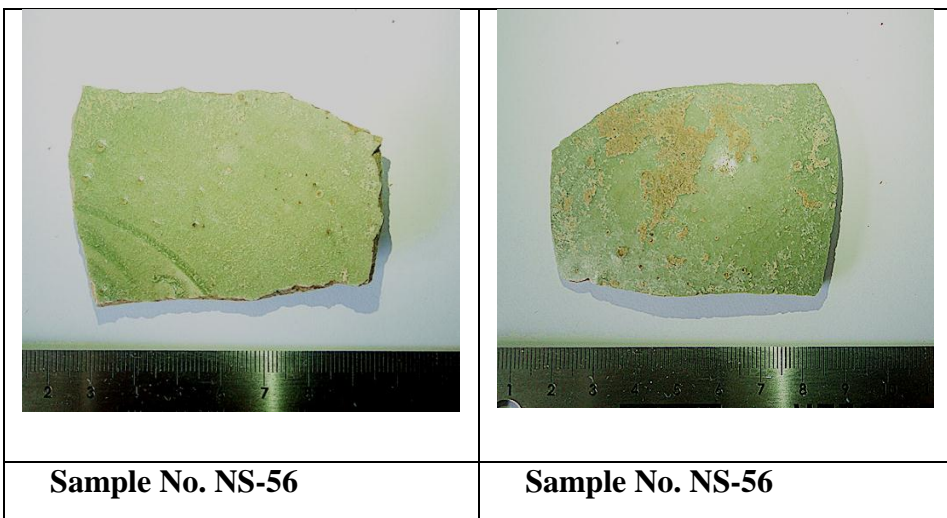
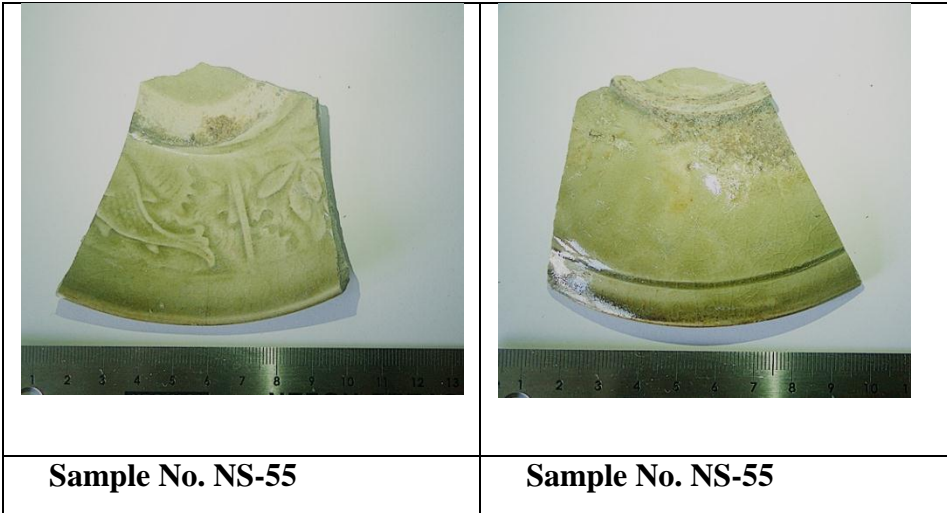
**Sample No. YZF-8**

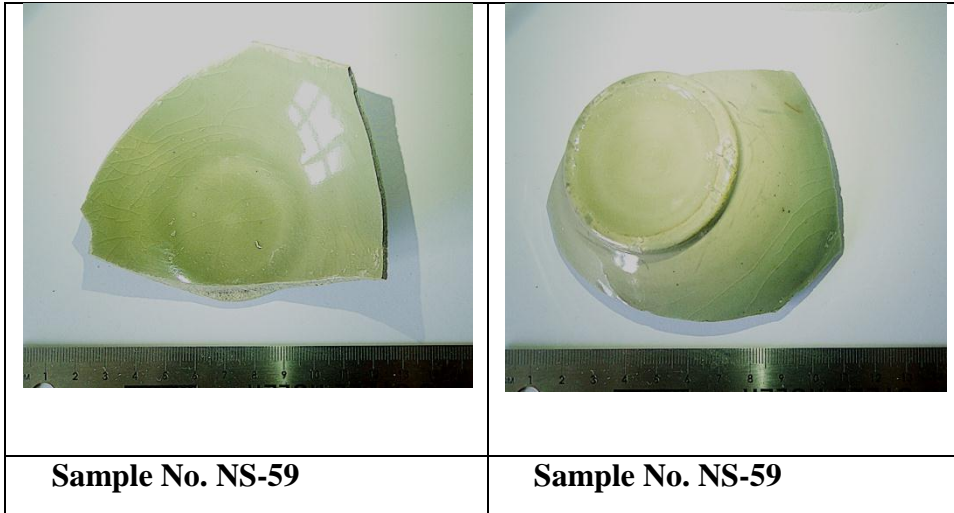


**Sample No. YZF-9**

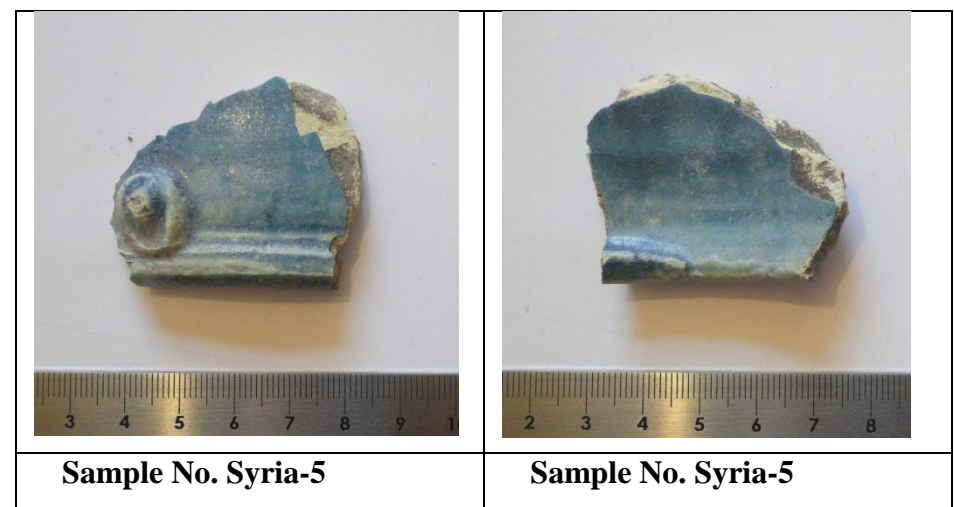
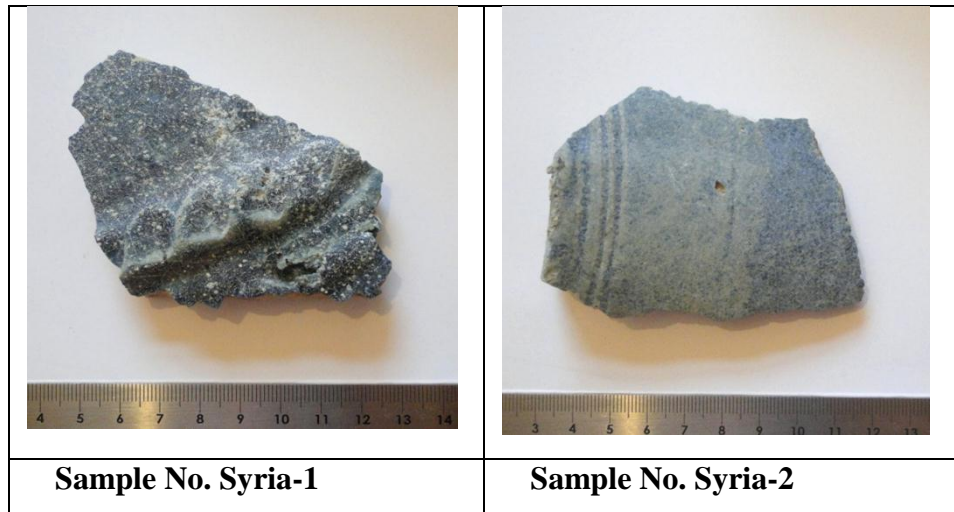




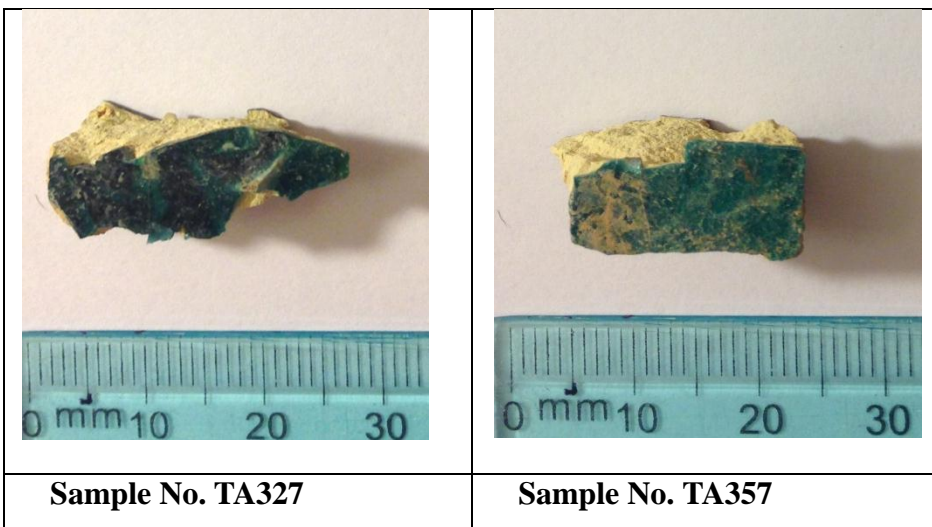
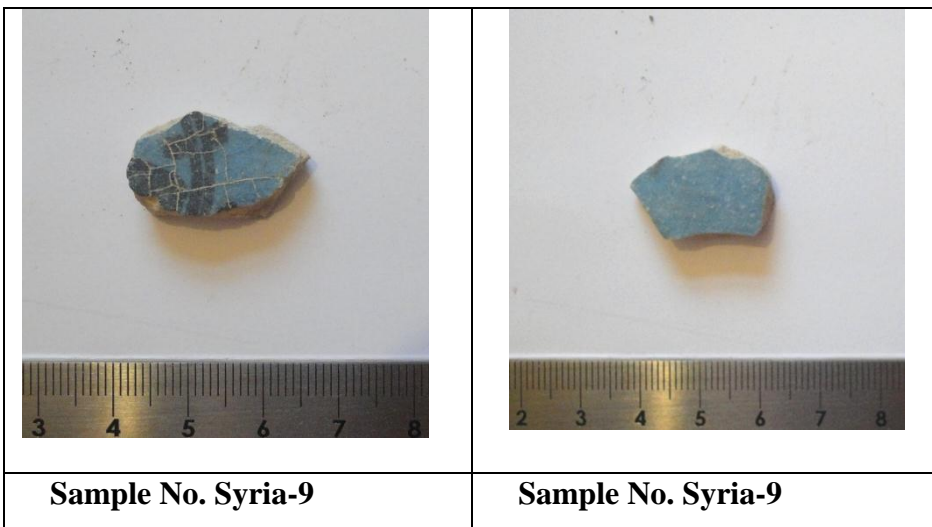
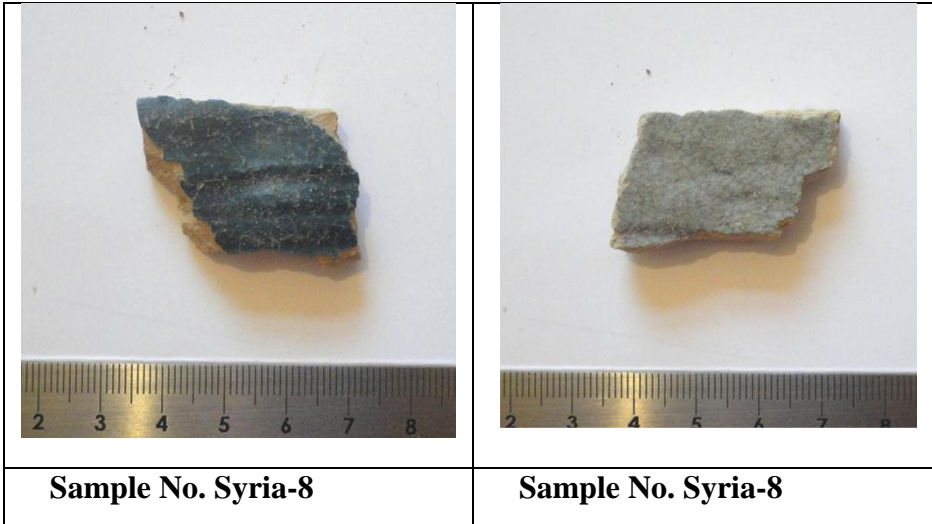




**A-20 the photos of 'Raqqa ware' samples**









**Sample No. TA 1043**